The homogeneous hydrogenation of esters and related compounds by a ruthenium triphosphine complex

Derek Vincent Tyers

THE HOMOGENEOUS HYDROGENATION OF ESTERS AND RELATED COMPOUNDS BY A RUTHENIUM TRIPHOSPHINE COMPLEX

THE HOMOGENEOUS HYDROGENATION OF ESTERS AND RELATED COMPOUNDS BY A RUTHENIUM TRIPHOSPHINE COMPLEX

Derek Vincent Tyers

Submitted for the Degree of
Doctor of Philosophy

University of Durham
Department of Chemistry
2002

To my Mum and Dad,
my brothers Anthony, Neil, Wayne and Simon,
and to Claire, my best friend.

"The journey which this little book is to describe was very agreeable and fortunate for me. After an uncouth beginning, I had the best of luck to the end. But we are all travellers in what John Bunyan calls the wilderness of this world – all, too, travellers with a donkey; and the best that we find in our travels is an honest friend. He is a fortunate voyager who finds many. We travel, indeed, to find them. They keep us worthy of ourselves; and, when we are alone, we are only nearer the absent."

Robert Louis Stevenson, a letter to Sidney Colvin, from Travels with a Donkey.

Acknowledgements

I would like to thank the members of lab 101, past and present, Nicky, Pete, Dave, Judith and Christopher. I would also like to thank my supervisors Dr. S. Crabtree (Davy Process Technology), Dr. A. Hughes and Dr. M. Kilner (University of Durham), a veritable embarrassment of riches.

My thanks, go also, to the staff at Davy Process Technology and the ancillary staff at the Department of Chemistry at the University of Durham for their invaluable help, and to Davy Process Technology for their sponsorship.

I would also like to thank my friends, especially Dave, Jan, John, Anne and Paul, and those of the Bowline Climbing Club.

Lastly, I must also thank Prof. K. Wade, who suggested, that I might like to consider what Durham had to offer.

The material in this thesis has not been submitted for examination for any other degree or part thereof, at the University of Durham or any other institution. The material contained herein is the sole work of the author except where formally acknowledged by reference.

Abstract

The homogeneous hydrogenation of esters and related compounds has been achieved by a catalyst-generated *in-situ* from the precursors $Ru(acac)_3$ and the tripodal phosphine ligand 1,1,1-tris(diphenylphosphinomethyl)ethane (Triphos). The catalyst is susceptible to deactivation in the presence of primary alcohols by their dehydrogenation to an aldehyde, which is subsequently decarbonylated to produce the $[Ru(Triphos)H_2(CO)]$ complex, characterised by ^1H and ^{31}P NMR spectroscopy, elemental analysis, IR and X-ray crystallography. The co-ordinated carbonyl ligand of $[Ru(Triphos)H_2(CO)]$ effectively blocks the co-ordination site required by the substrate for further hydrogenation, thus deactivating the catalyst.

Reactivation of the deactivated catalyst can be achieved, by introducing water to the reaction mixture, and removing the carbonyl ligand through the water gas shift reaction. The inclusion of water within the reaction solvent results in catalyst reactivation during the hydrogenation process.

Investigation of the hydrogenation of alkenes, in the absence of reagents susceptible to decarbonylation, resulted in the isolation of the solid dinuclear complex $[(Triphos)RuH(\mu\text{-}H)_2HRu(Triphos)]$, which was characterised by X-ray crystallography and ^{31}P NMR spectroscopy. Its information suggests that the active catalyst is $[Ru(Triphos)H_2]$.

The separation of the products from the catalyst and unconsumed reactants has been achieved by distillation of the product solution of the hydrogenation reaction. The recovered catalyst is sufficiently robust to be capable of multiple recycles, replicating the original and repeated result without loss of activity or selectivity.

Contents

Abbreviations

acac	acetylacetonato
Atm	atmosphere
BDO	1,4-butanediol
^{t}BuOH	2-methyl-2-propanol (*tert*-butanol)
BINAP	2,2'-bis(diphenylphosphino)-1,1'-binaphthyl
bipy	2, 2'-bipyridine
b.p.	boiling point
Cp	cyclopentadienyl
diglyme	diethylene glycol dimethyl ether (bis(2-methoxyethyl) ether)
DIOP	*O*-isopropylidene-2,3-dihydroxy-1,4-bis(diphenylphosphino)butane
diphos	1,2-bis(diphenylphosphino)ethane
DMF	*N*,*N*-dimethylformide
DMM	dimethyl maleate (*cis*-dimethyl-but-2-endioate)
DMS	dimethyl succinate (dimethyl butanedioate)
dppb	1,4-bis(diphenylphosphino)butane
gBL	γ-butyrolactone
homo	Highest occupied molecular orbital
iPA	propan-2-ol
lumo	Lowest unoccupied molecular orbital
m.o.	Molecular Orbital
NEt_3	triethylamine
NMR	Nuclear Magnetic Resonance
PBu_3	tributylphosphine
PCy_3	tricyclohexylphosphine
phen	1,10-phenanthroline
PPh_3	triphenylphosphine
PPr_3	tripropylphosphine (*n* or *i*)
*p*TSA	*p*-toluenesulphonic acid
py	pyridine
r.t.	Room Temperature

$mSP\text{ø}_2$	*m*-sulphophenyl-diphenylphosphine
THF	tetrahydrofuran
TMS	Tetramethylsilane
TPPMS	triphenylphosphine monosulphonate
TPPTS	triphenylphosphine trisulphonate
Triphos	1,1,1-tris(diphenylphosphinomethyl)ethane
ttp	bis(3-diphenylphosphino)propyl-phenylphosphine
WGS	Water-gas shift (reaction)

Chapter 1

Ruthenium Phosphine Hydride Chemistry

The hydrides of ruthenium-phosphine complexes are suitable for homogeneous catalytic hydrogenation. The use of the tripodal polyphosphine ligand 1,1,1-tris(diphenylphosphinomethyl)ethane allows the reactivity of the complex to be controlled to follow a specific reaction path.

1.1 Ruthenium Chemistry

Transition metal complexes are extensively used in catalytic applications. The platinum group metals in particular have been applied to a variety of catalytic reactions, both heterogeneous and homogeneous. Ruthenium has been found to catalyse reactions that include hydrogenation, hydroformylation, isomerisation, polymerisation, carbonylation and decarbonylation.[1] The intention of this review is to concentrate on the ruthenium chemistry associated with homogeneous catalytic hydrogenation; the overall chemistry of ruthenium has been extensively covered elsewhere.[2-6]

Ruthenium is in group eight of the periodic table and is one of the elements that forms the triad Fe, Ru and Os; it has the ground state electronic configuration of $[Kr]4d^7 5s^1$.[2] The chemistry of ruthenium is known to cover the oxidation states ranging from –II to VIII, but the organometallic chemistry is predominantly based on 0, II and III.[2, 5, 6, 7] Ruthenium (II) and (III) complexes favour octahedral geometry, with the co-ordinated ligands formally contributing 10 electrons to produce an 18 electron saturated arrangement. Although, ruthenium (II) 16 electron species, with square pyramidal geometry, can be obtained when sterically restrictive ligands stabilise the complex.[5]

Ruthenium forms an extensive range of phosphine complexes, which are primarily of the Ru(II), d^6 oxidation state, octahedral, t_{2g}^6 and diamagnetic.[7] Many ruthenium homogeneous catalysts are based on ruthenium-phosphine complexes, with two of the better known being $[RuCl_2(PPh_3)_3]$ (reacting probably as $[RuHCl(PPh_3)_3]$) and $[RuH_m(PPh_3)_n]$ (where m = 2 – 4, and n = 3 or 4).[1, 8] The ruthenium-phosphine dihydride complexes $[RuH_2(PPh_3)_n]$ (where n = 3 or 4) are easily obtained by

borohydride reduction of the dichloride.[7] The complexes will undergo the reversible addition of ligands such as CO and H_2, and can therefore be applied to hydrogenation reactions, etc..

1.2 Phosphine and Hydride Ligands

Ligands are denoted as being either an L or an X type ligand. The designation is for the purpose of electron accountancy, where an L type ligand donates two electrons to the metal whilst an X type ligand donates only one electron. X type ligands are σ-donors and typically are halides, amides, alkyls, aryls, alkoxides and the hydride. The L type ligands, as well as being a two-electron σ-donor to the metal, may also be π-acceptor ligands, such as alkenes, amines, CO or phosphines.

1.2.1 Phosphine Ligands

Phosphine ligands influence the chemistry of a metal complex through a combination of their electronic and steric properties, which are a direct consequence of the component substituents making up the ligand.

1.2.1.1 Electronic Effects of Phosphine Ligands

Phosphines are two-electron σ-donor, neutral L-type ligands that are able to act as π-acceptor ligands. The bond formed between the metal and the phosphine from the σ-donation involves the overlap of orbitals that are located directly between them, with two electrons formally donated by the phosphine (see Fig. 1.1, Sigma (σ) Bond). The phosphine, also acts as a π-acceptor ligand, through overlap of *d* orbitals of the respective metal and orbitals with the correct orientation from the phosphine. The traditional view is that vacant phosphine *d* orbitals overlap with filled metal *d* orbitals producing backbonding (see Fig. 1.1, $\pi_{d\text{-}d}$-Bond), but it is now understood that the σ*-orbitals of the phosphine P-R bonds are involved (see Fig. 1.1, $\pi_{d\text{-}\sigma^*}$-Bond).[9, 10] The contribution of the phosphorus 3*p* and 3*d* orbitals to the π bond, that accepts the transition metal backbonding, is believed to result in a hybrid orbital that is more suitable for energy and overlap requirements.[11] The π-acceptor properties of the phosphine increase as the electronegativity of the phosphine R group increases. The

resultant increased π-acceptor capacity of the phosphine reduces the electron density of the complex, that would otherwise have been absorbed by other π-acceptor ligands in the complex. This results in the other π-acceptor ligand's metal-ligand bond being lengthened and shortens that of the metal-phosphine bond.[10]

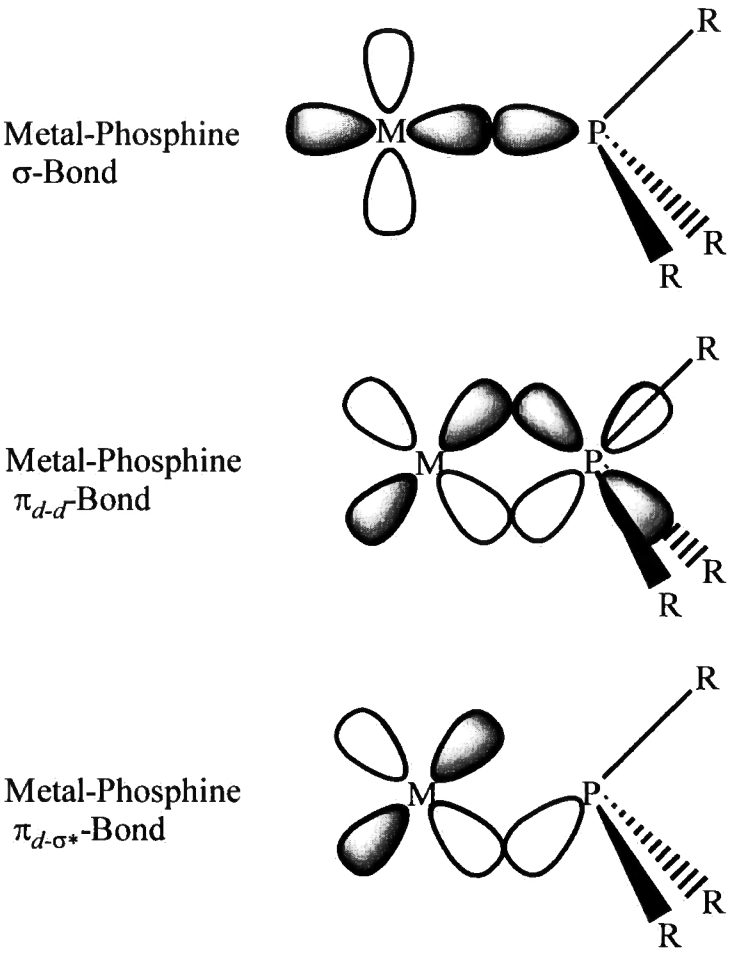

Figure 1.1 Metal-Phosphine Bonding Interactions

The availability of the phosphine's low energy *p* or *d* orbitals enables them to stabilise low oxidation states through back bonding. The high ligand field strength of phosphines can be important in catalysis, as the stabilisation of the low oxidation states prevents the reducing conditions of reactions, such as hydrogenation or hydroformylation, causing the precipitation of the metal, a problem encountered with the heavier transition metals.[12] Phosphine ligands have a relatively high *trans* effect. It is possible for up to

three phosphines to bond strongly to a metal, but any additional phosphines result in complexes that are susceptible to dissociation. Metal complexes containing labile ligands that easily dissociate, create free co-ordination sites suitable for activation of reactants and catalysis.[12]

1.2.1.2 Steric Effects of Phosphine Ligands

The steric bulk of a phosphine is a direct consequence of its respective substituent(s). The diversity of different substituents that can be incorporated into a phosphine produces a multitude of different individual steric properties. The steric effects of mono-phosphines was defined by Tolman in the cone angle θ, which for symmetrical ligands is measured as the apex angle of a cylindrical cone, that is centred 2.28 Å (228 pm) from the centre of the P atom of the phosphine, and which just touches the van der Waals radii of the outermost atoms of the respective substituents (see Fig. 1.2, Tolman Cone Angle).[13]

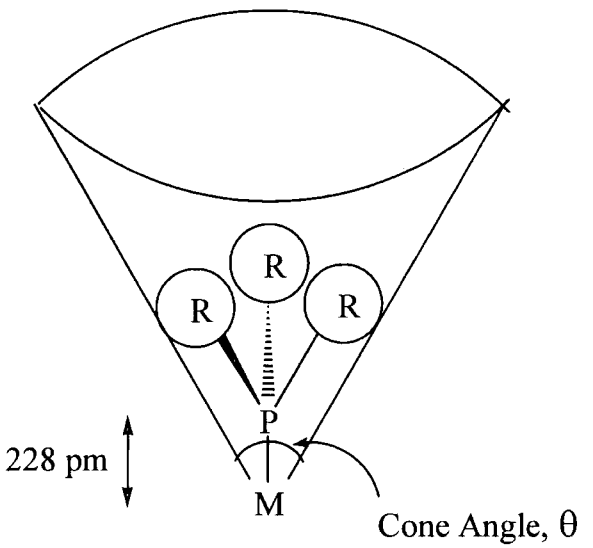

Figure 1.2 Tolman Cone Angle

The application of the cone angle as a quantification of the steric effects for phosphines is an effective tool for monodentate ligands, but is not so useful for diphosphines. The bite angle (see Fig. 1.3) is then a better parameter to apply for establishing the steric

implications.[14] The P-M-P angle of a transition metal complex is a result of a compromise between the bidentate phosphine's preferred bite angle and that of the metal. The bidentate phosphine's bite angle is predominantly dictated by the restrictions imposed by the nature of the ligand backbone and the steric interaction of the phosphine substituents, whereas, the preferred bite angle of the metal is primarily the result of the electronic requirements of the available *d* orbitals for the metal-phosphine bonds.

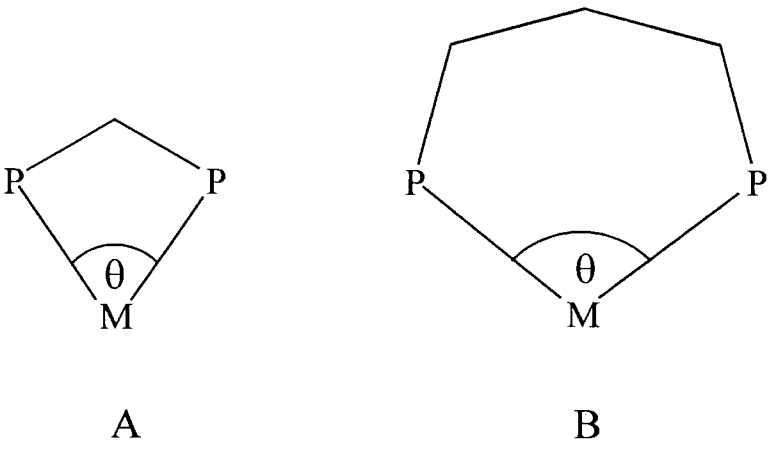

Figure 1.3 P-M-P Bite Angle
Note: P-M-P bite angle A < B.

The effect of P-M-P bite angles on the catalytic behaviour of metal-diphosphine complexes has been observed for platinum and rhodium catalysed hydroformylation, palladium catalysed cross coupling reaction and CO/alkene reactions, and nickel catalysed hydrocyanation reactions.[14] Hydroformylation reactions with rhodium catalysts, using diphosphine ligands with bite angles that are greater than 100°, produce mainly linear aldehydes and palladium catalysed reactions produce results with the best selectivity and activity when the diphosphine ligands have bite angles of roughly 100°. Dierkes and van Leeuwen concluded from this, that an optimum bite angle for each catalytic system exists.[14]

1.2.1.3 Tripodal Phosphine Ligands

A variety of different tripodal polyphosphine ligands has been synthesised and their chemistry investigated, but the majority of the studies has been focused on the triphosphine 1,1,1-tris(diphenylphosphinomethyl)ethane, $MeC(CH_2PPh_2)_3$, (Triphos) (see Fig. 1.4).[15]

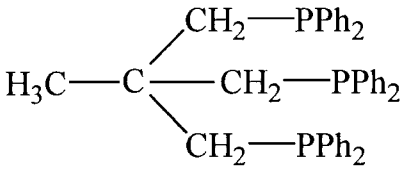

Figure 1.4 Triphos

Tripodal polyphosphine ligands, such as Triphos, co-ordinate to transition metals by occupying three *facial* sites of the co-ordination polyhedron (see Fig. 1.5).[16] The neopentyl skeleton of the $H_3CC(CH_2)_3$ *moiety* makes it possible for Triphos to occupy three *facial* sites of a square pyramidal, trigonal-bipyramidal or octahedral co-ordination sphere with almost no chelate ring strain.[15] The negligible chelate ring strain is due to the P-M-P bite angles of the transition metal-Triphos complexes, which are at their closest to being ideal in octahedral complexes where an almost unstrained geometry is obtained.

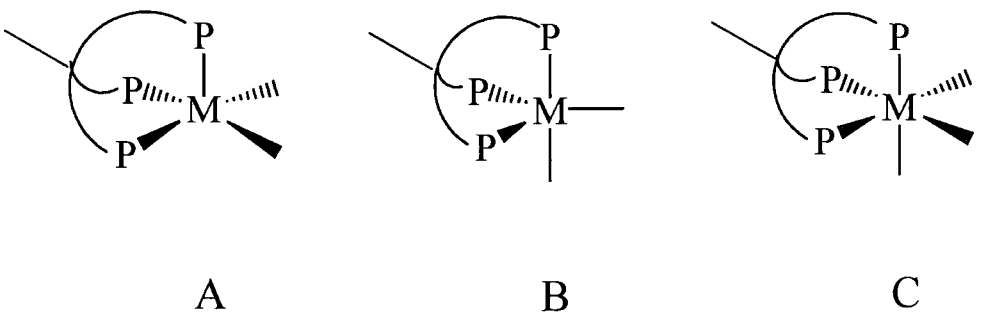

Figure 1.5 *Facial* Co-ordination of a Tripodal Polyphosphine Ligand (Triphos)
A: Square-pyramidal.
B: Trigonal-bipyramidal.
C: Octahedral.

Polyphosphine ligands, because of the chelate effect, allow control to be exercised over the electronic and structural properties of a complex, whilst maintaining its stoichiometry and stereochemistry. The application of polydentate phosphines makes it possible to alter the magnetic states, co-ordination geometries and the nucleophilicity of the metal, which can influence the reactivity of the complex.[12] Tripodal polyphosphines can form stable complexes with a variety of different oxidation states, and this results in many different metal co-ordination numbers being possible. The strength of bonding in tripodal triphosphines generates a strong *trans* effect, which can be used to direct the stereochemistry and stoichiometry of complexes formed in reactions.[17] Generally, the control is achieved by the use of the carefully considered selection of specific components for incorporation into a polydentate ligand, such as donor atoms, sterically hindering substituents and chelate bite angles. The tripodal triphosphine ligands are able to co-ordinate with most transition metals to form stable complexes, and with the platinum group metals in particular which has promoted their investigation as ligands in catalytic systems. Bianchini *et al* observed that tailoring the tripodal ligand and metal assembly could ensure that a particular substrate reaction followed a specific reaction pathway to produce the desired product.[17]

1.2.2 Hydride Ligands

The hydride (H^-) ligand is the simplest anionic ligand, and a metal hydride is defined as a complex that consists of a transition metal with one or more hydrogen atoms that are directly bonded to it.[10] The expression "metal hydride" suggests an ionic compound, or at least a covalent compound, polarised in the orientation of $M^+ H^-$, and possessing the associated nucleophilic properties of H^-.[18] This however, is usually only true for main group metal hydrides and not transition metal complexes.

The reactivity of boron and main group metal hydrides, with regard to reduction reactions, has made them indispensable reagents for laboratory based situations. They are, however, impractical for large scale or commercial use because they are both expensive and are not easily formed directly from H_2.[18] The capability of transition metals to form complexes directly from H_2, and to be regenerated in a similar manner has made them attractive for use in large scale catalytic reductions. This has resulted in considerable interest being shown in understanding the chemistry of transition metal hydride complexes.[1, 18-27]

Catalytic hydrogenation requires that molecular hydrogen be activated or divided by the catalyst, which for homogeneous transition metal complexes, was postulated as occurring by a combination of two interactions.[19] The first requires H_2 to be an electron donor, with its bonding orbital interacting with a vacant orbital of the metal.[28] The second interaction is the π-overlap of a filled metal π-orbital with the hydrogen σ*-orbital, facilitating the transfer of electron density from the metal to the hydrogen molecule. A combination of both these interactions is probably the means by which the hydrogen molecule is converted from a $M(\eta^2\text{-}H_2)$ complex to a dihydride, $M(H)_2$.[27] The electron donation from the filled H_2 σ orbital to a transition metal d_σ orbital results in the H-H bond being weakened, a two-electron three-centre bond forming for the three atoms. The H-H bond is broken when there is sufficient backbonding (electron transfer) from the transition metal's full d_π orbitals into the empty H_2 σ* orbital (see Fig. 1.6).[27]

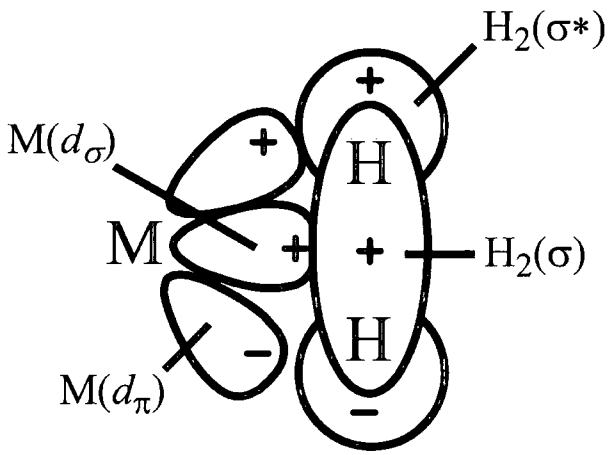

Figure 1.6 Proposed Metal-Hydrogen Bonding

The presence of electron withdrawing ligands bonded to the transition metal results in a reduction of the metal to H_2 backbonding, and therefore the H-H bond is not necessarily broken. This can result in the formation of a nonclassical hydride complex, $M(\eta^2\text{-}H_2)$ rather than the normal dihydride complex, $M(H)_2$ (see Fig. 1.7).[27]

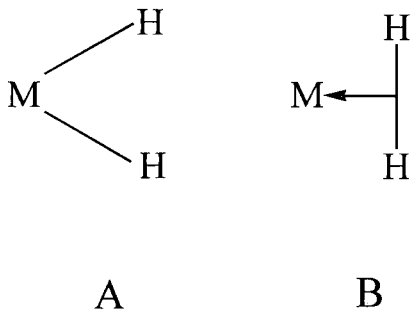

Figure 1.7 Classical and Nonclassical Metal Dihydrogen Complexes
A: Classical Dihydride.
B: Nonclassical Dihydride.

For transition metal-hydride complexes to hydrogenate substrates, the classical dihydride configuration of the complex is required. The metal complex also requires the availability of an adjacent vacant co-ordination site, which can be provided by dissociation of a labile ligand.[19] To enable hydrogenation to proceed the metal-hydride requires to be located *cis* to the vacant co-ordination site, so that it is able to interact with the incoming substrate that is to be hydrogenated.

1.3 Summary

Homogeneous hydrogenation with transition metal-phosphine complexes, where the phosphine is a tripodal polyphosphine, allows features that control of the reaction pathway to be incorporated into the complex. The complexation of ruthenium(II) with the tripodal Triphos phosphine produces an octahedral complex, where the *facial* co-ordination of the Triphos ensures that the three remaining co-ordination sites are all *cis* to each other. This guarantees that the hydride species of the complex is adjacent to any substrate and available for interaction for its hydrogenation. The *trans* effect and the steric hindrance of the Triphos, as a result of the phenyl substituents, influences the dissociation of the ligands and substrates co-ordinated to the ruthenium-complex.

1.4 References

1. B. R James, *Inorg. Chim. Acta, Res.*, 1970, 73.

2. N. N. Greenwood and A. Earnshaw, *Chemistry of the Elements*, Pergamon Press plc, Oxford, 1986.
3. E. A. Seddon and K. R. Seddon, *The Chemistry of Ruthenium*, Elsevier, Amsterdam, 1984.
4. E. W. Abel, F. G. A. Stone and G. Wilkinson, *Comprehensive Organometallic Chemistry*, Pergamon Press, Oxford, 1982, Vol. 4.
5. E. W. Abel, F. G. A. Stone and G. Wilkinson, *Comprehensive Organometallic Chemistry II*, Pergamon Press, Oxford, 1987, Vol. 7.
6. R. D. Gillard, J. A. McCleverty and G. Wilkinson, *Comprehensive Co-ordination Chemistry*, Pergamon Press, Oxford, 1987, Vol. 4.
7. F. A. Cotton and G. Wilkinson, *Advanced Inorganic Chemistry*, John Wiley & Sons, Chichester, 5th edn., 1988.
8. D. E. Linn, Jr., and J. Halpern, *J. Am. Chem. Soc.*, 1987, **109**, 2969.
9. A. G. Orpen and N. G. Connelly, *Organometallics*, 1990, **9**, 1206.
10. M. J. Winter, *d-Block Chemistry*, Oxford University Press, Oxford, 1994.
11. P. B. Dias, M. E. Minas de Piedade and J. A. Martinho Simões, *Coord. Chem. Res.*, 1994, **135/136**, 737.
12. *Homogeneous Catalysis with Metal Phosphine Complexes*, L. H. Pignolet, ed., Plenum Press, New York, 1983.
13. C. A. Tolman, *Chem. Res.*, **77**, 1977, 313.
14. P. Dierkes and P. W. N. M. van Leeuwen, *J. Chem. Soc., Dalton Trans.*, 1999, 1519.
15. C. Landgrafe, W. S. Scheldrick and M. Südfeld, *Eur. J. Inorg. Chem.*, 1998, 407.
16. C. Bianchini, A. Meli, M. Peruzzini and F. Vizza, *Organometallics*, 1990, **9**, 226.
17. C. Bianchini, A. Meli, M. Peruzzini, F. Vizza and F. Zanobini, *Co-ord. Chem. Rev.*, 1992, **120**, 193.
18. *Transition Metal Hydrides*, A, Dedieu, ed., VCH Publishers, Inc., New York, 1992.
19. R. E. Harmon, S. K. Gupta and D. J. Brown, *Chem. Rev.*, 1973, **73**, 22.
20. G. L. Geoffroy and J. R. Lehman, *Adv. Inorg. Chem., Radiochem.*, 1977, **20**, 189.
21. B. R. James, *Adv. Organomet. Chem.*, 1979, **17**, 319.
22. L. M. Venanzi, *Coord. Chem. Rev.*, 1982, **43**, 251.
23. G. G. Hlatky and R. H. Crabtree, *Coord. Chem. Rev.*, 1985, **65**, 1.
24. M. Y. Darensbourg and C. E. Ash, *Adv. Organomet. Chem.*, 1987, **27**, 1.
25. R. A. Henderson, *Transition Met. Chem.*, 1988, **13**, 474.
26. R. H. Crabtree and D. G. Hamilton, *Adv. Organomet. Chem.*, 1988, **28**, 299.
27. R. H. Crabtree. *Acc. Chem. Res.*, 1990, **23**, 4, 95.
28. J. A. Osborn, F. H. Jardine, J. F. Young and G. Wilkinson, *J. Chem. Soc. A*, 1966, 1711.

Chapter 2

Homogeneous Ester Hydrogenation

The homogeneous ruthenium-phosphine catalyst generated in situ from tris(acetylacetonate)ruthenium ($Ru(acac)_3$) and the tripodal phosphine 1,1,1-tris(diphenylphosphinomethyl)ethane (Triphos), will hydrogenate aliphatic and aromatic esters to their respective alcohols. The ester hydrogenation can be performed at 140°C with 6.8MPa of H_2 in the absence of a solvent and in the presence of water. An excess of water results in increased ester conversion.

2.1 Introduction

Ester reduction can be achieved by either chemical reduction or catalytic hydrogenation. The ester is cleaved to produce an alcohol that corresponds to the acid segment of the ester, and the alcohol derivative.

$$C_2H_5CO_2CH_3 \rightarrow CH_3(CH_2)_2OH + CH_3OH$$

Methyl propanoate — 1-Propanol — Methanol

Chemical reduction is carried out using lithium aluminium hydride, or where selectivity is required [1] with sodium and ethanol (the Bouvealt-Blanc reduction [2]). Catalytic hydrogenation is achieved using a copper chromite catalyst at high temperatures and pressures [3] (this is the preferred industrial process for ester hydrogenation).

The copper chromite hydrogenation catalyst used for ester reduction is a heterogeneous catalyst. Homogeneous catalysts for the hydrogenation of esters to alcohols have been reported, but none that are capable of producing comparable results to the heterogeneous copper chromite catalyst. The only reported homogeneous ester hydrogenation catalysts are ruthenium complexes.

2.1.1 Anionic ruthenium hydride catalyst

Anionic ruthenium hydride complexes were reported by Grey *et al* for the catalytic homogeneous hydrogenation of various polar organic compounds, including esters.[4] Grey *et al* had proposed that an anionic transition-metal hydride complex would act as a catalytic transfer agent,[5] the reduction being carried out by an equilibrium of hydrogen gas with the complex. Transition-metal hydride complexes have the ability to exhibit characteristics in the range of being mainly acidic ($L_nM^{\delta-}H^{\delta+}$) to mainly hydridic ($L_nM^{\delta+}H^{\delta-}$) in nature, depending on the character of the metal and the charge-transfer properties of the ligands. To achieve the maximum hydridic character and nucleophilicity of the hydride ligands Grey *et al* selected the anionic form. Grey *et al* investigated complexes of the general formula $A^+[L_nM{-}H_x]^-$, where A^+ is an alkali metal cation, M is a group 8 metal and L a tertiary phosphine ligand. Ruthenium was chosen as the group 8 metal because ruthenium complexes have the capacity to reversibly interact with polar organic substrates. Tertiary phosphine ligands were used due to their minimal electron withdrawing properties (compared with carbonyls, for example).[6] The potassium hydrido(phosphine)ruthenate complexes $K^+[(PPh_3)_2Ph_2PC_6H_4RuH_2]^-\cdot C_{10}H_8\cdot(C_2H_5)_2O$ [**1**] and $K_2[(PPh_3)_3(PPh_2)Ru_2H_4]^{2-}\cdot 2C_6H_{14}O_3$ [**2**] were synthesised and their properties as homogeneous catalysts studied.

Catalyst [**1**], in toluene at 90°C and 620 kPa of hydrogen for 20 hours, hydrogenated the activated esters dimethyl oxalate, methyl trifluoroacetate (both 10% conversion) and 2,2,2-trifluoroethyl trifluoroacetate (100% conversion) but not aliphatic or aromatic esters. Catalyst [**2**], under the same conditions, hydrogenated the activated esters dimethyl oxalate (70% conversion), methyl trifluoroacetate (88% conversion) and 2,2,2-trifluoroethyl trifluoroacetate (100% conversion). The hydrogenation of dimethyl oxalate by the catalysts, [**1**] and [**2**], produced methyl glycolate but not ethylene glycol. Neither catalyst was able to reduce the methyl glycolate to ethylene glycol.

Catalyst [**2**] was able to hydrogenate the aliphatic esters methyl acetate (22% conversion), ethyl acetate (8% conversion) and methyl propionate (5% conversion) but not aromatic esters (such as benzyl benzoate). When Grey *et al* replaced the catalysts [**1**] and [**2**] with their respective precursors, $[(PPh_3)_3RuHCl]\cdot$toluene and $\{[(PPh_3)_2RuHCl]\cdot\text{toluene}\}_2$, the % ester conversion decreased. Similarly, % ester

conversion decreased when the toluene solvent was replaced with THF or 18-crown-6. The cation-modifying ethers indicated that the hydridoruthenate catalysed reactions are cation assisted. Grey *et al* concluded that the anionic properties of [**1**] and [**2**] were necessary for the catalytic activity detected, which they interpreted as being nucleophilic hydride transfer. The results obtained also indicated that esters with electron-withdrawing groups adjacent to the unsaturated functional group, such as 2,2,2-trifluoroethyl trifluoroacetate, are more easily hydrogenated.

2.1.2 Neutral ruthenium hydride catalyst

Halpern and Linn reported that the neutral $[RuH_4(PPh_3)_3]$ catalyst is more active than the anionic $[RuH_3(PPh_3)_3]^-$ catalyst, for the hydrogenation of ketones and arenes.[7] Halpern and Linn investigated the anionic hydrido(phosphine)ruthenate complex $[(PPh_3)_2Ph_2PC_6H_4RuH_2]^-$ reported by Grey *et al* [4,5] in the mechanism of the hydrogenation of ketones and arenes. They discovered that $[(PPh_3)_2Ph_2PC_6H_4RuH_2]^-$ in the presence of H_2 was rapidly converted to *fac*-$[RuH_3(PPh_3)_3]^-$. In the catalytic hydrogenation of anthracene [8] *fac*-$[RuH_3(PPh_3)_3]^-$ reacts to form the bis(phosphine) complexes $[RuH(PPh_3)_2(anthracene)]^-$ and $[RuH_5(PPh_3)_2]^-$, possibly the catalytic intermediates in the reaction. Grey *et al* had reported that the anionic catalyst $[(PPh_3)_2Ph_2PC_6H_4RuH_2]^-$ is effective for the catalytic hydrogenation of polar compounds such as ketones, esters and nitriles.[4] Grey *et al* suggested that the anionic nature of the catalyst enhanced its efficacy as a hydride donor. The transfer of a hydride ion from the ruthenium hydride to the substrate proceeded because of the nucleophilic reactivity of $[(PPh_3)_2Ph_2PC_6H_4RuH_2]^-$. Halpern and Linn considered the mechanism of the catalysis and the nature of the catalyst to be unclear, as the products of ester and ketone hydrogenation are alcohols and anionic ruthenium hydride complexes are susceptible to protonation. They compared the catalytic properties of neutral and anionic complexes using $[RuH_4(PPh_3)_3]$ and $[RuH_3(PPh_3)_3]^-$ for the hydrogenation of cyclohexanone. The $[RuH_3(PPh_3)_3]^-$ catalysed hydrogenation of cyclohexanone is initially ineffective. The hydrogenation requires an induction period before the catalysis proceeds, at a rate identical for the hydrogenation using $[RuH_4(PPh_3)_3]$. The rationale proposed by Halpern and Linn is that $[RuH_3(PPh_3)_3]^-$ is inactive, but during the induction period is converted to $[RuH_4(PPh_3)_3]$, the active species. The higher catalytic activity of $[RuH_4(PPh_3)_3]$ arises because it is a η^2-dihydrogen complex, $[RuH_2(\eta^2\text{-}H_2)(PPh_3)_3]$,[9] and has the facility to lose H_2 more easily than $[RuH_3(PPh_3)_3]^-$. Halpern

and Linn concluded that it is the neutral complex rather than the anionic complex that is responsible for the hydrogenation.

2.1.3 Trialkylphosphine ruthenium carbonyl catalyst

Hydrogenation of dimethyl oxalate to methyl glycolate and the subsequent reduction of methyl glycolate to ethylene glycol by $[Ru(CO)_2(CH_3COO)_2(PBu_3)_2]$ has been reported by Matteoli *et al.*[10] Their study discovered that alkyl esters with a chain of five carbons or less could be homogeneously hydrogenated using trialkyl phosphine substituted ruthenium carbonyl complexes as catalyst precursors.

Matteoli *et al* investigated the ruthenium hydride $[H_4Ru_4(CO)_8P_4]$ and the ruthenium carbonyl carboxylates $[Ru_4(CO)_8(CH_3COO)_4P_2]$, $[Ru_2(CO)_4(CH_3COO)_2P_2]$ and $[Ru(CO)_2(CH_3COO)_2P_2]$ (where P = PBu_3, PPh_3 and PCy_3 (tricyclophosphine)), as catalysts for the hydrogenation of dimethyl oxalate.[11] The results showed that the ruthenium carbonyl complexes were more effective than the corresponding ruthenium hydride complexes, and that the mononuclear complex $[Ru(CO)_2(CH_3COO)_2P_2]$ is the most active of the catalysts studied. The effect of the phosphine ligands for all the complexes, is catalytic activity in the order $PBu_3 > PPh_3 > PCy_3$ (the PCy_3 derivative of the ruthenium hydride could not be synthesised). The use of alcohols as solvents, such as MeOH, methyl glycolate and ethylene glycol, improves the product yield. Matteoli *et al* found that when the solvent is MeOH, dimethyl oxalate reduction to methyl glycolate is 100% selective and is easily achieved, but the subsequent reduction of methyl glycolate to ethylene glycol is slower with a maximum yield of 31.6%. The addition of methyl glycolate or ethylene glycol, as a hydroxylated species, increases the ethylene glycol yield for the reduction, with the $[Ru(CO)_2(CH_3COO)_2(PBu_3)_2]$ catalyst. The concentration of ethylene glycol added has to be kept low, to avoid forming the decomposition or secondary products of carbon monoxide, methyl acetate, bis(2-hydroxyethyl)ether and 2-hydroxyethyl glycolate.

Matteoli *et al* found that a yield of 95% ethylene glycol is obtained for the catalytic system of $[Ru(CO)_2(CH_3COO)_2(PBu_3)_2]$ ($10mmol^{-1}$) in MeOH (15ml) and ethylene glycol ($12.4mmol^{-1}$) and benzene (0.5ml) at 180°C and 20Mpa of H_2 for 144 hours. The addition of benzene enables the catalyst to dissolve in the presence of ethylene glycol. Matteoli *et al*'s investigation of the catalytic precursor $[\{Ru(CO)_2(\mu\text{-}OOCCH_3)L\}_2]$,

where L = P^tBu_3, P^nBu_3, P^iPr_3, found that different results are obtained for the hydrogenation of dimethyl oxalate.[12] The catalytic activity for the complex is phosphine dependent, with L = P^tBu_3 > L = P^nBu_3 > L = P^iPr_3. The result was different to that expected,[13] since literature had suggested that the steric and electronic properties would give the order L = P^tBu_3 > L = P^iPr_3 > L = P^nBu_3.

From X-Ray crystallography the structure of $[\{Ru(CO)_2(\mu\text{-}OOCCH_3)L\}_2]$ was determined as two octahedrally co-ordinated ruthenium atoms joined by direct Ru-Ru interaction, with two *cis* bridging carboxylates (forming two Ru-O-C-O-Ru rings). Two *cis* carbonyls and a terminal phosphine complete the co-ordination about each ruthenium.

For hydrogenation to take place the substrate requires access to the metal atom. A free co-ordination site needs to be available to accommodate the substrate. Matteoli *et al* postulated that a bidentate ligand becomes monodentate to allow this. Comparison of the structural data of the different complexes showed that the only structural parameter that appears to be related to the catalytic activity, where P^tBu_3 > P^nBu_3 > P^iPr_3, is the P-Ru-Ru-P torsion angle. The P-Ru-Ru-P torsion angle, a measure of the distortion of the binuclear centre of the complex with respect to the phosphines, decreases from the most hindered P^tBu_3 to the more flexible P^nBu_3 and the less sterically crowded P^iPr_3. Matteoli *et al* suggested that the greater the distortion, the easier it is for the substrate to approach the vacant co-ordination site on the metal atom. They concluded that there is a correlation between catalytic activity of the catalyst, $[\{Ru(CO)_2(\mu\text{-}OOCCH_3)L\}_2]$, and the P-Ru-Ru-P torsion angle.

2.1.4 Cationic ruthenium phosphine hydride catalyst

Hara and Wada developed a catalyst for the hydrogenation of a carboxylic anhydride using tris(acetylacetonato)ruthenium ($Ru(acac)_3$), tri-n-octyl phosphine ($P(n\text{-}C_8H_{17})_3$) and a strong acid.[14] They had observed that the catalytic homogeneous hydrogenation of carboxylic anhydrides to the respective ester or lactone, using the catalysts $[RuCl_2(PPh_3)_3]$ [15], $[Ru_2Cl_4(dppb)_3]$ [16] and $[H_4Ru_4(CO)_8(P^nBu_3)_4]$ [17] did not achieve catalytic activity sufficient for a reaction to obtain greater than 50% conversion.

Hara and Wada discovered that the addition of a strong acid, such as *p*-toluenesulfonic acid, accelerated the rate of hydrogenation and improved selectivity for the respective ester or lactone. The Hara and Wada system achieved higher activity and selectivity than other ruthenium systems then reported, and that of the copper-chromite mixed oxide heterogeneous catalyst, the catalyst predominantly used for such hydrogenations. Their investigation found that the effect obtained using *p*-toluenesulfonic acid could be similarly reproduced using other strong acids, such as benzenesulfonic acid, methanesulfonic acid, ammonium tetrafluoroborate and ammonium hexafluorophosphate.

Hydrogenation of 3-hydroxyphthalic anhydride gave a substituted phthalide of which the sterically less hindered carbonyl group was hydrogenated exclusively, producing a 60% yield of 7-hydroxyphthalide and a 40% yield of 4-hydroxyphthalide. The use of ^{1}H NMR and ^{31}P NMR spectroscopy, at room temperature, led Hara and Wada to suggest the cationic complex, *mer*-$[HRu(P(^{n}C_8H_{17})_3)_3S_2]^+$, where S = solvent, is formed in the catalytic solution. They asserted that their cationic complex is more effective, than neutral complexes, at interacting with the carbonyl moiety of anhydrides, the greater interaction producing the higher catalytic activity observed.

Hara and Wada found that succinic anhydride could be hydrogenated to γ-butyrolactone (gBL), with 60% conversion and 95% selectivity, using the catalytic system of $Ru(acac)_3$, $P(n\text{-}C_8H_{17})_3$ and *p*-toluenesulfonic acid at 200°C with 5MPa of H_2 for 3 hours.[18] Replacing the *p*-toluenesulfonic acid with a phosphoric acid ester, produces succinic anhydride conversion of > 98%, with selectivity for 1,4-butanediol of > 40%, γ-butyrolactone with selectivity of between 20 and 50% (depending on the phosphoric acid ester) and small amounts of tetrahydrofuran (THF) < 10%.[19]

Hara and Wada investigated the relationship between structure and the additives employed (phosphoric acid esters) in ruthenium complexes. To do this $Ru(acac)_3$ and $P(n\text{-}C_8H_{17})_3$ in dioxane-d_8 were reacted at 200°C and 5MPa of H_2, producing the complexes A and B (See Fig. 2.1). When the reaction was repeated with 2.5 equivalents of $(n\text{-}BuO)_2PO(OH)$, the cationic monohydride ruthenium complex C was obtained. Addition of $(PhO)_2PO(OH)$ produced complex D. The dihydrogen structure of D was assigned because the spin-lattice relaxation time (T_1) of the ^{1}H NMR hydride signal at 253K was 65 minutes. Hara and Wada classified A and B as neutral complexes and C

and D as cationic complexes. They suggested that the cationic ruthenium complexes would activate the carbonyl group of the substrate and promote hydride transfer to the carbonyl group from the ruthenium.

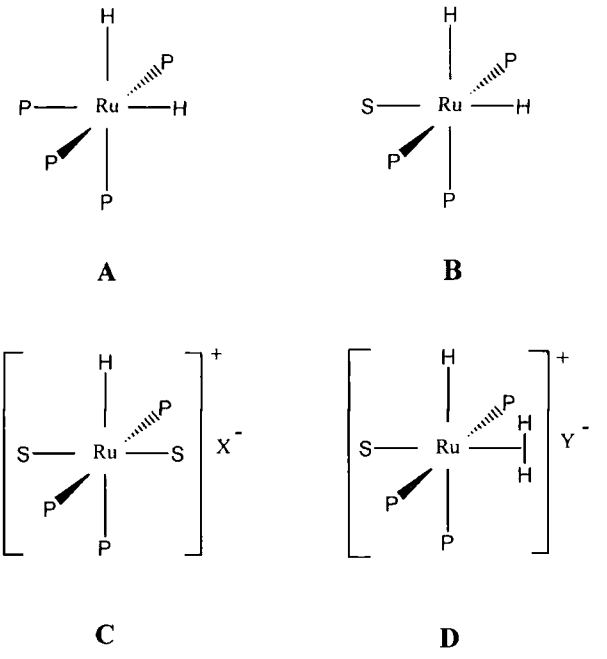

Figure 2.1 Proposed Structure for ruthenium complexes. S : solvent.

Hara and Wada concluded that succinic acid could be hydrogenated to γ-butyrolactone and 1,4-butanediol by a cationic catalyst generated from $Ru(acac)_3$, $P(n\text{-}C_8H_{17})_3$ and phosphoric acid esters.

2.1.5 Ruthenium carbonyl carboxylato complexes with nitrogen ligands

Frediani *et al* investigated the role of ligands in ruthenium complexes, and their application to catalytic homogeneous hydrogenation. They reported ruthenium carbonyl acetate complexes containing the nitrogen-based ligands, bipyridine and phenanthroline, as catalysts for hydrogenation of ketones, alkenes and alkynes.[20] The ruthenium complexes are active in polar solvents, including water, and the nitrogen-based ligands are unaltered on completion of hydrogenation. Frediani *et al* had noted that the catalytic activity of phosphine-substituted ruthenium complexes is often reduced at temperatures

above 120-130°C, probably due to cleavage of P-C bonds and to the formation of inactive ruthenium clusters with phosphido ligands.[21]

Frediani *et al* investigated ligands containing sp^2-hybridised nitrogen atoms in aromatic systems, as possible alternatives to phosphine ligands for hydrogenation catalysts. Nitrogen atoms generally, form stronger donor-acceptor bonds than phosphorus donors do.[22] Complexes of the form $[Ru_2(CO)_2(CH_3COO)(N\text{-}N)_2]$ and $[Ru(CO)_2(CH_3COO)(N\text{-}N)]$ (where N-N = a bidentate nitrogen donor), such as bipyridine or phenanthroline, were synthesised. Water soluble nitrogen ligands were selected to improve the solubility of the catalyst in water or polar solvents. Frediani *et al* found that at 140°C and 10MPa of H_2, with a water-methanol mixture as a solvent, the catalytic homogeneous hydrogenation of ketones, alkenes and alkynes is possible. The use of THF was less effective than the more polar water-methanol solvent. No decomposition of the catalyst was observed. Frediani *et al* found that the addition of a base improved catalytic activity. As phosphine substituted ruthenium carbonyl acetate complexes react with sodium carbonate when under H_2 pressure to form the hydride, Frediani *et al* investigated if the ruthenium complexes with nitrogen ligands would exhibit analogous behaviour to the ruthenium phosphine complexes. The improved activity observed was attributed to activation of the catalytic system as a result of the loss of a carboxylato ligand and the formation of a ruthenium carbonyl hydride species. Frediani *et al* concluded that ruthenium carbonyl carboxylato complexes containing nitrogen based ligands, in polar solvents in the presence of water, can hydrogenate C=O, C=C and C≡C bonds. The addition of a base improves the catalytic activity of the system, and the nitrogen containing ligands do not undergo any alteration at 140°C, and are unaltered on completion of the hydrogenation.

2.1.6 Ruthenium hydrido complexes with functionalized phosphine ligands

Frediani *et al* also looked at the role of functionalized phosphine ligands with hydrido ruthenium complexes, for the hydrogenation of carboxylic acids. Salvini *et al* reported that the complexes $[H_4Ru_4(CO)_8(P(CH_2OCOR)_3)_4]$ have greater catalytic activity for the hydrogenation of carboxylic acids than complexes with trialkyl- or triarylphosphines.[23] They observed that in the phosphine $P(CH_2OCOR)_3$, during carboxylic acid

hydrogenation, the ester is hydrogenated to produce an alcohol (RCH_2OH) and a $P(CH_2OH)$ moiety, which then reacts with the acid to renew the $P(CH_2OCOR)$ moiety. This was demonstrated by replacing the $P(CH_2OCOR)_3$ ligand with $P(CH_2OH)_3$, in the catalytic complex $[H_4Ru_4(CO)_8P_4]$, for a reaction with acetic acid. The ligand was converted to $P(CH_2OCOCH_3)_3$. Salvini *et al* found that the complexes $[H_4Ru_4(CO)_8(P(CH_2OCOR)_3)_4]$, irrespective of what R was, showed almost the same catalytic activity. If the phosphine ligand $P(CH_2CH_2COOCH_3)_3$ is used, then catalytic activity is low and the ester is not reduced. The $[H_4Ru_4(CO)_8(P(CH_2OCOR)_3)_4]$ was not as active as the tributylphosphine equivalent for the hydrogenation of alkenes and ketones.

2.1.7 Ruthenium tripodal phosphine catalyst

Teunissen and Elsevier reported the hydrogenation of aromatic and aliphatic esters to their respective alcohols, using a catalytic system of $Ru(acac)_3$ and the phosphine ligand $MeC(CH_2PPh_2)_3$ (Triphos) in a fluorinated alcohol solvent at 120°C and 8.5MPa of H_2.[24] Teunissen and Elsevier had investigated a ruthenium system based on the $Ru(acac)_3$ system of Hara and Wada.[14, 25] The investigation used the hydrogenation of dimethyl oxalate to methyl glycolate and ethylene glycol to quantify the catalytic activity of the system. Dimethyl oxalate reduces fairly easily to methyl glycolate, due to activation as a result of electron withdrawal, whereas reduction of methyl glycolate to ethylene glycol requires more extreme conditions ($p(H_2)$ 20MPa; 180°C)[10], as it is not activated by an electron withdrawing group.

Teunissen and Elsevier established that ruthenium catalysts with phosphine ligands have a higher catalytic activity than with the arsine $AsPh_3$ or the nitrogen ligands: 1,10-phenanthroline, 2,2':6',2"-terpyridine and tris(3,5-dimethylpyrazol-1-yl)borohydride.[25] The phosphine ligands studied also exhibited different levels of catalytic activity, in the order: $P(C_6H_{11})_3 < Ph_2PC_2H_4PPh_2 < PPh_3 < PhP(C_2H_4PPh_2)_2 \approx (CH_2P(Ph)C_2H_4PPh_2)_2 << MeC(CH_2PPh_2)_3$ (Triphos).[25] The result is comparable to that obtained by Moo-Jin Jun *et al*.[26] They examined the hydrogenation of propanal to propan-1-ol by $[RuHCl(CO)(PPh_3)(L\text{-}L')]$, where L-L' = dppe, $Ph_2PCH_2CH_2PPh_2$; arphos, $Ph_2AsCH_2CH_2PPh_2$; diarsine, $Ph_2AsCH_2CH_2AsPh_2$. The catalytic activity decreased in the order : dppe > arphos > diarsine > $[RuHCl(CO)(PPh_3)_3] \approx [RuHCl(CO)(AsPh_3)_3]$.

Moo-Jin Jun *et al* concluded that the catalytic activity of the ruthenium complex is greater with chelate ligands than non-chelate ligands, and for the bidentate ligands, is increased as the phosphine content is increased.

Teunissen and Elsevier found that the catalytic system using $Ru(acac)_3$ and the Triphos ligand, was the only catalyst they tested that hydrogenated dimethyl oxalate to ethylene glycol (95% yield). Catalytic systems incorporating the other ligands were only able to hydrogenate dimethyl oxalate to methyl glycolate. The catalytic properties of the $Ru(acac)_3$ and Triphos system led Teunissen and Elsevier to deduce that a ruthenium complex with a *facial* co-ordinating phosphine ligand was essential for high catalytic activity to be obtained. The low catalytic activity of the ligands $PhP(C_2H_4PPh_2)_2$ and $(CH_2P(Ph)C_2H_4PPh_2)_2$, which can co-ordinate in either the *facial* or *meridional* forms (but prefer the *meridional* form, to reduce steric interaction) supported the deduction.

The Teunissen and Elsevier system, of $Ru(acac)_3$ and Triphos in MeOH, when compared with that of Matteoli *et al* [10,27] has equal selectivity (95% ethylene glycol) a higher turnover frequency (160 against 136) and operates in milder conditions (100°C and 7MPa of H_2 for 16 hours against 180°C and 20MPa of H_2 for 39 hours). Teunissen and Elsevier discovered that by replacing the MeOH solvent with Propan-2-ol (iPA) and using triethylamine (NEt_3), dimethyl phthalate could be hydrogenated to phthalide with a yield of 82%. Replacing NEt_3 with tetrafluoroboric acid (HBF_4) resulted in a decrease in the hydrogenation of dimethyl phthalate, to 1,2-bis(hydroxymethyl)benzene, with a yield of 78%.

Grey *et al* reported that electron withdrawing groups made an ester easier to hydrogenate.[4] This led Teunissen and Elsevier to investigate the effects of fluorinated solvents.[24] They discovered that by using 1,1,1,3,3,3-hexafluoropropan-2-ol (FIPA), in the presence of NEt_3, the catalytic system could hydrogenate unactivated esters. The catalytic system, at 120°C and 8.5MPa of H_2, hydrogenated benzyl benzoate to benzyl alcohol (97% conversion, 95% yield), methyl palmitate (methyl hexadodecanoate) to hexadecan-1-ol (94% conversion, 94% yield) and dimethyl maleate (but-2-enedioate (DMM)) to 1,4-butanediol (BDO) (100% conversion, 100% yield).

Teunissen and Elsevier suggested that the ester reduction was a result of ionic hydrogenation. They had originally theorised that the ester hydrogenation was a

combination of transesterification (initiated by activation substituents) and hydrogenation. The use of the solvent 2,2,2-trifluoroethanol (TFE) for the hydrogenation of benzyl benzoate contradicted this theory, as a lower level of catalytic activity (than that obtained with FIPA) was observed. As a rule, a primary alcohol produces transesterification more easily than a secondary alcohol.[28] The higher catalytic activity of FIPA, a secondary alcohol, suggested that ionic hydrogenation was taking place. An experiment with a solvent mixture of TFE and FIPA resulted in a reduced level of catalytic activity, thus supporting the ionic hydrogenation theory.

Teunissen and Elsevier concluded that the catalytic system of $Ru(acac)_3$ and Triphos in FIPA at 120°C with 8.5MPa of H_2 can hydrogenate aliphatic and aromatic esters, and attributed this ability of the catalytic system to ionic hydrogenation of the ester.

2.1.8 Summary

The only reported catalysts for the homogeneous hydrogenation of esters are ruthenium complexes. Neutral, anionic and cationic ruthenium complexes have been investigated and varying levels of catalytic activity observed.

The hydrogenation of activated esters is possible with the anionic ruthenium hydride complex of Grey *et al*,[4,5] the ruthenium carbonyl carboxylate complexes of Matteoli *et al* [10,11,12,13,17] and the ruthenium triphosphine system of Teunissen and Elsevier.[24,25] The more difficult hydrogenation of unactivated esters has been attempted. Limited success has been achieved with the aforementioned systems and the cationic system of Hara and Wada, which uses a strong acid additive.[14,18,19]

Phosphine ligands have a greater activating effect than arsines or nitrogen containing ligands. Equally significant is the difference in performance between polydentate and monodentate phosphine ligands, with the monodentate ligand being less activating. The most active phosphine, reported, is the *facially* co-ordinating tripodal Triphos ligand.

The homogeneous catalytic hydrogenation of esters, aromatic and aliphatic, to their respective alcohols is possible. The most effective system reported is that generated *in situ* from $Ru(acac)_3$ and Triphos in an alcoholic solvent at 120°C with 8.5MPa of H_2.[24]

2.2 Results and discussion

The ruthenium-phosphine system reported by Teunissen and Elsevier,[24] which uses $Ru(acac)_3$ and the tripodal Triphos phosphine, was chosen as the starting point for the investigation into the homogeneous hydrogenation of esters.

2.2.1 Catalyst Conditions

The quality of a catalyst is measured by its performance for the properties of *activity*, *selectivity* and *life*. The conditions in which the catalysis takes place can have significant influence on the catalyst performance. The effect of solvent, additives, hydrogen pressure, temperature and time were studied to ascertain the optimum conditions to maximise catalyst performance.

2.2.1.1 Influence of Solvents

The most successful system for ester hydrogenation used alcohol as the solvent, with the best result being obtained with the fluorinated alcohol 1,1,1,3,3,3-hexafluoropropan-2-ol (FIPA).[24] Table 2.1 shows the different levels of ester conversion when a primary, secondary or tertiary alcohol is used in the hydrogenation of methyl dodecanoate. Methyl dodecanoate was selected for the initial investigation because its low volatility, and that of 1-dodecanol (a product of its hydrogenation), would assist product analysis.

Table 2.1. Alcohol influence on methyl dodecanoate hydrogenation.

Alcohol	Methyl Dodecanoate Conversion (%)
MeOH	4.1
IPA	49.0
^{t}BuOH	41.8

Conditions: 120°C, $p(H_2)$ = 6.8MPa, 16 hours.

The hydrogenation of methyl dodecanoate in MeOH resulted in only 4.1% conversion. This was lower than expected, as Teunissen and Elsevier had used MeOH as a solvent for the hydrogenation of the esters dimethyl oxalate and dimethyl phthalate, and reported conversion of 100% and 30%, respectively.[24, 25] The reason for this difference

is probably explained by the lower temperature of 100°C used by Teunissen and Elsevier (see 2.2.1.4 Influence of Temperature). When the MeOH solvent was replaced with propan-2-ol (iPA), the hydrogenation of methyl dodecanoate resulted in 49% conversion. Methyl dodecanoate was also hydrogenated when 2-methyl-2-propanol (^{t}BuOH) was used.

That the reaction occurs in ^{t}BuOH shows that the ester hydrogenation does not proceed by transfer hydrogenation, which can not occur for *tertiary*-alcohols as they do not have β-hydrogen atoms. An easily reduced substrate, such as iPA, is required for transfer hydrogenation to take place.

Hydrogenation of methyl dodecanoate produced methanol, 1-dodecanol, a small amount of transesterification (such products are not included in the ester conversion value) and a pale yellow crystalline solid. The solid was identified as monocarbonyldihydrido-1,1,1-tris(diphenylphosphinomethyl)ethaneruthenium(II), [Ru(Triphos)H_2(CO)] (See 2.2.4 for characterisation). The [Ru(Triphos)H_2(CO)] is the deactivated catalyst and is produced from the decarbonylation of an aldehyde of a dehydrogenated primary alcohol (See Chapter 3, Catalyst Deactivation).

The hydrogenation of the esters, methyl propanoate and propyl propanoate, was achieved in the absence of a solvent. Table 2.2 shows the level of ester hydrogenation obtained.

Table 2.2. Ester hydrogenation in the absence of a solvent.

Ester	Conversion (%)
Methyl propanoate	18.1
Propyl propanoate	28.6

Conditions: 120°C, $p(H_2)$ = 6.8MPa, 16 hours.

The products of the hydrogenation of both esters were their respective alcohols and the pale yellow solid [Ru(Triphos)H_2(CO)]. This indicates that the catalyst was generated *in situ* in the ester and that the mechanism of the hydrogenation is the same as when the catalysis is carried out in an alcohol solvent. The lower level of ester conversion in the absence of an alcohol solvent indicates that the alcohol solvent is beneficial, probably

allowing the catalyst to be formed more easily due to greater solubility of the $Ru(acac)_3$ and/or Triphos precursors in an alcohol.

The lower level of conversion of the methyl propanoate compared to that of the propyl propanoate is thought to arise because, although the hydrogenation of both esters produces 1-propanol, the methyl propanoate hydrogenation also produces methanol, which is more easily decarbonylated than 1-propanol, producing catalyst deactivation (See Chapter 3, Catalyst Deactivation). The lifetime of the catalyst is therefore lower in the hydrogenation of methyl propanoate than it is for the hydrogenation of propyl propanoate.

When water is used as the solvent and the reaction temperature is 140°C, the ester hydrogenation can be increased to greater than 98%. The change is explained as follows. At 140°C the water removes the carbonyl from the deactivated catalyst, $[Ru(Triphos)H_2(CO)]$, by the water gas shift reaction and thus reactivates the catalyst (See Chapter 4, Catalyst Reactivation). In Table 2.3, it can be seen that methyl propanoate was hydrogenated in water with 98.2% conversion, to the alcohols methanol and 1-propanol. The remainder of the product mixture comprised propyl propanoate (from transesterification), propionic acid (from hydrolysis) and unreacted methyl propanoate. The hydrogenation of dimethyl maleate (DMM) to 97.2% conversion in water is possible, the products being methanol, 1,4-butanediol (BDO), tetrahydrofuran (THF), γ-butyrolactone (gBL) and a small amount of decomposition products such as 1-propanol and 1-butanol (from the decarbonylation reaction).

Table 2.3 Ester hydrogenation using H_2O as a solvent

Ester	Conversion (%)
Methyl propanoate [a]	98.2
Dimethyl maleate [b]	97.2

Conditions: 140°C, $p(H_2)$ = 6.8MPa. a = 39 hours. b = 64 hours.

2.2.1.2 Influence of Additives

The influence of additives on ester hydrogenation was demonstrated by the use of phosphoric acid esters as promoters by Hara and Wada,[19] and the use of NEt_3 by Teunissen and Elsevier.[24] The cationic ruthenium catalyst of Hara and Wada, prepared

by the addition of phosphoric acid esters, was found to be more active than its neutral analogue. The catalysis by the ruthenium-phosphine complex of Teunissen and Elsevier was improved by the addition of the base NEt_3.

The effect of additives on the catalytic system of $Ru(acac)_3$ and Triphos in iPA, for the hydrogenation of methyl dodecanoate, is shown in Table 2.4. The addition of the acids *p*-toluenesulphonic acid (*p*TSA) and concentrated sulphuric acid both resulted in a reduction of ester conversion of more than 50%. The addition of NEt_3 had no observable benefit, achieving roughly the same level of methyl dodecanoate conversion as is attained in its absence.

Addition of the ionic liquid, 1-ethyl-3-methyl-1 *H*-imidazolium tetrafluoroborate, resulted in a decrease in ester hydrogenation and unexpectedly, a single-phase solution. The ionic liquid was added to ascertain whether the catalytic system could operate in a biphasic system. Homogeneous catalysis in biphasic systems, where the metal catalyst remains in a different phase to the product, avoids the problem of product and catalyst separation that is frequently an obstacle with homogeneous catalysis. Ionic liquids do not easily mix with many organic solvents, but will dissolve metal catalysts.[29] The intended biphasic product solution did not occur, and therefore the method of separately recovering the catalyst and product was not achieved. The reduction in conversion shows that addition of the ionic liquid is detrimental to the hydrogenation reaction.

The presence of water in catalytic systems can result in catalyst poisoning.[30] The catalytic system of Hara and Wada and that of Teunissen and Elsevier exhibited higher activity in the absence of water, as occurs in the present study.[19,24] Thus the addition of water to the system inhibited catalysis. However, in the studies conducted at 140°C, water became advantageous, with the catalyst reactivating by the water-gas shift reaction (See Chapter 4, Catalyst Reactivation).

Table 2.4 Influence of additives on the hydrogenation of methyl dodecanoate

Additive	Methyl Dodecanoate Conversion (%)
None	49.0
NEt_3	48.9
*p*TSA	17.9
Conc. Sulphuric Acid	24.8
Ionic Liquid [a]	36.2
H_2O	40.7

Conditions: 120°C, $p(H_2)$ = 6.8MPa, 16 hours.
a: 1-ethyl-3-methyl-1 *H*-imidazolium tetrafluoroborate.

None of the additives tested resulted in any improvement to the catalytic system.

2.2.1.3 Influence of Hydrogen Pressure

Reduced H_2 pressure for the homogeneous hydrogenation of esters resulted in a decrease in conversion to alcohols.[24] Conversely, increasing the H_2 pressure produced an increase in ester hydrogenation.[4,11,13]

Table 2.5 shows that for the hydrogenation of methyl dodecanoate, using the system of $Ru(acac)_3$ and Triphos in iPA, increasing the $p[H_2]$ by 50% resulted in an increase in ester conversion. The increase in ester conversion was not proportional to the $p[H_2]$ increase, as the overall ester conversion was an increase of 10%.

Table 2.5 Influence of increased $p[H_2]$ on the hydrogenation of methyl dodecanoate

$p[H_2]$ / MPa	Methyl Dodecanoate Conversion (%)
6.8	49.0
10.3	53.8

Conditions: 120°C, 16 hours.

In Table 2.6 it can be seen, using the system of $Ru(acac)_3$ and Triphos in iPA, for the hydrogenation of methyl propanoate the level of ester conversion is reduced when the $p[H_2]$ is decreased by roughly a third. The reduction in ester conversion was proportionally greater than the decrease in $p[H_2]$, being a 50% decrease in conversion to the 34% $p[H_2]$ decrease. When the $p[H_2]$ was zero the methyl propanoate conversion

was only 0.8%. The 0.8% conversion in the absence of $p[H_2]$ is probably as a result of transfer hydrogenation from the iPA. The low level of conversion indicates that transfer hydrogenation is not the preferred mechanism for the ester hydrogenation. Clearly $p[H_2]$ is required for ester hydrogenation to take place.

Table 2.6 Influence of decreased $p[H_2]$ on the hydrogenation of methyl propanoate

$p[H_2]$ / MPa	Methyl Propanoate Conversion (%)
6.8	41.2
4.5	20.6
0.0[a]	0.8

Conditions: 120°C, 16 hours. [a] $p[Ar]$ = 0.6MPa.

2.2.1.4 Influence of Temperature

The influence of temperature on the hydrogenation of methyl propanoate, using the $Ru(acac)_3$ and Triphos in iPA system, can be seen in Chart 2.1. The products of the hydrogenation comprised the alcohols, methanol and 1-propanol, some transesterification products and the pale yellow solid, $[Ru(Triphos)H_2(CO)]$, the respective yields of individual products varying with the level of methyl propanoate conversion. The lower conversion levels, which were obtained with the higher reaction temperatures, had higher levels of transesterification products. The highest level of conversion was obtained at 100°C, with 76.7%.

Chart 2.1 Methyl propanoate hydrogenation as a function of temperature

Conditions: $p(H_2)$ = 6.8MPa, 16 hours.

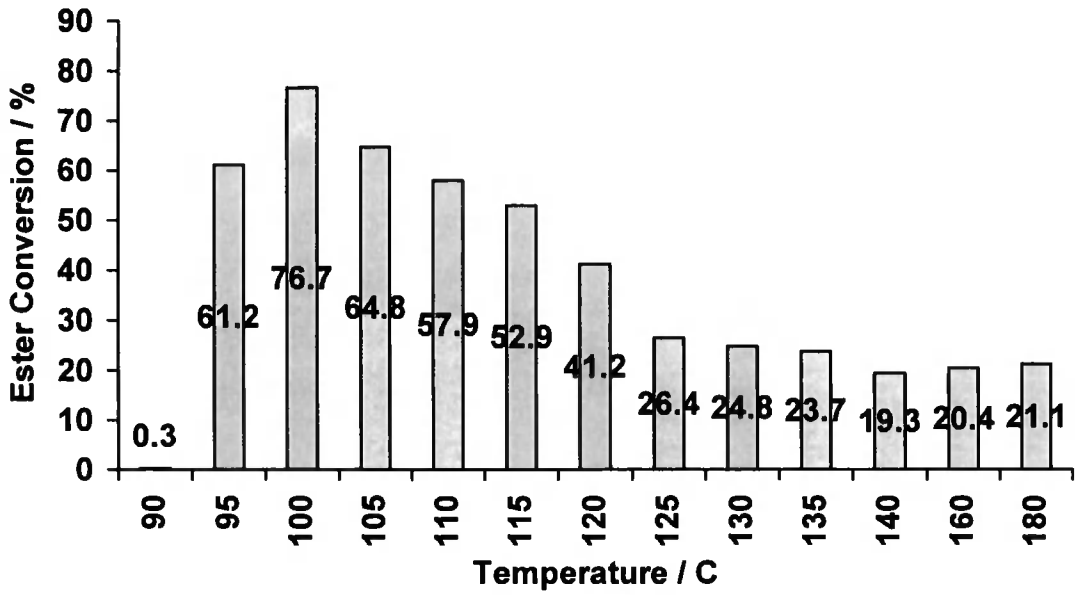

As temperature increased, the level of methyl propanoate hydrogenation decreased. The probable reason for this is that the increased temperature favours decarbonylation more than ester hydrogenation. The only temperature at which the solid, [Ru(Triphos)H_2(CO)], was not obtained was at 90°C.

The level of methyl propanoate hydrogenation at 90°C was almost zero, indicating that the rate of hydrogenation at that temperature is very slow, but as can be seen in Table 2.7, the rate of the decarbonylation reaction is slower. Increasing the reaction period tenfold resulted in a significant increase in hydrogenation of the methyl propanoate, with 84.4% conversion. The solid [Ru(Triphos)H_2(CO)] was obtained in the products, which indicates that catalyst deactivation via decarbonylation also occurs at 90°C, but at a slower rate than at any of the other temperatures tested.

Table 2.7 The effect of time on methyl propanoate hydrogenation @ 90°C

Time / Hours	Methyl Propanoate Conversion (%)
16	0.3
168	84.4

Conditions: $p(H_2)$ = 6.8MPa.

The indication that catalyst deactivation at 90°C is slower than at higher temperatures also applies to the hydrogenation of methyl propanoate at 100°C. The slower rate of decarbonylation (and therefore catalyst deactivation) explains the higher level of conversion achieved by the catalytic systems at that temperature, and suggests that the Teunissen and Elsevier [24, 25] system's ability to hydrogenate dimethyl oxalate and dimethyl phthalate at 100°C in MeOH is related to this (see 2.2.1.1 Influence of Solvents).

The hydrogenation of methyl dodecanoate was also affected by temperature. Chart 2.2 shows that the highest level of conversion for methyl dodecanoate is in the region of 105-110°C. Below 105°C, the level of hydrogenation is reduced significantly with only 2.2% conversion at 100°C.

Chart 2.2 Methyl dodecanoate hydrogenation as a function of temperature

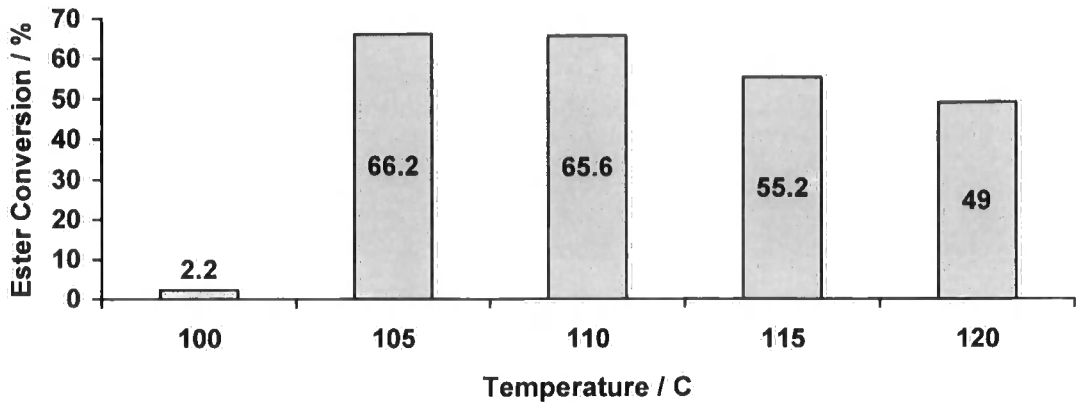

Conditions: $p(H_2)$ = 6.8MPa, 16 hours.

The highest level of hydrogenation of methyl propanoate, in 16 hours, was 76.7% at 100°C, whereas for methyl dodecanoate the highest level of hydrogenation took place at 105-110°C with 65-66% conversion. The difference in temperature at which methyl dodecanoate and methyl propanoate achieve their respective highest conversion levels, in the catalytic system, is due to their different volatility. Methyl dodecanoate is a long chain wax ester, which is a viscous solution with a b.p. of 262°C, whereas methyl propanoate with a b.p. of 79°C will be more volatile and more easily hydrogenated in the homogenous medium.

2.2.1.5 Influence of Time

The influence of the reaction period on the outcome of the catalytic reaction was demonstrated with the hydrogenation of methyl propanoate at 90°C (See 2.2.1.4 Influence of Temperature, Table 2.7). As expected, at 90°C a longer reaction period is required to obtain a comparable level of ester conversion with that acquired at a higher temperature.

At 90°C, the rates of both the hydrogenation and decarbonylation reaction are slower than at 120°C. Table 2.8 shows the results of the homogeneous hydrogenation of methyl dodecanoate for different reaction periods. The level of ester conversion after a 16-hour reaction period is not significantly greater than it is after 6 hours. This suggests that within 6 hours the decarbonylation reaction has deactivated the catalyst. When the reaction period was extended to 66 hours the level of ester hydrogenation was not

increased as the deactivated catalyst, [Ru(Triphos)H_2(CO)], was not capable of further hydrogenation. The extended reaction period resulted in a reduced level of ester conversion due to product alcohols being consumed by transesterification and decarbonylation.

Table 2.8 The hydrogenation of methyl dodecanoate as a function of time

Time / Hours	Ester Conversion (%)	iPA dodecanoate [a] (%)	Others [b] (%)
6	47.4	0.3	1.6
16	49.0	0.6	1.1
66	37.3	2.0	3.9

Conditions: 120°C, $p(H_2)$ = 6.8MPa.
a: Transesterification product.
b: Includes dodecyl dodecanoate, undecane and decomposition products.

The result obtained for the hydrogenation of methyl dodecanoate for the reduced reaction period of 6 hours, indicated that the reaction had achieved a level of conversion comparable with a 16-hour reaction period. In Graph 2.1 the level of methyl dodecanoate obtained at different times within a 16-hour reaction period can be seen. The first sample was taken after 40 minutes, which was the time taken for the autoclave to reach 120°C. The 7.0% conversion obtained is in keeping with the results of the temperature study (see section 2.2.1.4 Influence of Temperature), which demonstrated that hydrogenation of methyl dodecanoate takes place from *circa*100°C and above. Hydrogenation would have taken place during the time it took for the autoclave to be heated from 100°C to 120°C. From Graph 2.1 it can be seen that the ester conversion, and catalyst deactivation, is almost complete within 3 hours (180 minutes).

Graph 2.1 Methyl dodecanoate conversion as a function of time, during 16 hours

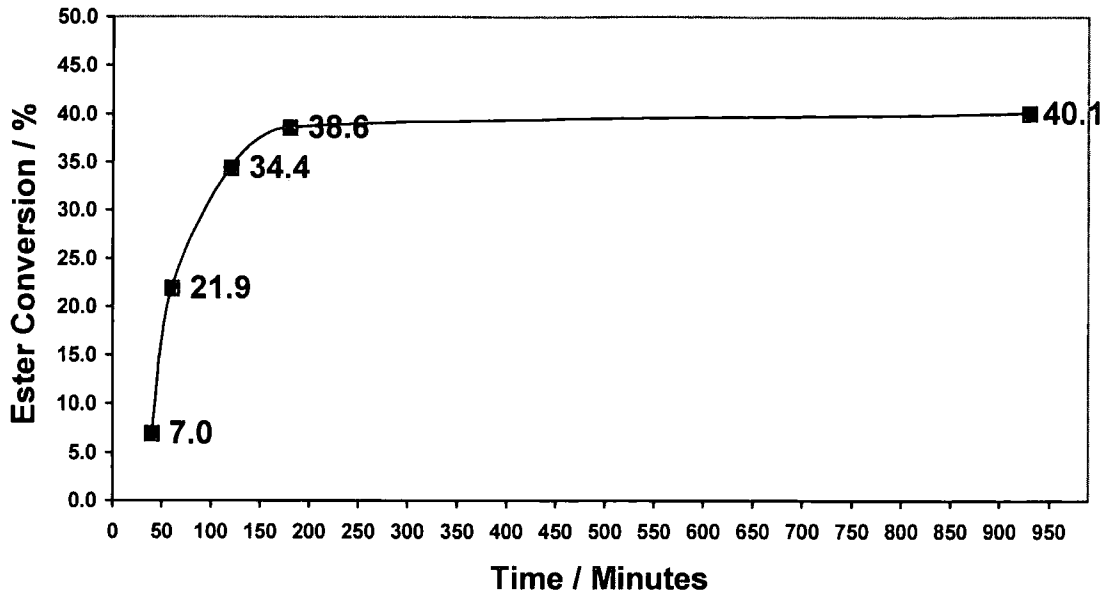

Conditions: 120°C, $p(H_2)$ = 6.8MPa.
Samples taken after 40, 60, 120, 180 and 930 minutes.
The lower level of overall conversion of methyl dodecanoate is attributed to the removal of catalyst and substrate during the sampling.

2.2.1.6 Air Sensitivity

The catalytic system of $Ru(acac)_3$ and Triphos in iPA was found to hydrogenate esters more effectively when using inert atmosphere handling techniques. The investigations previously described (see sections 2.2.1.1 to 2.2.1.5) were carried out using procedures that excluded air from the reaction (see 2.3 Experimental and Appendix 1). When the hydrogenations of methyl dodecanoate and methyl propanoate were carried out using reagents that had not been degassed and apparatus from which air had not been evacuated, the level of ester conversion was lower than when air was excluded (see Table 2.9).

Table 2.9 Comparison of Ester Conversion for Air Sensitivity

Ester	Conversion (%) / Air Sensitive Handling	Conversion (%) / Non Air Sensitive Handling
Methyl Dodecanoate	49.0	42.7
Methyl Propanoate	41.2	29.6

Conditions: 120°C, $p(H_2)$ = 6.8MPa, 16 hours.

The products obtained from the respective non air sensitive hydrogenations were the same as those for the hydrogenations carried out using the inert atmosphere techniques, including the pale yellow solid [Ru(Triphos)H_2(CO)]. Clearly from these results, the presence of air within the reagents or the apparatus inhibits and reduces the level of ester conversion.

2.2.1.7 Optimum Catalytic Conditions

The investigation of the optimum conditions for the hydrogenation of esters used a catalytic system generated from the precursors Ru(acac)$_3$ and Triphos with H_2. The influence of solvent, additives, $p[H_2]$, temperature and time were studied. The results indicated that ester hydrogenation was best achieved at 140°C in H_2O.

The ester hydrogenation could be achieved in the alcohols iPA and ^{t}BuOH as solvents, or in the absence of any solvent at all, but not without catalyst deactivation occurring. The best alternative to the H_2O and 140°C combination was achieved with iPA at 90-100°C for low molecular weight esters, but catalyst deactivation still took place. Temperatures above 120°C resulted in a decrease in ester conversion as a result of catalyst deactivation, which with increased temperature occurs at a faster rate than ester hydrogenation. Time was only found to be beneficial to hydrogenations at a low temperature (90°C), when the rate of catalyst deactivation is slow. The inclusion of additives to the hydrogenation process gave no detected advantage. Indeed, all of the additives investigated were actually detrimental apart from NEt_3, which had no effect at all.

2.2.2 Hydrogenation of a Range of Different Esters

The catalytic systems generated from Ru(acac)$_3$ and Triphos with the solvents iPA and H_2O were used for the study of homogeneous hydrogenation of a range of different esters. The catalytic systems were found capable of hydrogenating aliphatic esters, aromatic esters and diesters.

2.2.2.1 Hydrogenation of Aliphatic Esters

The aliphatic esters detailed in Table 2.10 were homogeneously hydrogenated by the catalytic system.

Table 2.10 Hydrogenation of aliphatic esters

Ester	Conversion (%)
Methyl dodecanoate	49.0
Isopropyl dodecanoate	24.6
Methyl propanoate	41.2

Conditions: 120°C, $p(H_2)$ = 6.8MPa, 16 hours.

The ester, propyl propanoate, in the absence of iPA, was also hydrogenated with 28.6% conversion by the same catalytic system (see Table 2.2). The pale yellow solid [Ru(Triphos)H_2(CO)] was identified amongst the products of all the hydrogenations. The level of ester conversion achieved was no greater than 50% for any of the esters, probably because, in all cases, the primary alcohol(s) produced decarbonylated to deactivate the catalyst. The low level of conversion of isopropyl dodecanoate is probably due to the steric hindrance created by the isopropyl group of the ester. The combination of the phenyl groups on the Triphos ligand co-ordinated to the ruthenium and the isopropyl group of the isopropyl dodecanoate make it difficult for the ester to approach closely the catalytic centre. The products of the hydrogenation of methyl propanoate and methyl dodecanoate both include methanol, with 1-propanol and 1-dodecanol respectively. The lower level of methyl propanoate conversion, compared with methyl dodecanoate, is probably because 1-propanol undergoes decarbonylation by the catalyst more easily than 1-dodcanol, and therefore deactivates the catalyst sooner.

2.2.2.2 Hydrogenation of Aromatic Esters

The catalytic system of $Ru(acac)_3$ and Triphos in iPA hydrogenated the aromatic esters benzyl benzoate and dimethyl phthalate, as detailed in Table 2.11.

Table 2.11 Hydrogenation of aromatic esters

Ester	Conversion (%)[a]	Alcohol Selectivity (%)
Benzyl benzoate	63.7	87.9
Dimethyl phthalate	72.5	0.0

Conditions: 120°C, $p(H_2)$ = 6.8MPa, 16 hours.
a: Transesterification products are not included.

2.2.2.2.1 Benzyl Benzoate Hydrogenation

The major product of the benzyl benzoate hydrogenation was benzyl alcohol (see Equation 2.1), with 87.9% selectivity. Transesterification products and the pale yellow solid [Ru(Triphos)H_2(CO)] were also obtained. Traces of benzaldehyde and benzene (see Equation 2.2) were detected, demonstrating that the primary alcohol benzyl alcohol undergoes dehydrogenation to benzaldehyde, which is then decarbonylated to benzene, the extracted carbonyl group producing the deactivated catalyst [Ru(Triphos)H_2(CO)].

$$\underset{\text{Benzyl benzoate}}{PhCO_2CH_2Ph} + 2H_2 \rightarrow \underset{\text{Benzyl alcohol}}{2PhCH_2OH} \qquad \textbf{Equation 2.1}$$

$$\underset{\text{Benzyl alcohol}}{PhCH_2OH} \rightarrow \underset{\text{Benzaldehyde}}{PhCHO} \rightarrow \underset{\text{Benzene}}{C_6H_6} + CO \qquad \textbf{Equation 2.2}$$

2.2.2.2.2 Dimethyl Phthalate Hydrogenation

The objective of the hydrogenation of dimethyl phthalate was to produce the alcohol 1,2-bis(hydroxymethyl)benzene (see Equation 2.3).

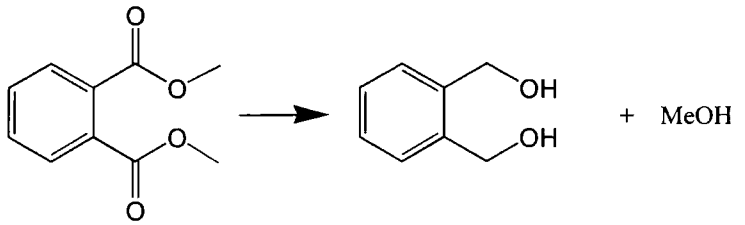

Dimethyl Phthalate 1,2-bis(hydroxymethyl)benzene

Equation 2.3

The hydrogenation achieved 72.5% conversion, but did not produce the alcohol 1,2-bis(hydroxymethyl)benzene, but isobenzofuranone and isobenzofuran instead (see Equation 2.4).

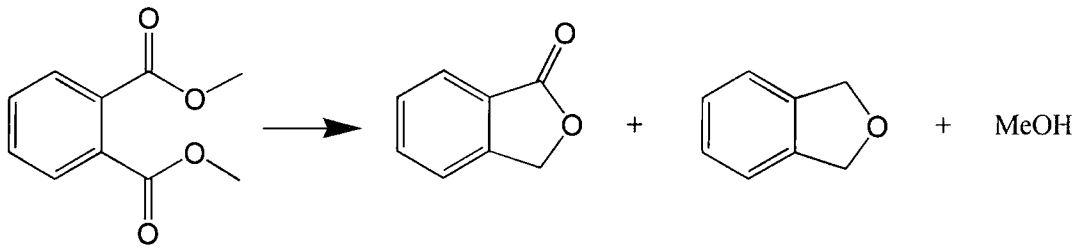

Dimethyl Phthalate Isobenzofuranone Isobenzofuran

Equation 2.4

Table 2.12 Dimethyl phthalate hydrogenation products [a]

Dimethyl phthalate conversion (%)	Isobenzofuranone selectivity (%)	Isobenzofuran selectivity (%)	Others [b] (%)
72.5	81.5	11.2	5.9

a: Excluding methanol.
b: The products of transesterification and decarbonylation / decomposition.

The product solution of the hydrogenation of dimethyl phthalate included traces of transesterification products and decarbonylation products. The target alcohol 1,2-bis(hydroxymethyl)benzene was not obtained, but traces of benzyl alcohol were detected by GCMS in the product solution. Dehydrogenation and decarbonylation of one of the two-hydroxymethyl groups of 1,2-bis(hydroxymethyl)benzene would have formed the benzyl alcohol. GCMS also indicated the presence of traces of phenyl acetate ($PhCO_2CH_3$) and benzene. The phenyl acetate is the product of the hydrogenation and decarbonylation of only one of the two-ester groups of dimethyl phthalate and the benzene is the product of the complete dehydrogenation and decarbonylation of 1,2-bis(hydroxymethyl)benzene.

Hydrogenation of an ester typically produces two alcohol molecules that correspond to the moieties adjacent to the ester functionality. The hydrogenation of dimethyl phthalate produced predominantly methanol and the lactone isobenzofuranone, not 1,2-bis(hydroxymethyl)benzene. For isobenzofuranone to be produced both ester groups of

the dimethyl phthalate have to be hydrogenated, as they would to produce the alcohol 1,2-bis(hydroxymethyl)benzene. If the catalytic hydrogenation proceeds by the co-ordination of the ester to a vacant site on the ruthenium, then simultaneous hydrogenation of both ester groups of dimethyl phthalate is unlikely. One possible route is that each ester group was independently hydrogenated to methanol and benzyl alcohol, and that when the second ester group of dimethyl phthalate had been hydrogenated to 1,2-bis(hydroxymethyl)benzene, immediate catalytic dehydrogenation of the diol to produce the lactone occurred, alternatively the lactone could be the product of transesterification following hydrogenation of one of the ester groups, allowing intramolecular interaction of the alcohol with the remaining ester group. The benzene backbone ensures that the orientation of the two alcohols is ideal for the intramolecular reaction to occur. The presence of isobenzofuranone and the absence of 1,2-bis(hydroxymethyl)benzene indicate that the lactone is the preferred product rather than the diol under the prevalent reaction conditions.

The capability of the catalyst to achieve both hydrogenation and dehydrogenation is demonstrated by the hydrogenation of esters to alcohols and their subsequent dehydrogenation and decarbonylation to deactivate the catalyst to produce [Ru(Triphos)H_2(CO)] (see Chapter 3). The dehydrogenation of a diol to a lactone is not unknown, 1,4-butanediol dehydrogenation to γ-butyrolactone can be achieved in the presence of a copper catalyst.[2]

2.2.2.3 Hydrogenation of Aliphatic Diesters

The catalytic system of Ru(acac)$_3$ and Triphos in iPA will also hydrogenate aliphatic diesters, both saturated and unsaturated. In particular, the saturated diesters diethyl carbonate, dimethyl malonate, dimethyl oxalate and dimethyl succinate were all hydrogenated by the catalytic system. Hydrogenation of diethyl carbonate and dimethyl malonate is detailed in Table 2.13, but in both cases, dehydrogenation and decarbonylation of the product alcohols resulted in formation of the pale yellow [Ru(Triphos)H_2(CO)].

Table 2.13 Hydrogenation of aliphatic diesters

Ester	Conversion (%)
Diethyl Carbonate	44.4
Dimethyl Malonate	57.2

Conditions: 120°C, $p(H_2)$ = 6.8MPa, 16 hours.

2.2.2.3.1 Diethyl Carbonate Hydrogenation

The hydrogenation of diethyl carbonate ($(EtO)_2CO$) produced ethanol and CO. The transesterification products isopropyl(ethyl)carbonate and diisopropyl carbonate were also obtained, with the isopropyl group coming from the iPA used as a solvent. Table 2.14 shows the product distribution and selectivity of the products of the diethyl carbonate hydrogenation.

Table 2.14 Diethyl Carbonate Hydrogenation Products

Diethyl Carbonate Conversion (%)	Ethanol Selectivity (%)	Isopropyl(ethyl)-carbonate Selectivity (%)	Diisopropyl Carbonate Selectivity (%)
44.4	53.1	37.4	4.2

Conditions: 120°C, $p(H_2)$ = 6.8MPa, 16 hours.

2.2.2.3.2 Dimethyl Malonate Hydrogenation

The objective of the hydrogenation of dimethyl malonate was to produce 1,3-propanediol (see Equation 2.5). However, although 57.2% conversion was achieved, the target alcohol of 1,3-propanediol was not obtained. The only alcohol obtained was methanol, all other products were transesterification products or decomposition products.

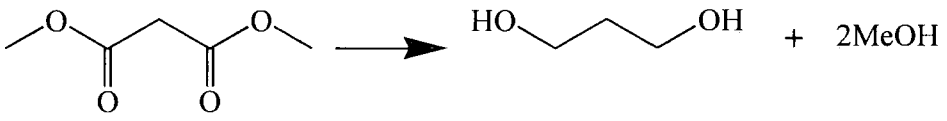

Equation 2.5

The major products of the hydrogenation of dimethyl malonate were methanol and the transesterification products isopropyl(methyl)malonate ($(CH_3)_2CHO_2CCH_2CO_2CH_3$) and diisopropyl malonate ($(CH_3)_2CHO_2CCH_2CO_2CH(CH_3)_2$). Also obtained were small amounts of methyl acetate and isopropyl acetate ($(CH_3)_2CHO_2CCH_3$), from hydrogenation/decarbonylation of one of the functional groups. Table 2.15 details the breakdown of the products.

Table 2.15 Dimethyl Malonate Hydrogenation Products [a]

Product	Selectivity (%)
Methanol	55.3
Methyl Acetate	2.8
Isopropyl Acetate	3.6
Isopropyl(methyl)malonate	16.2
Diisopropyl Malonate	10.5

Conditions: 120°C, $p(H_2)$ = 6.8MPa, 16 hours.
a: Esters identified by GCMS.

The higher boiling point of iPA compared with that of methanol, explains the transesterification of the dimethyl malonate to isopropyl(methyl)malonate and diisopropyl malonate. The transesterification is in keeping with the results of the hydrogenation of the esters detailed previously. The mono ester methyl acetate will be the result of hydrogenation of one of dimethyl malonate's ester groups to produce methyl glycolate, $H_3COCOCH_2CH_2OH$, (and methanol) which is subsequently dehydrogenated and decarbonylated by the catalyst to produce the methyl acetate and [Ru(Triphos)H_2(CO)]. The methyl acetate is then transesterified to produce the isopropyl acetate also obtained in the products.

2.2.2.3.3 Dimethyl Oxalate Hydrogenation

Dimethyl oxalate was hydrogenated by the catalytic system (see Table 2.16). The objective of the hydrogenation was to obtain ethylene glycol (see Equation 2.6).

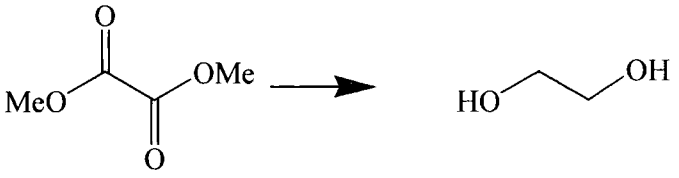

Equation 2.6

On completion of the hydrogenation no dimethyl oxalate was detected in the product solution. The hydrogenation did produce ethylene glycol, but in very low yield. The majority of the product, apart from methanol, comprises methyl glycolate and isopropyl glycolate. The yellow solid [Ru(Triphos)H_2(CO)] was also obtained.

Table 2.16 Dimethyl Oxalate Hydrogenation Products [a]

Product	Yield (%)	Selectivity (%)
Ethylene Glycol	1.8	1.9
Methyl Glycolate	23.6	25.9
Isopropyl Glycolate	69.4	76.4
Others [b]	5.2	5.8

Conditions: 120°C, $p(H_2)$ = 6.8MPa, 16 hours.
a: Methanol excluded.
b: Includes transesterification and decomposition products.
Note : Hydrogenation of dimethyl oxalate to ethylene glycol produces 2 moles of MeOH, but as the majority of the dimethyl oxalate was only hydrogenated to glycolates, only one mole per hydrogenation will have been obtained.

The composition of the products obtained from the dimethyl oxalate hydrogenation, being predominantly glycolates, indicates that the catalytic system was effective for the hydrogenation of one of the two-ester groups, but not for the hydrogenation of both. The low yield of ethylene glycol, by comparison with that of isopropyl glycolate, shows that transesterification occurs more readily than hydrogenation of the ester functionality of the methyl glycolate. The presence of [Ru(Triphos)H_2(CO)] in the products indicates that catalyst deactivation has occurred. Catalyst deactivation may have taken place before the hydrogenation of the second ester group could be achieved to any great extent, thus resulting in the low yield of ethylene glycol obtained.

The yield of ethylene glycol obtained in the dimethyl oxalate hydrogenation was significantly lower than that obtained by Teunissen and Elsevier [24, 25] and of Matteoli *et*

al [10, 27] where yields of > 95% were reported. Examination of these three catalytic systems indicates factors that may have influenced the different results. Comparison of the present system with that, that Teunissen and Elsevier used, shows a temperature of 100°C (not 120°C) and methanol (not iPA) as the solvent. The use of methanol as the solvent means that transesterification products are minimised, although the > 95% yield of ethylene glycol suggests that at 100°C ester hydrogenation is very favourable. Also, at 100°C the rate of catalyst deactivation is slower than at 120°C (see 2.2.1.1 Influence of Solvent and 2.2.1.4 Influence of Temperature), which would allow a greater level of ester conversion. Comparison with Matteoli *et al*'s system shows that they used a greater reaction period (of 39 hours) at a higher temperature of 180°C. Their use of benzene as a solvent reduced the options for formation of transesterification products. If the yield of ethylene glycol was low because the reaction period had only been sufficient to hydrogenate one of the ester groups under the catalytic conditions, then an extended reaction period as used by Matteoli *et al* would be required to achieve hydrogenation of the second ester group. Of the two alternative systems, the lower temperature of 100°C used by Teunissen and Elsevier would be more likely to be beneficial, as the higher temperature of 180°C used by Matteoli *et al* would increase the rate of decarbonylation and therefore catalyst deactivation (see 2.2.1.4 Influence of Temperature). The extended reaction period used by Matteoli *et al* might allow greater conversion, if the hydrogenation was carried out at the lower temperature to reduce catalyst deactivation through decarbonylation of the product alcohols. The hydrogenation of dimethyl succinate supports the premise that the lower temperature (100°C) and extended reaction period (64 hr) would be beneficial, as the levels of conversion were 89.9% and 99.9%, respectively (see 2.2.2.3.4 Dimethyl Maleate Hydrogenation) compared with 56.7% at 120°C over 16 hr.

2.2.2.3.4 Dimethyl Maleate Hydrogenation

The objective was to hydrogenate dimethyl maleate (*cis*-dimethyl-but-2-en-1,4-dioate) to 1,4-butanediol (see Equation 2.7). The catalytic system of $Ru(acac)_3$ and Triphos in H_2O at 140°C achieved the dimethyl maleate (DMM) hydrogenation, with a level of conversion of > 95%. The products obtained (see Table 2.17) were 1,4-butanediol, γ-butyrolactone (gBL) and tetrahydrofuran (THF) (see Equation 2.8). The yellow solid [$Ru(Triphos)H_2(CO)$] was not obtained but a small amount of 1-propanol, from the

decarbonylation of 1,4-butanediol, was obtained. This shows that the ruthenium-triphos catalyst was decarbonylating the product alcohols, but that catalyst reactivation took place due to the "water-gas shift reaction" (see Chapter 4, Catalyst Reactivation).

Table 2.17 Dimethyl Maleate Hydrogenation Products [a]

Dimethyl Maleate Conversion (%)	1,4-butanediol Selectivity (%)	γ-butyrolactone Selectivity (%)	Tetrahydrofuran Selectivity (%)
97.2	49.7	14.9	23.7

Conditions: 140°C, $p(H_2)$ = 6.8MPa, solvent = H_2O, 16 hours.
a: Excluding MeOH and decarbonylation products.

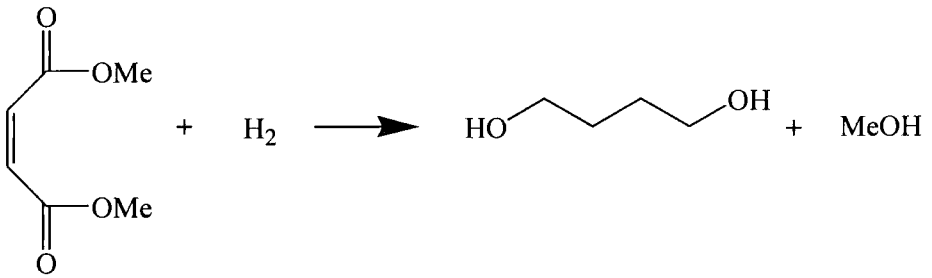

DMM BDO

Equation 2.7

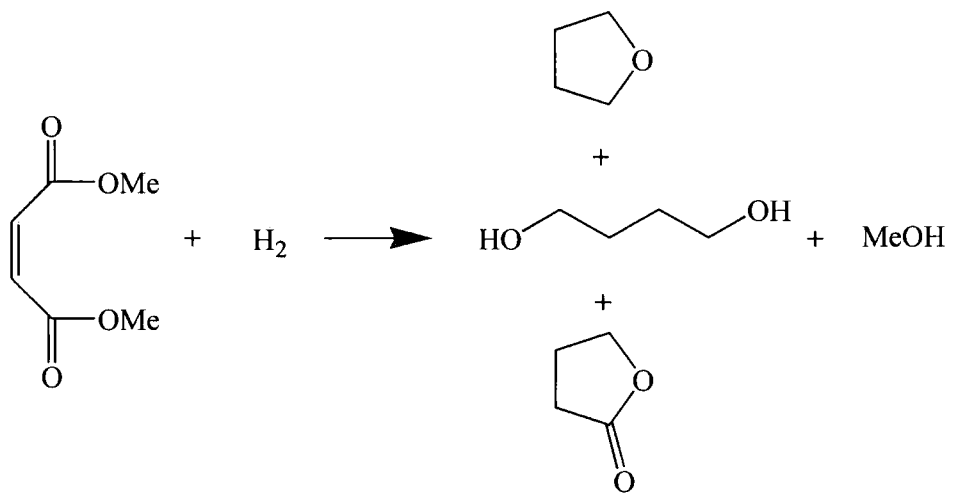

DMM THF + BDO + gBL

Equation 2.8

Attempts to hydrogenate DMM to 1,4-butanediol in the alcohol solvents MeOH and iPA were not very successful, with low levels of conversion being obtained (see Table 2.18).

Table 2.18 Hydrogenation of Unsaturated Diesters

Ester	Solvent	Conversion [a] (%)
Dimethyl maleate	MeOH	4.6
Dimethyl maleate	IPA	5.2
Dimethyl fumarate [b]	IPA	5.1

Conditions: 120°C, $p(H_2)$ = 6.8MPa, 16 hours.
a: To 1,4-butanediol, γ-butyrolactone and tetrahydrofuran.
b: Dimethyl fumarate is the *trans* isomer of dimethyl-but-2-en-1,4-dioate (dimethyl maleate being the *cis* isomer).

The level of conversion for DMM hydrogenation in iPA is not significantly different to that obtained in MeOH, in both cases very low levels of 1,4-butanediol being obtained.

To establish if the low level of DMM conversion was associated with steric interference, as a consequence of its *cis* configuration, the *trans* isomer dimethyl fumarate was investigated (see Fig. 2.2), the rationale being that the *trans* dimethyl fumarate would be able to approach a vacant co-ordination site on the ruthenium-triphos catalytic species more easily than the *cis*-DMM.

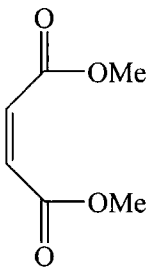

DMM

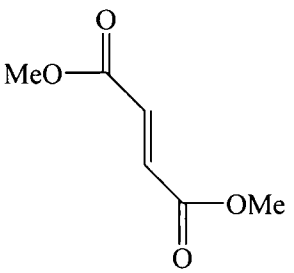

Dimethyl Fumarate

Figure 2.2 Dimethyl maleate and dimethyl fumarate

The hydrogenation of dimethyl fumarate to form 1,4-buatanediol achieved a comparable low level of conversion to that obtained for DMM. This demonstrated that the low level of ester hydrogenation was not due to steric interference. The hydrogenation of

dimethyl phthalate, which has a *cis* configuration like DMM, indicates that the orientation of the ester groups is not critical to which isomer is hydrogenated (see 2.2.2.2.2 Dimethyl Phthalate Hydrogenation).

The analysis of the product solutions of the hydrogenation of DMM and dimethyl fumarate showed that in both cases the alkene bond had been hydrogenated, and the saturated dimethyl succinate ($CH_3OCO(CH_2)_2OCOCH_3$) was produced. No trace of either DMM or dimethyl fumarate was observed on completion of the respective hydrogenations. Also obtained in the products of the hydrogenations was the yellow solid [Ru(Triphos)H_2(CO)]. This information indicates that the catalyst hydrogenates the C=C double bond to form the saturated ester, dimethyl succinate (DMS), and the low yield of 1,4-butanediol, with the presence of [Ru(Triphos)H_2(CO)], shows that the catalyst is deactivated before ester hydrogenation can occur to any great extent. This suggests that whilst hydrogenation of both the C=C double bond and the ester group are occurring, the C=C double bond being hydrogenated more easily, catalyst deactivation is also taking place. The hydrogenation of the C=C double bond and the dehydrogenation and subsequent decarbonylation of the products occur at greater rates than the ester hydrogenation; thus a low level of ester conversion is obtained.

The results of the hydrogenation of DMM and dimethyl fumarate suggested that although the catalyst hydrogenated both the C=C double bond and the ester group at the same time, the catalyst was susceptible to deactivation whilst hydrogenating the alkene. The hydrogenation of DMS by the catalytic system, of $Ru(acac)_3$ and Triphos in iPA, was investigated to establish the level of hydrogenation possible in the absence of the alkene (see Table 2.19).

Table 2.19 Dimethyl Succinate Hydrogenation

Solvent	Temperature / °C	Conversion (%)
MeOH	120	10.4
iPA	120	56.7
iPA	100	89.9
iPA	100	99.9 [a]

Conditions: $p(H_2)$ = 6.8MPa, 16 hours.
a: Reaction period = 64 hours.

The results of the hydrogenation of DMS show that in the absence of the C=C double bond of DMM, the ester groups can be hydrogenated to a greater extent, prior to the occurrence of catalyst deactivation. Comparison of the results for DMS hydrogenation with those for DMM, show that even in MeOH greater conversion is achieved for the former. When the lower temperature of 100°C is used the level of conversion can be increased to 89.9%, and when this temperature is combined with an increased reaction period the conversion can be increased to 99.9%. The higher conversion level obtained at 100°C is due to the slower rate of catalyst deactivation at the lower temperature, although the yellow solid [Ru(Triphos)H_2(CO)] is still obtained amongst the products, indicating that catalyst deactivation still occurs.

The hydrogenation of DMS produced 1,4-butanediol and γ-butyrolactone, and at 120°C a small amount of THF (see Table 2.20).

Table 2.20 Dimethyl Succinate Hydrogenation Product Selectivity [a]

Solvent & Temp. / °C	Conversion (%)	1,4-butanediol Selectivity (%)	γ-butyrolactone Selectivity (%)	THF Selectivity (%)
MeOH @ 120	10.4	7.9	38.9	0.4
iPA @ 120	56.7	29.8	23.6	3.4
iPA @ 100	89.9	14.7	68.2	0.0
iPA @ 100	99.9 [b]	49.5	47.0	0.0

Conditions: $p(H_2)$ = 6.8MPa, 16 hours.
a: Excludes MeOH and transesterification products.
b: Reaction period 64 hours.

From the products of the hydrogenation of DMS at 100°C (as detailed in Table 2.20), it can be seen that for the standard reaction period of 16 hours the major product is γ-butyrolactone, with a ratio to 1,4-butanediol of 4.6 : 1. However, when the reaction period is increased to 64 hours, the quantity of 1,4-butanediol obtained then exceeds that of γ-butyrolactone. This suggests that the DMS was hydrogenated into MeOH and γ-butyrolactone, which was subsequently hydrogenated into 1,4-butanediol (see Equation 2.9).

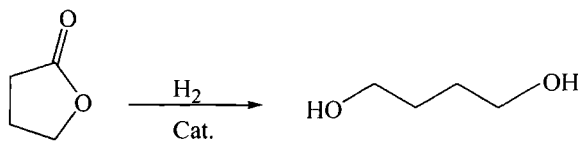

gBL BDO

Equation 2.9

The hydrogenation of γ-butyrolactone by the catalytic system produced 1,4-butanediol (see Table 2.21). This demonstrated that the 1,4-butanediol and γ-butyrolactone obtained in the DMS hydrogenation were the result of catalytic hydrogenation of DMS to γ-butyrolactone, followed by γ-butyrolactone hydrogenation to 1,4-butanediol. This shows that the ruthenium-triphos catalyst was not dehydrogenating the 1,4-butanediol to produce γ-butyrolactone (the synthesis of γ-butyrolactone can be achieved by the dehydrogenation of 1,4-butanediol, in the presence of a copper catalyst at 200°C [2]).

Table 2.21 γ-Butyrolactone Hydrogenation

Solvent & Temp. / °C	Conversion (%)	1,4-butanediol Selectivity (%)	THF Selectivity (%)
iPA @ 120°C	58.1	81.7	0.0
H_2O @ 120°C	2.0	67.4	3.8
H_2O @ 140°C	80.4	81.7	11.9

Conditions: $p(H_2)$ = 6.8MPa, 16 hours.

The low levels of tetrahydrofuran obtained for the hydrogenation of DMS indicate that the catalytic conditions are not favourable for its formation (see Table 2.19). The conversion of 1,4-butanediol to tetrahydrofuran can be achieved by an acid catalysed intramolecular H_2O extraction and cyclisation [2] (see Equation 2.10). The DMS hydrogenation was carried out in the alcohol iPA as a solvent, and produced the alcohols MeOH and 1,4-butanediol. Aliphatic alcohols typically have pK_as of > 15, and are consequently extremely weak acids. Consequently, the acid catalysed dehydration of 1,4-butanediol to tetrahydrofuran is therefore not going to be favoured by the reaction conditions of the DMS hydrogenation.

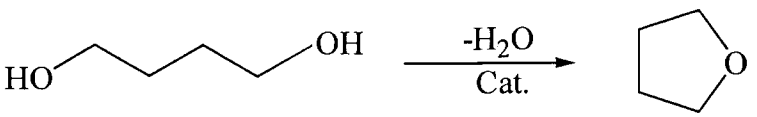

BDO THF

Equation 2.10

The highest levels of selectivity for tetrahydrofuran were obtained when the hydrogenation was carried out in H_2O as the solvent. The hydrogenation in H_2O of γ-butyrolactone (see Table 2.21) and DMM (see Table 2.17) resulted in significant increases of tetrahydrofuran, than when alcohol solvents were used. The hydrogenation of γ-butyrolactone in iPA did not produce any tetrahydrofuran, whereas in H_2O even at 120°C (which is not the favoured temperature for H_2O based hydrogenations) tetrahydrofuran was produced. The results indicate that selectivity for tetrahydrofuran requires H_2O. If the conversion of 1,4-butanediol to tetrahydrofuran by the catalytic system is as a result of acid-catalysis, this could be initiated by the H_2O. Although H_2O has a pK_a similar to most aliphatic alcohols,[31] the presence of dissolved CO_2 increases the acidity (see Equation 2.11).[32] It is perceived that catalysis is maintained by reactivation of the deactivated catalyst, [Ru(Triphos)H_2(CO)], by reaction with water through the water-gas shift reaction (see Chapter 4, Catalyst Reactivation) which produces CO_2, thus making the H_2O reaction solvent acidic. The acidity of the solvent may be sufficient to drive the acid-catalysed dehydration and cyclisation reactions to tetrahydrofuran.

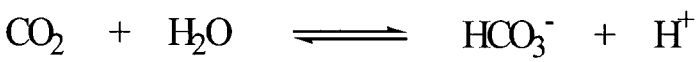

Equation 2.11

2.2.3 ^{31}P NMR Spectra Studies of the Product Solution

The ^{31}P NMR analyses of the respective product solutions of the ester hydrogenations in an alcohol solvent, indicate the presence of a series of ruthenium-triphos species that are predominantly common to all the systems studied. A typical spectrum, obtained is shown in Fig. 2.3, and was obtained from hydrogenation of methyl dodecanoate.

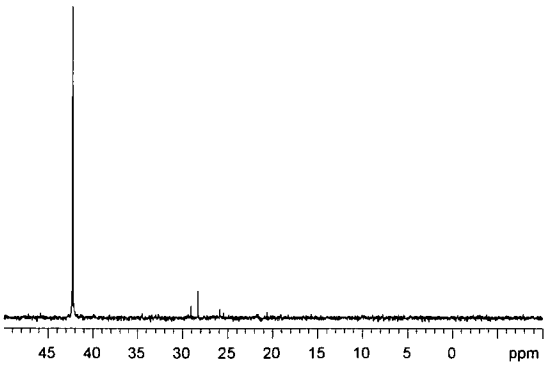

Figure 2.3 ^{31}P NMR Spectrum of the Product Solution of Methyl Dodecanoate Hydrogenation

Note: ^{31}P NMR @ r.t., $CDCl_3$.

From the above spectrum it can be deduced that none of the species generating the signals are paramagnetic, as the peaks are sharp, rather than broad peaks typically observed with paramagnetism. The spectrum (Fig. 2.3) contains three prominent singlets. The identity of the three species observed could not be determined due to insufficient experimental data, however, for a singlet to be obtained for a Triphos ligand, all the phosphorus atoms must be in identical environments. No hydride signal was detected in the ^{1}H NMR spectrum, which indicates that none of the species is a metal hydride, of any form.

Triphos contains three phosphorus atoms, [Triphos = $H_3CC(CH_2P(Ph)_2)_3$], which are able to bond directly to the ruthenium. This means interaction between the phosphorus atoms can take place through the ruthenium, giving rise to coupling. Any uncoordinated phosphorus atoms of the triphos will be in a different environment, and with being four bonds from the nearest other phosphorus atoms, (Ph_2P-CH_2-C-(CH_3)(CH_2-PPh_2)$_2$), P-P coupling will be small or non-existent. Also, uncoordinated phosphines, generally have negative δ values (Triphos = δ –24.5 (benzene-d_6) and -27.7 (chloroform-*d*) ppm), and therefore any uncoordinated phosphorus atom(s) of the triphos would be detected as a singlet with a negative δ value. In the absence of signals with negative δ in the ^{31}P NMR spectrum (Fig. 2.3), it is concluded that all three triphos phosphorus atoms are all co-ordinated to the ruthenium. Further, for the phosphorus atoms all to be in the same environment and co-ordinated, the ruthenium-triphos complexes must be of the form

[Ru(Triphos)L_n] (where n = 1 or 3). The ruthenium geometry has to therefore be either octahedral or tetrahedral (see Fig. 2.4). Note is also taken that ruthenium prefers to adopt octahedral geometry and favours the oxidation states of Ru^0, d^8 and Ru^{II}, d^6 (see Chapter 1).

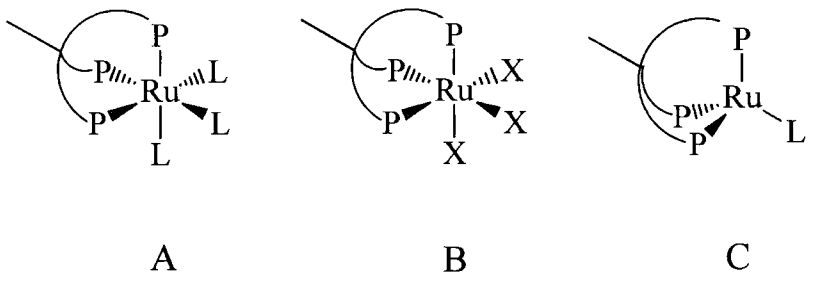

A B C

Figure 2.4 Octahedral and Tetrahedral Geometry of Ruthenium-triphos Complexes

The structures A and B in Fig. 2.4 show octahedral geometry, with both neutral (L) and anionic (X) ligands. In Structure A, the three ligands, in addition to the triphos, are neutral, the complex being therefore $[Ru(Triphos)L_3]^{2+}$ with Ru^{II}, d^6, whereas, in Structure B, the three ligands are anionic, and the complex is therefore $[Ru(Triphos)X_3]^-$ with Ru^{II}, d^6. Phosphine ligands are strong field ligands and the octahedral d^6 complex is low spin (see Chapter 1) and diamagnetic. It is possible that in both structures, A and B, the ligands could be bridging and that the ruthenium-triphos species could be, for example, a dimer, of the form $[(Triphos)Ru(\mu\text{-}L)_3Ru(Triphos)]^{4+}$ or $[(Triphos)Ru(\mu\text{-}X)_3Ru(Triphos)]^+$. Here, the ruthenium atoms remain octahedral, the bridging ligands are the same, and the phosphorus environments are identical. Such species would produce singlets in the ^{31}P NMR spectrum.

Structure C in Fig. 4 has tetrahedral geometry, with the fourth co-ordination position being occupied by a neutral ligand. The geometry of the four co-ordinate [Ru(Triphos)L] has to be tetrahedral, not square planner, due to the *fac* co-ordination of the triphos. The complex could therefore be a 16 electron unsaturated species [Ru(Triphos)L] with Ru^0, d^8. An unsaturated complex could result from the loss of H_2 from $[Ru(Triphos)H_2(CO)]$, to produce [Ru(Triphos)(CO)]. This might be achieved by

exposure to UV irradiation, as elimination of H_2 from the analogous $[RuH_2(CO)(PPh_3)_3]$ by UV irradiation has been reported [33] (see Chapter 4). Alternatively, the tetrahedral structure C, could be a ruthenium-triphos dimer with ruthenium-ruthenium bonding and take the form [(Triphos)RuRu(Triphos)], with a ruthenium-ruthenium quadruple bond. The ruthenium atoms of the dimer would still be tetrahedral, and therefore the phosphorus environments of the triphos molecules would be identical, and a singlet observed for the ^{31}P NMR spectrum.

From consideration of the reagents and products of the ester hydrogenation reaction, the possible identities of the ligands available, both L and X, can be elucidated. Table 2.22 details the possible ligands available, and include hydrogenation and decarbonylation products.

Table 2.22 Possible Ligands available from Ester Hydrogenation and Alcohol Decarbonylation.

Neutral Two Electron Ligands (L)	Anionic Two Electron Ligands (X) [a]
Triphos [b]	H^-
CO	$^-OCOR'$
H_2 (Non-classical)	^-OR
R-O-(CO)-R' [c]	R^- [d]
ROH	R'^- [d]
R'OH	$Acac^-$ [f]
iPA ($O{=}CMe_2$)	
2,4-Pentanediol [e]	

a: The attached atom is written first (except for acac$^-$).
b: Tridentate, therefore 3 x L.
c: Could be the initial ester or a transesterification product ester.
d: Alkyl, decarbonylation product.
e: acacH, hydrogenation product.
f: Can be X or LX.

It is unlikely that any of the singlets, in the ^{31}P NMR of Fig. 3, are as a result of two triphos ligands fully co-ordinating with a single ruthenium. Steric hindrance from the phenyl groups attached to each phosphorus atom would be significant, and the high *trans*-effect of the phosphines in such a situation, would result in a complex that was susceptible to dissociation [34] (see Chapter 1). The combination of the steric implications

and the electronic properties would result in an unstable complex, for which there is no evidence (no free phosphine, no exchange processes detected).

^{1}H NMR studies of the aliphatic ester hydrogenation product solutions did not detect the presence of a ruthenium hydride, terminal or bridging. The existence of $[Ru(Triphos)H_3]^-$ would be unlikely, as it would be expected to be as short lived as the analogous $[RuH_3(PPh_3)_3]^-$, considered by Halpern and Linn to be a precursor to the catalytic species $[RuH_2(\eta^2\text{-}H_2)(PPh_3)_3]$ [7].

The investigation of the effect of time on ester hydrogenation (see 2.2.1.5 Influence of Time), used sampling to establish the level of ester conversion as a function of time. Fig. 5 shows the ^{31}P NMR of the product solution of the methyl dodecanoate hydrogenation as a function of time.

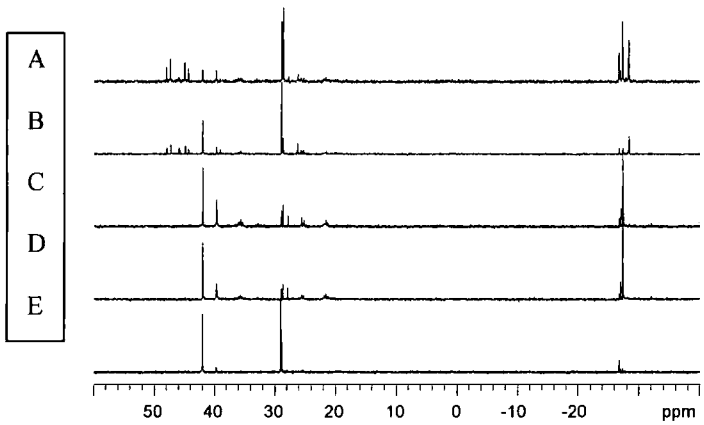

Figure 2.5 ^{31}P NMR Spectrum of the Product Solution of Methyl Dodecanoate Hydrogenation as a function of Time

Note: ^{31}P NMR @ r.t., $CDCl_3$.
A: Sample taken after 40 minutes.
$^{31}P\{^1H\}$NMR (25°C, chloroform-*d*): δ47.7 (**P**, d, $^2J_{p\text{-}p}$ = 49.2 Hz), 44.7 (**P**, d, $^2J_{p\text{-}p}$ = 49.2 Hz), 42.0 (**3P** ?, s), 39.8 (**3P** ?, s), 35.7 (**2P** ?, t, $^2J_{p\text{-}p}$ = 24.4 Hz), 28.9 (**3P** ?, s), 28.6 (**3P** ?, s), 27.8 (**3P** ?, s), 26.2 (**3P** ?, s), 21.6 (**2P** ?, t, $^2J_{p\text{-}p}$ = 24.4 Hz), -26.6 (**P** ?, s), -26.9 (**P** ?, s), -27.2 (**3P**, s), -28.2 (**?P** , s) ppm.
B: Sample taken after 60 minutes.
$^{31}P\{^1H\}$NMR (25°C, chloroform-*d*): δ47.7 (**P**, d, $^2J_{p\text{-}p}$ = 49.2 Hz), 44.7 (**P**, d, $^2J_{p\text{-}p}$ = 49.2 Hz), 42.0 (**3P** ?, s), 39.8 (**3P** ?, s), 39.0 (**3P** ?, s), 35.7 (**2P** ?, t, $^2J_{p\text{-}p}$ = 24.4 Hz), 28.9 (**3P** ?, s), 28.6 (**3P** ?, s), 27.8 (**3P** ?, s), 26.2 (**3P** ?, s), 21.6 (**2P** ?, t, $^2J_{p\text{-}p}$ = 24.4 Hz), -26.6 (**P** ?, s), -26.9 (**P** ?, s), -27.2 (**3P**, s), -28.2 (**?P** , s) ppm.
C: Sample taken after 120 minutes.

$^{31}P\{^{1}H\}$NMR (25°C, chloroform-*d*): δ 42.0 (**3P** ?, s), 39.8 (**3P** ?, s), 35.7 (**2P** ?, t, $^{2}J_{p\text{-}p}$ = 24.4 Hz), 28.9 (**3P** ?, s), 28.6 (**3P** ?, s), 27.8 (**3P** ?, s), 26.2 (**3P** ?, s), 21.6 (**2P** ?, t, $^{2}J_{p\text{-}p}$ = 24.4 Hz), -26.6 (**P** ?, s), -26.9 (**P** ?, s), -27.2 (**3P**, s) ppm.
D: Sample taken after 180 minutes.
$^{31}P\{^{1}H\}$NMR (25°C, chloroform-*d*): δ 42.0 (**3P** ?, s), 39.7 (**3P** ?, s), 35.7 (**2P** ?, t, $^{2}J_{p\text{-}p}$ = 24.4 Hz), 29.0 (**3P** ?, s), 28.7 (**3P** ?, s), 27.9 (**3P** ?, s), 26.2 (**3P** ?, s), 21.6 (**2P** ?, t, $^{2}J_{p\text{-}p}$ = 24.4 Hz), -26.6 (**P** ?, s), -26.9 (**P** ?, s), -27.2 (**3P**, s) ppm.
E: Sample taken after 930 minutes.
$^{31}P\{^{1}H\}$NMR (25°C, chloroform-*d*): δ 42.0 (**3P** ?, s), 39.7 (**3P** ?, s), 29.1 (**3P** ?, s), 28.8 (**3P** ?, s), -27.2 (**3P**, s) ppm.

The ^{31}P NMR spectra A to E, in Fig. 2.5 show that the species present during the hydrogenation reaction differ with time. The three singlets observed in the spectrum of the final solution (Fig. 2.3) can be seen in spectra A to E, gradually increasing in intensity. Spectrum E, the final sample comprises five singlets, three of which are observed in Fig. 2.3 and two additional singlets, of which, the additional singlet at δ -27 ppm is uncoordinated Triphos, whereas the identity and reason for the other additional signal is unknown. A series of multiplets and singlets is observed, in addition to the singlets, representing transient species not observed in the final product solution of spectra E. Spectrum A contains two doublets, at δ 47.7 and 44.7 ppm, which diminish in B and are absent in C. Two triplets, at δ 35.7 and 21.6 ppm, can be detected growing in intensity from A to C, diminishing in D and having disappeared from E. The presence of the doublets and triplets in the early ^{31}P NMR spectra (Fig. 2.5), suggests the presence of a catalyst intermediate. For the triphos ligand to produce a doublet ^{31}P NMR signal that is coupling with a second doublet, one of the three phosphorus atoms needs to be uncoordinated (and therefore produce a -δ value), and the two co-ordinated phosphorus atoms need to be in different environments from each other. The ruthenium-triphos complex would need to be of the formula $[Ru(\eta^2\text{-Triphos})X_2L_2]$, and with complex A structural geometry in Fig. 2.6. To obtain a ^{31}P NMR signal of two triplets, which are coupling with each other, a complex with four co-ordinated phosphorus would be required. Complex B in Fig. 6 illustrates a species that would generate a ^{31}P NMR spectrum of two triplets, coupling with each other, the four co-ordinating phosphorus atoms occupying two different environments. This is also achieved by two triphos ligands bonding with the ruthenium, and being *cis* in an equatorial plane. Each Triphos bonds using two phosphorus atoms, four phosphorus atoms in total. If the two triphos molecules were bonded *trans* to each other, as in C (Fig. 2.6), the ^{31}P NMR spectrum would be a singlet. The co-ordinated triphos phosphorus in B occupies two different environments, P_a and P_b (see Fig. 2.6), and each triphos would contain a phosphorus atom in a P_a and P_b environment. The phosphorus atoms P_a are *trans* to each

other and *cis* to the two P_b phosphorus atoms, whilst each of the phosphorus atoms P_b is *cis* to all the other phosphorus atoms (i.e. both of the P_a and the other P_b), generating two coupled triplets. The third phosphorus of each triphos would be uncoordinated and therefore generate a singlet with a negative shift. The remaining two co-ordination sites on the ruthenium would need to be occupied by the same ligand, such as two hydrides. The complex would have the formula $[Ru(\eta^2\text{-Triphos})_2X_2]$.

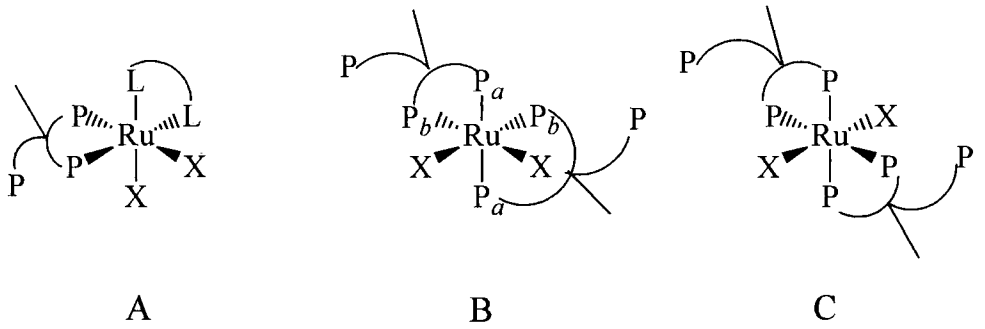

A B C

Figure 2.6 Possible Structures of Ruthenium-Triphos Complexes of $[Ru(\eta^2\text{-Triphos})X_2L_2]$ and $[Ru(\eta^2\text{-Triphos})_2X_2]$ Producing Singlet, Doublet and Triplet ^{31}P NMR Signals

To investigate if the multiplets obtained arise from catalytic intermediates, the reaction was repeated in the absence of the ester (methyl dodecanoate). The product solution from the reaction of $Ru(acac)_3$ and Triphos in iPA at 120°C with $p(H_2)$ of 6.8MPa, was an orange-red colour containing a micro-crystalline orange solid. The solution and the solid both gave ^{31}P NMR spectra (see Fig. 2.7) of the same species.

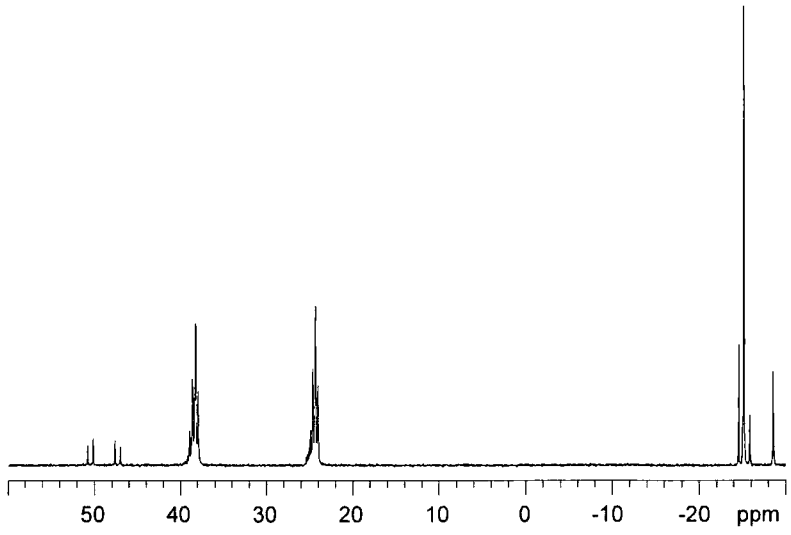

Figure 2.7 ^{31}P NMR Spectrum of the Solid Product from the Reaction of Ru(acac)$_3$ and Triphos in iPA at 120°C with $p(H_2)$ of 6.8MPa

Note: ^{31}P NMR is of the Product Solid in benzene-d_6, whereas Fig. 2.5 being the Product Solution was run as $CDCl_3$, the δ therefore differ accordingly.
$^{31}P\{^1H\}$NMR (25°C, benzene-d_6): δ 50.5 (**2P**, d, $^2J_{P\text{-}P}$ = 49.2 Hz), 47.3 (**2P**, d, $^2J_{P\text{-}P}$ = 49.2 Hz), 38.3 (**2P**, t, $^2J_{P\text{-}P}$ = 24.4 Hz), 24.6 (**2P**, t, $^2J_{P\text{-}P}$ = 24.4 Hz), -24.5 (**3P**, s), -25.0 (**P**, s), -25.8 (**P**, s), -28.5 (**?P**, s) ppm.

From Fig. 2.7 it can be seen that the two doublets and the two triplets observed in Fig. 2.5, were produced in the absence of methyl dodecanoate. This indicates that the two species are not hydrogenation products, and that the other ligands (L or X) are not from the ester hydrogenation or product alcohol decarbonylation. They could however, come from decarbonylation of 2,4-pentanediol the product of the acetylacetonate hydrogenation. On examination of the integration of the ^{31}P signals, it can be determined that the singlet at δ -25.8 ppm is the uncoordinated triphos phosphorus connected to the species that produces the two doublets, and that the singlet at δ – 24.5 ppm is part of the species that generates the two triplets. ^{1}H NMR studies of the product solution did not detect a hydride signal, whereas a study of the product solid produced two broad peaks in the hydride region (see Fig. 2.8).

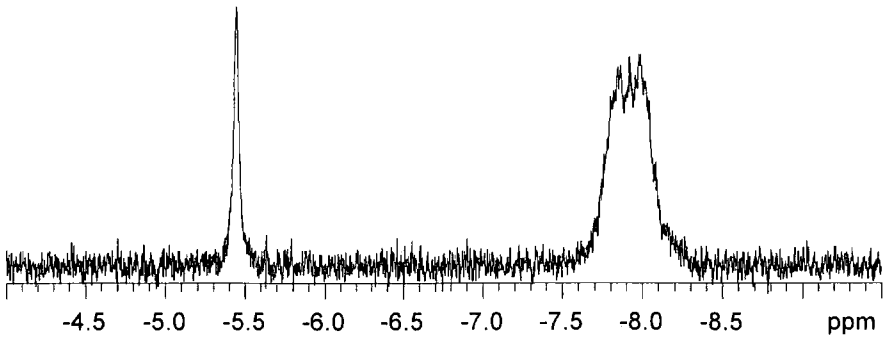

Figure 2.8 ^{1}H NMR Spectrum of the Solid Product from the Reaction of Ru(acac)$_3$ and Triphos in iPA at 120°C with $p(H_2)$ of 6.8MPa

Note: ^{1}H NMR is of the product solid.

^{1}H NMR (25°C, benzene-d_6): δ - 5.4 (**2H**, br s), - 7.8 (**2H**, br s) ppm.

The ^{1}H NMR hydride region, in Fig. 2.8, indicates that two different ruthenium hydride species are present in the products of the reaction. Both of the signals exhibit line width that indicates the absence of paramagnetic Ru(III), but that the species are probably undergoing exchange. The combination of the ^{31}P NMR (Fig. 2.7) and the ^{1}H NMR (Fig. 2.8) measurements indicate that the two species are [Ru(η^2-Triphos)H_2L_2] and [Ru(η^2-Triphos)$_2H_2$] (see Fig 2.9, A and B respectively).

Addition of chloroform-*d* to the product solid caused, the two doublets and two triplets to be replaced a singlet at δ 44.6 ppm [^{31}P{^{1}H} NMR (25°C, benzene-d_6 and chloroform-*d*): δ 44.6 (**3P**, s) ppm]. This suggests that the hydrides have been replaced by chlorides (metal-hydrides react with halogens, and halogen compounds, producing the corresponding halide.[6]), and that a complex of the formula [Ru(Triphos)Cl_3]$^-$ or [(Triphos)Ru(μ-Cl)$_3$Ru(Triphos)]$^+$ has formed. The identity of the ligands, L, in [Ru(η^2-Triphos)H_2L_2] is unknown, but the possibilities are restricted to the reagents contained in the reaction. They could be solvent molecules (iPA), the acetylacetonato-ligand and its hydrogenation products, giving, for example [Ru(η^2-Triphos)H_2S_2] (S = solvent) or [Ru(η^2-Triphos)H_2(acac)]$^-$.

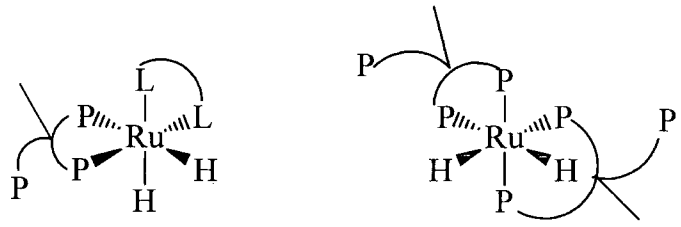

A B

Figure 2.9 Possible Structures of Hydride Complexes giving ^{1}H NMR Signals at δ -5.4 and –7.8 ppm. [Ru(η^2-Triphos)H_2L_2] and [Ru(η^2-Triphos)$_2H_2$]

A: [Ru(η^2-Triphos)H_2L_2]
B: [Ru(η^2-Triphos)$_2H_2$]

The two triplets observed in the ^{31}P NMR spectrum of the product solution disappear after 2-3 days, whereas the two doublets remain. A ^{1}H NMR spectrum of this aged solution contains only one peak in the hydride region, at δ - 5.4 ppm, indicating that [Ru(η^2-Triphos)$_2H_2$], the species that generates the two triplets, is less stable than the species producing the two doublets, i.e. [Ru(η^2-Triphos)H_2L_2]. As the triplets are produced by [Ru(η^2-Triphos)$_2H_2$], which has four phosphine groups bonded to the metal, their disappearance is not surprising as the combination of the *trans* effect and steric crowding by the phosphines produces a labile complex.

For a complex to be capable of catalysis, it will need to be able to allow the co-ordination of the substrate (ester) and hydrogen. Also for the intramolecular hydrogenation of the co-ordinated ester to occur, the hydrogen needs to be in a *cis* location with respect to the ester. Literature [24, 25] reports and the results detailed previously (see 2.2.2 Hydrogenation of Esters), indicate that the Triphos component is instrumental to the process, being a tridentate tripod ligand, which co-ordinates in a *fac* geometry through all three phosphorus atoms, and ensuring that vacant co-ordination sites are mutually *cis* to each other (see Fig. 2.10, complex A). The *fac* co-ordination of the triphos also results in the steric properties and the *trans* effect of the phosphines being focused on the three remaining co-ordination sites. This suggests that the active catalyst would take the form of [Ru(Triphos)H_2S], where S is a labile ligand such as solvent, substrate or dihydrogen (see Fig. 2.10, complex B). The dissociation of the labile S ligand would produce [Ru(Triphos)H_2], the necessary 16-electron co-

ordinatively unsaturated species, required to allow the ester to be co-ordinated, and hydrogenated. The isolation of the complex [(Triphos)HRu(μ-H)$_2$RuH(Triphos)] from the hydrogenation of 1-hexene (See Chapter 7), provides support for the proposal that the active catalyst is [Ru(Triphos)H$_2$], formed by the loss of a labile ligand from [Ru(Triphos)H$_2$S]. The complex [(Triphos)HRu(μ-H)$_2$RuH(Triphos)] would be obtained by dimerisation of [Ru(Triphos)H$_2$] (see Equation 2.12).

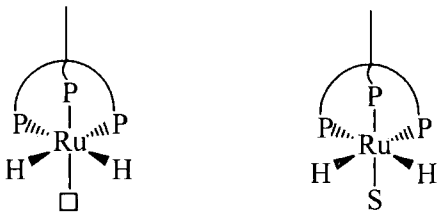

A B

Figure 2.10 *fac* Co-ordination of Triphos and Ligand Dissociation
A: = a vacant co-ordination site.
B: S = H$_2$, solvent or substrate molecule.

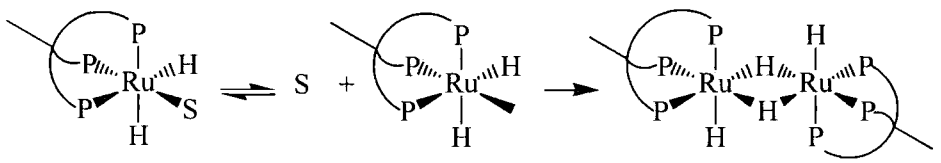

Equation 2.12

To form the ruthenium-triphos catalyst, the Ru(acac)$_3$ starting material would undergo a series of acac replacements leading to the creation of the active catalytic form, possibly [Ru(Triphos)H$_2$S]. During the ligand replacement process, intermediates would include species that contain both acac and partially co-ordinated triphos ligands. The composition of the complex [Ru(η^2-Triphos)H$_2$L$_2$], which is observed in the early stages of the hydrogenation of methyl dodecanoate, but not in the products on completion of the reaction, would fall into that category and could therefore be a precursor to the catalyst. The complex [Ru(η^2-Triphos)$_2$H$_2$], which is also observed in the initial stages of the methyl dodecanoate hydrogenation but not in the products, is more likely to arise from a competing side reaction. For the hydrogenation of an ester by [Ru(η^2-Triphos)$_2$H$_2$], a vacant co-ordination site would be required. This would

probably arise as a result of dissociation of one of the phosphorus atoms. It would then be more likely that the chelate effect would result in the third phosphorus atom of the remaining η^2-ligand co-ordinating, rather than the ester. This would ultimately lead to the dissociation of the η^1-triphos ligand and probably to a ruthenium complex with one η^3-triphos ligand co-ordinated. The absence of the species in the ^{31}P NMR of the final product solution of the ester hydrogenation (see Fig. 2.5), indicates that the bis-triphos complex is a transient species. What contribution (if any) it makes to the overall mechanism of the hydrogenation remains unknown.

Ester hydrogenations in the absence of an alcohol as a solvent, or using H_2O as the solvent, produce ^{31}P NMR spectra that contain species not detected in the ^{31}P NMR spectra of ester hydrogenations in alcohol solvents. Hydrogenation of methyl propanoate was carried out with and without iPA as a solvent, and with H_2O as the solvent. With iPA, ^{31}P NMR spectra were the same as those obtained for the other aliphatic esters hydrogenated in iPA (see Fig.2.3), whereas when the hydrogenation took place in the absence of a solvent, the ^{31}P NMR included additional signals (see Fig. 2.11).

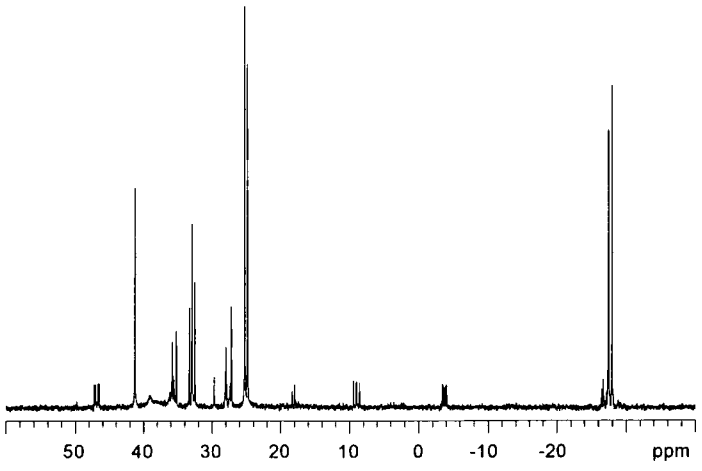

Figure 2.11 ^{31}P NMR of Methyl Propanoate Hydrogenation in the Absence of Solvent

$^{31}P\{^1H\}$NMR (25°C, chloroform-*d*): δ 46.9 (**P**, dd, $^2J_{P\text{-}P}$ = 40 Hz and 17 Hz), 41.3 (**3P**, s), 35.8 (**3P**, s), 35.2 (**3P**, s), 32.9 (**P**, t, $^2J_{P\text{-}P}$ = 32 Hz), 28.0 (**3P**, s), 27.9 (**3P**, s), 25.0 (**2P**, d, $^2J_{P\text{-}P}$ = 32 Hz), 18.3 (**3P**, s), 17.9 (**3P**, s), 9.0 (**P**, dd, $^2J_{P\text{-}P}$ = 40 Hz and 32 Hz), -3.8 (**P**, dd, $^2J_{P\text{-}P}$ = 32 Hz and 17 Hz), -27.1 (**3P**, s), -27.5 (**3P**, s), -27.9 (**3P**, s), ppm.

From the ^{31}P NMR spectrum (Fig. 2.11) additional singlets and a series of multiplets are observed. The hydrogenation of propyl propanoate in the absence of iPA as a solvent gave a ^{31}P NMR spectrum that was similar to that obtained for methyl propanoate, (Fig. 2.11). The only significant difference was that the three doublets of doublets were not observed.

The singlets (Fig. 2.11) represent species where the triphos phosphorus atoms are all in identical environments, i.e. [Ru(Triphos)L_n] (n = 1 or 3) as previously described, and the multiplets represent species where the triphos phosphorus atoms are in different environments. There is a species of the form [Ru(Triphos)X_2L] or [Ru(Triphos)LL'] generating a triplet and doublet at δ 32.9 and 25.0 ppm, and a species [Ru(Triphos)XLX'] generating three doublets of doublets at 46.9, 9.0 and –3.8 ppm. A triplet and doublet would be observed for the five co-ordinate [Ru(Triphos)LL'] species, as the three triphos phosphorus atoms exist in two different environments, shown as P_a and P_b in Fig. 2.12. The [Ru(Triphos)LL'] species would be Ru^0, d^8, if L are neutral ligands.[35] The variety of possible identities for L and X, detailed in Table 2.22, apply to the hydrogenation of methyl propanoate. In the absence of data for model complexes, it is not possible to be more precise about the nature of L, L' and S.

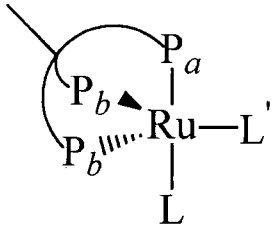

Figure 2.12 Structure of [Ru(Triphos)LL']

The hydrogenation of the methyl propanoate in H_2O also produced a reaction product solution giving a ^{31}P NMR spectrum containing a series of multiplets, in addition to the usual singlets (see Fig. 2.13). The spectrum includes three doublet-triplet combinations, representing three different species of the form [Ru(Triphos)X_2L] or [Ru(Triphos)LL']. A doublet and triplet at δ 32.5 and 3.4 ppm are coupling, as are the triplet and doublet at δ 22.2 and –1.4 ppm respectively, and the doublet and triplet at δ 15.5 and 3.9 ppm

respectively. From the available data it is not possible to make assignments of the identities of any of the species observed, or whether the multiplet combinations are [Ru(Triphos)X_2L] or [Ru(Triphos)LL'].

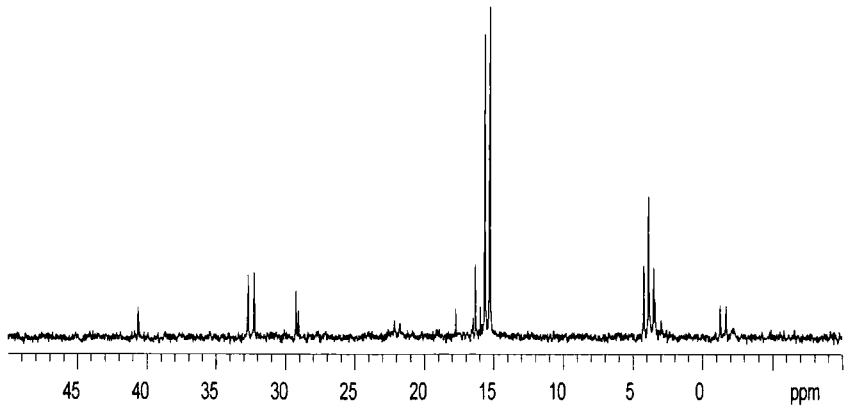

Figure 2.13 ^{31}P NMR of Methyl Propanoate Hydrogenation in H_2O

$^{31}P\{^1H\}$NMR (25°C, chloroform-*d*): δ 40.6 (**3P**, s), 32.5 (**2P**, d, $^2J_{P\text{-}P}$ = 35 Hz), 29.3 (**3P**, s), 29.0 (**3P**, s), 22.2 (**P**, t, $^2J_{P\text{-}P}$ = 32 Hz), 17.7 (**3P**, s), 16.3 (**3P**, s), 15.9 (**3P**, s), 15.5 (**2P**, d, $^2J_{P\text{-}P}$ = 28 Hz), 3.9 (**P**, t, $^2J_{P\text{-}P}$ = 28 Hz), 3.4 (**P**, t, $^2J_{P\text{-}P}$ = 35 Hz), -1.4 (**2P**, d, $^2J_{P\text{-}P}$ = 32 Hz) ppm.

The hydrogenation of the aromatic esters and the aliphatic diesters (see sections 2.2.2.2 and 2.2.2.3) produced ^{31}P NMR spectra that are similar to those obtained for the hydrogenation of methyl propanoate in the absence of iPA. In particular, the esters dimethyl phthalate, diethyl carbonate, dimethyl malonate, benzyl benzoate and dimethyl maleate were all hydrogenated in iPA as a solvent, and produced ^{31}P NMR spectra that included a triplet and doublet at *ca.* δ 32 and 25 ppm respectively, with $^2J_{P\text{-}P}$ = 32 Hz, a combination observed in methyl propanoate hydrogenation without iPA (see Fig. 2.12). In contrast, the hydrogenation of dimethyl oxalate in iPA produced a ^{31}P NMR spectrum that was comparable to that obtained for the hydrogenation of methyl propanoate in H_2O, which included three doublet-triplet combinations with the same δ and $^2J_{P\text{-}P}$ values (see Fig. 2.13). The ^{31}P NMR spectrum of the product solution of the hydrogenation of benzyl benzoate suggests that the species giving different doublet-triplet patterns may be related (see Fig. 2.14).

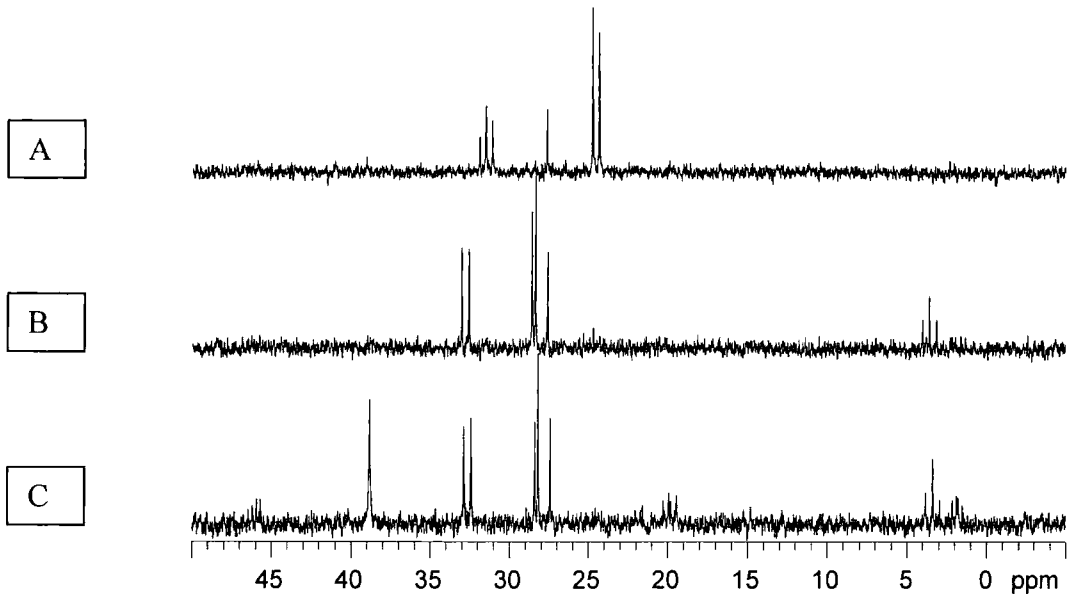

Figure 2.14 ^{31}P NMR Spectra for Benzyl Benzoate Hydrogenation

A: Immediately after completion of the reaction.
^{31}P{^{1}H}NMR (25°C, chloroform-*d*): δ 31.5 (**P**, t, $^{2}J_{P\text{-}P}$ = 32 Hz), 27.7 (**3P**, s), 24.6 (**2P**, d, $^{2}J_{P\text{-}P}$ = 32 Hz) ppm.
B: 14 days after completion of the reaction.
^{31}P{^{1}H}NMR (25°C, chloroform-*d*): δ 32.8 (**2P**, d, $^{2}J_{P\text{-}P}$ = 35 Hz), 28.6 (**3P**, s), 28.4 (**3P**, s), 27.6 (**3P**, s), 3.6 (**P**, t, $^{2}J_{P\text{-}P}$ = 35 Hz) ppm.
C: 6 months after completion of the reaction.
^{31}P{^{1}H}NMR (25°C, chloroform-*d*): δ 45.9 (**P**, dd, $^{2}J_{P\text{-}P}$ = 40 Hz and 19 Hz), 38.8 (**3P**, s), 32.7 (**2P**, d, $^{2}J_{P\text{-}P}$ = 35 Hz), 28.4 (**3P**, s), 28.2 (**3P**, s), 27.5 (**3P**, s), 19.9 (**P**, dd, $^{2}J_{P\text{-}P}$ = 40 Hz and 28 Hz), 3.4 (**P**, t, $^{2}J_{P\text{-}P}$ = 35 Hz), 1.9 (**P**, dd, $^{2}J_{P\text{-}P}$ = 28 Hz and 19 Hz) ppm.

The ^{31}P NMR spectra in Fig. 2.14 show the species present change as a function of time. Spectrum A was obtained on completion of the hydrogenation reaction, whilst B was acquired 14 days later and C, 6 months after that. Comparison of Spectra A and B shows that the triplet and doublet at δ 31 and 25 ppm, with $^{2}J_{P\text{-}P}$ = 32 Hz, observed in A have disappeared in B, and been replaced with the doublet and triplet at δ 33 and 3.6 ppm, $^{2}J_{P\text{-}P}$ = 35 Hz. Spectrum C contains the species observed in B, and two additional species that generate a singlet at δ 38 ppm, and three doublets of doublets at δ 45.9, 19.9 and 1.9 ppm. The triplet-doublet combinations observed in the ^{31}P NMR spectrum are consistent with complexes of the form [Ru(Triphos)X_2L]. The changes observed in the three ^{31}P NMR spectra will be as a result of ligand replacement. The change between A and B is most likely to be because the ligand L in the complex [Ru(Triphos)X_2L] was replaced by L', to produce [Ru(Triphos)X_2L']. Replacement of X in the complex [Ru(Triphos)X_2L] would also be possible, but would require both of the ligands to be replaced with a new ligand X' to produce [Ru(Triphos)X'_2L] to obtain the doublet-

triplet combination. However, it is likely that the replacement would also produce the intermediate [Ru(Triphos)XLX'], which would be detected as three doublets of doublets, and these are not seen in B, suggesting that the ligand L is replaced not the ligands X. The three doublets of doublets in C would be produced by a complex of the form [Ru(Triphos)XLX'], and as previously suggested this is likely to be as a result of replacement of one of the two X ligands in the complex [Ru(Triphos)X_2L'] with X'. Addition of chloroform-*d* to a sample of the solution that generated B, had no effect on the ^{31}P NMR signal obtained, which indicates that the X ligand is not a hydride. The identity of the various species observed is unknown as the L and X ligands are unidentified.

The multiplets in the ^{31}P NMR spectra obtained from the hydrogenation of aromatic esters and diesters in alcohol solvents, and aliphatic esters in the absence of iPA are probably not generated by the active catalytic species, because, if [Ru(Triphos)H_2], it would be unstable due to its reactivity and decay rapidly. The complexes are more likely to be of the [Ru(Triphos)X_2L] type, where the X ligand is from the partial ester hydrogenation or a decarbonylation product such as an alkyl group. The presence of multiplets in the ^{31}P NMR spectra of the product solutions for the hydrogenation of aliphatic esters in the absence of iPA, aromatic esters and diesters in iPA but not in the hydrogenation of aliphatic esters hydrogenated in iPA remains unexplained.

The complex [(Triphos)HRu(μ-H)$_2$RuH(Triphos)] was isolated from the hydrogenation of 1-hexene (See Chapter 7). The hydrogenation achieved 100% conversion to produce hexane, and in the absence of alcohols susceptible to decarbonylation, the active catalyst dimerised to form [(Triphos)HRu(μ-H)$_2$RuH(Triphos)]. The ^{31}P NMR spectrum of the product did not contain any multiplets, but contained a signal at similar ppm to that obtained for the aliphatic esters in iPA. This supports the argument that the multiplets observed in the ^{31}P NMR spectra of the products are not of the catalytic species. The ^{31}P NMR spectra obtained of the products of the hydrogenation of propanoic acid or maleic acid (see Chapter 5) are the same as that observed for the hydrogenation of methyl propanoate in H_2O. The acid hydrogenation achieves conversion of > 98%, and the species in the ^{31}P NMR spectrum change with time in the same manner as those previously described. The similarity of the ^{31}P NMR spectra for the different ester hydrogenations is probably due to the similarity of the decarbonylation products that would be obtained from their respective alcohols from their hydrogenation. Many of the

hydrogenations produce the primary alcohol MeOH, or similar short chain aliphatic alcohols, which decarbonylate to produce CO and an alkyl group, both of which would form more stable [Ru(Triphos)X_2L] complexes than the proposed active catalyst [Ru(Triphos)H_2] or its probable precursor [Ru(Triphos)H_2S]. The stability of the solid [Ru(Triphos)H_2(CO)] demonstrates this feature.

2.2.4 [Ru(Triphos)H_2(CO)] Characterisation

[Ru(Triphos)H_2(CO)], the product of catalyst deactivation was characterised by X-ray crystallography, ^{1}H, ^{31}P NMR and IR spectroscopy, mass spectrometry and elemental analysis.

The solid [Ru(Triphos)H_2(CO)] was obtained when ester hydrogenation was carried out in an alcohol solvent or with the ester itself as the solvent. The pale yellow coloured solid was observed as a ring (1-2 cm wide) of precipitate, deposited on the internal surfaces of the autoclave that were immersed in the reaction solution whilst the mixture was rapidly stirred, but occurring on the autoclave wall immediately above the product solution on opening the vessel. The solid usually took the form of a fine particled crystalline material, although fine needle shaped crystals, 0.5 x 0.2 x 0.08 mm^3, were obtained when the reaction product solution was cooled slowly. The [Ru(Triphos)H_2(CO)] is not very soluble, as is demonstrated by its precipitation in the predominantly alcohol, product solutions of the different ester hydrogenations. The [Ru(Triphos)H_2(CO)] was found to be poorly soluble in diethyl ether, THF, furan, acetonitrile-d_3, benzene-d_6, toluene-d_8, acetic-d_3 acid-*d* and D_2O but readily soluble in chloroform-*d*. The [Ru(Triphos)H_2(CO)] was sufficiently soluble in benzene-d_6 and chloroform-*d* to allow investigation by ^{1}H and ^{31}P NMR.

The crystals of [Ru(Triphos)H_2(CO)] obtained were suitable for X-ray crystallography and a structure determination was performed by H. Puschmann. The structure details the connectivity and spatial relationship between the ruthenium, triphos and carbonyl, but not the hydrides. Metal hydrides are difficult to detect by crystallographic techniques, due to the small X-ray scattering cross section of the H atom, which is usually obscured by the electron density of the transition metal to which it is bonded. Hydride detection can occur as a result of X-ray scattering from the metal-hydride bond (X-rays are scattered by electron density), but not the hydrogen nuclei.[36, 37] The crystal structure of

[Ru(Triphos)H_2(CO)] shows that the triphos and CO occupy positions consistent with an octahedral complex in keeping with two hydrides occupying the remaining sites (see Figure 15).

Figure 2.15 The Crystal Structure of [Ru(Triphos)H_2(CO)]
(see Appendix 2 for crystallographic data)

The ^{31}P NMR spectrum obtained of [Ru(Triphos)H_2(CO)] consists of a coupled triplet and doublet (see Fig. 2.16). As the magnetically active isotopes of ruthenium are ^{99}Ru, abundance 12.81%, with I = 3/2 and ^{101}Ru, abundance 16.98%, with I = 5/2, the coupling observed is between the different phosphorus environments of the [Ru(Triphos)H_2(CO)].[^{31}P{^{1}H} NMR (C_6D_6): δ 37.2 (**P**, t, $^2J_{P\text{-}P}$ = 32 Hz), 28.4 (**2P**, d, $^2J_{P\text{-}P}$ = 32 Hz) ppm].

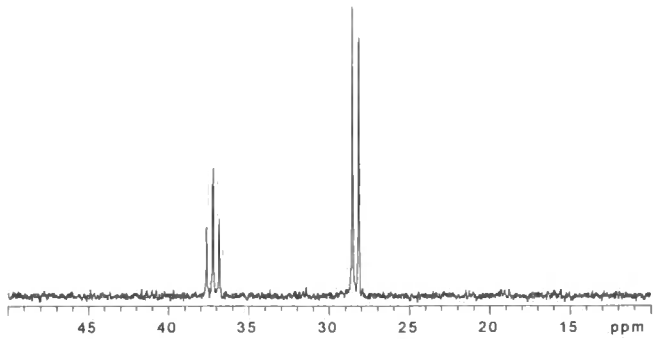

Figure 2.16 The ^{31}P NMR of [Ru(Triphos)H_2(CO)]

The ^{31}P NMR spectrum confirms that [Ru(Triphos)H_2(CO)] has an octahedral geometry, the triplet and doublet observed are as a result of two different environments for the three phosphorus atoms of the triphos (see Fig. 2.17). In the absence of the hydrides the complex would adopt a tetrahedral geometry, which would generate a singlet in the ^{31}P NMR spectrum as the Triphos phosphorus atoms would be in identical environments. The two different phosphorus environments are identified in Fig. 2.17 as P_a and P_b, P_a being *trans* to the carbonyl and *cis* to both hydrides, whereas P_b are both *cis* to the carbonyl, *trans* to one hydride and *cis* to the other hydride. The triplet observed in the ^{31}P NMR is from phosphorus P_a and the doublet from the phosphorus P_b.

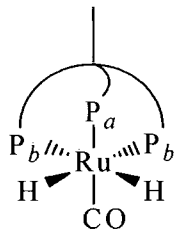

Figure 2.17 The Different Phosphorus Environments of [Ru(Triphos)H_2(CO)]

Metal hydride ligands can be detected by ^1H NMR, as their resonance is lower frequency of TMS, an area that is usually free of resonation from other ligands.[36] The hydride undergoes strong shielding from the transition metal, which results in negative δ ^1H NMR values. The chemical shifts for transition metal hydrides can be observed in the region 0.0 to –50.0 ppm, with terminal hydrides typically being ca. –2 to –12 ppm. [38, 39, 40] The hydride will couple with transition metals, where the metal has spin ½, and with phosphines, *cis* (J = 15-30 Hz) and *trans* (J = 90-150 Hz). The difference of the *cis* and *trans* phosphine couplings can be useful for the structural determination of a complex.[36] The ^1H NMR spectrum of [Ru(Triphos)H_2(CO)] in the region 0.0 to –50.0 ppm consisted of a doublet of doublets (see Figure 2.18). [^1H NMR (C_6D_6) δ -6.4 (**2H**, dd, $^2J_{P\text{-}H}$ = 51 Hz, $^2J_{P\text{-}H}$ = 18 Hz) ppm].

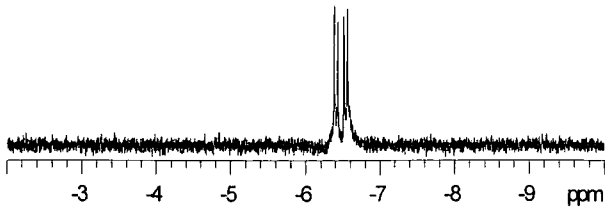

Figure 18 The ^{1}H NMR Spectrum of [Ru(Triphos)H_2(CO)]

This doublet of doublets was a simpler signal than expected, as the two protons are connected through the ruthenium to the three phosphorus atoms of the Triphos, which exist in two different environments (see Figure 17). The coupling constant of 18 Hz obtained, suggests coupling with the *cis* phosphorus, but the coupling constant of 51 Hz is not so easily assigned, as it is greater than the value for *cis*(^{2}J) coupling but lower than that for *trans*(^{2}J) coupling. From Figure 19, it can be seen that both hydrides are interacting with two *cis* phosphorus and one *trans* phosphorus. Hydride $H_{(I)}$ is *trans* to phosphorus $P_{b(II)}$ and *cis* to both P_a and $P_{b(I)}$, whilst hydride $H_{(II)}$ is *trans* to phosphorus $P_{b(I)}$ and *cis* to both P_a and $P_{b(II)}$.

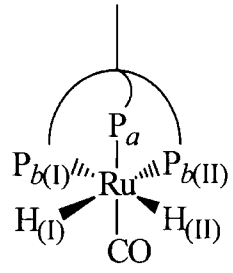

Figure 2.19 The *cis* and *trans* interactions of the hydrides with the phosphorus of [Ru(Triphos)H_2(CO)]

The ^{1}H NMR spectrum of [Ru(Triphos)H_2(CO)] obtained using selective ^{31}P decoupling (see Figure 2.20) enabled the coupling constants, 18 and 51 Hz, to be assigned to the respective hydride- phosphine interaction. The selective ^{31}P decoupling of the triplet and doublet reduce the ^{1}H NMR hydride signal to a doublet for each ^{31}P decoupling. The $^{2}J_{P\text{-}H}$ = 51 Hz is generated by hydride interaction with the ^{31}P triplet and the $^{2}J_{P\text{-}H}$ = 18 Hz is from hydride interaction with the ^{31}P doublet. From Figure 2.19 it can be seen that

the phosphorus P_a generates the ^{31}P triplet, which is *cis* to both of the hydrides, $H_{(I)}$ and $H_{(II)}$, and therefore the coupling $^{2}J_{P\text{-}H}$ 51 Hz is *cis*(J). The $^{2}J_{P\text{-}H}$ 18 Hz is as a result of the decoupling of the ^{31}P doublet, which is produced by the phosphorus P_b. The phosphorus P_b relationship with the hydrides is from a *cis* and a *trans* interaction. The 18 Hz value for the $^{2}J_{P\text{-}H}$ coupling is lower than would be expected for a *trans* interaction, and is therefore more likely due to the *cis* interaction. If this is the case, then the *trans* coupling is not observed.

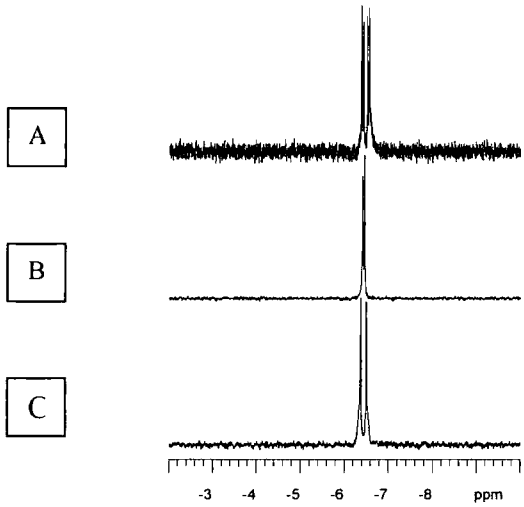

Figure 2.20 The ^{1}H NMR Spectra of [Ru(Triphos)H_2(CO)] with Phosphorus Decoupling

A: No ^{31}P Decoupling.
B: Decoupling ^{31}P Doublet.
C: Decoupling ^{31}P Triplet.
Note: For ^{31}P NMR spectrum, see Fig. 2.16.

The interaction of metal-hydrides with halogens, or halogen compounds, will normally result in the corresponding halide.[6] The ^{31}P NMR spectra of [Ru(Triphos)H_2(CO)] in chloroform-*d* initially gave a triplet and doublet. $^{31}P\{^{1}H\}$ NMR ($CDCl_3$): δ 35.3 (**P**, t, $^{2}J_{P\text{-}P}$ = 32 Hz), 27.8 (**2P**, d, $^{2}J_{P\text{-}P}$ = 32 Hz) ppm (the same as in benzene-d_6, apart from the δ ^{31}P, see Fig. 2.16). The spectra rapidly changed to become a more complicated spectrum (see Fig. 2.21), suggesting that in chloroform-*d* the [Ru(Triphos)H_2(CO)] hydrides are replaced by Cl, either to produce [Ru(Triphos)Cl_2(CO)] or [Ru(Triphos)H(CO)Cl].

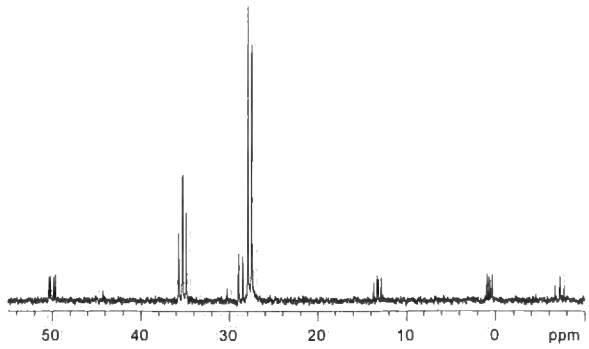

Figure 2.21 The ^{31}P NMR Spectrum of [Ru(Triphos)H_2(CO)] in chloroform-*d*

The ^{31}P NMR spectrum (Fig. 2.21) indicates the presence of three species, represented by; (i) three doublets of doublets, (ii) a triplet with a doublet and (iii) a doublet with a triplet [$^{31}P\{^1H\}$ NMR (chloroform-*d*): (i) δ 50.0 (**P**, dd, $^2J_{P-P}$ = 40 Hz and 17 Hz), 13.3 (**P**, dd, $^2J_{P-P}$ = 40 Hz and 32 Hz), 0.7 (**P**, dd, $^2J_{P-P}$ = 32 Hz and 17 Hz) ppm, (ii) δ 35.3 (**P**, t, $^2J_{P-P}$ = 32 Hz), 27.8 (**2P**, d, $^2J_{P-P}$ = 32 Hz) ppm, and (iii) δ 28.8 (**2P**, d, $^2J_{P-P}$ = 41 Hz), -7.2 (**P**, t, $^2J_{P-P}$ = 41 Hz) ppm]. The coupling constants and a ^{31}P COSY (see Fig. 2.22) confirm the three species.

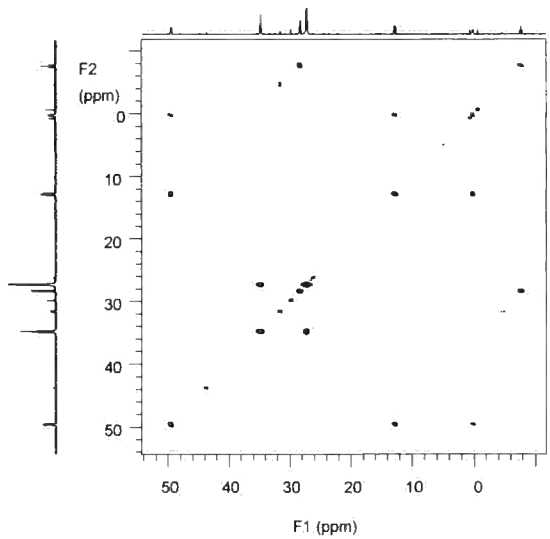

Figure 2.22 The ^{31}P COSY Spectra of [Ru(Triphos)H_2(CO)] in chloroform-*d*

The ^{31}P NMR spectrum of [Ru(Triphos)H_2(CO)] in chloroform-*d* indicates that of the three species present, two produce a triplet-doublet combination and the third three doublets of doublets. The ^{31}P spectra of the three species show that in each case the three phosphorus atoms of the triphos are co-ordinated to the ruthenium, suggesting that they are all octahedral complexes. The triplet-doublet combination is caused by the three triphos phosphorus atoms being in two different environments, whereas the three doublets of doublets indicates that the three triphos phosphorus atoms are all in different environments. From the initial ^{31}P NMR spectrum, the triplet and doublet at δ 35.3 and 27.8 ppm arise from [Ru(Triphos)H_2(CO)]. The chloroform interaction with the ruthenium-hydrides of [Ru(Triphos)H_2(CO)] results in [Ru(Triphos)Cl_2(CO)], which generates a triplet-doublet combination. Synthesis and spectral study of [Ru(Triphos)Cl_2(CO)] (see Experimental, 2.3.3) confirmed the assignment of the second doublet and triplet, at δ 28.8 and -7.2 ppm respectively, to [Ru(Triphos)Cl_2(CO)]. Three doublets of doublets in the ^{31}P NMR spectrum arise when, three phosphorus atoms are in different environments, suggesting that the species is [Ru(Triphos)H(CO)Cl]. Attempts to synthesise, isolate and characterise [Ru(Triphos)H(CO)Cl] were unsuccessful, and therefore no independent confirmation for this interpretation was obtained.

The ^{31}P NMR of [Ru(Triphos)H_2(CO)] in chloroform-*d* demonstrates that the hydrides will interact with chloro-compounds to produce [Ru(Triphos)H(CO)Cl] and [Ru(Triphos)Cl_2(CO)] (see Equation 2.13).

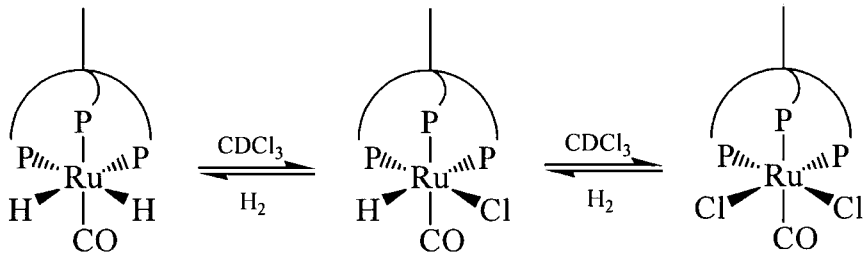

Equation 2.13

The [Ru(Triphos)H_2(CO)] characterisation was corroborated by IR spectroscopy, mass spectrometry and elemental analysis. IR spectroscopy detected the ν (CO) but not the ν (M-H). The metal-hydride stretching frequencies are predominantly in the range 1500-

2200 cm^{-1}, but the intensities are often weak and therefore difficult to detect. [36, 41] [IR (r.t., cm^{-1}) ν (CO) = 1921 cm^{-1} (Nujol Mull) and 1943 cm^{-1} (benzene-d_6). Mass spectral data: molecular ion peak (M^+), 756.22 (calculated M_r 756.14); $[M-H_2]^+$, 754; $[M-CO-H_2]^+$, 726; $[M-Ph-CO-H_2]^+$, 649; $[M-PPh_2-H_2]^+$, 569; $[M-PPh_2-CO-H_2]^+$, 541; $[M-PPh_2-PPh]^+$, 463; $[M-2PPh_2-CO-CH_3]^+$, 363; $[M-3PPh_2]^+$, 201; largest intensity peak $[M-CO-H_2]^+$, 726. Elemental analysis: Found : C, 66.58; H, 5.44. $C_{42}H_{39}OP_3Ru$, requires: C, 66.65; H, 5.46].

2.2.5 The Catalytic Cycle

The homogeneous hydrogenation of esters has been achieved by the catalytic system of $Ru(acac)_3$ and Triphos. Fig. 2.23 is a proposed catalytic cycle.

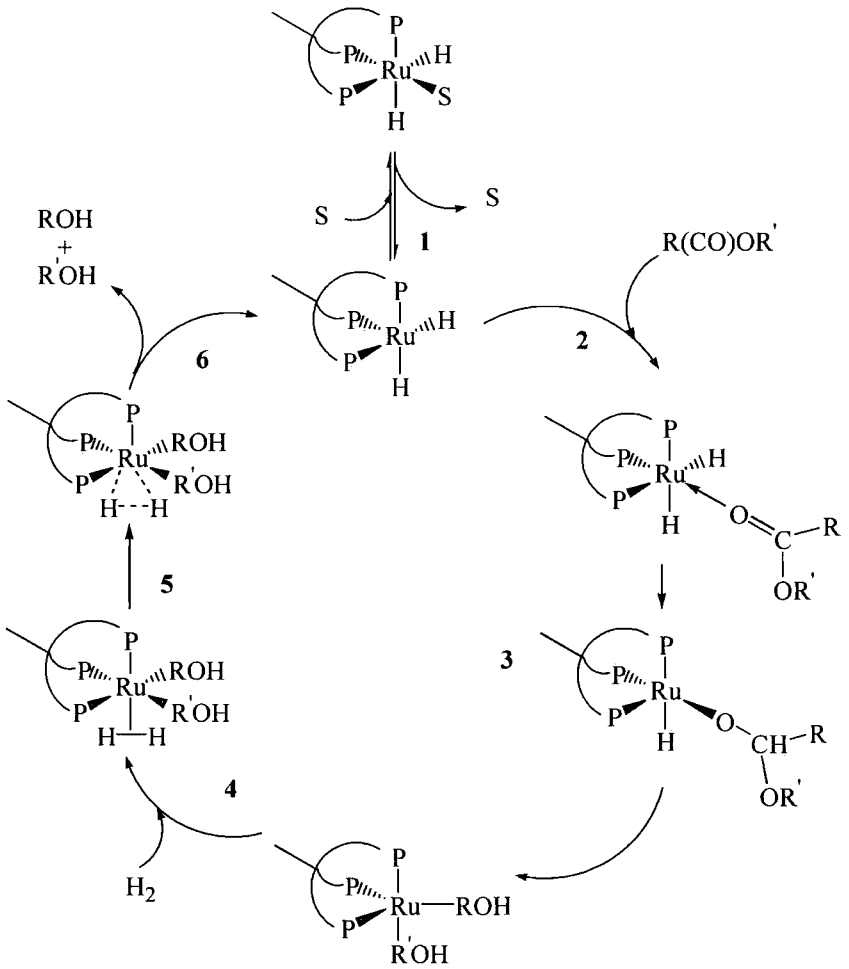

Figure 2.23 Proposed Catalytic Cycle for Homogeneous Ester Hydrogenation

Step **1**. Dissociation of labile ligand S (S = solvent or H_2), to form [Ru(Triphos)H_2] a co-ordinatively unsaturated 16 electron [Ru] complex.

Step **2**. Co-ordination of ester at vacant co-ordination site on Ru.

Step **3**. Intramolecular hydrogen transfer.

Step **4**. Co-ordination of H_2.

Step **5**. Agostic intermediate for the oxidative addition of H_2.

Step **6**. Loss of alcohol products and oxidative addition of H_2 to [Ru] complex recycles catalyst.

2.2.6 Conclusion

The homogeneous hydrogenation of esters is possible with a catalyst produced *in-situ* from $Ru(acac)_3$ and the tridentate tripod phosphine ligand Triphos. The hydrogenation can be achieved in alcohols (e.g. iPA or ^tBuOH) at 120°C or in H_2O at 140°C. A hydrogen pressure of 6.8 MPa was found to give the best results, although both higher and lower pressures will still achieve hydrogenation.

The primary alcohol products of the ester hydrogenation deactivate the catalyst, and result in reduced levels of conversion. The primary alcohols are dehydrogenated and then decarbonylated by the ruthenium catalyst to form the inactive complex [Ru(Triphos)H_2(CO)]. The effect of catalyst deactivation can be minimised by using H_2O as a solvent and operating the hydrogenation at 140°C, at which temperature the water-gas shift reaction reactivates the catalyst and maintains hydrogenation.

The active catalyst is believed to be[Ru(Triphos)H_2], which is obtained from the dissociation of a labile ligand from [Ru(Triphos)H_2S] (where S = solvent, substrate or molecular H_2).

2.3 Experimental

2.3.1 Hydrogenations

All hydrogenations were carried out using a 300-ml Hasteloy™ autoclave equipped with overhead stirrer. The autoclave was loaded with $Ru(acac)_3$, Triphos and other solid

reagents required, and then the air was removed by three cycles of vacuum followed by refilling with argon. The selected solvent and ester were purged under argon for 1 hour, and then added to the autoclave by canula. The autoclave was then pressurised at r.t. with hydrogen (4.4 MPa), heated to the chosen temperature, at which the hydrogen Mass Flow Controller would be set to 6.8 MPa, and then heated and stirred for the allocated period of time. On completion of the reaction period, the heating was stopped and the autoclave allowed to slowly cool. The headspace gases within the autoclave were slowly vented and the products removed. The product solution was analysed by GC, GCMS and NMR spectroscopy. The product solid was analysed by ^{31}P NMR spectroscopy, X-ray crystallography (where appropriate), and on selected samples by ^{1}H NMR and IR spectroscopy, mass spectrometry and elemental analysis. No special precautions were taken at this stage to preclude air.

Quantity of Reagents used:

Table 2.23 General Reactions:

Reagent	Quantity
$Ru(acac)_3$	4.5×10^{-4} mol
Triphos	6.1×10^{-4} mol
Solvent [a]	50.0 cm^3
Ester [b] (or other substrate)	20.0 cm^3 [c]

Table 2.24 Additives, Included in 2.2.1.2 Influence of Additives

Reagent	Quantity
NEt_3	5.0 cm^3
*p*TSA	0.3816 g
Conc. Sulphuric Acid	5.0 cm^3
Ionic Liquid [d]	2.5 cm^3
H_2O	5.0 cm^3

a: Alcohol or H_2O.
b: All esters tested were liquids, except dimethyl oxalate, which is a solid at r.t., ∴20.4416 g used.
c: 70.0 ml when no solvent included.
d: 1-ethyl-3-methyl-1 *H*-imidazolium tetrafluoroborate.

2.3.2 NMR Spectroscopy

The NMR spectra of the product solutions were measured against an external reference of chloroform-*d* containing Triphos, which was used to lock and shim the NMR spectrometer. The product solids were dissolved in the appropriate *deuterated* solvent and the NMR spectrometer locked and shimmed accordingly, prior to running the sample for the required NMR measurements.

2.3.3 Synthesis of [Ru(Triphos)Cl_2(CO)]

The synthesis of [Ru(Triphos)Cl_2(CO)] was carried out according to the literature method.[42] Elemental analysis for [Ru(Triphos)Cl_2(CO)]: Found : C, 60.51; H, 4.70. $C_{42}H_{37}Cl_2OP_3Ru$ requires: C, 61.07; H, 4.77. $^{31}P\{^1H\}$ NMR (chloroform-*d*): δ 28.8 (**2P**, d, $^2J_{P\text{-}P}$ = 40 Hz) and -7.2 (**P**, t, $^2J_{P\text{-}P}$ = 40 Hz) ppm.

2.4 References

1. J. March, *Advanced Organic Chemistry*, John Wiley & Sons, New York, 4th edn., 1992.
2. H. Beyer and W. Walter, *Handbook of Organic Chemistry*, Simon and Schuster International Group, Hemel Hempstead, 1996.
3. H. Adkins, *Org. React.*, 1954, **8**, 1.
4. R. A. Grey, G. P. Pez and A. Wallo, *J. Am. Chem. Soc.*, 1981, **103**, 7536.
5. G. P. Pez, R. A. Grey and J. Corsi, *J. Am. Chem. Soc.*, 1981, **103**, 7528.
6. F. A. Cotton and G. Wilkinson, *Advanced Inorganic Chemistry*, John Wiley & Sons, Chichester, 5th edn., 1988.
7. D. E. Linn, Jr., and J. Halpern, *J. Am. Chem. Soc.*, 1987, **109**, 2969.
8. W. A. Fordyce, R. Wilczynski and J. Halpern, *J. Organomet. Chem.*, 1985, **296**, 115.
9. R. H. Crabtree and D. G. Hamilton, *J. Am. Chem. Soc.*, 1986, **108**, 3124.
10. U. Matteoli, G. Menchi, M. Bianchi and F. Piacenti, *J. Mol. Catal.*, 1988, **44**, 347.
11. U. Matteoli, G. Menchi and F. Piacenti, *J. Organomet. Chem.*, 1986, **299**, 233.
12. U. Matteoli, G. Menchi, M. Bianchi and F. Piacenti, *J. Mol. Catal.*, 1991, **64**, 257.
13. U. Matteoli, G. Menchi, M. Bianchi, F. Piacenti, S. Ianelli and M. Nardelli, *J. Organomet. Chem.*, 1995, **498**, 177.
14. Y. Hara and K. Wada, *Chem. Soc. Jpn., Chem. Lett.*, 1991, 553.
15. J. E. Lyons, *J.C.S. Chem Commun.*, 1975, 412.
16. T. Ikariya, K. Osakada, Y. Ishii, S. Osawa, M. Saburi and S. Yoshikawa, *Bull. Chem. Soc. Jpn.*, 1984, **57**, 897.
17. M. Bianchi, G. Menchi, F. Francalanci, F. Piacenti, U. Matteoli, P Frediani and C. Botteghi, *J. Organomet. Chem.*, 1980, **188**, 109.
18. Y. Hara, H. Inagasaki, S. Nishimura and K. Wada, *Chem. Soc. Jpn., Chem. Lett.*, 1992, 1983.

19. H. Inagasaki, S. Nishimura, Y. Hara and K. Wada, *Science and Technology in Catalysis 1994*, 1995, 327.
20. P. Frediani, M. Bianchi, A. Salvini, R. Guarducci, L. C. Carluccio and F. Piacenti, *J. Organomet. Chem.*, 1995, **498**, 187.
21. P. E. Garrou, *Chem. Rev.*, 1985, **85**, 171.
22. A. Togni and L. M. Venanzi, *Angew. Chem., Int. Edn. Engl.*, 1994, **33**, 497.
23. A. Salvini, P. Frediani, M. Bianchi, F. Piacenti, L. Pistolesi and L. Rosi, *J. Organomet. Chem.*, 1999, **582**, 218.
24. H. T. Teunissen and C. J. Elsevier, *J.C.S. Chem Commun.*, 1998, 1367.
25. H. T. Teunissen and C. J. Elsevier, *J.C.S. Chem Commun.*, 1997, 667.
26. K-L. Na, S. Huh, K-M. Sung and M-J. Jun, *Polyhedron*, 1996, Vol. 15, **11**, 1841.
27. U. Matteoli, M. Bianchi, G. Menchi, P. Frediani and F. Piacenti, *J. Mol. Catal.*, 1984, **22**, 353.
28. J. Otera, *Chem. Rev.*, 1993, **93**, 1449.
29. H. Carmichael, *Chemistry in Britain*, Vol. 36, **1**, 36.
30. *Catalyst Handbook*, ed. M. V. Twigg, Manson Publishing Ltd., Frome, 2cnd edn., 1996.
31. M. A. Fox and J. K. Whitesell, *Organic Chemistry*, Jones and Bartlett Publishers International, London, 1994.
32. D. C. Harris, *Quantitative Chemical Analysis*, W. H. Freeman and Co., New York, 4th edn., 1995.
33. G. L. Gregory and M. G. Bradley, *Inorg. Chem.*, 1977, Vol. 16, **4**, 744.
34. L. H. Pignolet (Ed), *Homogeneous Catalysis with Metal Phosphine Complexes*, Plenum Press, New York, 1983.
35. E. W. Abel, F. G. A. Stone and G. Wilkinson, *Comprehensive Organometallic Chemistry*, Pergamon Press, Oxford, 1987, Vol. 4.
36. R. H. Crabtree, *The Organometallic Chemistry of the Transition Metals*, John Wiley & Sons, New York, 2nd edn., 1994.
37. R. Bau, R. G. Teller, S. W. Kirtley and T. F. Koetzle, *Acct. Chem. Res.*, 1979, **12**, 176.
38. J. A. Iggo, *NMR Spectroscopy in Inorganic Chemistry*, Oxford University Press, Oxford, 1999.
39. G. O Spessard and G. L . Miessler, *Organometallic Chemistry*, Prentice-Hall International (UK) Ltd., London, 1997.
40. Ch. Elschenbroich and A. Salzer, *Organometallics a Concise Introduction*, VCH Publishers Inc., New York, 2nd edn., 1992.
41. D. M. Adams, *Metal-Ligand and Related Vibrations*, Edward Arnold (Publishers) Ltd., London, 1967.
42. W. O. Siegl, S. J. Lapporte and J. P. Collman, *Inorg. Chem.*, 1973, Vol. 12, **3**, 674.

Chapter 3

Catalyst Deactivation

The primary alcohol products obtained from the hydrogenation of esters deactivate the homogeneous ruthenium-triphosphine catalyst (generated in-situ from $Ru(acac)_3$ and Triphos). The primary alcohol is dehydrogenated to an aldehyde, which is subsequently decarbonylated stoichiometrically to produce [$Ru(Triphos)H_2(CO)$] and the respective alkane.

3.1 Introduction

The irreversible removal of CO from organic molecules is possible with transition metal reagents. The decarbonylation of primary alcohols and aldehydes can be achieved both catalyticaly and stoichiometrically, proceeding via an acyl intermediate species.[1] The processes are sequential, since the initial stage in decarbonylation of a primary alcohol requires dehydrogenation to the analogous aldehyde, which subsequently decarbonylates (see Equation 3.1). [2, 3] Industrially the reaction is achieved by the use of a metal centre, either for example a metal particle on a support or a metal centre in a complex, which is easily reduced.[4]

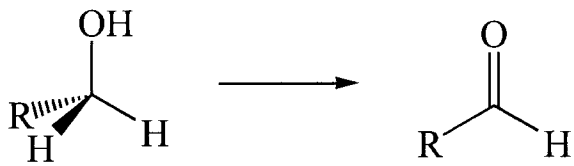

Equation 3.1

The accepted mechanism for the aldehyde decarbonylation [5, 6] proceeds via the oxidative addition of the aldehyde to an unsaturated metal, the aldehyde then undergoes the reverse of carbonyl insertion with migration of the alkyl group to the metal, which is then followed by reductive elimination of an alkane (see Equation 3.2).

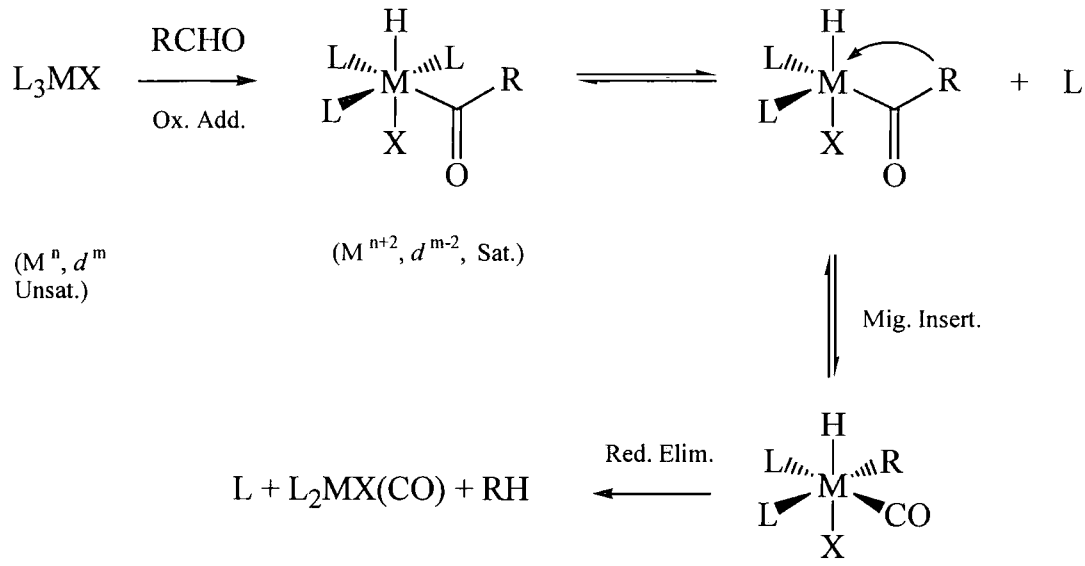

Equation 3.2

Note: L = PR_3, X = H or a halide.

A most efficient decarbonylation reagent is $[RhCl(PPh_3)_3]$, Wilkinson's hydrogenation catalyst, but it is not a catalyst for decarbonylation, as the product $[RhCl(CO)(PPh_3)_3]$, is unreactive due to its inability to co-ordinate further aldehyde.[7] $[RhCl(PPh_3)_3]$ is therefore regarded, as a stoichiometric decarbonylation reagent.

3.1.1 Ruthenium Catalysed Decarbonylation

The decarbonylation of oxygen-containing solvents (frequently alcohols) is used as a synthetic route to several hydrido/halido-carbonyl ruthenium complexes.[8] Chatt *et al* reported [9] that the complex $[RuH(CO)Cl(PEt_2Ph)_3]$ could be obtained from reacting the $[Ru_2Cl_3(PEt_2Ph)_6]Cl$ salt with ethanol and potassium hydroxide. They suggested that the first step is for an ethoxide-ruthenium complex to be formed, followed by the transfer of a hydride to the ruthenium to create an acetaldehyde complex, which then decomposed, possibly via an isocarbonyl complex (instead of acetaldehyde elimination), to produce the ruthenium-carbonyl complex and methane (see Equation 3.3).

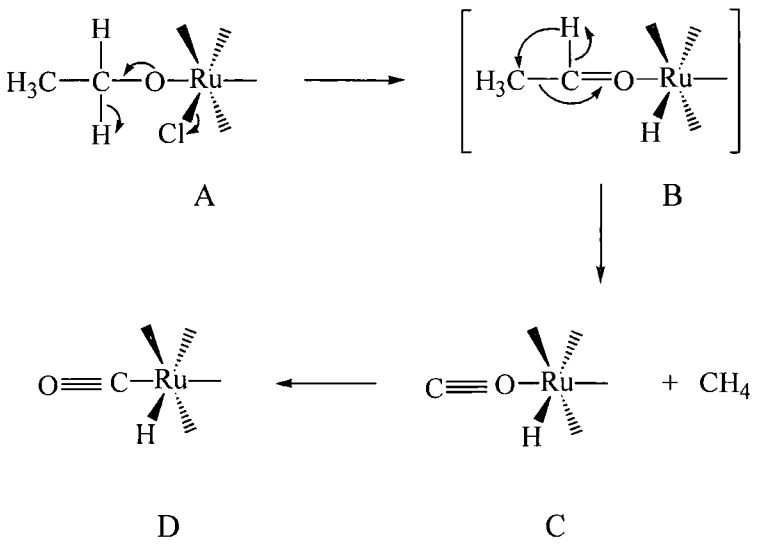

Equation 3.3

A: Ruthenium-ethoxide complex
B: Ruthenium-acetaldehyde complex.
C: Ruthenium-isocarbonyl complex.
D: Ruthenium-carbonyl complex.

The ability of ruthenium to remove CO from organic molecules is demonstrated by the synthesis of a variety of mono-ruthenium carbonyl complexes. The complexes $[RuCl_2(CO)(PPh_3)_3]$, $[RuHCl(CO)(PPh_3)_3]$, $[RuH_2(CO)(PPh_3)_3]$, $[Ru(CO)_3(PPh_3)_3]$, $[Ru(CO)_3(P(C_6H_4\text{-}p\text{-}CH_3)_3)_2]$ and $[Ru(CO)_3(P(C_6H_4\text{-}p\text{-}OCH_3)_3)_2]$ can be synthesised by tailoring the reaction of the hydrated $RuCl_3$ decarbonylation of aqueous formaldehyde, in a boiling solution of the relevant phosphine in ethanol. [10, 11] The $[RuH_2(\eta^2\text{-}H_2)(PPh_3)_3]$ complex was found to decarbonylate the alcohols methanol, ethanol, 1-propanol and benzyl alcohol to form $[RuH_2(CO)(PPh_3)_3]$. [12]

Grey *et al* [13], whilst investigating ester hydrogenation, found that the catalysts $K^+[(Ph_3P)_2Ph_2PC_6H_4RuH_2]^-\cdot C_{10}H_8\cdot(C_2H_5)_2O$ and $K_2^+[(Ph_3P)_3(Ph_2P)Ru_2H_4]^{2-}\cdot 2C_6H_{14}O_3$ decarbonylated formate esters to carbon monoxide and the corresponding alcohols. The decarbonylation and catalyst deactivation were stoichiometric, as the reaction ceased when the catalyst was precipitated as a white solid. Analysis of the solid indicated the presence of metal carbonyls.

3.1.2 Ruthenium Catalysed Aldehyde Reduction

The use of homogeneous ruthenium catalysts for the reduction of aldehydes to alcohols has been reported, [13, 14, 15] The aldehyde reduction is frequently accompanied by some level of decarbonylation product being obtained. Ito *et al* [16] found that hydridoruthenium complexes, such as $[RuH_2(PPh_3)_4]$, will catalyse aldehyde conversion to esters (see Equation 3.4).

$$2\ Pr^nCHO \longrightarrow Pr^nCOOBu^n$$

Equation 3.4

The conversion of the $[RuH_2(PPh_3)_4]$ catalyst to $[Ru\ H_2(CO)(PPh_3)_2]$ during the reaction, showed that aldehyde decarbonylation had also taken place. Sánchez-Delgado *et al* [17] discovered that after the aldehyde hydrogenation, the catalysts $[RuCl_2(PPh_3)_3]$ and $[RuHCl(PPh_3)_3]$ were recovered as their respective carbonyl containing species, indicating that aldehyde decarbonylation had also occurred during the reaction, although the formation of the carbonyl species was not found to be detrimental to the catalytic activity. The ruthenium catalysed conversion of cinnamaldehyde ($C_6H_5(CH)_2CHO$) to 3-phenylpropionic acid, with the catalyst $[RuH_2(PPh_3)_4]$ and a catalyst generated *in situ* from $RuCl_3/PCy_3$, was reported by De Vries *et al* [18] as being susceptible to decarbonylation of the aldehyde. Murahashi *et al* discovered that although the ruthenium catalysts $[RuH_2(PPh_3)_4]$ and $[RuH_2(CO)(PPh_3)_3]$ will catalyse the transformation of alcohols and aldehydes to esters and lactones, the decarbonylation of aldehyde intermediates is also obtained. [19]

3.1.3 Ruthenium Catalysed Transfer Hydrogenation

Ruthenium catalysts have been found to be capable of promoting transfer hydrogenation. Sasson and Blum [20] discovered that the ruthenium complex $[RuCl_2(PPh_3)_3]$ could promote hydrogen transfer from alcohols, hydrocarbons, aldehydes, acids and amides. The advantages of transfer hydrogenation in organic synthesis, where hydrogen is transferred from one organic molecule to another, is the avoidance of the associated handling problems of molecular hydrogen and that a

homogeneous catalyst focuses and increases the local concentration of the reductant. The capacity of ruthenium complexes to dehydrogenate alcohols has been used for transfer hydrogenation reactions, in particular that involving ketones. The work of Bäckvall *et al* [21, 22, 23] investigated the ruthenium-catalysed transfer hydrogenation of ketones by alcohols. They found that secondary alcohols were more suitable than primary alcohols for transfer hydrogenation, as they are not susceptible to decarbonylation. The aldehyde formed from dehydrogenation of a primary alcohol deactivates the catalyst by undergoing decarbonylation. The ruthenium catalysed dehydrogenation of unsymmetrical α,ω-diols to produce lactones, by using an α,β-unsaturated ketone as the hydrogen acceptor was reported by Ishii *et al.* [24] The diol is dehydrogenated by a ruthenium catalyst of the form $[RuH_2(PR_3)_4]$ (R= PPh_3, $PMePh_2$, PMe_2Ph, $PHPh_2$) and the hydrogen transferred to the ketone acceptor.

The dehydrogenation of methanol was investigated, as the product of the dehydrogenation is free of water (which is produced with the oxidative dehydrogenation using O_2), and therefore will not be susceptible to solution gelation. Shinoda *et al* [25] reported that methanol dehydrogenation can be achieved by the catalysts $[Ru_2(OAc)_4Cl]$ with a *tertiary*-phosphine (PPh_3 or $PEtPh_2$) or $[Ru(OAc)Cl(PR_3)]$, whilst Smith and Maitlis [26] demonstrated that $[RuCl_2(PPh_3)_3]$ was also suitable. Morton and Cole-Hamilton [27] found that the complex $[RuH_2(N_2)(PPh_3)_3]$, catalysed the dehydrogenation of a range of alcohols tested, including diols and a triol as well as primary alcohols. A mechanism proposed for the dehydrogenation (see Fig. 1), suggested that the active catalyst is formed by the loss of N_2 from $[RuH_2(N_2)(PPh_3)_3]$, to allow an alkoxide complex to be formed. Morton and Cole-Hamilton reported that a base, such as NaOH, was required for the reaction to enable a more nucleophilic alkoxide ion to be generated, which would then rapidly attack the ruthenium dehydrogenation catalyst. Loss of aldehyde produces $[RuH_3(PPh_3)_3]^-$ which is then easily protonated to the $[RuH_2(H_2)(PPh_3)_3]$ complex, from which the labile H_2 leaves to reproduce the active catalyst. The decarbonylation product $[RuH_2(CO)(PPh_3)_3]$ was observed in the products of the dehydrogenation of ethanol and butanol.

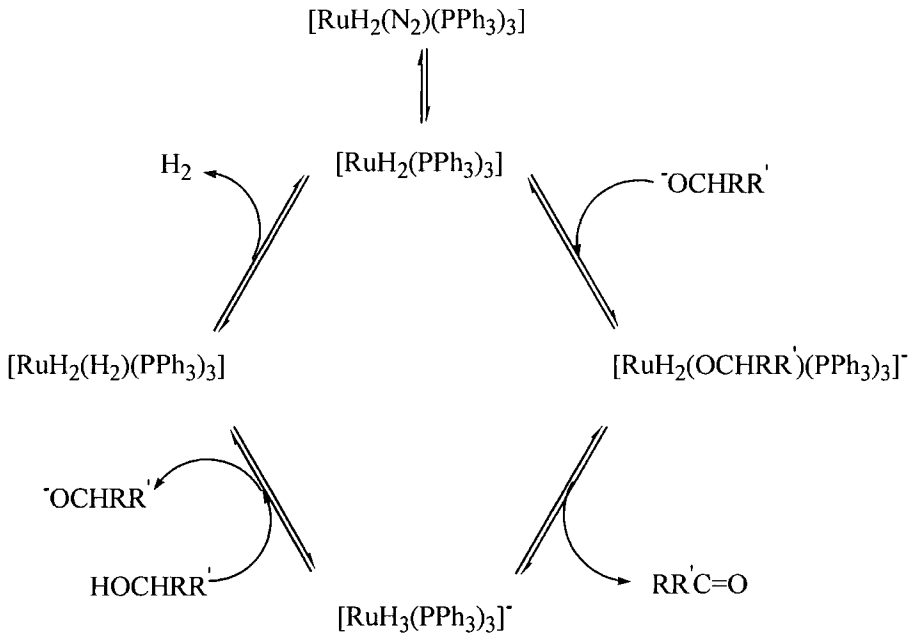

Figure 1 Mechanism for alcohol dehydrogenation by $[RuH_2(N_2)(PPh_3)_3]$ [27]

3.1.4 Summary

The decarbonylation of alcohols and aldehydes can be achieved with transition metals. Ruthenium-phosphine complexes are particularly effective at CO extraction from organic molecules, the property being used as a synthetic route to many mono-ruthenium carbonyl complexes. The synthesis proceeds by dehydrogenation of a primary alcohol by the ruthenium complex and the subsequent decarbonylation of the resultant aldehyde.

The ability of ruthenium-phosphine complexes to remove hydrogen from alcohols has led to the development of a variety of complexes for transfer hydrogenation. To avoid stoichiometric deactivation of the ruthenium catalyst as a result of decarbonylation, secondary alcohols such as iPA (which forms acetone) are used.

The deactivation of ruthenium catalysts, used for the hydrogenation of aldehydes and esters, occurs as a result of direct substrate decarbonylation or as a result of dehydrogenation of alcohol products, followed by decarbonylation of the corresponding aldehyde.

3.2 Results and discussion

The products of the hydrogenation of esters (see Chapter 2) with the catalyst generated *in situ* from $Ru(acac)_3$ and Triphos included the pale yellow solid [$Ru(Triphos)H_2(CO)$], which was obtained from the decarbonylation of the dehydrogenated primary alcohol product of the ester hydrogenation. The low level of ester conversion obtained when the primary alcohol methanol was used as a solvent, rather than iPA (see Chapter 2, Influence of Solvents), demonstrates the susceptibility of the catalytic system to deactivation by decarbonylation. The ester hydrogenations carried out in solvents that do not decarbonylate, produce, in addition to the solid [$Ru(Triphos)H_2(CO)$], organic decarbonylation products (see Chapter 2, Hydrogenation of Esters). For example, the products of the hydrogenation of benzyl benzoate contained traces of benzene and benzaldehyde from benzyl alcohol decarbonylation, the hydrogenation of dimethyl maleate included traces of 1-propanol from partial decarbonylation of 1,4-butanediol, and in the hydrogenation of methyl dodecanoate a small amount of undecane from 1-dodecanol decarbonylation was obtained in the products.

The hydrogenation of methyl propanoate with the solid [$Ru(Triphos)H_2(CO)$] was attempted. The reaction used [$Ru(Triphos)H_2(CO)$] obtained from previous hydrogenations, and was carried out under the conditions used to investigate ester hydrogenations, with iPA as the solvent at 120°C with 6.8MPa of H_2 for 16 hours. The result was a low level of ester conversion, that is probably attributed to the free Triphos (observed) and a small amount of uncoordinated $Ru(acac)_3$ in the [$Ru(Triphos)H_2(CO)$] starting material or to a low level of CO liberation from the [$Ru(Triphos)H_2(CO)$]. The ^{31}P NMR of both the product solution and solid obtained at the end of the reaction were identical to those previously obtained for ester hydrogenation. The level of methyl propanoate hydrogenation with the solid [$Ru(Triphos)H_2(CO)$] was so low, that the [$Ru(Triphos)H_2(CO)$] is considered to be catalyticaly inactive.

3.2.1 Reaction of Alcohols with $Ru(acac)_3$ and Triphos

The decarbonylation of primary alcohols was investigated by using the reaction conditions for the catalytic hydrogenation of esters, but with the ester replaced by the alcohol under study (see Table 3.1). The solid [$Ru(Triphos)H_2(CO)$] was obtained when

the ester was replaced with the alcohols methanol, 1-propanol, 1-dodecanol and 1,4-butanediol. The ^{31}P NMR of the product solutions from the reactions with methanol, 1-propanol, 1-dodecanol and 1,4-butanediol were similar to those for the hydrogenation of aliphatic esters (see Chapter 2, Product Solution ^{31}P NMR data), comprising only of singlets in approximately the same corresponding positions. $^{31}P\{^{1}H\}$NMR (25°C, chloroform-*d*): δ41.6 (**3P**, s), 28.0 (**3P**, s), 27.5 (**3P**, s), -27.7 (**3P**, s) ppm. Only the singlet at δ –27.7 ppm can be assigned (to free Triphos) all the other signals being unassigned due to lack of data. The ^{31}P NMR's of the product solutions of the reactions with iPA and ^{t}BuOH were the same as those detailed in Chapter 2, with the Product Solution ^{31}P NMR indicating the presence of species of the form $[Ru(\eta^2\text{-Triphos})H_2L_2]$ and $[Ru(\eta^2\text{-Triphos})_2H_2]$.

Table 3.1 Alcohols Investigated for Decarbonylation

Solvent [a]	Alcohol Investigated [b]
iPA	Methanol
^{t}BuOH	Methanol
iPA	1-Propanol
iPA	1-Dodecanol
iPA	1,4-Butanediol
iPA	iPA [c]
^{t}BuOH	^{t}BuOH [c]

Conditions: 120°C, $p(H_2)$ = 6.8 MPa, 16 hours.
a: 50.0 ml.
b: 20.0 ml.
c: No additional alcohol added, reaction solution = 50.0 ml in total.

The primary alcohols methanol and 1-propanol both produced the solid $[Ru(Triphos)H_2(CO)]$, but analysis of their respective product solutions by GC and GCMS did not detect any trace of aldehyde or alkane. The lack of alkane is not surprising as both are volatile gases, and would have been vented in the headspace gas with depressurisation of the autoclave, on completion of the reaction (as would any formaldehyde produced). The lack of aldehyde from the 1-propanol reaction (propanal is a liquid at r.t.), suggests that it is probably immediately decarbonylated when formed, and little or none of it is released into the reaction medium on dehydrogenation of the alcohol. The reaction with 1-dodecanol also produced the solid $[Ru(Triphos)H_2(CO)]$. Analysis of the product solution by GCMS detected a small amount of undecane and a

trace of dodecanal. The presence of the undecane after the reaction with 1-dodecanol, confirms that the carbonyl in the solid [Ru(Triphos)H_2(CO)] comes from the alcohol. The trace of dodecanal detected on completion of the reaction with 1-dodecanol, supports the proposal that alcohol dehydrogenation followed by aldehyde decarbonylation is the source of the carbonyl found in the solid [Ru(Triphos)H_2(CO)].

The reaction with the diol 1,4-butanediol also produced the solid [Ru(Triphos)H_2(CO)]. No trace of any other decarbonylation products was detected in the product solution. The product solution did contain a small amount of γ-butyrolactone, which is a product of the dehydrogenation of 1,4-butanediol. The lack of any decarbonylation products other than the [Ru(Triphos)H_2(CO)] and the presence of the dehydrogenation product γ-butyrolactone, indicate that the product of the diol dehydrogenation does not necessarily undergo immediate decarbonylation, but may undergo cyclisation.

The reactions with only the solvent (iPA or ^{t}BuOH) present and no additional alcohol did not produce the solid [Ru(Triphos)H_2(CO)]. A solid was obtained, but the analysis indicated that the products were of the form [Ru(η^2-Triphos)H_2L_2] and [Ru(η^2-Triphos)$_2H_2$] (see Chapter 2, Product Solution ^{31}P NMR). The decarbonylation of iPA and ^{t}BuOH by the catalyst did not occur, although traces of acetone in the product solutions indicated that some iPA was dehydrogenated.

3.2.2 Reaction of Aldehydes with Ru(acac)$_3$ and Triphos

The decarbonylation of aldehydes was investigated by using the reaction conditions for the catalytic hydrogenation of esters, but with the ester replaced by the aldehyde under study. The solid [Ru(Triphos)H_2(CO)] was obtained when the ester was replaced with the aldehydes propanal and dodecanal. The reactions with propanal and dodecanal both resulted in the aldehydes being hydrogenated to their respective primary alcohols, 1-propanol and 1-dodecanol. The ^{31}P NMR of the product solutions were similar to those for the hydrogenation of aliphatic esters (see Chapter 2, Product Solution ^{31}P NMR data), comprising of only singlets in approximately the same positions. ^{31}P{^{1}H}NMR (25°C, chloroform-*d*): δ 42.0 (**3P**, s), 28.5 (**3P**, s), 27.7 (**3P**, s), -27.7 (**3P**, s) ppm. Only the singlet at δ –27.7 ppm can be assigned (as free Triphos) with confidence, all the other signals being unassigned due to lack of further data.

The reaction with propanal resulted in 100% conversion. The product solution contained predominantly 1-propanol with a small amount of propyl propanoate. The ester, propyl propanoate, was probably produced by the dehydrogenation of a hemiacetal. Hemiacetals are produced by the addition of a nucleophilic alcohol molecule to the carbonyl group of an aldehyde (or ketone).[28] The dissolving of an aldehyde in an alcohol produces an equilibrium between the alcohol and the aldehyde and forms a hemiacetal (see Fig. 3.2).[4] Hemiacetals are usually unstable, and rarely isolated, and it is therefore possible that the ruthenium catalyst could dehydrogenate the hemiacetal in the same way that it does an alcohol (see Equation 3.3). This would result in an ester being produced (see Fig. 3.3). The dehydrogenation of the hemiacetal that would be produced from propanal and 1-propanol would result in the ester propyl propanoate observed in the product solution (see Fig. 3.3).

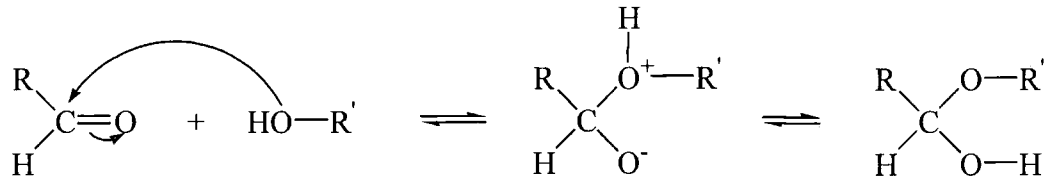

Figure 3.2 Mechanism for Hemiacetal Formation

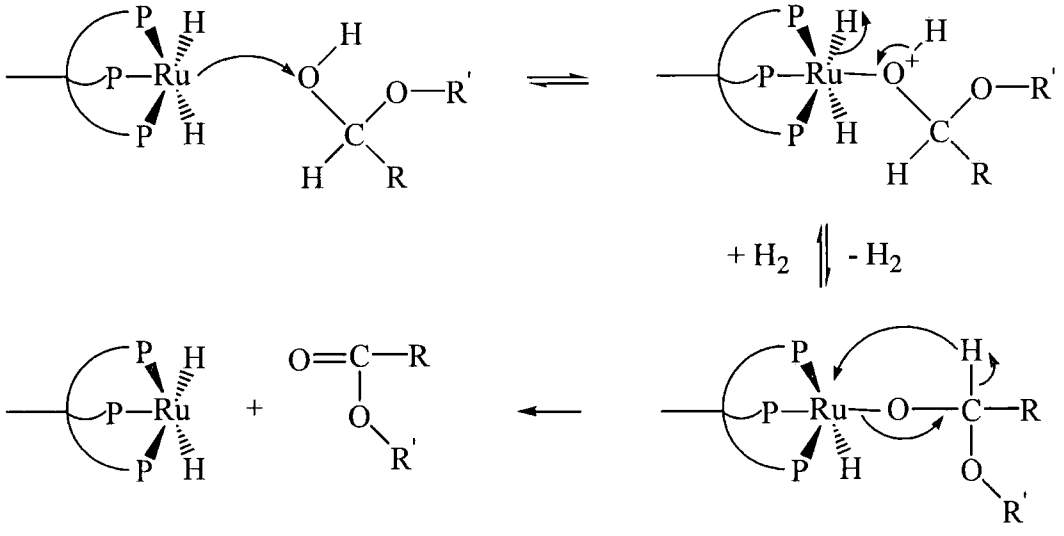

Figure 3.3 Hemiacetal Dehydrogenation

The reaction with dodecanal also resulted in 100% aldehyde conversion. The major product detected was 1-dodecanol, with a small amount of undecane, the decarbonylation product. The undecane and the solid [Ru(Triphos)H_2(CO)] indicate that decarbonylation has occurred. The analysis of the product solution did not detect the ester dodecyl dodecanoate, the analogous ester to that detected in the propanal experiment.

The presence of the solid [Ru(Triphos)H_2(CO)] in both reactions products, and undecane in the dodecanal reaction, indicates decarbonylation had occurred.

3.2.3 Influence of Additives on Ester Conversion

The level of ester conversion obtained was reduced when additives, which provided a more readily available source of CO, were included in the reaction. The hydrogenation of methyl dodecanoate by the catalytic system of $Ru(acac)_3$ and Triphos in iPA was used as the model, for the investigation. The additives selected were the alcohol 1,4-butanediol, the aldehyde propanal and carbon monoxide (see Table 3.2).

Table 3.2 Influence of additives on methyl dodecanoate hydrogenation

Additive	Methyl Dodecanoate Conversion (%)
None	49.0
CO	1.0
1,4-butanediol	24.3
Propionaldehyde	34.0

Conditions: 120°C, $p(H_2)$ = 6.8 MPa, 16 hours.

As can be seen from the results detailed in Table 3.2, the level of methyl dodecanoate conversion decreased on inclusion of the additives. The pale yellow solid [Ru(Triphos)H_2(CO)] was obtained on completion of each reaction.

The lowest level of conversion was obtained with the addition of CO. The analysis of the product solution found that a very small amount of hydrogenation had taken place. The ^{31}P NMR spectrum of the product solution was a complicated spectrum containing several different species, the majority of which had not been seen in the ^{31}P NMR spectrum of previous ester hydrogenations (see Chapter 2, Product Solution ^{31}P NMR

data), or the ^{31}P NMR spectra of the alcohol and aldehyde investigations (see 3.2.1 and 3.2.2). $^{31}P\{^{1}H\}$NMR (25°C, chloroform-*d*): δ 47.3 (**P**, dd, $^{2}J_{P\text{-}P}$ = 40 Hz and 19 Hz), 35.2 (**3P**, s), 30.3 (**2P**, d, $^{2}J_{P\text{-}P}$ = 38.1 Hz), 28.6 (**3P**, s), 27.8 (**3P**, s), 25.3 (**2P**, d, $^{2}J_{P\text{-}P}$ = 38.9 Hz), 18.3 (**P**, dd, $^{2}J_{P\text{-}P}$ = 40 Hz and 28 Hz), 2.9 (**P**, dd, $^{2}J_{P\text{-}P}$ = 28 Hz and 19 Hz), 2.6 (**P**, t, $^{2}J_{P\text{-}P}$ = 38.9 Hz), -5.5 (**P**, t, $^{2}J_{P\text{-}P}$ = 38.1 Hz), -27.7 (**3P**, s), ppm. A ^{1}H NMR study of the hydride region did not detect a signal representing the presence of a metal hydride. The ^{31}P NMR multiplet signals indicate that the possible species are of the form [Ru(Triphos)LX_2] or [Ru(Triphos)L_2] for the two doublet-triplet combinations and [Ru(Triphos)LXX'] for the three doublets of doublets. The absence of further data means no further assignment can be made.

The addition of 1,4-butanediol resulted in a lower level of ester conversion than when the propionaldehyde was added. This appears to contradict the rationale that the catalyst is deactivated by the aldehyde obtained from dehydrogenation of a primary alcohol. The analysis of the product solutions of ester hydrogenations has shown that aldehydes are not usually detected, but when they are present, only in trace quantities (see Chapter 2, Hydrogenation of Esters). The replacement of the ester with an aldehyde (see 3.2.2) for the hydrogenation, resulted in 100% conversion to the corresponding alcohol. The presence of the solid [Ru(Triphos)H_2(CO)] on completion of the aldehyde reaction indicates that decarbonylation has also occurred. The lack of aldehyde and the presence of the corresponding alcohol with the solid [Ru(Triphos)H_2(CO)] indicates that the route to catalyst deactivation is not directly from the aldehyde, but via the alcohol. The reason for this could be that the catalyst deactivation is as a result of alcohol dehydrogenation and decarbonylation occurring consecutively, as part of the alcohol co-ordination, as per the mechanism proposed by Chatt *et al* [9] (see Equation 3.3). The aldehyde is not eliminated from the complex but decarbonylated immediately after the dehydrogenation of the alcohol, which is then followed by alkane elimination. This could be because aldehyde co-ordinates to the ruthenium catalyst differently for hydrogenation, than it does for decarbonylation, and that it is only when the aldehyde is co-ordinated to the ruthenium catalyst as a result of alcohol dehydrogenation, that the orientation of its co-ordination allows decarbonylation. The alcohol dehydrogenation proceeds via co-ordination to the ruthenium complex by the oxygen atom, and aldehyde hydrogenation proceeding via co-ordination of the carbonyl to the ruthenium complex (see Fig 3.4). Cornils and Herrmann [29] suggested that the ruthenium catalyst [RuH_2P_4] (where P = water soluble phosphines such as TPPTS and mSP$ø_2$) co-ordinated

aldehydes *via* the carbonyl in an agostic intermediate involving both the carbonyl and the oxygen, with direct nucleophilic attack of one of the hydrides on the carbonyl oxygen producing the alcohol.

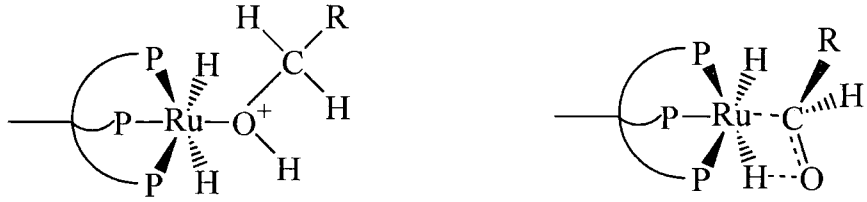

A B

Figure 3.4 Proposed method of Alcohol and Aldehyde co-ordination to the Ruthenium Catalytic Complex

A: Alcohol co-ordination through the oxygen atom.
B: Aldehyde co-ordination through an agostic intermediate with the carbonyl.

This would mean that the aldehyde has to be hydrogenated to an alcohol before the deactivation process can begin. The alcohol 1,4-butanediol would therefore initiate catalyst deactivation sooner than the aldehyde propanal, which would result in a lower level of ester hydrogenation occurring as the alcohol is able to undergo decarbonylation sooner than the aldehyde. The earlier catalyst deactivation by the alcohol, would reduce the available catalyst for the hydrogenation sooner than with the aldehyde, which would therefore result in a lower level of substrate conversion.

The requirement for aldehyde to be hydrogenated to the corresponding alcohol (see Fig.3.5), and the alcohol dehydrogenation and subsequent consecutive decarbonylation (see Fig. 3.6) explains the almost total lack of aldehyde observed in the product solutions of the different hydrogenation reactions and the lower level of ester hydrogenation achieved with the alcohol additive.

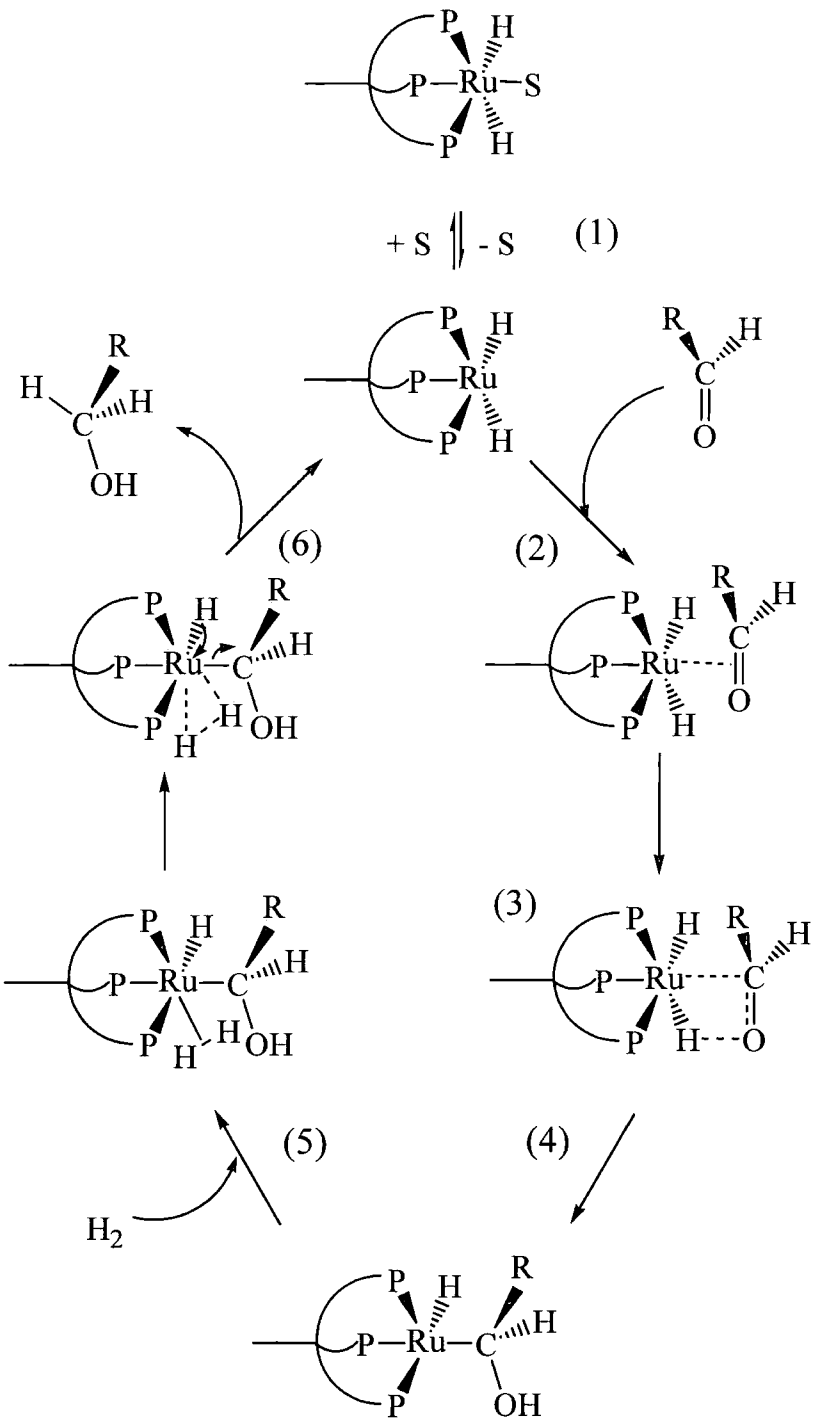

Figure 3.5 Proposed Aldehyde Hydrogenation by the Ruthenium Catalyst

(1) Dissociation of labile ligand, S, to form the 16 electron unsaturated catalytic species [Ru(Triphos)H_2] (S= Solvent or H_2).
(2) Co-ordination of aldehyde to the vacant co-ordination site on ruthenium, possibly via (3).
(3) Agostic intermediate.
(4) Hydride Transfer.
(5) Co-ordination of H_2, possibly simultaneously with (4) and (6).
(6) Loss of alcohol (RCH_2OH) and oxidative addition of H_2 to reproduce the catalytic species [Ru(Triphos)H_2].

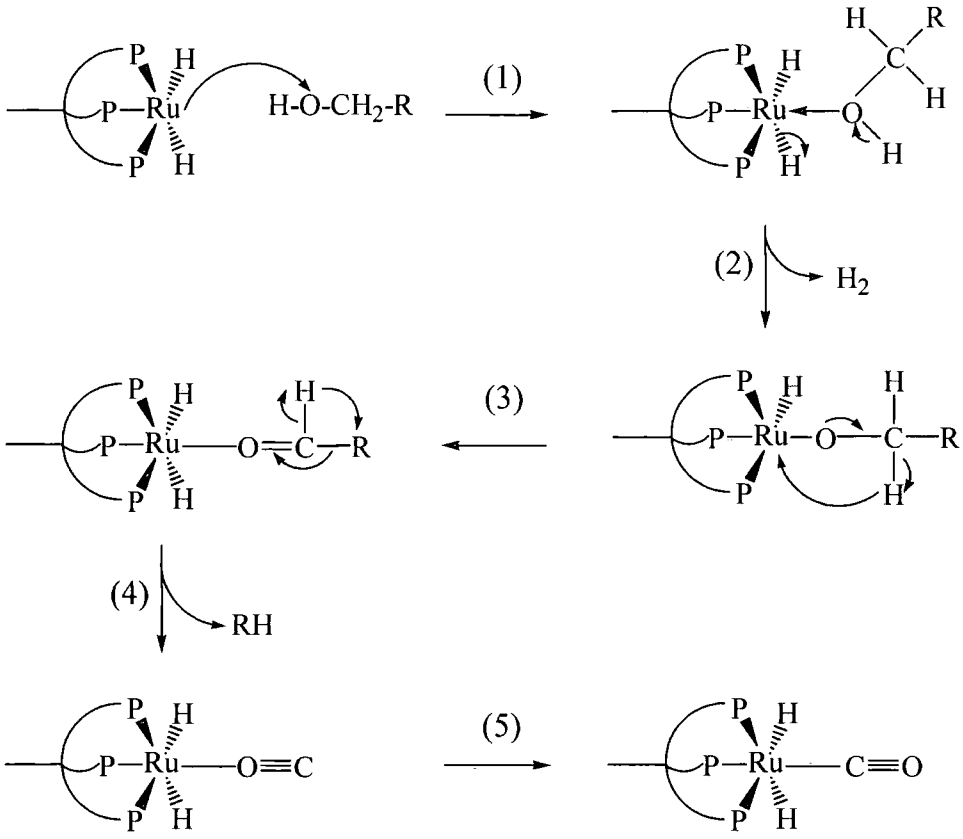

Figure 3.6 Proposed Alcohol Dehydrogenation and Decarbonylation by the Ruthenium Catalyst

(1) Co-ordination of alcohol to 16 electron unsaturated [Ru(Triphos)H_2(CO)].
(2) Loss of H_2 to form ruthenium-ethoxide complex.
(3) Hydride transfer to ruthenium.
(4) Elimination of alkane from ethoxide decomposition (possibly via an isocarbonyl complex).
(5) [Ru(Triphos)H_2(CO)] formed.

3.2.4 Conclusion

The catalyst generated from the $Ru(acac)_3$ and Triphos in iPA is susceptible to decarbonylation of primary alcohols, to form [Ru(Triphos)H_2(CO)], in the same way as related ruthenium-phosphine complexes. The mechanism probably proceeds by dehydrogenation of the primary alcohol to a co-ordinated aldehyde, which is decarbonylated not eliminated, to form a metal carbonyl complex and alkane which is eliminated.

The decarbonylation reaction is stoichiometric and therefore the overall result is that the co-ordinated carbonyl results in the catalyst being deactivated for ester hydrogenation, as the necessary vacant co-ordination site is occupied by carbon monoxide, a non labile ligand.

3.3 Experimental

3.3.1 Hydrogenations

All hydrogenations were carried out using a 300-ml Hasteloy^{TM} autoclave equipped with overhead stirrer. The autoclave was loaded with the $Ru(acac)_3$, Triphos (see Table 3.3), and the air removed by three cycles of vacuum action followed by refilling with argon. The selected solvent and substrate (see Table 3.3) were purged under argon for 1 hour, and then added to the autoclave by canula. The autoclave was then pressurised at r.t. with hydrogen (4.4 MPa). The autoclave was then heated to 120°C, at which the hydrogen mass flow controller would be set to 6.8 MPa, and then heated and stirred for 16 hours. On completion of the reaction period the heating was stopped and the autoclave allowed to slowly cool, over 2 hours. The headspace gases within the autoclave were slowly vented and the products removed. The product solution was analysed by GC, GCMS and NMR spectroscopy. The product solid was analysed by ^{31}P NMR spectroscopy, and on selected samples by ^{1}H NMR spectroscopy, IR, and elemental analysis.

Table 3.3 Quantity of Reagents used

Reagent	Quantity
$Ru(acac)_3$	4.5×10^{-4} mol
Triphos	6.1×10^{-4} mol
Solvent [a]	50.0 ml
Substrate [b]	20.0 ml [c]
Additive [d]	5.0 ml
CO	0.4 MPa

a: iPA or ^{t}BuOH.
b: Ester, alcohol or aldehyde.
c: Nil, when iPA or ^{t}BuOH investigated.
d: Propanal or 1,4-butanediol.

3.3.2 NMR Spectroscopy

The NMR spectra of the product solutions were measured against an external reference of chloroform-*d* containing Triphos, which was used to lock and shim the NMR spectrometer. The product solids were dissolved in the appropriate *deuterated* solvent and the NMR spectrometer locked and shimmed accordingly, prior to recording the spectrum.

3.4 References

1. F. A. Cotton and G. Wilkinson, *Advanced Inorganic Chemistry*, John Wiley & Sons, Chichester, 5th edn., 1988.
2. M. A. Fox and J. K. Whitesell, *Organic Chemistry*, Jones and Bartlett Publishers International, London, 1994.
3. H. Beyer and W. Walter, *Handbook of Organic Chemistry*, Simon and Schuster International Group, Hemel Hempstead, 1996.
4. T. W. G. Solomons, *Fundamentals of Organic Chemistry*, John Wiley & Sons, Chichester, 5th edn., 1997.
5. L. S. Hegedus, *Transition Metals in the Synthesis of Complex Organic Molecules*, University Science Books, Mill Valley, California, 1994.
6. G. W. Parshall and S. D. Ittel, *Homogeneous Catalysis*, John Wiley & Sons, Chichester, 2nd edn., 1992.
7. R. H. Crabtree, *The Organometallic Chemistry of the Transition Metals*, John Wiley & Sons, New York, 2nd edn., 1994.
8. E. W. Abel, F. G. A. Stone and G. Wilkinson, *Comprehensive Organometallic Chemistry*, Pergamon Press, Oxford, 1987, Vol. 4.
9. J. Chatt, B. L. Shaw and A. E. Field, *J. Chem. Soc.*, 1964, 3466.
10. N. Ahmad, S. D. Robinson and M. F. Uttley, *J. Chem. Soc., Dalton Trans.*, 1972, 843.
11. N. Ahmad, J. J. Levison, S. D. Robinson and M. F. Uttley, *Inorg. Synth.*, 1974, **15**, 45.
12. L. S. Van Der Sluys, G. J. Kubas and K. G. Caulton, *Organometallics*, 1991, **10**, 1033.
13. R. A. Grey, G. P. Pez and A. Wallo, *J. Am. Chem. Soc.*, 1981, **103**, 7536.
14. J. Tsuji and H. Suzuki, *Chem. Letters*, 1977, 1085.
15. K-L. Na, S. Huh, K-M. Sung and M-J. Jun, *Polyhedron*, 1996, Vol. 15, **11**, 1841.
16. T. Ito, H. Horino, Y. Koshiro and A. Yamamoto, *Bull. Chem. Soc. Jpn.*, 1982, **55**, 504.
17. R. A. Sánchez-Delgado, N. Valencia, R. Márquez-Silva, A. Andriollo and M. Medina, *Inorg. Chem.*, 1986, **25**, 1106.
18. J. G. de Vries, G. Roelfes and R. Green, *Tetrahedron Letters*, 1998, **39**, 8329.
19. S. Murahashi, T. Naota, K. Ito, Y. Maeda and H. Taki, *J. Org. Chem.*, 1987, **52**, 4319.
20. Y. Sasson and J. Blum, *J. Org. Chem.*, 1975, Vol. 40, **13**, 1887.
21. Y. R. Santosh Laxmi and J. E. Bäckvall, *J.C.S. Chem. Commun.*, 2000, 611.
22. J. E. Bäckvall, R. L. Chowdhury and U. Karlsson, *J.C.S. Chem. Commun.*, 1991, 473.

23. R. L. Chowdhury and J. E. Bäckvall, *J.C.S. Chem. Commun.*, 1991, 1063.
24. Y. Ishii, K. Osakada, T. Ikariya, M. Saburi and S. Yoshikawa, *J. Org. Chem.*, 1986, **51**, 2034.
25. S. Shinoda, H. Itagaki and Y. Saito, *J.C.S. Chem. Commun.*, 1985, 860.
26. T. A. Smith and P. M. Maitlis, *J. Organomet. Chem.*, 1985, **289**, 385.
27. D. Morton and D. J. Cole-Hamilton, *J.C.S. Chem. Commun.*, 1988, 1154.
28. R. T. Morrison and R. N. Boyd, *Organic Chemistry*, Prentice Hall International (UK) Ltd., London, 6th edn., 1992.
29. *Aqueous-Phase Organometallic Catalysis*, eds. B. Cornils and W. A. Hermann, Wiley-VCH, Weinheim, 1998.

Chapter 4

Catalyst Reactivation

The deactivated catalyst [Ru(Triphos)H_2(CO)] *can be reactivated by the water gas shift reaction when an excess of water and temperatures of 140°C (or greater) are used. The reactivation of the catalyst using an amine oxide to remove the carbonyl from* [Ru(Triphos)H_2(CO)] *was found to be ineffective.*

4.1 Introduction

The catalyst [Ru(Triphos)H_2S] (S = Solvent or H_2), generated from the *in situ* reaction of Ru(acac)$_3$ and Triphos with hydrogen, is deactivated by the co-ordination of carbon monoxide to form the complex [Ru(Triphos)H_2(CO)] (see Chapter 3, Catalyst Deactivation). The co-ordinated carbonyl is insufficiently labile to allow the active catalyst, believed to be [Ru(Triphos)H_2], to form. This carbonyl group in effect blocks the vacant co-ordination site required for co-ordination of the substrate and therefore deactivates the catalyst. The removal of the carbonyl to reform [Ru(Triphos)H_2] is thus an important objective towards reactivation of the catalyst, and extending its lifetime.

4.1.1 Properties of the Carbonyl Ligand

The carbon monoxide ligand stabilises metal complexes with low oxidation states by accepting electron density from the metal, then as a π-acceptor ligand (or π-acid) uses an unoccupied π* orbital to accept electron density from a transition metal and forms a strong metal-ligand bond. The unoccupied orbital has the correct symmetry to overlap a filled *d*-orbital of the transition metal. Most π-acceptor ligands are high field ligands and therefore usually result in octahedral metal complexes being 18-electron systems and thus low spin.

The bonding is illustrated in Fig. 4.1.[1, 2] The carbonyl donates a lone pair of electrons from the carbon to an empty σ-orbital on the metal forming a co-ordinate bond. The transition metal uses its d_π orbitals to bond *via* the empty π^* orbital of the carbonyl

group. Transition metals, which are electron rich, can delocalise electron density from their full *d*-orbitals to empty antibonding π^* orbitals on the carbonyl, a capability known as backbonding. The interaction occurs because the metal *d*-orbitals (t_{2g} for an octahedral complex) have the correct symmetry to overlap with the carbonyl π^* orbitals. This transition metal-carbon interaction is bonding, whereas antibonding between carbon and oxygen. The combination of σ and π-bonding between the metal and carbon is synergistic, because the metal's ability to delocalise electron density into the carbonyl π^* orbital is proportional to the electron density possessed by the metal which is enhanced by σ-electron donation from the carbonyl group and other ligands attached to the metal. The metal-carbonyl bond strength, which can be high,[3] is however influenced by the whole ligand environment and the charge on the complex. Whilst strengthening the bond between the metal and carbon, backbonding weakens the oxygen bond and causes bond lengthening. Thus metal-carbon bond strengthening is therefore created at the expense of the carbon-oxygen bond weakening. The greater the electron density transferred to the LUMO of the carbonyl ligand, the longer and weaker the CO bond becomes, a property that can be observed and monitored by IR and X-ray crystallography.

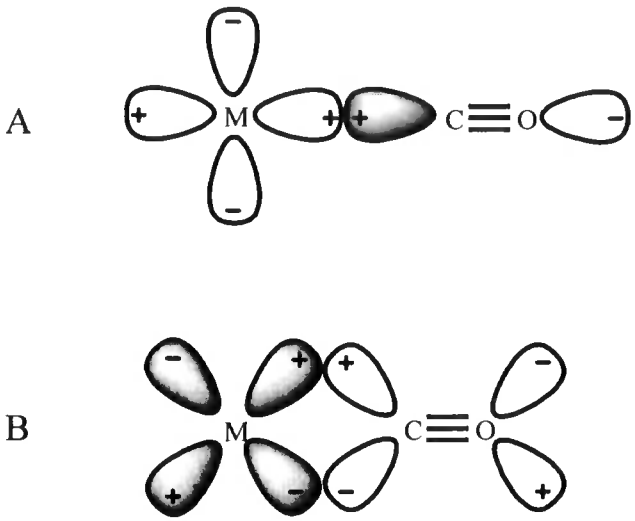

Figure 4.1 Bonding between Transition Metals and Carbon Monoxide

Orbital shading represents the source of the electron density responsible for the bonding. The + and – signs indicate the symmetry of the orbital.
A: Metal-carbonyl σ-Bond.
Carbonyl ligand donates a lone pair of electrons on the carbon atom to an empty metal *d*-orbital.
B: Metal-carbonyl π Bond.
Electron density is delocalised from full metal *d*-orbitals (t_{2g}) to empty π^* orbitals on the carbon atom of the carbonyl ligand (in two orthogonal planes).

The co-ordinated carbonyl is polarised by bonding to a transition metal. The carbon becomes more positive and the oxygen more negative. Free CO is weakly polar, with the polarisation being C^{-}-O^{+}, its inconsistency with the principle of maintaining tetravalency is unusual for carbon, as is its formulation with a triple bond to oxygen and its associated superimposed ionic character, which explains the ability of CO to act as a *Lewis* base.[4] From a m.o. diagram of a π bond of CO (see Fig. 4.2), it can be seen that the CO π homo is polarised toward the oxygen and the CO π^{*} lumo is polarised toward the carbon.[2] This polarisation explains why the metal-carbonyl bond is more favourable at the carbon. The filled metal d_{π} orbital donates electron density to the carbonyl through the CO π^{*} lumos.

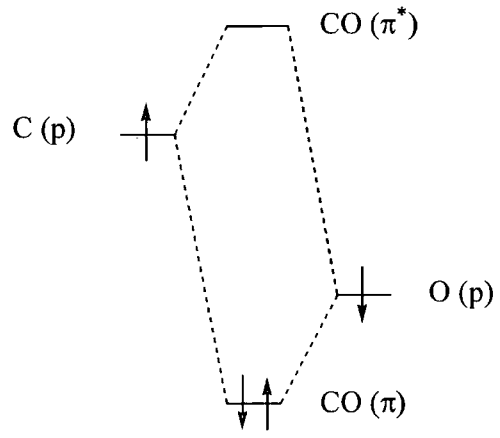

Figure 4.2 An m.o. diagram of a CO π bond [2]

The polarity of the co-ordinated carbonyl ligand results in it being chemically activated, with the carbon receptive to nucleophilic attack and the oxygen to electrophilic attack.[2] The ligand environment of the metal and any charge on the complex influence the polarisation of the CO and its susceptibility to attack..

4.1.2 Carbonyl Substitution and Removal

Substitution reactions of co-ordinatively saturated 18 electron metal-carbonyls are usually activated by ligand dissociation, which though not always easy, can be promoted by heat, photolysis, catalysis or a reagent.[5] The rate of carbonyl substitution in six co-ordinated metal-carbonyls frequently decreases as the carbonyls are replaced by ligands that are more strongly σ-donors.[1] The substitution limit is often only two or

three ligand replacements, and the steric properties of bulky phosphine ligands are often detrimental to extensive carbonyl substitution. Replacement of a π-acceptor ligand with a ligand that is a σ-donor increases the electron density on the metal centre and results in greater back donation to the π acceptor ligands present, thereby strengthening the respective metal-ligand bonds, and reducing the rate of further ligand dissociation.

This study focuses on carbonyl substitution and removal by nucleophilic attack of amine oxides and the water gas shift reaction. Carbonyl dissociation has been achieved by other methods, such as photochemical reactions,[2] but these are not discussed here.

4.1.2.1 Amine Oxide Promoted Carbonyl Substitution

One of the few ways of removing a carbonyl group from a metal complex is by nucleophilic attack with an amine oxide.[2, 6] The electrophilic nature of the carbonyl carbon promotes the attack by the nucleophilic amine-oxide (see Fig. 4.3) at the carbonyl carbon [7, 8] to produce a species that then breaks down to produce CO_2 (which is a good leaving group), the corresponding amine and a co-ordinatively unsaturated metal complex.

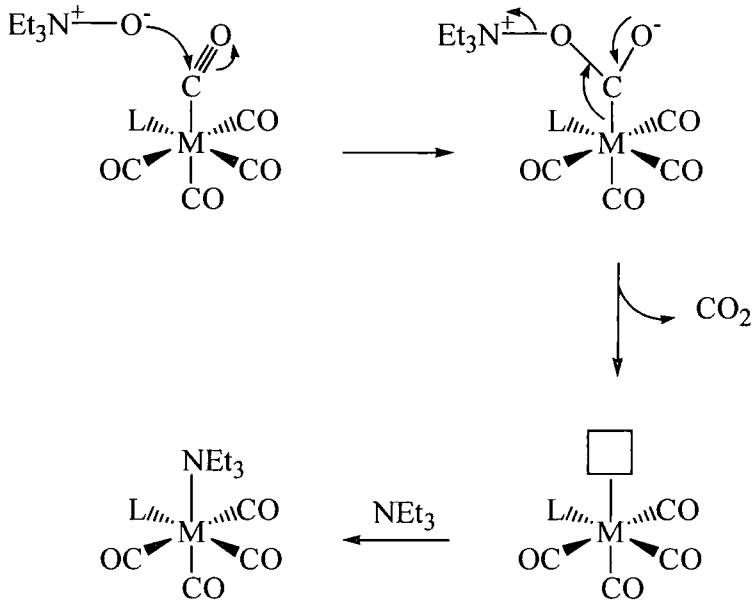

Figure 4.3 CO Removal by Amine Oxide

In Fig. 4.3 the nucleophilic oxygen of the amine-oxide attacks a carbonyl that is *trans* to another carbonyl (*trans* effect), rather than one that is *trans* to a ligand such as PR_3. This is because *trans* carbonyl groups compete with each other for electron density in the same d_π-orbital, and have a lower level of metal back donation than a carbonyl that is *trans* to the weaker PR_3 ligand. The lower level of metal back donation makes the metal-carbonyl bond weaker, and therefore the carbonyl is more susceptible to nucleophilic attack.

Basolo *et al* [8, 9, 10] studied the rates of reaction and the mechanism of carbonyl substitution in metal-carbonyl complexes, in the presence of the amine oxide $(CH_3)_3NO$. They reported that a CO ligand could be substituted by PPh_3 in the ruthenium complexes $[Ru(CO)_5]$ and $[Ru_3(CO)_{12}]$ by the nucleophilic attack using $(CH_3)_3NO$. The removal of one carbonyl ligand from $[Ru(CO)_2X_2L_2]$ complexes (where X = Cl, Br, CF_3CO_2; L_2 = phen, bipy, $(PPh_3)_2$) was achieved with $(CH_3)_3NO$ in pyridine (see Equation 4.1), but the second carbonyl remained co-ordinated to the metal.[11, 12] The inability to remove the second carbonyl supports the suggestion that amine oxide promoted decarbonylations are restricted to carbonyls with $\nu(CO) > 2000\ cm^{-1}$.[7] However, Black *et al* found that the removal of both carbonyls from $[Ru(CO)_2X_2L_2]$ could be accomplished by using 2-methoxyethanol as the solvent with $(CH_3)_3NO$ in the presence of a bidentate ligand (see Equation 4.1).[12] Thus, the removal of both carbonyls of the $[Ru(CO)_2X_2L_2]$ complex indicated that amine oxide promoted decarbonylation could also be achieved for carbonyls with $\nu(CO) < 2000\ cm^{-1}$.

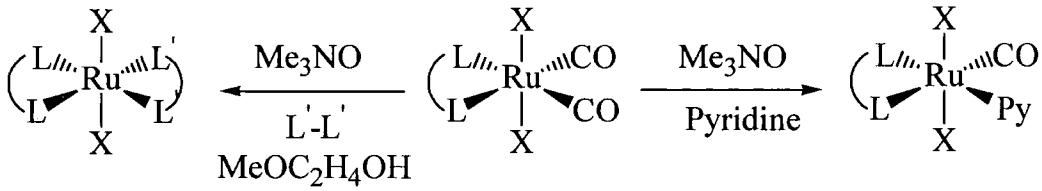

Equation 4.1

4.1.2.2 Carbonyl Removal by the Water Gas Shift Reaction

The water-gas shift (WGS) reaction (see Equation 4.2) converts CO and H_2O into H_2 and CO_2. The reaction allows the proportion of hydrogen obtained in the production of synthesis gas (see Equation 4.2) to be increased.[13] Industrially, the reaction is catalysed

heterogeneously by transition metals, either at high temperatures (300-400°C) using an iron-chromite catalyst or at lower temperatures (≈ 200°C) using zinc-copper based catalysts.[14] Investigations of homogeneous catalysts for the WGS reaction have been conducted with a variety of different transition metal carbonyls and carbonyl complexes, but none so far have been commercially viable alternatives to the heterogeneous catalysts.[15, 16]

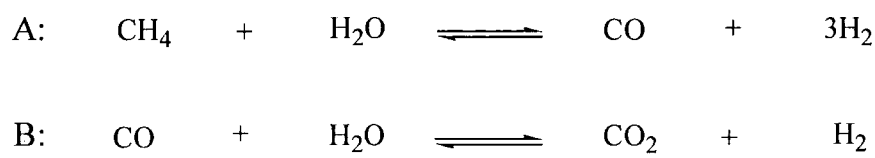

Equation 4.2

A: Synthesis gas reaction (Steam reforming).
B: Water gas shift reaction.

The WGS reaction has been investigated by Ford *et al* [17] and a mechanism proposed (see Scheme 4.1). The reaction proceeds by the nucleophilic attack of water (or hydroxide) at the carbon of a metal co-ordinated carbon monoxide. The metal carboxylic acid formed, undergoes decarboxylation to produce a metal hydride. Protonation of the metal hydride with subsequent elimination of hydrogen results in an unsaturated metal complex, which can co-ordinate further CO.

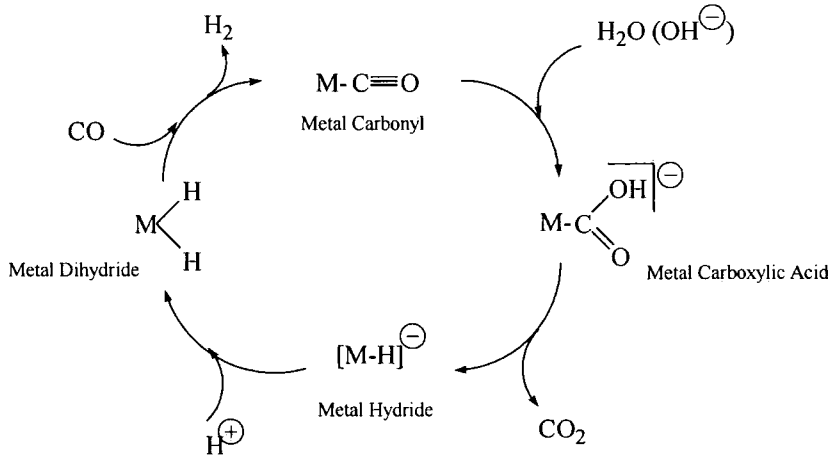

Scheme 4.1 Water Gas Shift Mechanism [17]

The WGS reaction can be an undesired side reaction of homogeneous catalysis where CO and H_2O are being utilised, or are present as part of the reaction, especially as most of the late transition metals are capable of some form of the reaction.[18, 19] Metals or metal complexes that can deprotonate water will favour the WGS reaction.

Ruthenium complexes are found to be capable of catalytic WGS reaction, both heterogeneously [20] and homogeneously [21]. Ruthenium carbonyl complexes are active, with homogeneous catalysis in an alkaline solution being reported by Ford [22] for $[Ru_3(CO)_{12}]$, $[Ru_4H_4(CO)_{12}]$, $[Ru_6C(CO)_{17}]$, $[Ru_4H_2(CO)_{13}]$ and $[FeRu_3H_2(CO)_{13}]$. The reaction proceeds by the proposed mechanism detailed in Scheme 4.1. The reductive elimination of H_2, assisted by the co-ordination of CO, was proposed as the rate-limiting step. Interestingly, the iron-ruthenium mixed metal carbonyl species, $[FeRu_3H_2(CO)_{13}]$, is catalyticaly more active than a catalyst consisting of only one of the two metals,[22] the greater activity being attributed to a superior reactivity for hydrogen elimination. The irradiation of an aqueous solution of the ruthenium complex $[RuCl(bipy)_2(CO)]Cl$, was reported by Cole-Hamilton [23] to catalyse the WGS reaction to produce H_2, CO and CO_2. $[RuCl(bipy)_2(CO)]^+$ and $[Ru(bipy)_2(CO)]^{2+}$, were reported by Tanaka *et al*, [24] to be active under mild conditions of 70-150°C with 3-20 kg/cm^2 (0.3-2.0 MPa) of CO. Their study resulted in the isolation of the intermediates of the different stages of the WGS reaction. The IR spectrophotometric characterisation of the intermediates provided support for the mechanism detailed in Scheme 4.1.

The requirement for nucleophilic attack at the metal-carbonyl carbon and the need therefore for both the CO and the H_2O to be activated, has meant that many of the systems investigated for the WGS reaction involve a basic medium. The homogeneous catalysis of the WGS reaction in the absence of base and in acidic solutions has also been investigated.[22] To proceed in neutral or acidic conditions, the CO must be activated by co-ordination to the metal, such that nucleophilic attack by H_2O, as against hydroxide, can take place. Alternatively, a metal complex can activate the CO and deprotonate the H_2O to promote the WGS reaction. $[(P(i\text{-Propyl})_3)_nPt]$ in the absence of added base was reported by Yoshida *et al*, [25] to co-ordinate CO, and water. Subsequent carbonyl insertion to produce a metal carboxylic acid species (see Scheme 4.2), decarboxylation and protonation results in a platinum dihydride, which undergoes reductive elimination of hydrogen.[2, 3]

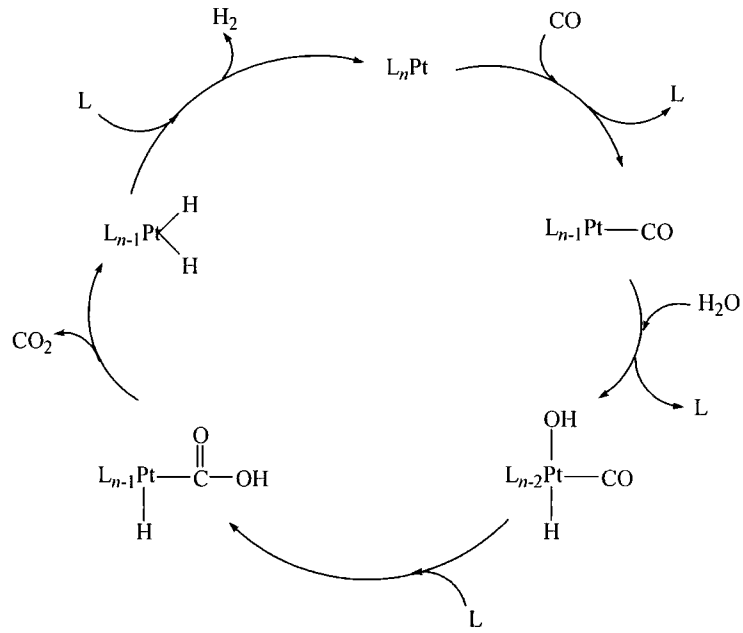

Scheme 4.2 Platinum Catalysed Water Gas Shift Reaction [3]

A rhodium complex has been reported by Eisenberg *et al* that catalyses the WGS reaction in an acidic medium.[26] The catalyst is prepared from $[Rh(CO)_2Cl]_2$, glacial acetic acid, concentrated HCl, and NaI in H_2O, and in its active form includes predominantly the monomeric rhodium species $[RhI_2(CO)_2]^-$, $[RhI_5(CO)]^{2-}$ and $[RhI_4(CO)_2]^-$. The two important components of the reaction (see Equation 4.3) are the reduction of Rh(III) by CO to Rh(I) and the oxidation of Rh(I) by H_2O to Rh(III).

A: $Rh(III) + CO + H_2O \longrightarrow Rh(I) + CO_2 + 2H^+$

B: $Rh(I) + 2H^+ \longrightarrow Rh(III) + H_2$

Equation 4.3

The study of rhodium bipyridine complexes for the homogeneous catalysis of the WGS reaction by Creutz *et al* [27] discovered that a pH $\approx$ 3 produced the optimum conditions for maximum catalytic activity. Increasing the pH resulted in a gradual decline in activity, whereas a decrease in pH resulted in a rapid reduction in activity. The rationale offered, is that oxidation of the CO of $[HRh(bipy)_2(CO)]^{2+}$ (see Equation 4.4: A), is the

rate limiting step, and that the CO activation is inversely dependent on $[H^+]$. Thus a low pH inhibits the reaction. The CO co-ordinated to the rhodium(III) complex is activated to nucleophilic attack, and is reflected in the mechanism proposed by Creutz *et al* as nucleophilic attack and subsequent CO_2 elimination (see Equation 4.4:B). The decreased activity for the WGS reaction when the pH was increased (pH 3 to pH 7 resulted in a rate reduction of almost an order of magnitude), was thought to be due to changes in the rhodium complex as a result of bipyridine displacement by the CO.

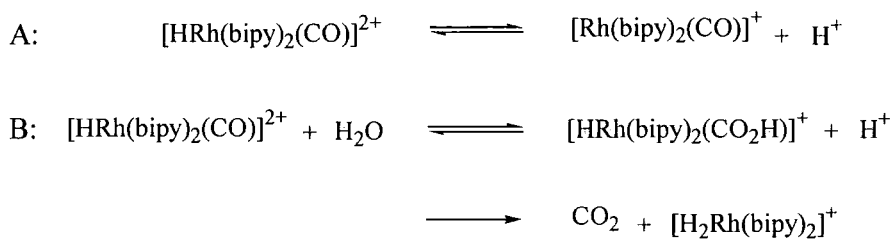

Equation 4.4

A: CO oxidation.
B: Nucleophilic attack.

The work of Eisenberg *et al*[26] led to the investigation by Ford *et al* of metal carbonyls in acidic media.[28] They found that, although $[Ir_4(CO)_{12}]$ and $[Fe(CO)_5]$ in a solution of H_2SO_4, H_2O and ethoxyethanol were inactive as WGS catalysts, the analogous solution with $[Ru_3(CO)_{12}]$ or $[H_4Ru_4(CO)_{12}]$ was active, but unstable due to the resulting complex being susceptible to undergoing sublimation out of solution. A more stable, but still active, system was obtained by using diethyleneglycol dimethyl ether (diglyme) as the solvent. Their investigation resulted in the conclusion that the WGS reaction was based on the dinuclear anion $[HRu_2(CO)_8]^-$. The reaction of $[HRu_2(CO)_8]^-$ with CO, to break the ruthenium-ruthenium interaction, and produce $[Ru(CO)_5]$ and $[HRu(CO)_4]^-$ was believed to be the rate limiting step. The $[HRu(CO)_4]^-$ ion was considered to be sufficiently basic that it could be protonated to the dihydride and subsequently lose hydrogen (see Scheme 4.3).

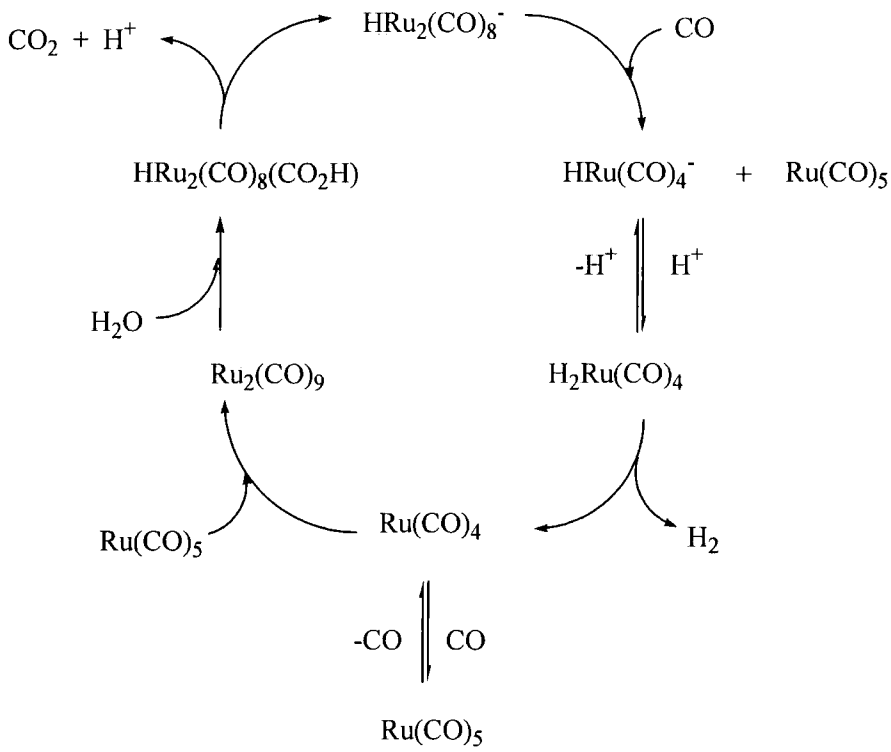

Scheme 4.3 Ruthenium Catalysed Water Gas Shift Reaction in Acidic Conditions

A low pressure of CO is thought to be necessary, to ensure that the ruthenium species present is $[HRu_2(CO)_8]^-$, as at higher CO pressure the catalysis is inhibited by an equilibrium between CO and $[Ru_2(CO)_9]$ (see Equation 4.5).

$$CO + [Ru_2(CO)_9] \rightleftharpoons 2[Ru(CO)_5]$$

Equation 4.5

4.1.3 Summary

The strength of the metal-carbonyl bond, makes removal of the CO ligand from metal complexes difficult to achieve. The nature of the σ and π bonding interaction between the metal and the carbonyl results in a polarisation of the co-ordinated CO that results in the carbonyl carbon being susceptible to nucleophilic attack.

The removal of CO from metal carbonyls (mononuclear and clusters) and from metal complexes containing carbonyl ligands is possible using an amine oxide. The reaction proceeds by the attack of the extremely nucleophilic oxygen of the amine oxide at the δ^+ metal-carbonyl carbon. This produces a species that ultimately breaks down to produce the corresponding amine, CO_2 (a good leaving group) and a co-ordinatively unsaturated metal complex. The ease of CO removal from metal complexes is dependent on the ligand environment of the metal and any charge on the metal complex. A metal that is electron rich will result in strong back donation to the carbonyl ligand and a proportionally strong metal-carbonyl bonding interaction, which makes removal of the carbonyl more difficult.

The water-gas shift (WGS) reaction removes transition metal co-ordinated carbonyls, by a reaction of H_2O at the co-ordinated CO to produce H_2, CO_2 and a co-ordinatively unsaturated metal complex. The WGS reaction originates from the nucleophilic attack of water (hydroxide) at a metal co-ordinated carbon monoxide carbon, to form a metal carboxylic acid, which then undergoes decarboxylation and protonation to produce a metal hydride. Protonation of the metal hydride with subsequent elimination of hydrogen results in an unsaturated metal complex, which can co-ordinate further CO. The WGS reaction requires activation of the metal co-ordinated carbonyl carbon and the H_2O, which is usually achieved by using an alkaline solution. However, the reaction can proceed in both neutral and acidic media, if the metal complex is sufficiently basic to provide the activation.

The removal of carbonyls from ruthenium complexes has been accomplished by both the nucleophilic attack of amine oxides and by the WGS reaction.

4.2 Results and discussion

The investigation for a method to reactivate the deactivated catalyst, the ruthenium complex [Ru(Triphos)H_2(CO)], by the removal of the carbonyl ligand, examined two techniques. The use of amine oxides for direct nucleophilic attack at the co-ordinated carbonyl and the water gas shift reaction to remove the co-ordinated carbonyl as carbon dioxide by introducing H_2O into the reaction conditions.

The [Ru(Triphos)H_2(CO)] used in the investigations was the solid product obtained from the hydrogenation of esters, as previously described (see Chapter 2, Homogeneous Ester Hydrogenation).

4.2.1 Reaction of [Ru(Triphos)H_2(CO)] with Amine Oxides

The investigation of the amine oxide, Me_3NO, as a method of removing CO from [Ru(Triphos)H_2(CO)] produced results that suggested that it was ineffective. The data obtained, indicated that the amine oxide removed the hydrides and not the carbonyl. The difficulty in recovering the products of the reaction and their respective characterisation led to the conclusion that the use of the amine oxide, under the conditions applied, was an unreliable method of reactivating the catalyst.

The difficulty in obtaining suitable data on the progress of the reaction and the general scarcity of data prevented identification of the species produced. However, consideration of the limited information obtained, presented below, suggested that a ruthenium cluster complex, could be the product, the cluster complex being [{Ru(Triphos)}$_4$(μ_3-CO)$_4$] having a "cubic" structure (see Fig. 4.4).

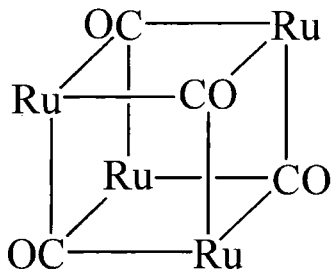

Figure 4.4

Note: Triphos omitted from each octahedral ruthenium for clarity.

The addition of Me_3NO to [Ru(Triphos)H_2(CO)] produces a species that generates a ^{31}P NMR spectrum that comprises a singlet at δ 28.3 ppm, a ^1H NMR spectrum with no hydride signal and an IR spectrum that has a stretch ν at 1682 cm^{-1}. The same product can be obtained either when [Ru(Triphos)H_2(CO)] is heated in benzene under reflux, or with time, when the [Ru(Triphos)H_2(CO)] is exposed to air under ambient conditions. Here the product can not include any replacement ligand such as NEt_3. The loss of the two hydrides from [Ru(Triphos)H_2(CO)], in air with time is conceivably possible, but

the loss of both the hydrides and / or the CO under the same conditions is less likely. The exposure of the analogous complex $[RuH_2(CO)(PPh_3)_3]$ to UV light was reported by Geoffroy and Bradley [29] to result in the loss of H_2, but not CO, producing $[Ru(CO)(PPh_3)_3]$. These data support the suggestion that the product of the reaction of [Ru(Triphos)H_2(CO)] with Me_3NO, heating under reflux or degradation with time still contains the CO but not the hydrides. The results of Geoffroy and Bradley [29] also suggest that the product obtained with time may be due to a photochemical reaction.

^{1}H NMR data indicate that the hydrides have been removed or lost from [Ru(Triphos)H_2(CO)]. The IR data show that although the carbonyl stretch, ν(CO), at 1943 cm^{-1} has disappeared, a new stretch is observed at 1682 cm^{-1}. This indicates that the CO has not been removed, but is in a new bridging environment. The ν(CO) for metal-carbonyl complexes are observed in the range ≈ 1600 – 2200 cm^{-1}, with triply bridging CO groups absorbing at the low end.[30, 31] The singlet obtained in the ^{31}P NMR spectrum (at δ 28.3 ppm) indicates that the three phosphorus atoms of the triphos are all in the same environment. If the IR stretch at 1682 cm^{-1} is assigned to a ruthenium-carbonyl, then the species must contain ruthenium, triphos and the CO. For a ruthenium complex containing only triphos and CO to provide a ^{31}P NMR of a singlet, it would have to adopt a highly symmetrical geometry e.g. a tetrahedron, which would result in the complex being Ru^0, d^8. The observation of both ^{1}H and ^{31}P NMR spectra containing sharp, clear signals indicates that the complex is diamagnetic. The singlet observed in the ^{31}P NMR spectrum is therefore produced by an octahedral ruthenium-triphos complex, with three identical ligands. The IR stretch observed at 1682 cm^{-1}, which is in the range of the ν(CO) for a symmetrical μ_3-CO, indicates that the three identical ligands are triply bridging CO groups. The CO bonds to three ruthenium atoms (see Fig. 4.5, A) and the ruthenium-triphos co-ordinates three carbonyls (see Fig. 4.5, B). The simplest symmetrical structure containing these components is the tetramer cluster compound [Ru(Triphos)(CO)]$_4$ which is [{Ru(Triphos)}$_4$(μ_3-CO)$_4$], and has a "cubic" structure (see Fig. 4.5, C).

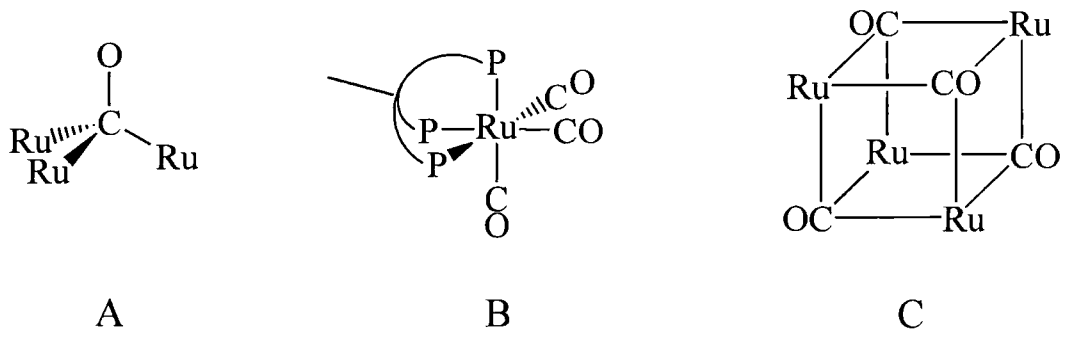

A B C

Figure 4.5 [Ru(Triphos)(CO)]$_4$

A: Symmetrical μ_3-CO, with ruthenium (Triphos omitted from each ruthenium for clarity).
B: Octahedral ruthenium-triphos with $(\mu_3\text{-CO})_3$.
C: Possible structure suggested by the NMR and IR data (Triphos omitted from each ruthenium for clarity).

The tetrameric cluster compound [Fe(η^5-C_5H_5)(CO)]$_4$ (see Fig.4.6) contains CO groups that are triply bridging, with a ν(CO) of 1620 cm^{-1}.[32] The [Fe(η^5-C_5H_5)(CO)]$_4$ data support the suggestion that the observed low IR stretch at 1682 cm^{-1} is that of triply bridging CO groups.

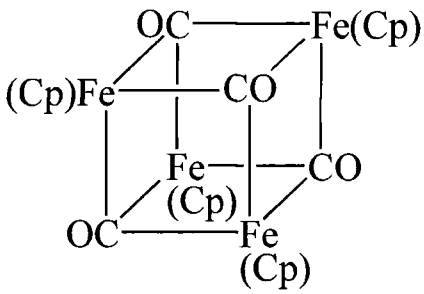

Figure 4.6 [Fe(η^5-C_5H_5)(CO)]$_4$

4.2.1.1 Reaction of [Ru(Triphos)H$_2$(CO)] with Me$_3$NO

The [Ru(Triphos)H$_2$(CO)] reacts with Me$_3$NO in the presence of acetonitrile (MeCN), which was included to provide a replacement ligand for the CO. MeCN was chosen because it is not sterically demanding (being pencil-shaped), and can usually be displaced from the metal complex, under relatively mild reaction conditions.[5] The reaction solution, of benzene, was initially clear pale yellow at r.t., due to the [Ru(Triphos)H$_2$(CO)] with the white Me$_3$NO being undissolved. After an hour, under

reflux at 80°C, the solution was still a pale yellow colour, which then became a translucent brown 45 minutes later. Analysis whilst it was pale yellow, showed that [Ru(Triphos)H_2(CO)] remained in solution, whereas analysis of the brown coloured solution showed that significant change had occurred, the ^{31}P NMR spectrum now comprising five singlets. The ^{1}H NMR spectrum of the brown solution had no signal within the hydride region and the IR spectrum did not show a ν(CO) at 1943 cm^{-1}. The ^{31}P NMR spectrum of the brown solution (; ^{31}P{^{1}H} NMR (25°C, benzene-d_6): δ 47 (**3P**, s), 46 (**3P**, s), 35 (**3P**, s, br), 33 (**3P**, s, br), 28 (**3P**, s) ppm) had the five singlets with an integration ratio of 1:1:2:1:18. These singlets suggest that the species present all have their respective triphos phosphorus atoms in identical environments, and of the form [Ru(Triphos)L_n] (where n = 1 or 3). The ligands available in the product solution include the solvent benzene-d_6, MeCN, Me_3N and H_2O. The two broad ^{31}P NMR spectrum signals at δ 35 and 33 ppm suggest that either the two species are fluxional, or possibly paramagnetic. The singlet at 28 ppm represents the main product. The IR spectrum of the brown coloured product solution showed a new stretch at ν1682 cm^{-1}. The change in colour, ^{31}P NMR and IR spectra of the solution indicated the absence of [Ru(Triphos)H_2(CO)], and was confirmed by the absence of a hydride signal in the ^{1}H NMR spectrum. The absence of the ν(CO) stretching frequency at 1943 cm^{-1} indicated that either the CO had been removed, or a change in environment at the ruthenium, following loss of the hydrides.

4.2.1.2 CO Substitution by MeCN and Me_3N in [Ru(Triphos)H_2(CO)]

To establish the roles of the amine oxide Me_3NO and the MeCN, the same reaction was attempted, firstly without the MeCN and then without either the Me_3NO or the MeCN. The reaction, performed in benzene under reflux at 80°C, in the absence of MeCN produced the same result as that obtained when it was included. The MeCN therefore did not participate in the reaction. When the reaction was performed without the Me_3NO, the reaction solution changed colour as it did with the Me_3NO to become a pale yellow before becoming a brown colour. The colour change took longer to occur, requiring almost 8 hours to become the translucent brown colour. Analysis of the product solution by ^{31}P NMR indicated that two species were present. ^{31}P{^{1}H} NMR (25°C, benzene-d_6): δ 37.2 (**P**, t, $^{2}J_{P\text{-}P}$ = 32 Hz), 28.4 (**2P**, d, $^{2}J_{P\text{-}P}$ = 32 Hz), 28.3 (**3P**, s) ppm. The two species were [Ru(Triphos)H_2(CO)], which generates the ^{31}P NMR triplet

and doublet, and a species that produces a singlet being recognised as the same product as that from the Me_3NO reaction. When the reaction was repeated using an extended reaction period, to investigate whether all the [Ru(Triphos)H_2(CO)] could be converted, to the new species, samples were taken periodically and monitored by ^{31}P NMR spectroscopy. Initially only the triplet and doublet of the [Ru(Triphos)H_2(CO)] were observed, but as the reaction proceeded an increasing level of the new species (singlet at δ 28.3 ppm) was observed. The IR spectrum of a sample of the solution taken after it had become a brown colour, contained carbonyl stretches at ν(CO) 1943 cm^{-1} and 1682 cm^{-1}. After 10.75 days the ^{31}P NMR spectrum of the product solution contained only the singlet at δ 28.3 ppm. A metal hydride was not detected in the ^{1}H NMR spectrum of the hydride region of the product solution. Attempts to recover the product as a solid by recrystallization or solvent removal were unsuccessful.

4.2.1.3 Degradation of [Ru(Triphos)H_2(CO)] with Time

The species represented by a singlet at δ 28.3 ppm in the ^{31}P NMR was also observed in a sample of [Ru(Triphos)H_2(CO)], which had been exposed to light and air over a period of approximately six months - the colour had darkened from pale yellow to a darker golden yellow colour. A subsequent ^{31}P NMR spectrum of the sample showed the triplet and doublet associated with the [Ru(Triphos)H_2(CO)] and also the singlet at δ 28.3 ppm. The singlet at δ 28.3 ppm had not been present in the original ^{31}P NMR spectrum of the dissolved solid; only the triplet and doublet that identify [Ru(Triphos)H_2(CO)] were observed. This suggests that the species represented by the new δ 28.3 ppm species is a decomposition product of [Ru(Triphos)H_2(CO)]. That the [Ru(Triphos)H_2(CO)] is present with the new species, indicates that the decomposition is not a facile process, although it does suggest that [Ru(Triphos)H_2(CO)] is air/light sensitive. Variable temperature (VT) ^{31}P NMR spectroscopy studies on the new sample were conducted at ambient temperature, 30°C and 50°C [$^{31}P\{^{1}H\}$ NMR (25°C, benzene-d_6): δ 37.2 (**P**, t, $^{2}J_{P\text{-}P}$ = 32 Hz), 28.4 (**2P**, d, $^{2}J_{P\text{-}P}$ = 32 Hz), 28.6 (**3P**, s) ppm. $^{31}P\{^{1}H\}$ NMR (30°C, benzene-d_6): δ 37.3 (**P**, t, $^{2}J_{P\text{-}P}$ = 32 Hz), 28.4 (**2P**, d, $^{2}J_{P\text{-}P}$ = 32 Hz), 28.4 (**3P**, s) ppm. $^{31}P\{^{1}H\}$ NMR (50°C, benzene-d_6): δ 37.4 (**P**, t, $^{2}J_{P\text{-}P}$ = 32 Hz), 28.5 (**2P**, d, $^{2}J_{P\text{-}P}$ = 32 Hz), 28.2 (**3P**, s) ppm]. The chemical shift of the singlet in the ^{31}P NMR spectrum can clearly be seen to slightly change position with increase in temperature, whilst the triplet doublet combination remains in roughly the same location. The

changes strongly indicate loss of hydrogen and formation of the symmetrical complex $[Ru(Triphos)(CO)]_4$.

4.2.2 Reaction of $[Ru(Triphos)H_2(CO)]$ with H_2O

The reactivation of $[Ru(Triphos)H_2(CO)]$ for catalytic hydrogenation can be achieved by it being heated in water at 140°C. The $[Ru(Triphos)H_2(CO)]$ can be used as the catalytic precursor for the hydrogenation of esters and carboxylic acids when an excess of water is included in the reaction and a temperature of 140°C, or above, is applied. The carbonyl ligand is removed by the water gas shift reaction from $[Ru(Triphos)H_2(CO)]$ and released as CO_2. The site made vacant by the removal of the CO, allows catalysis to proceed.

The hydrogenation of the ester, methyl propanoate, and the carboxylic acids, propionic acid and maleic acid, were used for the investigation of catalyst reactivation, by the water gas shift mechanism. The deactivated catalyst $[Ru(Triphos)H_2(CO)]$ was found to be ineffective for the hydrogenation of the ester, methyl propanoate, in iPA at 120°C, whereas, when the solvent iPA was replaced by H_2O and the temperature increased to 140°C, the ester conversion to 1-propanol obtained was 97.9 % (see Table 4.1). Similarly, the deactivated catalyst $[Ru(Triphos)H_2(CO)]$ in H_2O at 120°C achieved almost no hydrogenation of propionic acid. An increase in the reaction temperature, to 140°C was required for the hydrogenation of the propionic acid to occur (see Table 4.1).

Table 4.1 Hydrogenation with $[Ru(Triphos)H_2(CO)]$

Substrate Hydrogenated	Temperature (°C)	Conversion (%)
Methyl Propanoate [a]	140	97.9
Propionic Acid	120	1.2
Propionic Acid	140	98.7 [b]

Conditions: $p(H_2)$ = 6.8MPa, 16 hours.
a : 26-hour reaction period.
b : Conversion calculated by acid titration, with 0.1M KOH.

The hydrogenation of maleic acid by $[Ru(Triphos)H_2(CO)]$ in H_2O was also achieved (the hydrogenation of maleic acid can be accomplished using the catalytic precursors of $Ru(acac)_3$ and Triphos, see Chapter 5, Acid Hydrogenation). The hydrogenation of the

maleic acid, by the water treatment of the deactivated catalyst, resulted in a conversion of 66.8 % (see Table 4.2), to tetrahydrofuran (THF), γ-butyrolactone (gBL) and 1,4-butanediol (BDO).

Table 4.2 Hydrogenation of Maleic Acid by [Ru(Triphos)H_2(CO)]

Maleic Acid Conversion (%)	THF Selectivity (%)	gBL Selectivity (%)	BDO Selectivity (%)
66.8 [a]	50.4	29.9	12.8

Conditions: $p(H_2)$ = 6.8MPa, 140°C, 112 hours.

At the end of the maleic acid hydrogenation, when using [Ru(Triphos)H_2(CO)], the headspace gas within the autoclave was analysed and found to contain CO_2 and a trace of CO, the presence of which suggested that the ruthenium carbonyl complex ([Ru(Triphos)H_2(CO)]), had been reactivated by removal of the carbonyl in the water gas shift reaction, to produce CO_2. The CO component of the headspace gas was probably released by dissociation from the deactivated catalyst as a result of the increased temperature.

To demonstrate that [Ru(Triphos)H_2(CO)] was the source of the CO_2 and CO in the headspace gas, [Ru(Triphos)H_2(CO)] was dissolved in THF with an excess of H_2O and heated at 140°C under H_2. Analysis of the headspace gas found both CO_2 and CO, whilst the product solution was found to contain both THF and H_2O but not any decarbonylation products. The CO_2 and CO had therefore come from the [Ru(Triphos)H_2(CO)]. A ^{31}P NMR spectrum of the product solution differed from that of [Ru(Triphos)H_2(CO)]. The spectrum obtained from [Ru(Triphos)H_2(CO)], as detailed in Chapter 2, contains a triplet and a doublet at δ 37 and 28 ppm respectively (see Figure 4.7), whereas the spectrum obtained from heating [Ru(Triphos)H_2(CO)] in H_2O was more complicated and changed with time (see Figure 4.8). As neither of the two spectra in Fig. 4.8 include the triplet and a doublet at δ 37 and 28 ppm, it is clear that [Ru(Triphos)H_2(CO)] is not present in the product. The presence of triplets and doublets that are coupling, indicate that complexes where the three phosphorus atoms of the Triphos exist in two different environments are present, whilst the broad signals observed in both spectra suggest species that are undergoing exchange. The transient nature of the doublet and triplet at δ 15.3 and 3.7 ppm, seen in the initial spectrum but

not the later (Figure 4.8A and 4.8B), could be generated by [Ru(Triphos)H_2] or [Ru(Triphos)H_2(THF)].

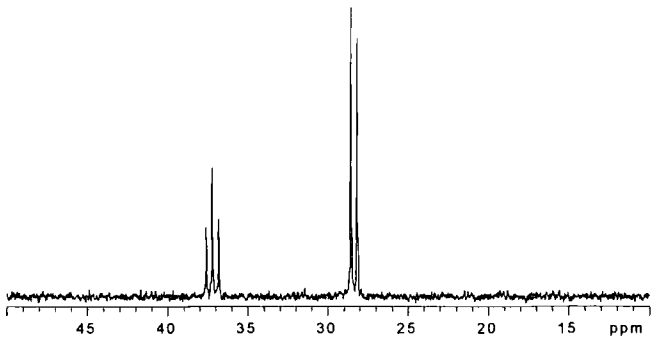

Figure 4.7 The ^{31}P NMR of [Ru(Triphos)H_2(CO)]

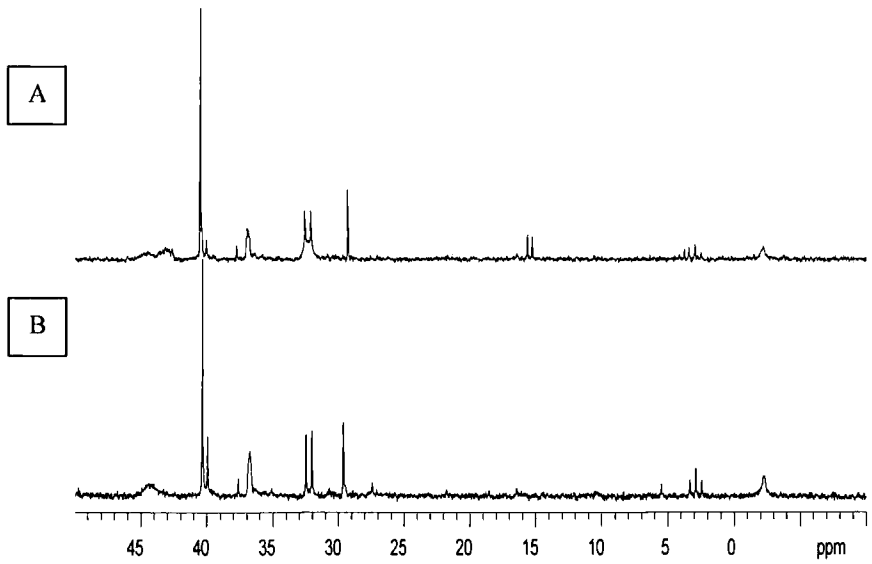

Figure 4.8 ^{31}P NMR Spectrum of the Product of [Ru(Triphos)H_2(CO)] + H_2O

A, initial spectrum.
$^{31}P\{^1H\}$NMR (25°C, chloroform-*d*): δ 44.5 (**?P**), 43.1 (**?P**), 40.5 (**3P**, s), 40.0 (**3P**, s), 37.5 (**3P**, s), 37.0 (**?P**), 32.5 (**2P**, d, $^2J_{P\text{-}P}$ = 35 Hz), 29.3 (**3P**, s), 15.3 (**2P**, d, $^2J_{P\text{-}P}$ = 28 Hz), 3.7 (**P**, t, $^2J_{P\text{-}P}$ = 28 Hz), 2.9 (**P**, t, $^2J_{P\text{-}P}$ = 35 Hz), –2.0 (**?P**) ppm.
B, spectrum seven days later.
$^{31}P\{^1H\}$NMR (25°C, chloroform-*d*): δ 44.2 (**?P**), 40.5 (**3P**, s), 40.5 (**3P**, s), 37.5 (**3P**, s),), 37.0 (**?P**), 32.5 (**2P**, d, $^2J_{P\text{-}P}$ = 35 Hz), 29.6 (**3P**, s), 27.5 (**3P**, s), 5.5 (**3P**, s), 2.9 (**P**, t, $^2J_{P\text{-}P}$ = 35 Hz) –2.2 (**?P**) ppm.

4.2.3 Hydrogenation with $Ru(acac)_3$ and Triphos in the presence of H_2O

The hydrogenation of ester and acid substrates using [Ru(Triphos)H_2(CO)] as the catalytic precursor (subsequently activated for catalysis by the water gas shift reaction), suggested that greater levels of substrate conversion could be obtained in hydrogenations using the catalytic precursors $Ru(acac)_3$ and Triphos with the inclusion of an excess of water in the reaction conditions.

When an excess of water was included and the temperature increased to 140°C, hydrogenations using the $Ru(acac)_3$ and Triphos catalytic system obtained levels of substrate conversion comparable with those attained when [Ru(Triphos)H_2(CO)] was used with water. The ester and acid substrates were hydrogenated almost to completion (see Table 4.3) for hydrogenation of methyl propanoate and dimethyl maleate (DMM), and Table 4.4 for maleic acid (see also Chapter 5).

Table 4.3 Ester Hydrogenation by $Ru(acac)_3$ and Triphos in H_2O

Ester	Conversion (%)	Product & Selectivity For (%)
Methyl Propanoate	98.2	1-Propanol (98.4) [a]
Dimethyl Maleate (DMM)	97.2	THF (23.1) [b] gBL (14.5) BDO (48.4)

Conditions: $p(H_2)$ = 6.8MPa, 140°C, methyl propanoate 40 hours and DMM 64 hours.
a: Propyl propanoate and propionic acid also obtained, in low yield.
b: Dimethyl succinate also obtained, in low yield.
Note : MeOH was also produced in both cases, but not included in above.

Table 4.4 Maleic Acid Hydrogenation by $Ru(acac)_3$ and Triphos in H_2O

Maleic Acid Conversion (%) [a]	THF Selectivity (%)	gBL Selectivity (%)	BDO Selectivity (%)
98.4 [b]	67.05	12.71	15.15

Conditions: $p(H_2)$ = 6.8MPa, 180°C, 18 hours.
a: Conversion calculated by acid titration, with 0.1M KOH.
b: Succinic acid also obtained, in low yield.

The analysis of the respective headspace gases, on completion of the hydrogenations, detected the presence of CO_2 and CO. This indicates that although a greater level of substrate conversion occurs, for the hydrogenations using the catalytic precursors $Ru(acac)_3$ and Triphos with H_2O, the catalyst still decarbonylates the products to produce [Ru(Triphos)H_2(CO)] and it is the water gas shift reaction reactivation of the catalyst that enables the substrate conversion to continue.

4.2.3 Synthesis of [Ru(Triphos)H_2(CO)]

The complex [Ru(Triphos)H_2(CO)] was synthesised by an alternate route to that of the hydrogenation reactions, and characterised by NMR spectroscopy, IR spectroscopy and elemental analysis. The objective was to use the synthesised [Ru(Triphos)H_2(CO)] for investigations of the chemistry of the carbonyl removal. The synthetic route used $NaBH_4$ to replace Cl ligands in [Ru(Triphos)Cl_2(CO)] (which was prepared as per the literature [33]). The synthesis used, produced [Ru(Triphos)H_2(CO)], but the product was difficult to purify. Analysis indicated that unconsumed [Ru(Triphos)Cl_2(CO)] was present, and a second product believed to be [Ru(Triphos)H(CO)Cl]. The ^{31}P NMR spectrum of the synthesis product indicates the presence of three species, represented by; (i) three doublets of doublets ([Ru(Triphos)H(CO)Cl]), (ii) a triplet with a doublet ([Ru(Triphos)H_2(CO)]) and (iii) a doublet with a triplet ([Ru(Triphos)Cl_2(CO)]). $^{31}P\{^1H\}$ NMR (chloroform-*d*): (i) δ 50.0 (**P**, dd, $^2J_{P-P}$ = 40 Hz and 17 Hz), 13.3 (**P**, dd, $^2J_{P-P}$ = 40 Hz and 32 Hz), 0.7 (**P**, dd, $^2J_{P-P}$ = 32 Hz and 17 Hz) ppm, (ii) δ 35.3 (**P**, t, $^2J_{P-P}$ = 32 Hz), 27.8 (**2P**, d, $^2J_{P-P}$ = 32 Hz) ppm, and (iii) δ 28.8 (**2P**, d, $^2J_{P-P}$ = 41 Hz), -7.2 (**P**, t, $^2J_{P-P}$ = 41 Hz) ppm.

4.2.4 Conclusion

The water gas shift reaction can be used to reactivate the deactivated catalyst, [Ru(Triphos)H_2(CO)]. The addition of water to the reaction and the use of temperatures above 140°C removes the carbonyl ligand from [Ru(Triphos)H_2(CO)] to produce the required vacant site for catalysis.

The hydrogenation of ester and acid substrates using the catalyst system of $Ru(acac)_3$ and Triphos can achieve conversion to completion, when the reaction conditions include water and the higher temperature (of 140°C and above).

The amine oxide, Me_3NO was ineffective at reactivating the deactivated [Ru(Triphos)H_2(CO)] catalyst, as it was unable to remove the carbonyl ligand.

4.3 Experimental

4.3.1 Reactions of [Ru(Triphos)H_2(CO)] with Amine Oxides

All operations involving experimentation with amine oxides were carried out under dry nitrogen using standard Schlenk techniques unless otherwise stated. The reactions were carried out in benzene-d_6 to allow NMR spectroscopy to be combined with IR spectroscopy to monitor the reactions. The NMR spectrum of [Ru(Triphos)H_2(CO)] is distinctive, with the ^{31}P NMR generating a triplet and doublet at δ 37 and 28 ppm and the ^{1}H NMR hydride region displaying a doublet of doublets at δ -6.4 ppm. The IR of [Ru(Triphos)H_2(CO)] in benzene-d_6 has a carbonyl stretching band, ν(CO), at 1943 cm^{-1} (see Chapter 2, Homogeneous Ester Hydrogenation, 2.2.4 [Ru(Triphos)H_2(CO)] Characterisation).

4.3.1.1 [Ru(Triphos)H_2(CO)] + Me_3NO + C_6D_6

[Ru(Triphos)H_2(CO)] (0.01g, 1.3 x 10^{-5} mol) and Me_3NO (0.005g, 6.6 x 10^{-5} mol) were dissolved in benzene-d_6 (3.0 ml) and the mixture heated to reflux temperature under nitrogen for 2 hours, then allowed to cool, before a sample was removed for analysis by NMR and IR spectroscopy.

4.3.1.2 [Ru(Triphos)H_2(CO)] + Me_3NO + C_6D_6 + MeCN

[Ru(Triphos)H_2(CO)] (0.01g, 1.3 x 10^{-5} mol) and Me_3NO (0.005g, 6.6 x 10^{-5} mol) were dissolved in a solution of benzene-d_6 (3.0 ml) and MeCN (0.5 ml), and then the mixture heated to reflux temperature under nitrogen for 2 hours, then allowed to cool, before a sample was removed for analysis by NMR and IR spectroscopy.

4.3.1.3 [Ru(Triphos)H_2(CO)] + C_6D_6

[Ru(Triphos)H_2(CO)] (0.01g, 1.3 x 10^{-5} mol) was dissolved in benzene-d_6 (3.0 ml) and heated to reflux temperature under nitrogen, then allowed to cool, before a sample was removed for analysis by NMR and IR spectroscopy.

4.3.2 Hydrogenations

All hydrogenations were carried out using a 300-ml Hasteloy^{TM} autoclave equipped with overhead stirrer. The autoclave was loaded with the reagents (see Table 4.5) and then the air was removed by flushing three times with hydrogen. The autoclave was then pressurised at r.t. with hydrogen (4.4 MPa). The autoclave was then heated to the respective reaction temperature, the hydrogen mass flow controller set to 6.8 MPa, and the autoclave heated and stirred for 16 hours. On completion of the reaction period, the heating was stopped and the autoclave allowed to slowly cool, over approximately two hours. The headspace gases within the autoclave were slowly vented and the products removed. The product solution was analysed by GC, GCMS and NMR. The product solid was analysed by ^{31}P NMR spectroscopy, and on selected samples by ^{1}H NMR spectroscopy, IR spectroscopy, and elemental analysis. The headspace gas was analysed by Draeger tubes and refinery gas analyser GC.

Table 4.5 Quantity of Reagents used

Reagent	Quantity
[Ru(Triphos)H_2(CO)]	4.5 x 10^{-4} mol
Ru(acac)$_3$	4.5 x 10^{-4} mol
Triphos	6.1 x 10^{-4} mol
Substrate (with H_2O)	20.0 ml
Substrate (with iPA)	20.0 ml
Substrate Only	70.0 ml
IPA	50.0 ml
H_2O	50.0 ml

4.3.3 [Ru(Triphos)H_2(CO)] Synthesis.

[Ru(Triphos)H_2(CO)] was prepared by the conversion of [$RuCl_2(CO)_2(PPh_3)_2$] to [Ru(Triphos)Cl_2(CO)], which is subsequently converted to [Ru(Triphos)H_2(CO)].

[$RuCl_2(CO)_2(PPh_3)_2$] was synthesised as per the procedure of Robinson *et al.*[34] Added successively to a boiling solution of triphenylphosphine (0.78 g, 3.0 mmol) in 2-methoxyethanol (20 cm^3), were hydrated ruthenium trichloride (0.13 g, 0.5 mmol) in 2-methoxyethanol (10 cm^3), aqueous formaldehyde (5 cm^3, 40% w/v solution), potassium hydroxide (0.2 g) in 2-methoxyethanol (10 cm^3), and carbon tetrachloride (5 cm^3). The mixture was heated under reflux for 30 minutes, cooled and then diluted with methanol (30 cm^3). The precipitate was washed with ethanol, water and ethanol before recrystallization from dichloromethane-methanol to produce white crystals.
Yield 0.23 g, 62.1 % (Found: C, 59.99; H, 4.10. $C_{38}H_{30}Cl_2O_2P_2Ru$ requires: C, 60.65; H, 4.02).

[Ru(Triphos)Cl_2(CO)] was synthesised as per the procedure of Collman *et al.*[33] [$RuCl_2(CO)_2(PPh_3)_2$] (g, 0.1 mmol) and Triphos (g, 0.1 mmol) were added to toluene (10 cm^3) and heated for 6 hours at 120°C. The yellow precipitate was collected by filtration and washed in *n*-hexane, and dried.
Yield 74 % (Found: C, 60.51; H, 4.70. $C_{42}H_{39}Cl_2OP_3Ru$ requires: C, 61.07; H, 4.77).

[Ru(Triphos)H_2(CO)] was prepared by the addition of [Ru(Triphos)Cl_2(CO)] and $NaBH_4$ to a boiling solution of ethanol (20 cm^3). The yellow precipitate was washed with ethanol, water and ethanol and recrystallized in toluene.
Yield (Found: C, 65.14; H, 5.28. $C_{42}H_{41}OP_3Ru$ requires: C, 66.65; H, 5.46). IR: (r.t., cm^{-1}) ν(CO) = 1920 cm^{-1} (Nujol Mull). $^{31}P\{^1H\}$ NMR (chloroform-*d*): (i) δ 50.0 (**P**, dd, $^2J_{P\text{-}P}$ = 40 Hz and 17 Hz), 13.3 (**P**, dd, $^2J_{P\text{-}P}$ = 40 Hz and 32 Hz), 0.7 (**P**, dd, $^2J_{P\text{-}P}$ = 32 Hz and 17 Hz) ppm, (ii) δ 35.3 (**P**, t, $^2J_{P\text{-}P}$ = 32 Hz), 27.8 (**2P**, d, $^2J_{P\text{-}P}$ = 32 Hz) ppm, and (iii) δ 28.8 (**2P**, d, $^2J_{P\text{-}P}$ = 41 Hz), -7.2 (**P**, t, $^2J_{P\text{-}P}$ = 41 Hz) ppm.

4.3.4 NMR Spectroscopy

The NMR spectra of the product solutions were measured against an external reference of chloroform-*d* containing Triphos, which was used to lock and shim the NMR spectrometer. The product solids were dissolved in the appropriate *deuterated* solvent and the NMR spectrometer locked and shimmed accordingly, prior to recording the spectrum.

4.4 References

1. D.F. Shriver, P. W. Atkins and C. H. Langford, *Inorganic Chemistry*, Oxford University Press, Oxford, 2nd edn., 1995.
2. R. H. Crabtree, *The Organometallic Chemistry of the Transition Metals*, John Wiley & Sons, New York, 2nd edn., 1994.
3. G. O. Spessard and G. L. Miessler, *Organometallic Chemistry*, Prentice-Hall International (UK) Ltd., London, 1997.
4. H. Beyer and W. Walter, *Handbook of Organic Chemistry*, Simon and Schuster International Group, Hemel Hempstead, 1996.
5. M. O. Albers and N. J. Coville, *Coord. Chem. Rev.*, 1984, **53**, 227.
6. A. Albini, *Synthesis*, 1993, 263.
7. D. J. Blumer, K. W. Barnett and T. L. Brown, *J. Organomet. Chem.*, 1979, **173**, 71.
8. J. K. Shen, Y. C. Gao, Q. Z. Shi and F. Basolo, *J. Organomet. Chem.*, 1991, **401**, 295.
9. J. K. Shen, L. L. Shi, Y. C. Gao, Q. Z. Shi and F. Basolo, *J. Am. Chem. Soc.*, 1988, **110**, 2414.
10. J. K. Shen, Y. C. Gao, Q. Z. Shi and F. Basolo, *Organometallics*, 1989, **8**, 2144.
11. D. S. C. Black, G. B. Deacon and N. C. Thomas, *Inorg. Chim. Acta*, 1981, **54**, L143.
12. D. S. C. Black, G. B. Deacon and N. C. Thomas, *Inorg. Chim. Acta*, 1982, **65**, L75.
13. F. A. Cotton, G. Wilkinson and P. L. Gaus, *Basic Inorganic Chemistry*, John Wiley & Sons, Inc., Chichester, 3rd edn.,1995.
14. *Catalyst Handbook*, ed. M. V. Twigg, Manson Publishing Ltd., Frome, 2cnd edn., 1996.
15. J. P. Collman, L. S. Hegedus, J. R. Norton and R. G. Finke, *Principles and Applications of Organotransition Metal Chemistry*, University Science Books, Mill Valley, CA, 2cnd edn., 1987.
16. F. A. Cotton and G. Wilkinson, *Advanced Inorganic Chemistry*, John Wiley & Sons, Inc., Chichester, 5th edn., 1988.
17. P. C. Ford and A. Rokicki, *Adv. Organomet. Chem.*, 1988, **28**, 139.
18. *Aqueous-Phase Organometallic Catalysis*, eds. B. Cornils and W. A . Hermann, Wiley-VCH, Weinheim, 1998.
19. *Applied Homogeneous Catalysis with Organometallic Compounds*, eds. B. Cornils and W. A . Hermann, Wiley-VCH, Weinheim, 2000.
20. T. Venäläinen,, T. A. Pakkenen, T. T. Pakkenen and E. Iiskola, *J. Organomet. Chem.*, 1986, **314**, C49.
21. E. W. Abel, F. G. A. Stone and G. Wilkinson, *Comprehensive Organometallic Chemistry*, Pergamon Press, Oxford, 1987, Vol. 4.
22. P. C. Ford, *Acc. Chem. Res.*, 1981, **14**, 31.

23. D. J. Cole-Hamilton, *J. Chem. Soc., Chem. Commun.*, 1980, 1213.
24. H. Ishida, K. Tonka, M. Morimoto and T. Tanaka, *Organometallics*, 1986, **5**, 724.
25. T. Yoshida, T. Yamagata, T. H. Tulip, J. A. Ibers and S. Otsuka, *J. Am. Chem. Soc.*, 1978, **100**, 2063.
26. C. H. Cheng, D. E. Hendrikson and R. Eisenberg, *J. Am. Chem. Soc.*, 1977, **99**, 2791.
27. P. Mahajan, C. Creutz and N. Suitin, *Inorg. Chem.*, 1985, **24**, 2063.
28. P. C .Ford, R. G. Rinker, R. M. Laine, C. Ungermann, V. Landis and S. A. Moya, *J. Am. Chem. Soc.*, 1978, **100**, 4595.
29. G. L. Geoffroy and M. G. Bradley, *Inorg. Chem.*, 1977, Vol. 16, **4**, 744.
30. D. M. Adams, *Metal-Ligand and Related Vibrations*, Edward Arnold (Publishers) Ltd., London, 1967.
31. E. A. V. Ebsworth, D. W. H. Rankin and S. Cradock, *Structural Methods in Inorganic Chemistry*, Blackwell Scientific Publications, London, 2nd edn., 1991.
32. N. N. Greenwood and A. Earnshaw, *Chemistry of the Elements*, Pergamon Press plc, Oxford, 1986.
33. W. O. Siegl, S. J. Lapporte and J. P. Collman, *Inorg. Chem.*,1973, **12**, **3**, 674.
34. N. Ahmad, S. D. Robinson and M. F. Uttley, *J. Chem. Soc., Dalton Trans.*, 1972, 843.

Chapter 5

Homogeneous Acid Hydrogenation

The homogeneous hydrogenation of the carboxylic acids propanoic, dodecanoic, maleic, fumaric and succinic, the anhydride of maleic acid, and the amino acid (+/-) 2-phenylglycine was achieved by the catalyst generated in situ from $Ru(acac)_3$ and the tripodal triphosphine Triphos. The hydrogenation of the monocarboxylic acids produced predominantly alcohols, whilst the products of the bicarboxylic acids and anhydride hydrogenations included the diol 1,4-butanediol with both the cyclic ether tetrahydrofuran and the lactone γ-butyrolactone. The ratio of the products obtained was controlled by adjustment of the reaction temperature.

5.1 Introduction

The hydrogenation of carboxylic acids produces primary alcohols (see Equation 5.1). The reduction can be achieved using either reducing agents or catalytic hydrogenation. The more common reducing agents are metal hydrides, such as $LiAlH_4$, which are particularly effective, and BH_3.[1] Catalytic hydrogenation is predominantly based on heterogeneous systems operating at high temperatures (150-250°C) and pressures (20-30 MPa), usually containing copper chromite or zinc chromite catalysts, although ruthenium and rhenium catalysts have also been reported.[2, 3] The limited hydrogenation of carboxylic acids can be accomplished homogeneously with ruthenium catalysts, although they demonstrate greater reactivity with the analogous anhydrides.[4] The catalytic hydrogenation of carboxylic acids is difficult to achieve, with most catalytic systems producing the associated ester or lactone rather than the corresponding alcohol.

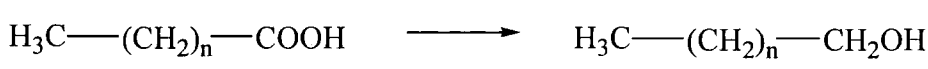

Carboxylic Acid — Primary Alcohol

Equation 5.1

The work of Tóth *et al* [5] on the solublisation of ruthenium catalysts with sulphonated phosphines, was applied to the hydrogenation of unsaturated carboxylic acids (such as crotonic acid) and 2-oxo-carboxylic acids (such as pyruvic acid).[5] Their investigation of the catalysts $[RuCl_2(mSP\text{ø}_2)_2]$, $[HRuCl(mSP\text{ø}_2)_3]$ and $[HRu(OAc)(mSP\text{ø}_2)_3]$ (where $mSP\text{ø}_2$ = *m*-sulphophenyl-diphenylphosphine) found hydrogenation of the unsaturated carboxylic acid C=C bonds and the C=O bond of the 2-oxo-carboxylic acids, but that the acid functional group was unaffected (see Equation 5.2).

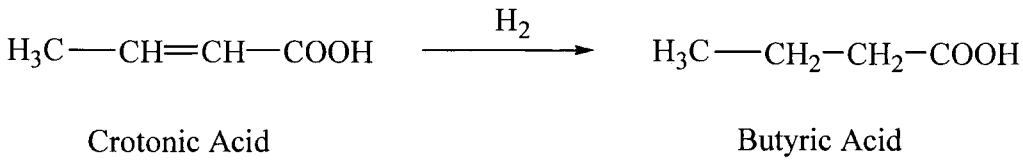

Crotonic Acid Butyric Acid

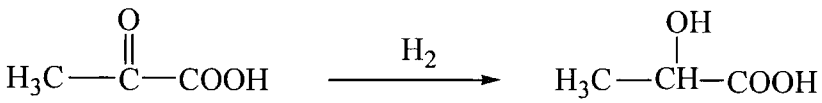

Pyruvic Acid Lactic Acid

Equation 5.2

The hydrogenation of carboxylic acid anhydrides to γ-lactones with $[RuCl_2(PPh_3)_3]$ was reported by Lyons.[6] Succinic anhydride and phthalic anhydride were reduced, at 100°C and 0.02 Pa of hydrogen, to γ-butyrolactone and phthalide respectively (see Equation 5.3). The reaction products also included the corresponding acids, probably as a result of hydrolysis between unreacted anhydride and the water generated by the hydrogenation. Lyons found that the same reduction could not be repeated when the ruthenium catalyst was replaced with the hydrogenation catalysts, $[IrCl(CO)(PPh_3)_2]$, $[RhCl(CO)(PPh_3)_2]$, $[RhCl(PPh_3)_3]$, and $[Co_2(CO)_8]$.

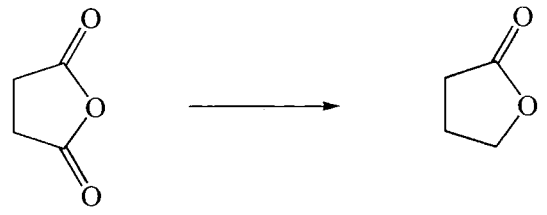

Succinc Anhydride γ-Butyrolactone

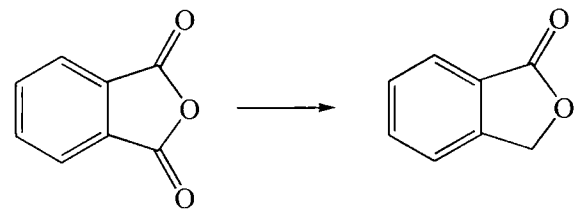

Phthalic Anhydride Phthalide

Equation 5.3

Lyons suggested that the catalytic hydrogenation of the carboxylic anhydrides proceeds by the cleavage of the C=O bond by a ruthenium hydride species, probably $[RuHCl(PPh_3)_3]$. The hydrogenation of the carbonyl and subsequent elimination of water then produces the respective lactone (see Fig. 5.1).

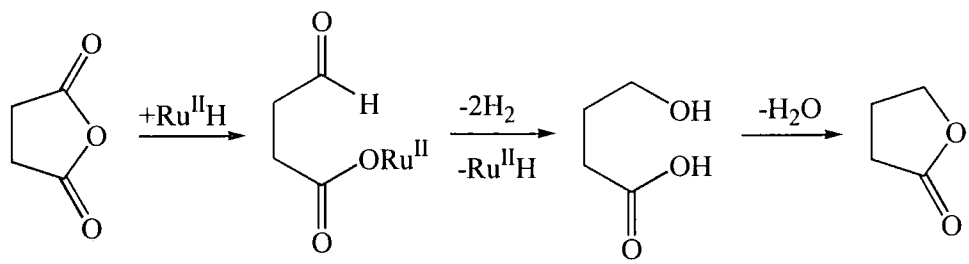

Figure 5.1 Carboxylic Acid Hydrogenation to a Lactone [6]

The regioselective hydrogenation of unsymmetrical substituted cyclic anhydrides is achieved by ruthenium-phosphine catalysts, producing the two isomeric γ-lactones (see Equation 5.4). Morand and Kayser found that $[RuCl_2(PPh_3)_3]$ selectively hydrogenated

the carbonyl group on the unhindered side of the anhydride, which is in contrast to reductions using $LiAlH_4$, which attacks the carbonyl group adjacent to the hindered carbon with the substituent(s).[7] The ruthenium catalysts $[RuCl_2(PPh_3)_3]$, $[Ru_2Cl_4(dppb)_3]$, $[Ru_2Cl_4(diop)_3]$ and $[RuCl_2(ttp)]$ were investigated for the regioselective hydrogenation of substituted anhydrides by Ikariya *et al.*[8] The study established that the regioselectivity of hydrogenation was due to steric interaction between the catalysts bulky phosphine ligands and the respective substituents. The steric hindrance of the substituent on the lactone was greater than any electronic effect, with the exception of phenyl substituents when the electron withdrawing phenyl group weakens the adjacent C=O bond, thus allowing hydrogenation on the hindered side to proceed. The hydrogenation of the respective anhydride halted at the γ-lactone, no alcohols being produced.

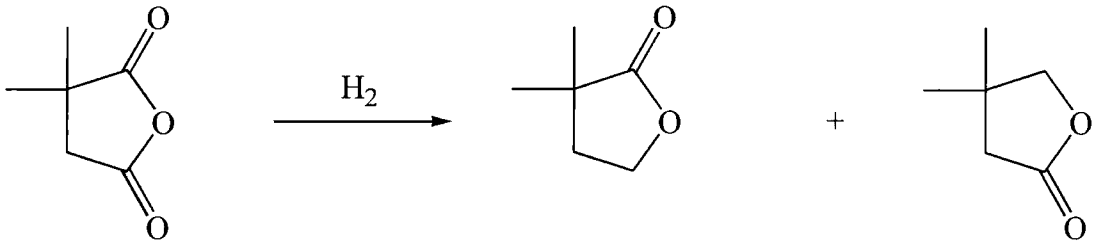

2,2-dimethylsuccinic Anhydride

Lactones

Equation 5.4

The homogeneous hydrogenation of carboxylic acids by a ruthenium carbonyl hydride cluster was investigated by Matteoli *et al.*[9] They reported the hydrogenation of citraconic and mesaconic acids by $[H_4Ru_4(CO)_8\{(-)\text{-DIOP}\}_2]$, to produce predominantly (-)(s)-methyl succinic acid and a mixture of γ-lactones, in low yields (see Equation 5.5). The homogeneous hydrogenation of saturated monocarboxylic acids (up to C_6), some bicarboxylic acids and the analogous anhydrides with the catalyst $[H_4Ru_4(CO)_8(PBu_3)_4]$ was more successful. Matteoli *et al* reported that the carboxylic group of alkanoic acids could be hydrogenated in high yields to produce the respective alcohols, which in most cases was then consumed to create the associated ester with the original acid.[10] The catalyst's inability to hydrogenate the ensuing ester resulted in no, or low, yields of alcohols being present among the products.

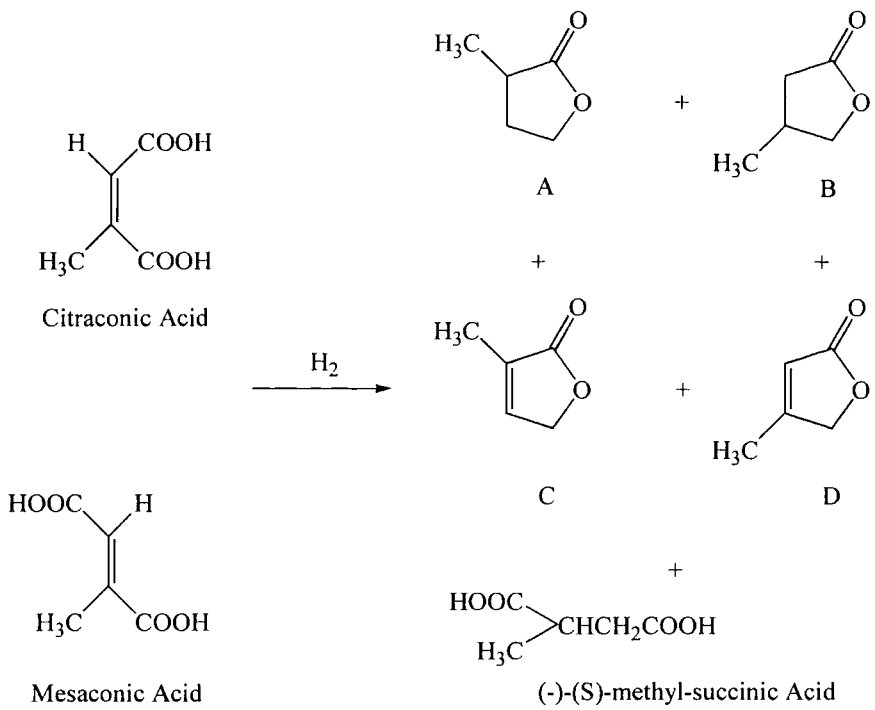

Equation 5.5

A: α-methyl-γ-butyrolactone
B: β-methyl-γ-butyrolactone
C: α-methyl-$\Delta^{\alpha,\beta}$-butenolide
D: β-methyl-$\Delta^{\alpha,\beta}$-butenolide

The ruthenium catalytic system developed by Hara and Wada *et al* can hydrogenate succinic anhydride to produce 1,4-butanediol (BDO) (see Equation 5.6).[11-16] The catalytic system comprises a catalyst generated *in situ* from $Ru(acac)_3$ and trioctylphosphine with a phosphoric acid ester additive. The reaction is carried out under H_2 (5 MPa) at 200-210°C. The ruthenium complex was determined as being cationic with a structure that was deduced as being $[RuH(H_2)(PR_3)_3S]X$ or $[RuH(PR_3)_3S_2]X$ (where S = solvent). The cationic complex was found to be effective for the hydrogenation of both succinic acid and γ-butyrolactone to produce BDO, the effectiveness being attributed to the complex activating the carbonyl group and therefore accelerating hydride transfer.

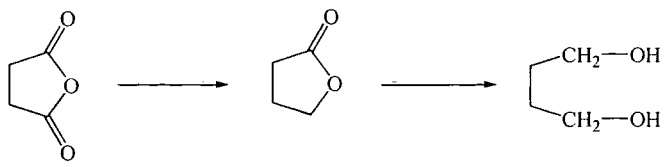

Succinc Anhydride γ-Butyrolactone 1,4-Butanediol

Equation 5.6

5.1.1 Summary

The industrial catalytic reduction of carboxylic acids uses predominantly heterogeneous catalysts. The products of the reduction are usually the associated ester, with little or no alcohol products present. The homogeneous hydrogenation of carboxylic acids is possible using ruthenium complexes, although as with the majority of the heterogeneous systems, the products are usually the respective ester of the original acid. The catalytic system of Hara and Wada *et al* is the only homogeneous system reported, that is capable of producing alcohol as a major product of the reaction, in good yield with roughly 40% selectivity for BDO in the hydrogenation of succinic anhydride.[14, 16]

The inability of the catalysts investigated to hydrogenate the esters produced from the acid reduction is the barrier to producing alcohols by direct reduction of carboxylic acids.

5.2 Results and discussion

The catalyst, that is generated *in-situ* from $Ru(acac)_3$ and the tripodal triphosphine Triphos, was investigated for the hydrogenation of carboxylic acids.

5.2.1 Hydrogenation of Monocarboxylic Acids

Hydrogenation of monocarboxylic acids was achieved by the catalyst. Propionic acid and dodecanoic acid were hydrogenated to their respective alcohols, with high levels of conversion and in high yield (see 5.2.1.1). The hydrogenation of the amino acid (+/-) 2-phenylglycine ($PhCH(NH_2)CO_2H$) was also investigated. The reduction produced a large number of different products (see 5.2.1.2).

5.2.1.1 Hydrogenation of Propionic and Dodecanoic Acids

Propionic acid can be hydrogenated to 1-propanol with a conversion of almost 100% and with selectivity for the alcohol product of greater than 95% (see Table 5.1). The hydrogenation of dodecanoic acid achieved a conversion of > 90% and selectivity for 1-dodecanol of almost 80% (see Table 5.1).

Table 5.1 Hydrogenation of Propionic and Dodecanoic Acids

Acid	Specific Conditions	Conversion (%)	Alcohol Selectivity (%)	Ester Selectivity (%)
Propionic	120°C iPA (Solvent)	30.3 [a]	27.64	3.61
Propionic	140°C No Solvent	42.1	16.08	40.44
Propionic	140°C H_2O	98.6	95.94	2.97
Dodecanoic	140°C H_2O	92.3 [b]	79.1	1.5

Common reaction conditions: $p(H_2)$ = 6.8 MPa, 16 hours.
a: The products included [Ru(Triphos)H_2(CO)].
b: The products of the hydrogenation of dodecanoic acid included undecane.

To obtain the maximum conversion of propanoic acid the reaction requires the presence of water and a temperature of 140°C (or greater). The water and 140°C temperature allows the water gas shift (WGS) reaction to reactivate the catalyst, which is deactivated by decarbonylation of the hydrogenation products (see Chapter 3, Catalyst Deactivation, and Chapter 4, Catalyst Reactivation). From Table 5.1, it can be seen that when the propionic acid hydrogenation was conducted at 120°C, with iPA as a solvent, only a 30% conversion was obtained. The products of the reaction included the deactivated catalyst [Ru(Triphos)H_2(CO)], as a precipitate. The [Ru(Triphos)H_2(CO)] indicates that catalyst reactivation has not occurred. Reduction of carboxylic acids produces a primary alcohol and H_2O (see Equation 5.7), but for the catalyst reactivation to occur, *via* the WGS reaction, the temperature is required to be greater than 120°C. When the reaction was performed at 140°C a greater level of propionic acid conversion was achieved and the deactivated catalyst [Ru(Triphos)H_2(CO)] was not observed in the products. The higher level of ester product obtained when the reaction is carried out in the absence of a solvent, iPA or water, is probably due to the higher concentration of acid available to esterify the product alcohols. The ability of the catalyst to hydrogenate esters would allow an extended reaction period to eventually consume the ester by-product, and generate predominantly alcohol as the reaction product.

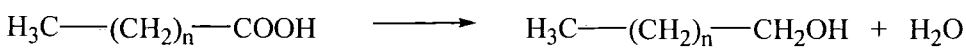

Carboxylic Acid Primary Alcohol

Equation 5.7

The optimum reaction conditions from the propionic acid reduction were applied to the dodecanoic acid hydrogenation. The product comprised a biphasic solution, with a dark brown coloured organic upper layer and a clear aqueous lower layer. From Table 5.1 it can be seen that the level of conversion achieved was over 90%. The level of esterification of the product was low, with almost 80% selectivity for 1-dodecanol. The product solution contained undecane from the decarbonylation of the alcohol and traces of dodecanal from dehydrogenation of the alcohol (see Chapter 3), but the deactivated catalyst [Ru(Triphos)H_2(CO)] was not observed. The presence of undecane and dodecanal in the products accompanied by a lack of [Ru(Triphos)H_2(CO)] demonstrates that the WGS reaction has maintained catalytic activity during the reaction.

5.2.1.2 Hydrogenation of (+/-) 2-Phenylglycine

The hydrogenation of the amino acid (+/-) 2-phenylglycine was carried out in water at a temperature of 180°C. The higher temperature of 180°C was used because although (+/-) 2-phenylglycine has a melting point of ca. 300°C the combination of the water and the higher temperature would allow the amino acid to become sufficiently soluble to be hydrogenated. The catalyst hydrogenated (+/-) 2-phenylglycine, to produce a variety of different products. The large number of different products required analysis by GCMS, and due to the presence of a significant number of unidentified compounds the analysis was qualitative only. Fig. 5.2 details the products of the hydrogenation that were identified.

Figure 5.2 (+/-) 2-Phenylglycine Hydrogenation Products

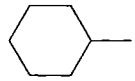

Methyl Cyclohexane

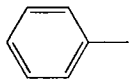

Toluene

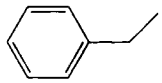

Ethyl Benzene

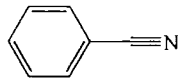

Benzonitrile

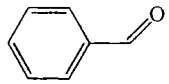

Benzaldehyde

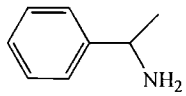

1-methylbenzylamine

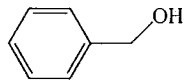

Benzyl Alcohol

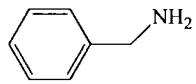

Benzylamine

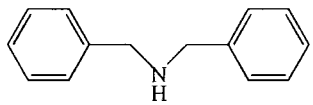

Dibenzylamine

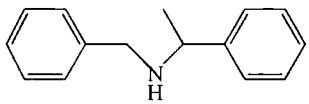

Benzyl-1-methylbenzylamine

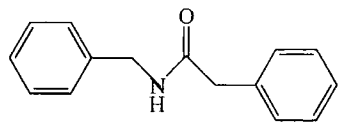

Benzylbenzenacetamide

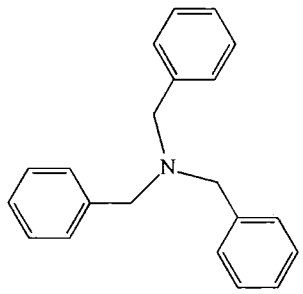

Tribenzylamine

The products obtained indicate that, under the catalytic conditions used, the catalyst is a powerful reducing agent. The lack of selectivity of the catalyst produced a homogeneous mixture of products that included amines, alcohols, aryls and alkyls. The major hydrogenation products were the amines dibenzylamine and benzylamine, and the alcohol benzyl alcohol. Toluene, 1-methylbenzamine and benzyl-1-methylbenzylamine were also obtained as minor products. All the other products detailed in Fig. 5.2 were detected only as traces.

5.2.2 Hydrogenation of Bicarboxylic Acids

The $Ru(acac)_3$ and Triphos catalytic system will hydrogenate maleic and fumaric acids, *via* succinic acid, to produce a mixture of γ-butyrolactone (gBL), tetrahydrofuran (THF) and 1,4-butanediol (BDO) (see Fig. 5.3).

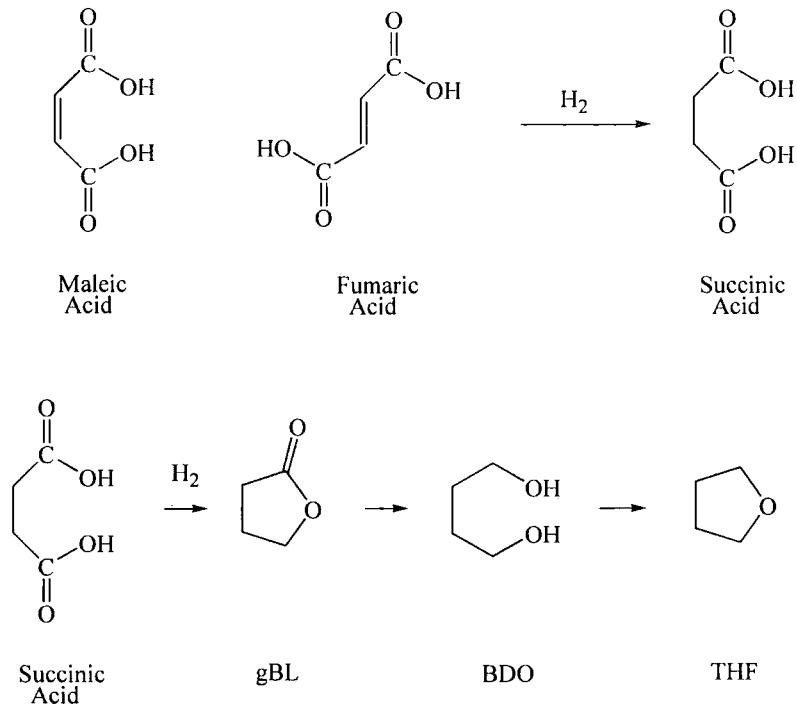

Figure 5.3 Maleic Acid Hydrogenation

The reduction of malonic acid ($H_2OCCH_2CO_2H$) to alcohol products was also attempted, but this reaction was not so successful, with acetic acid being the major

product, no further reduction products being observed. This result was comparable to that obtained by Matteoli *et al* for the hydrogenation of malonic acid.[9, 10]

5.2.2.1 Hydrogenation of Maleic and Fumaric Acids

The hydrogenation of maleic acid was conducted in water as a solvent and at temperatures of 140-200°C. The conditions selected for the hydrogenation reactions took account of the melting point of maleic acid (c.a. 140°C) and succinic acid, the first hydrogenation product (180°C) (see Fig 5.4).

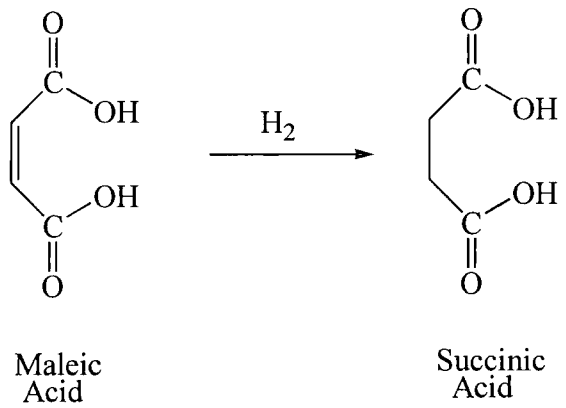

Figure 5.4 Maleic Acid Hydrogenation to Succinic Acid

The hydrogenation of maleic acid can achieve almost 100% conversion (see Table 5.2) at 180°C to 200°C. The lower level of conversion obtained at the temperature of 140°C is possibly due to the poor solubility of succinic acid in the reaction medium at that temperature. The catalytic system is able to hydrogenate both isomers, maleic and fumaric, to the same level of conversion at 180°C. As fumaric acid has a melting point of c.a. 300°C, the comparable level of conversion with maleic acid, is probably because the hydrogenation of the C=C double bond is *facile* and allows the reaction equilibrium to drive the solubility of the fumaric acid favourably in the desired direction. The catalyst is also able to hydrogenate the anhydride of maleic acid to the same level of conversion (see Table 5.2).

Table 5.2 Hydrogenation of Maleic, Fumaric Acids and Maleic Anhydride

Substrate	Temperature (°C)	Conversion (%) [a, b]
Maleic Acid	140	53.5
Maleic Acid	180	98.4
Maleic Acid	200	97.4
Fumaric Acid	180	98.2
Maleic Anhydride	180	98.4

Common reaction conditions: $p(H_2)$ = 6.8 MPa, 16 hours.
a: Conversion calculated by titration as the acid component.
b: Conversion to gBL, THF and BDO.

The products of the hydrogenation of maleic or fumaric acid are succinic acid, gBL, THF and BDO. Small amounts of the primary alcohol 1-propanol are also obtained, and analysis of the head space gas at the end of the reaction detected CO_2. The presence of CO_2 in the products indicates that catalyst deactivation and reactivation *via* the WGS reaction occurred.

The ratio of products obtained in the hydrogenation of maleic acid is dependent on the reaction conditions employed. Table 5.3 details the selectivity of the products obtained at 140°C, 180°C and 200°C. At 140°C the ratio of THF:gBL:BDO is of the order 6:8:1, and at 180°C it is 12:2:3, whereas at 200°C it is 2:2:1. This shows that the reaction temperature influences the ratio of the products obtained, and suggests that control of the reaction conditions would lead to a greater yield of a desired product i.e. 180°C preferentially produces THF as the major product.

Table 5.3 Maleic Acid Product Ratio as a Function of Temperature

Temperature (°C)	THF Selectivity (%)	gBL Selectivity (%)	BDO Selectivity (%)	THF:gBL:BDO ≈ Ratio
140	35.2	47.8	6.6	6:8:1
180	66.3	12.9	15.4	12:2:3
200	42.4	36.6	18.1	2:2:1

5.2.3 NMR Spectroscopy of Products

The ^{31}P NMR spectra generated from the product solutions of the successful carboxylic acid hydrogenations all displayed the same signals. The initial spectra include three different "triplet-doublet" combinations, which with time, results in one of the "triplet-doublet" combinations disappearing (see Fig. 5.5). The triplet and doublets observed are coupled, which indicates that they represent complexes where the three phosphorus atoms of the Triphos exist in two different environments. The transient nature of the doublet and triplet at δ 15.3 and 3.7 ppm, which were detected in the initial spectra but not the later (Figure 5.5A and 5.5B), could be due to the [Ru(Triphos)H_2] or [Ru(Triphos)H_2Solv.] species. Unfortunately, the proton rich product solution made it impossible to obtain a ^{1}H NMR of the metal-hydride region to confirm this.

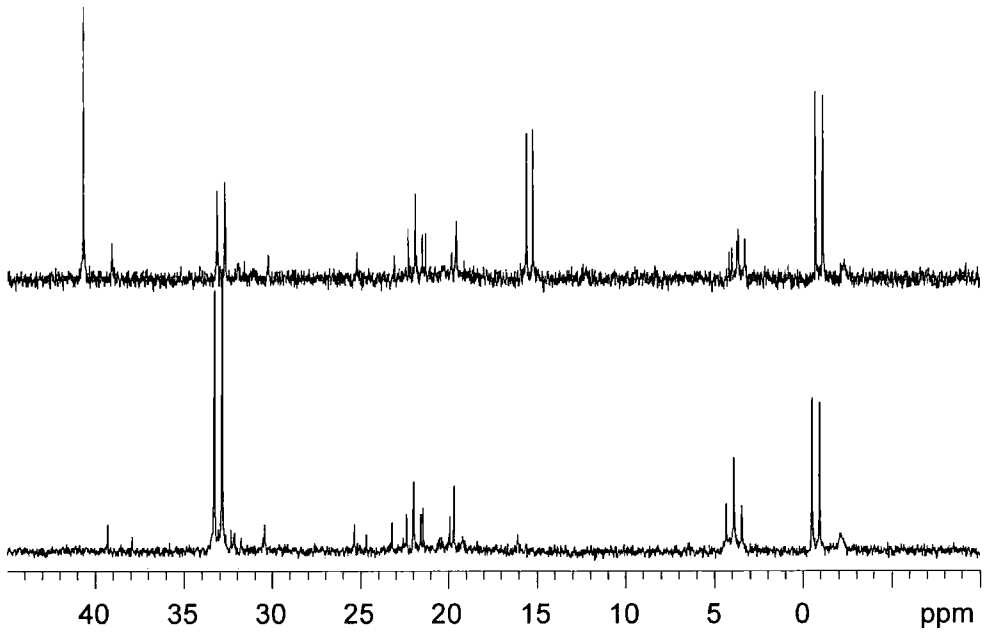

Figure 5.5 ^{31}P NMR Spectrum of Carboxylic Acid Product Solution

A, initial spectrum.
$^{31}P\{^{1}H\}$NMR (25°C, chloroform-*d*): δ 40.7 (**3P**, s), 39.1 (**3P**, s), 32.8 (**2P**, d, $^{2}J_{P\text{-}P}$ = 35 Hz), 30.4 (**3P**, s), 25.4 (**3P**, s), 23.1 (**3P**, s), 22.2 (**P**, t, $^{2}J_{P\text{-}P}$ = 32 Hz), 21.3 (**3P**, s), 19.6 (**3P**, s), 15.3 (**2P**, d, $^{2}J_{P\text{-}P}$ = 28 Hz), 3.7 (**P**, t, $^{2}J_{P\text{-}P}$ = 35 Hz), 3.6 (**P**, t, $^{2}J_{P\text{-}P}$ = 28 Hz), – 0.8 (**2P**, d, $^{2}J_{P\text{-}P}$ = 32 Hz) ppm.
B, spectrum seven days later.
$^{31}P\{^{1}H\}$NMR (25°C, chloroform-*d*): δ 39.3 (**3P**, s), 37.9 (**3P**, s), 33.1 (**2P**, d, $^{2}J_{P\text{-}P}$ = 35 Hz), 30.4 (**3P**, s), 25.3 (**3P**, s), 23.2 (**3P**, s), 21.9 (**P**, t, $^{2}J_{P\text{-}P}$ = 32 Hz), 21.4 (**3P**, s), 19.9 (**3P**, s), 19.7 (**3P**, s), 16.0 (**3P**, s), 3.9 (**P**, t, $^{2}J_{P\text{-}P}$ = 35 Hz) – 0.6 (**2P**, d, $^{2}J_{P\text{-}P}$ = 32 Hz) ppm.

The ^{31}P NMR spectra obtained from the product solutions of the acid hydrogenations are significantly different from those obtained for the hydrogenation of esters, where only a series of singlets is observed (see Chapter 2, Fig. 2.3). The reason for this is probably because the ^{31}P NMR of the ester hydrogenation is generated at the end of the catalytic process by catalyticaly inactive or deactivated species, whereas the ^{31}P NMR of the acid hydrogenations is generated by species that either continue to be catalyticaly active or are the stable intermediates/precursors of them.

5.2.4 Conclusion

The catalytic system of $Ru(acac)_3$ and Triphos in the presence of H_2O at 140°C is able to hydrogenate carboxylic acids completely to alcohols in high yield. The catalyst's ability also to hydrogenate esters ensures that alcohols are the products of hydrogenation. The reaction conditions can be adjusted to allow the products of the reaction to be influenced, enabling the ratio of alcohols and other derived products to be controlled.

The mixture of products obtained in the hydrogenation of the amino acid (+/-) 2-phenylglycine demonstrated that the catalyst is a powerful reducing agent, enabling other transformations to be achieved additional to the acid to alcohol conversion. The result of the maleic acid hydrogenations, where the ratio of products obtained was influenced by control of the conditions, suggests that it may be possible also to control the (+/-) 2-phenylglycine hydrogenation products, possibly also through either careful choice of temperature or the duration of the reaction.

5.3 Experimental

5.3.1 Hydrogenations

All hydrogenations were carried out using a 300-ml Hasteloy™ autoclave equipped with overhead stirrer. The autoclave was loaded with the reagents (see below, 5.3.1.1) and then the air was removed by flushing three times with hydrogen under pressure. The autoclave was then pressurised at r.t. with hydrogen (4.4 MPa), then heated to the respective reaction temperature, at which the hydrogen mass flow controller was set to 6.8 MPa. The reaction mixture was then heated and stirred for 16 hours. On completion

of the reaction period, the heating was stopped and the autoclave allowed to slowly cool under pressure, over approximately two hours. The headspace gases within the autoclave were slowly vented and the products removed. The product solution was analysed by GC, GCMS, NMR spectroscopy and titration with KOH (0.100 M). The product solid was analysed by ^{31}P NMR spectroscopy and selected samples by ^{1}H NMR spectroscopy, IR, mass spectrometry and elemental analysis. The headspace gas was analysed by Draeger tubes and a GC refinery gas analyser.

5.3.1.1 Quantity of Reagents Used

Table 5.4 Catalyst used for all Reactions

Reagent	Quantity
$Ru(acac)_3$	4.5×10^{-4} mol
Triphos	6.1×10^{-4} mol

Table 5.5 Propionic Acid Hydrogenation Reactions

Reaction	Components	Quantity
@ 120°C	Propionic Acid	20.0 cm^3
	iPA (Solvent)	50.0 cm^3
@ 140°C	Propionic Acid	70.0 cm^3
@ 140°C	Propionic Acid	50.0 cm^3
	H_2O	20.0 cm^3

Table 5.6 Dodecanoic Acid Hydrogenation Reaction

Reagent	Quantity
Dodecanoic Acid	9.98×10^{-2} mol
H_2O	70.0 cm^3

Table 5.7 (+/-) 2-Phenylglycine Hydrogenation Reagents

Reagent	Quantity
(+/-) 2-Phenylglycine	1.38×10^{-1} mol
H_2O	70.0 cm^3

Table 5.8 Maleic and Fumaric Acid, and Maleic Anhydride Hydrogenation Reagents

Reagent	Quantity
Maleic Acid	1.72×10^{-1} mol
Fumaric Acid	1.72×10^{-1} mol
Maleic Anhydride	2.04×10^{-1} mol
H_2O	70.0 cm^3

Table 5.9 Malonic Acid Hydrogenation Reagents

Reagent	Quantity
Malonic Acid	1.92×10^{-1} mol
H_2O	70.0 cm^3

5.3.2 NMR Spectroscopy

The NMR spectra of the product solutions were measured against an external reference of chloroform-*d* containing Triphos, which was used to lock and shim the NMR spectrometer. The product solids were dissolved in the appropriate *deuterated* solvent and the NMR spectrometer locked and shimmed accordingly, prior to running the sample for the required NMR measurements.

5.4 References

1. J. March, *Advanced Organic Chemistry*, John Wiley & Sons, New York, 4th edn., 1992.
2. H. Beyer and W. Walter, *Handbook of Organic Chemistry*, Simon and Schuster International Group, Hemel Hempstead, 1996.
3. M. Toba, S. Tanaka, S. Niwa, F. Mizukami, Z. Koppány, L. Guczi, K. -Y. Cheah and T. -S. Tang, *Applied Catalysis A*, 1999, **189**, 243.
4. E. W. Abel, F. G. A. Stone and G. Wilkinson, *Comprehensive Organometallic Chemistry*, Pergamon Press, Oxford, 1987, Vol. 4.
5. Z. Tóth, F. Joó and M. T. Beck, *Inorg. Chim. Acta*, 1980, **42**, 153.
6. J. E. Lyons, *Chem. Commun.*, 1975, 412.
7. P. Morand and M. Kayser, *Chem. Commun.*, 1976, 315.
8. T. Ikariya, K. Osakada, Y. Ishii, S. Osawa, M. Saburi and S. Yoshikawa, *Bull. Chem. Soc. Jpn.*, 1984, **57**, 897.
9. M. Bianchi, F. Piacenti, P. Frediani, U. Matteoli, C. Botteghi, S. Gladiali and E. Benedetti, *J. Organomet. Chem.*, 1977, **141**, 107.

10. M. Bianchi, G. Menchi, F. Francalanci, F. Piacenti, U. Matteoli, P Frediani and C. Botteghi, *J. Organomet. Chem.*, 1980, **188**, 109.
11. Y. Hara and K. Wada, *Chem. Soc. Jpn., Chem. Lett.*, 1991, 553.
12. K. Wada, Y. Hara and K. Sasaki, U.S. Patent No. 4 892 955 (assigned to Mitsubishi Chemical Industries Ltd.)
13. K. Wada, Y. Hara and K. Sasaki, U.S. Patent No. 5 021 589 (assigned to Mitsubishi Kasei Corporation)
14. Y. Hara and H. Inagaki, U.S. Patent No. 5 077 442 (assigned to Mitsubishi Kasei Corporation)
15. Y. Hara, H. Inagasaki, S. Nishimura and K. Wada, *Chem. Soc. Jpn., Chem. Lett.*, 1992, 1983.
16. H. Inagasaki, S. Nishimura, Y. Hara and K. Wada, *Science and Technology in Catalysis 1994*, 1995, 327.

Chapter 6

Catalyst Recovery and Recycling

The recovery of the catalyst and the separation of the products of the homogeneous hydrogenation of both ester and acid were achieved by distillation of the product solution. The catalyst was recycled and shown to be capable of further substrate hydrogenations in a series of batch reactions. The recovered catalyst was also found to be able to hydrogenate different substrates to those of the original hydrogenation, i.e. acids by the catalyst recovered from ester hydrogenation and vice versa.

6.1 Introduction

The quality of a catalyst is measured against the three major properties of activity, selectivity and life.[1] A successful catalyst will ultimately be required to perform well in all three of these categories. For homogeneous catalysis the last category, life, is the category that poses the most problems for the catalyst, the difficulty of recovery and recycling impinging on its life. The recovery and recycling of homogeneous catalysts in commercial processes usually requires additional stages, which are often expensive. It is the high costs associated with the homogeneous catalyst recovery, which provide a major obstacle in their development and introduction into commercially viable industrial applications. The integrity of the catalyst is important to ensure the purity of the product, although some industrial processes have been developed that allow the catalyst residue to be left in the product, as in the production of the polymer polyethylene.[2, 3] The cost of the catalyst, which frequently comprises expensive late transition metals and ligands, also makes recovery important so as to reduce the expense associated with catalyst loss.

A fundamental property of homogeneous catalysts is their solubility in the reaction medium, and it is this characteristic that is responsible for the difficulties encountered with their separation from products and unconsumed reagents. Separation of homogeneous catalysts is usually achieved by distillation or the application of a specific chemical technique. The use of distillation is only possible where the volatility of the products or reagents is significantly different from that of the dissolved catalyst.

Homogeneous catalysts can be damaged by thermal or chemical stress during recovery.[4] To address this problem, a variety of possible solutions have been investigated. These fall into two main groups: (i) the heterogenisation of the catalyst, and (ii) biphasic catalysis, although biphasic catalysis could also be described as the heterogenisation of homogeneous catalysis, with the catalyst being immobilised by a liquid support.[4]

6.1.1 Anchored Homogenous Catalysts

Heterogenisation of the catalyst is where a homogeneous catalyst is anchored to some form of support. Anchoring the catalyst to the support is usually achieved by displacement of a ligand from the metal-catalyst by a ligand bonded to the support. The linkage between the support and the catalyst is predominantly through covalent bonding, but other systems have been reported that use ionic bonding, chemisorption or physisorption, or the saturation of a solid with a solution containing a homogeneous catalyst. A variety of different supports using both organic and inorganic systems have been studied, with anchoring the metal-catalyst to a polymer being one of the more common methods applied.[5, 6]

The most common organic supports are polymers based on polystyrene, although other polymers such as polyvinyls, polyacrylates and cellulose have also been utilised. The metal-catalyst is predominantly bonded to the support via a ligand attached to the polymer support; direct bonding between the metal and a carbon of the polymer backbone is unusual. The ligands used to provide a link between the support and the metal-catalyst have included amongst others, phosphines, amines, thiols, nitriles, and cyclopentadienes. The polymer usually incorporates some degree of crosslinking, to minimise interaction of the functional group ligands and ensure their availability for the anchoring of the metal-catalyst.[6]

Although the technique of heterogenisation of homogeneous catalysts using organic polymers has seen various systems investigated, none has been sufficiently successful to provide a practical solution that is suitable for commercial development for industrial use. The homogeneous catalysts that have successfully undergone heterogenisation have only done so at loss of activity or selectivity. A major problem still to be solved, is that many of these systems suffer from the metal leaching from the support, accompanied by a reduction in activity and ultimately leading to loss of the catalyst.[6] Soluble polymers

have been investigated by Bergbreiter [7] and Augustine [8] as a solution to catalyst leaching, and as a method to enhance diffusion in an attempt to increase activity and selectivity. The catalysis is conducted under homogeneous conditions and catalyst separation has been achieved by either membrane filtration, for high molecular weight metal complex systems, or by the addition of a polymer-insoluble-solvent to create precipitation of the metal complex.

The use of inorganic materials for the heterogenisation of homogeneous catalysts has not been applied to the same extent as organic polymers. The inorganic supports investigated have included silica, ceramics, clay, glass, magnesia, γ-alumina and zeolites etc.[6] Of these, silica has been favoured because the form and size of its particles produces an environment that is suitable for the anchoring of homogeneous catalysts, due to the number of pores of a compatible size and the availability of suitable functional groups on its surface. When strong acidic or basic supports have been required, γ-alumina and magnesia have been utilised. The application of zeolites for anchoring homogeneous catalysts has been limited by the size restriction of their pores, which are usually too small.[9] As with organic supports, anchoring the metal catalyst is usually via a ligand rather than by direct bonding between the metal and the support. The problems of leaching and diffusion, which are encountered with organic supports, also pose problems for inorganic supports.[6]

6.1.2 Biphasic Catalysis

The concept of biphasic catalysis is based on the principle that the homogeneous catalyst resides in a different phase to that of the reaction products. The immiscibility of the two phases allows the products to be removed by decantation of the respective phase, the catalyst being recovered in the remaining phase. Catalysis in biphasic systems occurs, either at the interface of the two phases of the biphasic solution, almost as a heterogeneous catalyst, or as a result of the immiscibility of the two phases disappearing with temperature to produce a single phase solution, which allows the catalyst to interact with the substrate in accordance with homogeneous catalysis. The two phases are restored on cooling and contain the catalyst and products respectively.

Various different biphasic systems have been investigated, including the use of aqueous-organic biphases that incorporate water-soluble catalysts, fluorinated solvent

biphases where the catalyst is soluble in the fluorous phase due to the co-ordination of fluorinated ligands, and biphases created by utilising ionic liquids.

Biphasic catalysis with aqueous-organic systems requires that the catalyst be soluble in water, which is unusual for most organometallic catalytic complexes. The solubility of the catalyst can be achieved by the co-ordination of ligands containing highly polar substituents. The incorporation into phosphine ligands of polar substituents such as $-SO_3H$, -COOH, -OH, and $-NH_2$ can be used to create the necessary characteristics for a ligand to be hydrophilic, and thus when bonded to a metal result in solubility of the complex in aqueous media. The different possibilities provided by the substituents allow ligands to be designed that are compatible with specific conditions. Phosphine ligands containing carboxy- or amino- functional aryl groups, dissolve in only basic or acidic conditions respectively, whereas inclusion of sulfo functional groups results in the ligand dissolving at any *p*H. An advantage of the use of water in biphasic catalytic systems is that, due to its polarity, the partition coefficient between it and the organic phase is frequently advantageous for product separation.[4]

Unlike the systems investigated that utilise a solid support to heterogenise the homogeneous catalyst, biphasic systems have been successfully developed and applied to an industrial process. A biphasic aqueous catalytic system has been developed for the hydroformylation of alkenes, and has been in commercial use on an industrial scale since 1984.[10] The process was the result of a collaboration between the companies Ruhrchemie AGH and Rhône-Poulenc, to develop a continuous biphasic system for the conversion of propene to *n*-butyraldehyde. The system is based on the water-soluble catalyst $[HRh(CO)(TPPTS)_3]$ (where TPPTS is triphenylphosphine trisulfonate).

The development of a biphasic aqueous catalyst for hydrogenation has, to date been less successful.[6] The hydrogenation of a variety of substrates, such as alkenes and carbonyls, has been investigated using catalytic systems comprised predominantly of late transition metals with the water soluble ligands TPPTS and TPPMS (where TPPMS is triphenylphosphine monosulfonate). Tóth *et al* reported a series of ruthenium complexes that were capable of hydrogenating unsaturated C-C and C-O compounds in aqueous biphasic solutions.[11] The ruthenium catalysts were made soluble by the use of the phosphine ligand *m*-sulfophenyl-diphenylphosphine. Whereas, the hydrogenation of sorbic acid to 4-hexanoic acid in an aqueous biphasic system was achieved by Drießen-

Hölscher *et al* using a ruthenium catalyst that contained the hydrophilic tris(3-hydroxypropyl)phosphine ligand.[12]

Aqueous biphasic catalytic systems are not suitable for all chemical systems, because the presence of water with the components of some reactions results in undesired interactions, detrimental to the overall process. Also, many organic compounds have too low a solubility in water for use with an aqueous catalyst. The use of nonaqueous biphasic systems avoids the problems of such chemical processes. A successful non-aqueous liquid-liquid biphasic system is dependent on the differences between the solvent properties of the product and the catalyst-containing phase, for example, polar products require an apolar catalyst phase. As with aqueous systems the catalyst has to be designed so that it is soluble in the designated catalyst phase. Various organic biphasic systems have been studied, with different combinations of alcohols, ethers and alkanes having been considered.[4] Loh *et al*, for example, looked at the use of systems that contained poly(ethyleneoxide), heptane and methanol or dichloromethane for the hydrogenation of 1-hexene using rhodium catalysts.[13] Alcohols have been used as the catalyst phase for systems with apolar products. Various systems have been investigated, of which the Shell Higher Olefin Process (SHOP) is probably that most successful developed for industrial use.[6] The Shell Higher Olefin Process, the oligomerisation of ethylene, uses a nickel catalyst that is soluble in alkanediols such as 1,4-butanediol but in which the products, α-olefins, are almost insoluble. The solubility of the nickel catalyst is achieved using ligands that are diorganophosphino acid derivatives.

Non-aqueous biphasic systems that use a fluorinated solvent as one of the phases have also been investigated.[14] Fluorinated solvents are nonpolar and, because of low miscibility with most organic solvents, can be used in biphasic systems with acetone, alcohols, THF and toluene. The solubility of an organometallic catalytic complex in the fluorinated solvent is achieved by the inclusion of fluorocarbon constituents to the co-ordinated ligands.

The use of ionic liquids as one of the phases in biphasic catalysis has provided a further medium in which to immobilise a homogeneous catalyst.[15] Ionic liquids are easily able to dissolve most catalytic metal complexes and their immiscibility with most organic solvents, makes them suitable for the catalytic phase of biphasic catalytic systems.

Biphasic systems containing ionic liquids have seen a wide level of catalytic applications investigated, including methods to produce cleaner diesel, butene dimerisation, and linear alkyl benzenes amongst others.[15] The ionic liquid 1-*n*-butyl-3-methylimidazolium tetrafluoroborate has been used with ruthenium catalysts for the hydrogenation of olefins,[16] 2-arylacrylic acids [17] and arenes.[18]

The investigation of supercritical fluids (SCFs) in catalysis has demonstrated that their properties can also be advantageous for catalyst recovery and product separation. In keeping with the previous biphasic systems, the catalyst requires being soluble in the SCF. The solubility of organometallic complexes in SCFs has been achieved by co-ordination of perfluorinated aryl phosphine ligands, which are also advantageous for product recovery, as it results in the catalyst being immiscible with the organic products.[19] The most extensively investigated SCF is supercritical CO_2 ($scCO_2$), which has been used in various catalytic systems but is especially effective for hydrogenation of organic compounds due to the miscibility of hydrogen in $scCO_2$.[20]

6.1.3 Summary

The recovery of homogeneous catalysts is a problem that has seen many novel solutions proposed, and continues to attract interest as process and industrial requirements demand further innovation, application and technique refinement.

The use of chemical treatment or distillation to separate catalyst and product can be detrimental to the catalyst, and may result in irrecoverable damage. Such processes require the catalyst to be robust, and in the case of distillation, that the products are more volatile than the catalyst.

The heterogenisation of the homogeneous catalyst, by its attachment to some form of support (usually polymeric), attempts to harness the "best of both worlds", with the ease of separation associated with heterogeneous catalysts and the selectivity of homogeneous catalysts. At present, problems associated with lower levels of activity and selectivity, combined with loss of catalyst from leaching, still have to be addressed before systems based on this technique are used commercially.

The simplest system for homogeneous catalyst and product recovery is based on biphasic systems, where the product is isolated in a different phase to the catalyst, and separation is easily achieved by decantation of the relevant phase. Such systems require careful consideration of the characteristics of the individual components of the reaction, and frequently necessitate that the catalyst be designed with specific properties to make it compatible with a particular phase. Biphasic systems have been successfully developed, that have seen application in industry, by Shell (SHOP) and Ruhrchemie AGH/ Rhône-Poulenc (hydroformylation).

Biphasic catalytic systems offer the best solution to the problem of homogeneous catalyst recovery, providing a suitable system can be designed that is compatible to the requirements of the desired catalytic reaction.

6.2 Results and discussion

The deactivated catalyst [Ru(Triphos)H_2(CO)], precipitated during ester hydrogenation (see Chapter 2), was found to be capable of being reactivated via the water gas shift reaction (see Chapter 4). The reactivation of the [Ru(Triphos)H_2(CO)], and the further hydrogenation subsequently achieved, demonstrates that catalyst recovery and recycling is possible, albeit in a limited way. The ^{31}P NMR analysis of the product solutions of the ester hydrogenations indicate the presence of ruthenium-triphos species, as does similar analysis of the product solutions of the reactivation experiments and the acid hydrogenation reactions (see Chapter 5). This indicates that the product solutions contain either soluble catalytic complexes or soluble ruthenium-triphos by-products, and from consideration of the ^{31}P NMR data most probably both (see the respective Chapters Results and Discussion for the appropriate data).

The precipitated [Ru(Triphos)H_2(CO)] is obtained when the substrate hydrogenation occurs in the absence of H_2O, and is accompanied by low substrate conversion and the solution based ruthenium-triphos species. Although the recovery of the [Ru(Triphos)H_2(CO)] precipitate is straightforward, the low levels of conversion and the presence of the further solution based species suggest that this is probably not the most economical point at which to undergo catalyst recovery and product separation. The exposure of the [Ru(Triphos)H_2(CO)] to air and its resilience to temperature (see

Chapter 4) suggested that the catalyst might be sufficiently robust to withstand the products being separated by distillation.

The [Ru(Triphos)H_2(CO)] used in the investigations was the solid product obtained from the hydrogenation of esters, as previously described (see Chapter 2, Homogeneous Ester Hydrogenation).

6.2.1 Catalyst Recovery by Distillation

The investigation of distillation as a technique for catalyst recovery and product separation used a series of batch reactions, based on an initial catalyst charge generated *in-situ* from the catalytic precursors $Ru(acac)_3$ and Triphos. Propionic acid was chosen as the substrate to be hydrogenated, as the products would allow for a straightforward unambiguous analysis. After each batch reaction, the product solution was distilled by rotary evaporation to remove the products and the unreacted substrate. The products of the respective reactions were decanted into a rotary evaporator for the product removal and to recover the catalyst. The product solution was reduced to a volume of 5 cm^3, which contained a concentrate of the soluble catalyst in a solution of predominantly propionic acid, which is less volatile than the reaction products (1-propanol and propyl propanoate). A further charge of propionic acid substrate was then added to the recovered catalyst. The autoclave was not cleaned after the removal of the product solution of each reaction, in an attempt to minimise the loss of any catalyst that may have been precipitated during product removal. The catalyst recycle and the new charge of substrate were then added to the uncleaned autoclave. The batch reactions were each run for a period of four hours to ensure that total substrate conversion did not occur, and thus allowing the results of each recycle to be compared. After the initial reaction and the first six recycles, a blank reaction containing only the propionic acid substrate, without the recycled catalyst was carried out. No hydrogenation was achieved. Table 6.1 details the results of the propionic acid hydrogenation in the initial reaction and the subsequent catalyst recycles, including the blank reaction. The data detailed in Table 6.1 were obtained from the distillate. A ^{31}P NMR of the distillate did not detect the presence of any phosphorus species. Graph 6.1 shows the level of propionic acid conversion achieved per catalyst recycle.

Table 6.1 Catalyst Recycle Test :

Propionic Acid Hydrogenation Products and Conversion

Recycle No	1-Propanol / %	Propyl Propanoate / %	Propionic Acid / %	Molar Conversion / Propionic Acid
Initial Reaction	14.11	42.60	28.21	45.0
1	15.16	46.97	24.41	47.4
2	15.16	44.43	26.23	46.6
3	15.00	47.96	23.89	47.6
4	21.00	49.47	16.94	53.9
5	14.97	48.27	23.93	47.6
6	18.18	48.45	20.32	50.9
7[a]	0.00	0.00	100.00	0.0
8[b]	11.61	40.93	31.57	41.8
9	9.83	44.62	31.47	41.1
10	8.12	40.67	35.5	37.8

Conditions: 180°C, $p(H_2)$ = 6.8MPa.
a: Blank reaction. Charge of Propionic Acid, but without the recycled catalyst.
b: Quantity of catalyst reduced due to sample being removed for ^{31}P NMR analysis.

Graph 6.1 Propionic Acid Conversion Per Catalyst Recycle

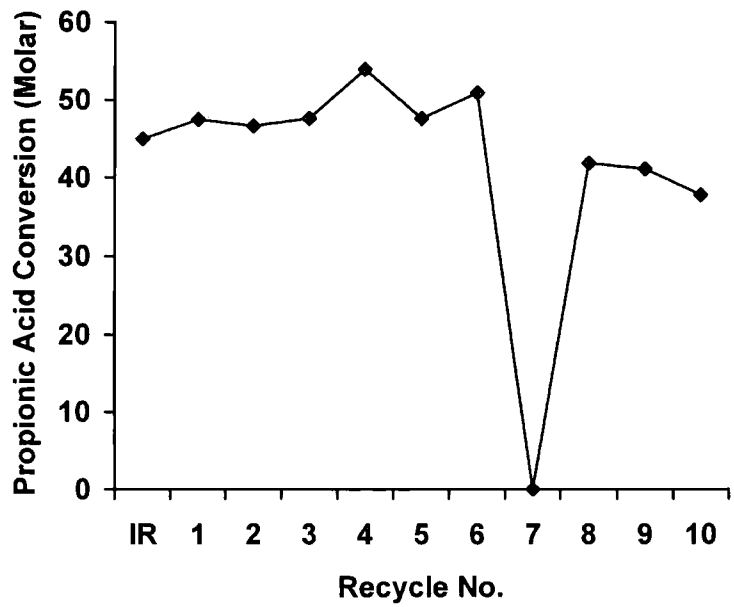

The results detailed in Table 6.1 and Graph 6.1 show the product compositions found for recycled catalyst for further batch hydrogenation reactions. Although the method used to investigate the viability of distillation as a procedure for the catalyst recovery and product separation was rudimentary, the results clearly show that the technique was successful. The batch reaction procedure exposed the catalyst to the air at each recycle, and an opportunity to lose catalyst due to handling during the transfer between autoclave to rotary evaporator. Despite this, the catalyst produced results that showed roughly consistent levels of substrate conversion, and suggests that the catalyst is robust under such recycle conditions. The blank reaction (recycle number 7) demonstrated, not only that the material recovered after the distillation (contained in the concentrated solution) is the catalytic substance, but also that the catalyst was not an unseen substance on the inner surface of the autoclave i.e. not a heterogeneous catalyst.

The ^{31}P NMR spectrum of the concentrated solution containing the catalyst (see Fig 6.1) produced a spectrum that was consistent with those previously observed during the investigation of the acid hydrogenation (see Chapter 5).

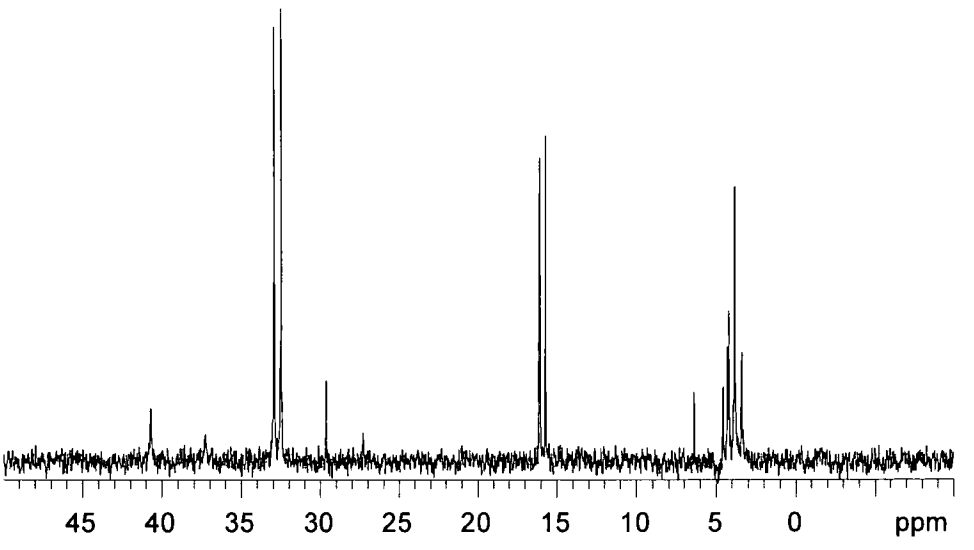

Fig 6.1 ^{31}P NMR Spectrum of the Concentrated Product Solution Containing the Catalyst

$^{31}P\{^{1}H\}$NMR (25°C, chloroform-*d*): δ 40.5 (**3P**, s), 37.5 (**3P**, s), 32.5 (**2P**, d, $^{2}J_{P\text{-}P}$ = 35 Hz), 29.3 (**3P**, s), 16.3 (**2P**, d, $^{2}J_{P\text{-}P}$ = 28 Hz), 6.2 (**3P**, s), 3.8 (**P**, t, $^{2}J_{P\text{-}P}$ = 28 Hz), 3.4 (**P**, t, $^{2}J_{P\text{-}P}$ = 35 Hz) ppm.

6.2.2 Hydrogenation of Different Substrates with the Recovered Catalyst

The recovered catalytic precursor, whether it is solid [Ru(Triphos)H_2(CO)] or the residual solution following distillation, can be used successfully in the hydrogenation of substrates other than that from which it was derived. This indicates that in both cases the catalyst or catalytic precursor has been separated from the hydrogenation reaction product and recycled.

The solid deactivated catalyst precursor [Ru(Triphos)H_2(CO)] obtained in the hydrogenation of esters (see Chapter 2) was used for hydrogenation of both propionic acid and maleic acid (see Chapter 4). The distillate containing the concentrated catalyst recovered from the separation of the product of an ester hydrogenation was found to show the same activity in the second reaction involving hydrogenation of an acid as it had in the initial ester hydrogenation.

The ester methyl propanoate was hydrogenated using the *in-situ* generated catalyst, from Ru(acac)$_3$ and Triphos. The reaction, carried out in the presence of H_2O at a temperature of 140°C resulted in the absence of [Ru(Triphos)H_2(CO)] in the products because of the catalyst reactivation water gas shift reaction (see Chapter 4). The residual distillate following rotary evaporation, was then used in the hydrogenation of propionic acid (see Table 6.2).

Table 6.2 Hydrogenation of Methyl Propanoate and Propionic Acid using the same Sample of Catalyst.

Substrate	Conversion / %
Methyl Propanoate [a]	98.8
Propionic Acid [b]	75.5 [c]

Conditions: 140°C, $p(H_2)$ = 6.8MPa.
a: Reaction period 42 hours.
b: Reaction period 22 hours.
c: Products of conversion are 1-propanol and propyl propanoate.

6.2.3 Catalyst Life

The life of a catalyst is usually defined as the time that a catalyst maintains a level of activity and/or selectivity before becoming deactivated.[1, 21] Measures by which the life of a catalyst can be assessed are the turn over number (TON) and the turn over frequency (TOF). The TON is defined as being the moles of product obtained per mole of catalyst and the TOF is defined as being the TON per hour.

The limitations of the recycling experiment, described in 6.2.1 above mean that any calculation has to be based on assumptions on the amount of catalyst present at each stage of the recycling. The calculation in Table 6.3, below, is based on the assumption that the same quantity of catalyst (ruthenium metal) is present at all stages of the recycle, and is the same amount as was used in the initial reaction. As some loss of the catalyst was inevitable using the method of recycling employed for the catalyst recycle test, and a small quantity of catalyst was removed for analysis after recycle number 6, this is clearly not the case.

Table 6.3 Estimated Turn Over Numbers for the Catalyst Recycle Test

Recycle No.	TOF [a]	TON [b]
Initial Reaction	187.7	938.4
1	204.8	989.8
2	220.0	971.5
3	253.6	993.1
4	270	1124.9
5	253.4	992.6
6	260.3	1062.7
7 [c]	0.0	0.0
8	227.6	872.4
9	214.3	857.1
10	205.8	789.0

Note:
a: TOF (Turn Over Frequency) = TON / Hours.
b: TON (Turn Over Number) = Moles of Product / Moles of Catalyst.
c: Recycle 7 was a blank reaction and contained no catalyst.

The assumption that the quantity of catalyst remains unaltered throughout, produces a result, which is conservative of a true value, but provides an approximate indication of the life of the catalyst during the recycle test. The cumulative value for the TON is in excess of 9600. As the recycle experiment was incomplete, in that the catalyst was still active in recycle 10, the overall life of the catalyst for batch recycling is unknown.

6.2.4 Conclusion

The separation of the products and recovery of the catalyst from the homogenous hydrogenation reactions, using a catalyst generated *in-situ* from $Ru(acac)_3$ and Triphos, was achieved by distillation. The catalyst recovered by distillation was sufficiently stable and robust to be used in a succession of ten batch recycle reactions without any indication of significant degradation of catalyst performance.

The use of a different substrate to that from which the catalyst was initially produced illustrates a common catalytic species for ester and acid hydrogenations, and demonstrates its potential in different areas.

6.3 Experimental

6.3.1 Hydrogenations

All hydrogenations were carried out using a 300-ml Hasteloy^{TM} autoclave equipped with overhead stirrer. The autoclave was loaded with the $Ru(acac)_3$, Triphos or $[Ru(Triphos)H_2(CO)]$, and then the air was removed by three cycles of vacuum followed by refilling with argon. The selected solvent and substrate were purged by bubbling argon through them for 1 hour, and then added to the autoclave by canula. The autoclave was then pressurised at r.t. with hydrogen (4.4 MPa). The autoclave was then heated to the relevant reaction temperature, at which the hydrogen mass flow controller was set to 6.8 MPa, and stirred for the selected reaction period. On completion of the reaction period the heating was stopped and the autoclave allowed to cool slowly. The headspace gases within the autoclave were slowly vented and the products removed. The product solution was analysed by GC, GCMS and ^{31}P NMR spectroscopy.

Table 6.4 Quantity of Reagents used.

Reagent	Quantity
$Ru(acac)_3$	4.5×10^{-4} mol
Triphos	6.1×10^{-4} mol
Propionic Acid	70.0 cm^3
Methyl Propanoate	20.0 cm^3
H_2O [a]	50.0 cm^3

a: Used only with the hydrogenation of methyl propanoate.

6.3.2 NMR Spectra

The NMR spectra of the product solutions were measured against an external reference of chloroform-*d* containing Triphos, which was used to lock and shim the NMR spectrometer. The product solids were dissolved in the appropriate *deuterated* solvent and the NMR spectrometer locked and shimmed accordingly, prior to recording the spectrum.

6.3.3 Rotary Evaporation

Rotary evaporation of the product solutions was carried out at 60 Torr and 70-80°C. The concentrated solution containing the catalyst precursor, was removed by washing from the vessel into the autoclave. The propionic acid charge was split into two equal volumes and used to wash the catalyst into the autoclave from the rotary evaporator vessel, to minimise catalyst loss.

6.4 References

1. *Catalyst Handbook*, ed. M. V. Twigg, Manson Publishing Ltd., Frome, 2nd Edn., 1996.
2. G. W. Parshall and S. D. Ittel, *Homogeneous Catalysis*, John Wiley & Sons, Chichester, 2nd edn., 1992.
3. M. A. Hamilton, D. A. Harbourne, C. G. Russell, V. G. Zboril and R. M. Mulhaupt, EPO 0,131,420, 1988, and C. G. Russell, U.S. Patent 4,612,382, 1986 (both assigned to Du Pont Canada).
4. *Aqueous-Phase Organometallic Catalysis*, eds. B. Cornils and W. A. Hermann, Wiley-VCH, Weinheim, 1998.
5. J. C. Bailar, Jr., *Cat. Rev.-Sci. Eng.*, 1974, **10(1)**, 17.

6. *Applied Homogeneous Catalysis with Organometallic Compounds*, eds. B. Cornils and W. A . Hermann, Wiley-VCH, Weinheim, 2000.
7. D. E. Bergbreiter, *Catalysis Today*, 1998, **42**, 389.
8. R. L. Augustine, *Catalysis Today*, 1997, **37**, 419.
9. B. C. Gates, *Chem. Rev.*, 1995, **95**, 511.
10. B. Cornils and E. G. Kuntz, *J. Organomet. Chem.*, 1995, **502**, 177.
11. Z. Tóth, F. Joó and M. T. Beck, *Inorg. Chim. Acta*, 1980, **42**, 153.
12. J. Heinen, M. S. Tupayachi and B. Drießen-Hölscher, *Catalysis Today*, 1999, 273.
13. R. C. da Rosa, L. Martinelli, L. H. M. da Silva and W. Loh, *Chem. Commun.*, 2000, 33.
14. I. T. Horvath, *Acc. Chem. Res.*, 1998, **31**, 641.
15. H. Carmichael, *Chemistry in Britain*, 2000, Vol. 36, **1**, 36.
16. P. A. Z. Suarez, J. E. L. Dullius, S. Einloft, R. F. de Souza and J. Dupont, *Inorg. Chim. Acta*, 1997, **255**, 207.
17. A. L. Monteiro, F. K. Zinn, R. F. de Souza and J. Dupont, *Tetrahedron: Asymmetry*, 1997, Vol. 8, **2**, 177.
18. P. J. Dyson, D. J. Ellis, D. G. Parker and T. Welton, *Chem. Commun.*, 1999, 25.
19. J. A. Darr and M. Poliakoff, *Chem. Rev.*, 1999, **99**, 495.
20. M. G. Hitzler and M. Poliakoff, *Chem. Commun.*, 1997, 1667.
21. *Homogeneous Catalysis with Metal Phosphine Complexes*, ed. L. H. Pignolet, Plenum Press, London, 1983.

Chapter 7

Exploratory Homogeneous Hydrogenation of Alkenes and Nitrogen Compounds

The catalytic system generated in-situ from $Ru(acac)_3$ and Triphos is able to homogeneously hydrogenate the alkenes, 1-hexene and cyclohexene, and the nitrogen compounds nitrotoluene, propionitrile and propionamide.

7.1 Introduction

Ruthenium catalysts have been reported for the homogenous hydrogenation of a variety of different substrates that contain C=C, C=O and nitrogen containing functional groups.[1-4]

7.1.1 Hydrogenation of Alkenes

The hydrogenation of the activated alkenes maleic acid and fumaric acid was one of the first homogeneous hydrogenations of alkenes to be characterised. The hydrogenation was catalysed by a Ru(III)chloride species in an aqueous solution. The proposed mechanism (see Fig 7.1) proceeds via the generation of a ruthenium(II)-alkene complex, which on addition of hydrogen undergoes rearrangement to an alkyl intermediate. This stage is followed by proton attack at the ruthenium bonded carbon, resulting in the reformation of the catalyst.

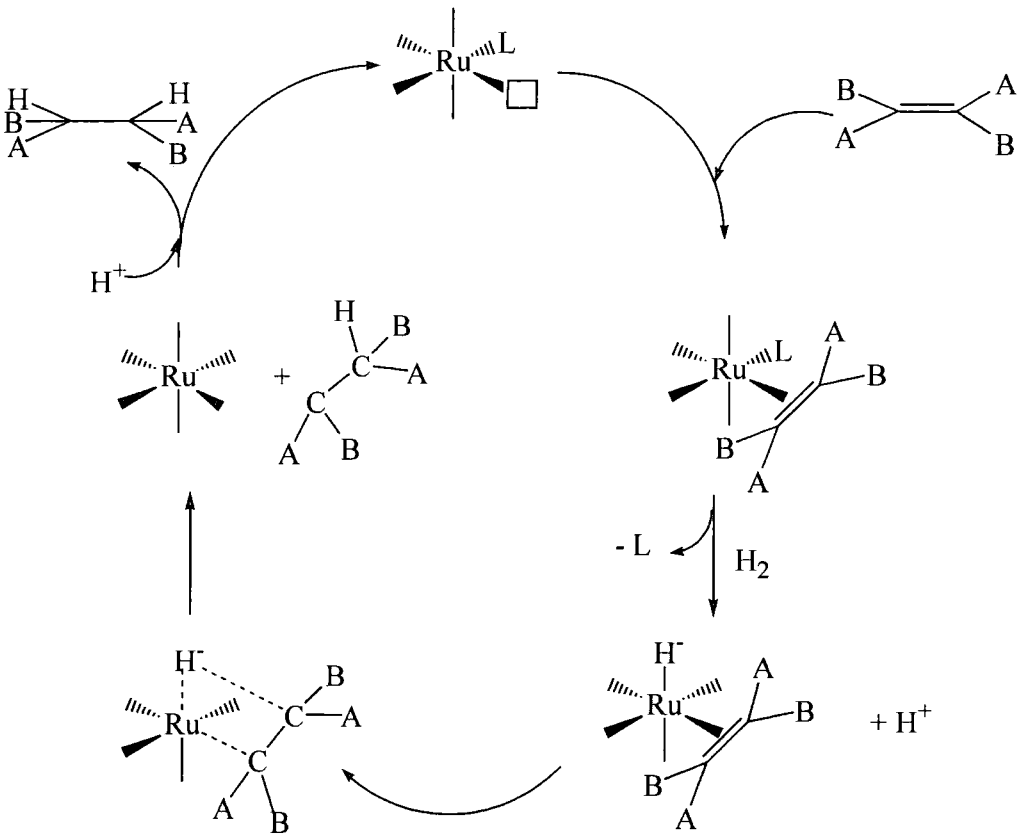

Fig. 7.1 Homogeneous Hydrogenation of an Activated Alkene by a Ruthenium Catalyst [1]

Two of the most common ruthenium catalysts investigated are $[RuCl_2(PPh_3)_3]$ and $[RuHCl(PPh_3)_3]$, which have been found to be successful for the hydrogenation of terminal alkenes.[5] The study of the $[RuHCl(PPh_3)_3]$ complex by Wilkinson *et al* was based on the results obtained using the catalytic rhodium(I) complex $[RhCl(PPh_3)_3]$.[6,7] The ability of the $[RhCl(PPh_3)_3]$ complex to dissociate in solution suggested that the analogous ruthenium(II) complexes $[RuCl_2(PPh_3)_n]$ (where n = 3, 4) would exhibit comparable properties. Their experimentation established that the active catalyst was a $[RuHCl(PPh_3)_3]$ complex, and that the possible mechanism (see Fig 7.2) would be similar to the analogous rhodium system and involve the dissociation of a triphenylphosphine ligand followed by the creation of an alkyl complex.

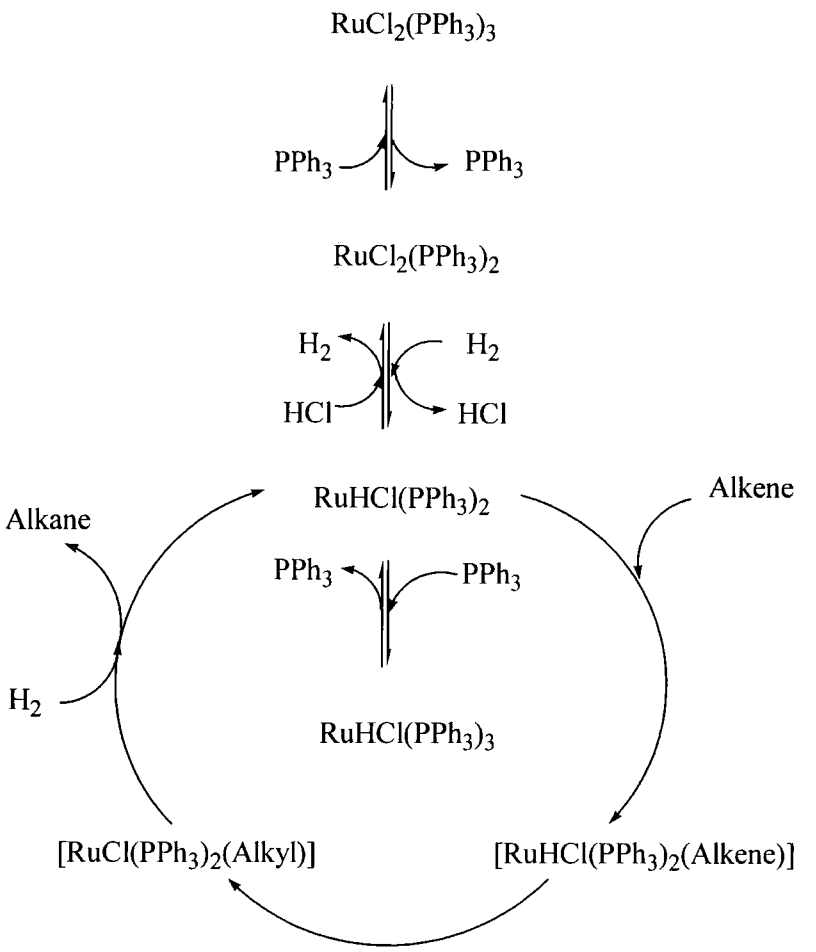

Fig. 7.2 Homogeneous Hydrogenation of an Alkene by a Ruthenium Catalyst [3]

The ruthenium-phosphine hydride complexes have been found to be effective hydrogenation catalysts. The tetrahydride species $[RuH_4(PPh_3)_3]$ (shown to be $[RuH_2(\eta^2\text{-}H_2)(PPh_3)_3]$)[8, 9] has been investigated and reported as catalytic for the hydrogenation of terminal alkenes and anthracene, whereas, the dihydride $[RuH_2(PPh_3)_3]$ was shown to hydrogenate 1-hexene, propene and styrene but not cyclohexene or internal alkenes.[10, 11] The anionic dihydride ruthenium complex $K[RuH_2(C_6H_4PPh_2)(PPh_3)_2]\cdot C_{10}H_8(Et_2O)$ investigated by Grey *et al*, was found to hydrogenate polynuclear aromatics.[12]

The use of sulphonated phosphine ligands allowed water soluble biphasic catalytic systems to be investigated.[13, 14] The catalysts $[RuHCl(NaL)_3]$, $[RuCl_2(NaL)_2]$ and $[RuH(OAc)(NaL)_3]$ (where NaL = *m*-$Ph_2PC_6H_4SO_3Na$) hydrogenated the activated

alkenes, such as the unsaturated acids, crotonic, maleic, fumaric, cinnamic, itaconic and butadiene-1-carboxylic acids, as well as the alkenes 1-hexene and styrene.

The homogenous hydrogenation of cyclic alkenes can be achieved by the ruthenium complex $[RuCl_2(CO)_2(PPh_3)_2]$.[3] The active catalyst is understood to be $[RuHCl(CO)_2(PPh_3)_2]$ with dissociation of PPh_3 allowing the unsaturated substrate to bond. The catalyst was found to hydrogenate alkenes and dienes with rates in the order : conjugated dienes > unconjugated dienes > terminal alkenes > internal alkenes. The ruthenium-hydride complex $[RuCl(CO)H(PPh_3)_3]$ has been reported by Wakatsuki and Yamazaki for catalytic hydrogenation of enynes.[15] Wakatsuki and Yamazaki found that the $[RuCl(CO)H(PPh_3)_3]$ complex reacts with the double bond of *cis*-enynes and the triple bond of *trans*-enynes.

The use of chiral ligands has allowed chiral catalysts to be developed, which due to the importance of control of enantioselectivity in drug design and development is of great value. Diphosphine ligands have been developed for homogeneous catalysis, of which the bidentate ligands have proven the most effective. The chiral property can be introduced through either the carbon skeleton or via the phosphorus centre. Ruthenium chiral catalysts have been investigated for the hydrogenation of prochiral alkenes by Genet *et al.*[16] The first chiral ruthenium catalyst, $[Ru_2DiopCl_4]$, was prepared by James *et al.*[17] The catalyst $[Ru_2DiopCl_4]$ complex was obtained from reacting $[RuCl_2(PPh_3)_3]$ with an excess of DIOP. Since then, a variety of different ligands that confer chirality have been investigated, of which BINAP has proved the most effective for the hydrogenation of prochiral substrates that include alkenes, carbonyls and imines.[18]

7.1.2 Hydrogenation of Nitrogen Compounds

7.1.2.1 Reduction of Nitro Compounds

The reduction of nitro groups (see Equation 7.1) is fairly easily achieved. Both aliphatic and aryl nitro-compounds can be reduced (to primary amines) in solution by hydrochloric acid with tin, iron, a metal salt such as $SnCl_2$ or by catalytic hydrogenation.[19-22]

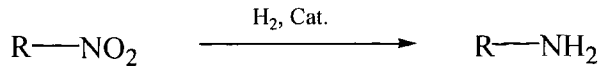

Nitro Compound Amine

Equation 7.1

The reduction of nitro compounds can result in the production of unwanted compounds, such as azo compounds, as the reaction proceeds via nitroso and oxime intermediates (see Figure 7.3). The extent to which the reduction of nitro compounds proceeds is dependent upon the *p*H of the reaction solution. In the case of the reduction of nitrobenzene, if the reaction is conducted in a mineral acid the product is aniline, whereas if the reaction medium is a neutral or a weakly acidic solution then the product is *N*-phenylhydroxylamine, whilst an alkaline medium results in the bimolecular hydrazobenzene, C_6H_5-NH-NH-C_6H_5.[19]

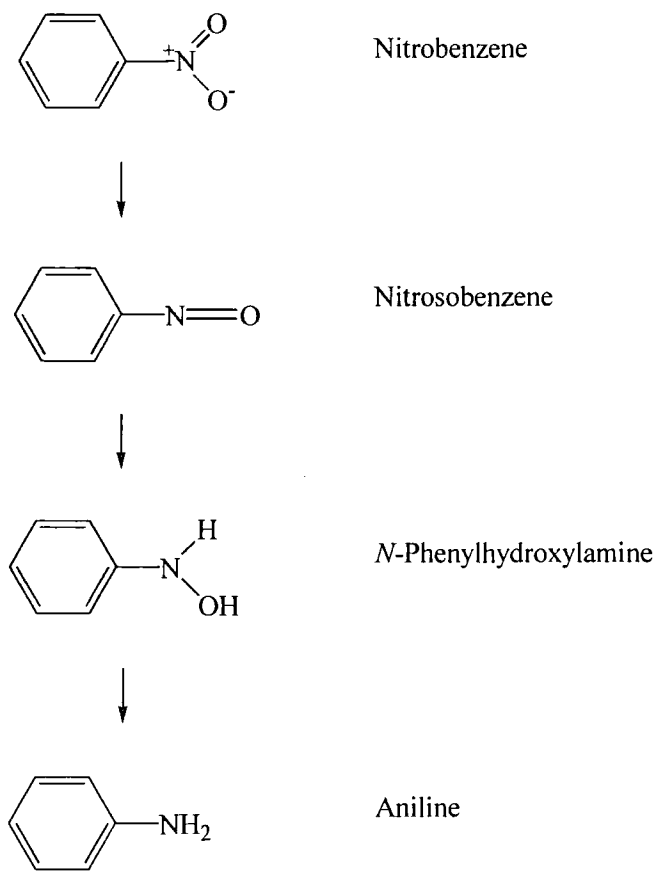

Fig. 7.3 Nitrobenzene Conversion to Aniline

The reduction of aromatic nitro compounds can be achieved by rhodium and cobalt oxo catalysts. McQuillin and Love reported that the rhodium complex $[RhCl_2(BH_4)(DMF)(py)_2]$ hydrogenated aromatic nitro compounds, including cross-linked polystyrenes.[23] The stoichiometric reduction of aromatic nitro compounds with $Fe_3(CO)_{12}$ in a biphasic system by phase-transfer catalysis (PTC) has been reported by Alper *et al.*[24] The reaction is understood to proceed *via* the $[HFe_3(CO)_{11}]^-$ intermediate, which is produced *in-situ* at the interface of the biphasic system, and is transferred to the organic phase as an ion pair with a quaternary ammonium cation. Alper *et al* also found that the reduction could be achieved by replacing the $Fe_3(CO)_{12}$ with catalytic $Ru_3(CO)_{12}$.[25] The PTC reduction of nitro compounds by the ruthenium catalyst $[RuCl_2(PPh_3)_3]$ in an atmosphere of CO-H_2 (1:1) has also been reported by Miura *et al.*[26] The homogenous hydrogenation of aromatic and aliphatic nitro compounds was investigated by Knifton, using the $[RuCl_2(PPh_3)_3]$ catalyst.[27] The reduction probably occurs *via* a ruthenium hydride intermediate. The homogenous reduction of nitrobenzene to aniline with hydrogen and carbon monoxide has been reported for systems using the ruthenium compounds $[Ru_3(CO)_{12}]$, $[Ru(CO)_5]$ and $[Ru(acac)_3]$ as catalyst precursors.[28]

7.1.2.2 Reduction of Nitrile Compounds

The hydrogenation of nitrile compounds is not so easily achieved as the reduction of nitro compounds. As with nitro compounds, the reduction of nitriles to amines can be achieved using $LiAlH_4$ or with hydrogen and a catalyst (see Equation 7.2).[21] As with the majority of organic syntheses or catalytic reactions, most are unsuitable for application to industrial use. The commercial production of diamines is predominantly by hydrogenation of the respective dinitrile.[29] Industrially, the reduction uses cobalt or nickel catalysts at high temperatures and pressures, with the hydrogenation taking place in the presence of large quantities of ammonia to ensure that primary amines are the major product.[19, 29]

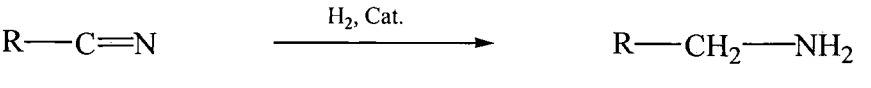

Nitrile

Primary Amine

Equation 7.2

The catalytic homogeneous hydrogenation of nitriles was found to be possible using phosphine complexes of transition metals.[30] Levering described in a U.S. Patent the use of $Fe(CO)_5$ and $Ni(CO)_4$ complexes for the hydrogenation of nitriles, at hydrogen pressures of 14 MPa at 200°C.[31] The rhodium complex, $[RhH(PPr_3)_3]$, was reported by Yoshida *et al* as being able to effectively hydrogenate nitriles under the extremely mild conditions of 1 atm. and 20°C.[32] The ruthenium complex $[(diphos)_2Ru(NCMe)_2]^{2+}$ and the scandium complex $^*Cp_2ScR$ (where R = H, Me, *p*-toluene) were reported, by Bercaw *et al*, for catalytic reduction of nitriles.[33]

The investigation of homogeneous catalysts based on ruthenium complexes for nitrile hydrogenation has seen varying degrees of success. The potassium hydrido(phosphine)ruthenate complexes $K^+[(PPh_3)_2Ph_2PC_6H_4RuH_2]^-\cdot C_{10}H_8\cdot(C_2H_5)_2O$ and $K_2[(PPh_3)_3(PPh_2)Ru_2H_4]^{2-}\cdot 2C_6H_{14}O_3$ synthesised by Grey *et al* were found to be capable of nitrile reduction to amines, albeit slowly and with the products comprising a mixture of primary, secondary and tertiary amines.[34] The hydrogenation of nitriles by catalytic systems using $[RuCl_2(PPh_3)_3]$, $[RuCl(CO)H(PPh_3)_3]$ and other ruthenium complexes at 4 MPa and 130°C was patented by Dewhirst.[35] At DuPont, the work of Beatty and Paciello on nitrile hydrogenation with ruthenium catalysts using mono phosphines, such as PCy_3, was patented.[36]

7.1.2.3 Reduction of Amide Compounds

The reduction of amides can produce alcohols, aldehydes, amines or hydrocarbons, depending on the chemical composition of the amide and the method of reduction employed (see Equation 7.3).[37] However, the major application for amide reduction is to convert them to amines. Amides can be reduced to amines with $LiAlH_4$ or by catalytic hydrogenation, the latter usually requiring high pressures and temperatures.[19] As with nitriles, the reduction does not occur as easily as that of the reduction of nitro compounds.[38]

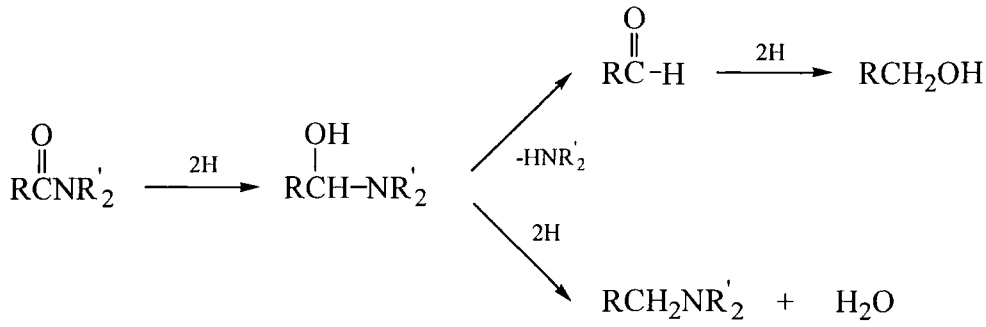

Amide Amine

Equation 7.3

The catalytic hydrogenation of amides to amines can be achieved with a copper chromite catalyst, at 210-250°C with 1-3 Pa 10^7.[37] The high temperature of the reduction results in a mixture of primary, secondary and tertiary amines as the products, as a consequence of the associated side reactions inherent with the reaction conditions. The intrinsic difficulties of the high temperature catalytic amide hydrogenation are only avoided by the use of the reducing agents based on metal hydrides of the alkali metals, aluminium and borohydride complexes.[37-39]

7.1.3 Summary

Ruthenium complexes, with varying levels of success, have achieved the catalytic homogeneous hydrogenation of alkenes and nitrogen compounds. Not surprisingly, for hydrogenation catalysts, the ruthenium hydride complexes $[RuH_n(P_3)]$ (where P = a monodentate phosphine and n = 2 – 4), generated from $[RuCl_2(P_3)]$, are the most common form of the catalyst reported and frequently the most effective. The ruthenium complex, $[RuH_n(PPh_3)_3]$, will hydrogenate aliphatic alkenes [9-11] whilst analogous complexes have been reported for the hydrogenation of aromatic nitro compounds [27] and nitrile compounds [35, 36].

7.2 Results and Discussion

The catalyst generated *in-situ* from $Ru(acac)_3$ and the tripodal triphosphine Triphos was investigated for the hydrogenation of alkenes and nitrogen compounds. The

hydrogenation of the alkenes was carried out in iPA as a solvent whilst the hydrogenation of the nitrogen compounds was in a solvent comprising THF and water.

7.2.1 Hydrogenation of 1-Hexene and Cyclohexene

The catalytic hydrogenation of terminal, internal and cyclic alkenes can be achieved by the catalyst system generated *in-situ* from $Ru(acac)_3$ Triphos. The hydrogenation of internal alkenes has been observed by the conversion of dimethyl maleate and dimethyl fumarate to dimethyl succinate, as described in Chapter 2, and the conversion of maleic acid and fumaric acid to succinic acid, as described in Chapter 5 (see Equation 7.4).

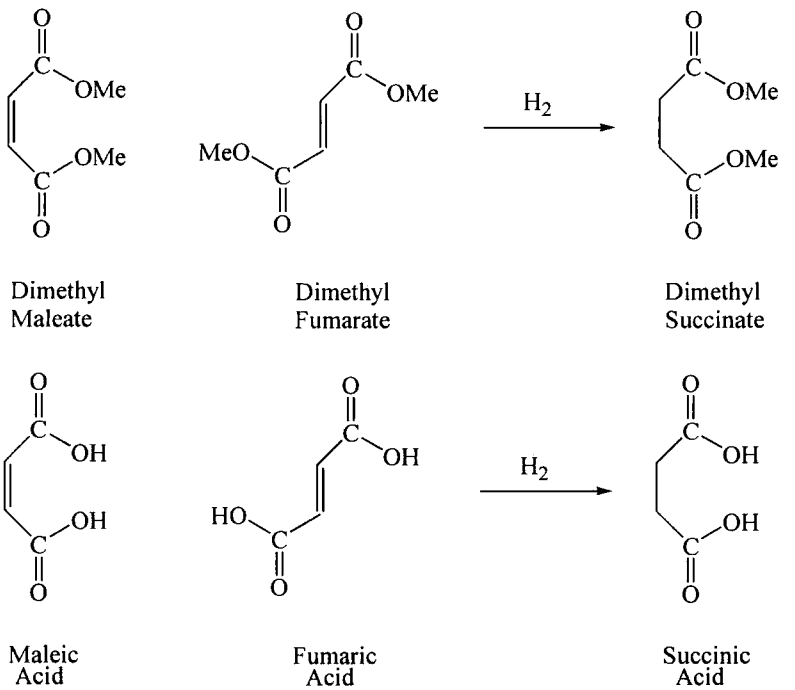

Equation 7.4

The internal alkenes of both the diester and the dicarboxylic acid are both easily hydrogenated to 100% conversion, irrespective of whether they are of *cis* or *trans* configuration. The hydrogenation of the terminal alkene, 1-hexene, converted it entirely to hexane, whereas for the cyclohexene, hydrogenation was incomplete with a conversion to cyclohexane of 78 % (see Table 7.1). The lower level of hydrogenation of cyclic alkenes, to that of terminal alkenes, was interpreted by Wilkinson *et al* as being due to the steric effects caused by bulky phosphine ligands.[3] The steric effects

associated with the hydrogenation of the diesters and the dicarboxylic acids will be as great as those for the cyclic alkene, possibly even greater, and yet under comparable reaction conditions they achieved 100 % conversion. The difference is probably because of the electronic properties of the respective functional groups, whereby the alkene is activated through electron withdrawal.

Table 7.1 Hydrogenation of Cyclohexene and 1-Hexene

Substrate	Conversion / %
Cyclohexene	78.43
1-Hexene	100.00

Conditions: 120°C, $p(H_2)$ = 6.8 MPa, 16 hours.

7.2.1.1 Isolation of [(Triphos)HRu(μ-H)$_2$RuH(Triphos)]

The catalytic hydrogenation of 1-hexene produced small dark red crystals which were identified by X-ray crystallography as [(Triphos)HRu(μ-H)$_2$RuH(Triphos)], with a structure determination by A. Batsanov (see Fig. 7.4). The [(Triphos)HRu(μ-H)$_2$RuH(Triphos)] is probably the product of the dimerisation of [Ru(Triphos)H$_2$], which would probably be unstable.

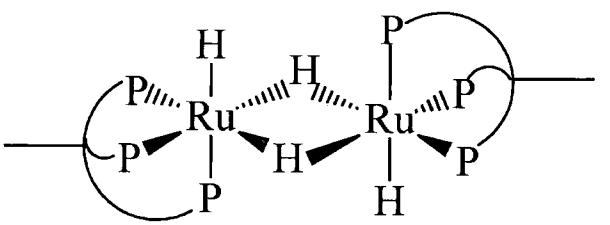

Figure 7.4 Structure of [(Triphos)HRu(μ-H)$_2$RuH(Triphos)]
(see Appendix 3 for crystallographic structure and data)

The [(Triphos)HRu(μ-H)$_2$RuH(Triphos)] was produced in the 100% hydrogenation of 1-hexene to hexane. The reaction occurred in the absence of alcohols that are susceptible to decarbonylation, and therefore deactivation of the catalyst by co-ordination of an extracted carbonyl ligand was not possible. The [(Triphos)HRu(μ-H)$_2$RuH(Triphos)] obtained on completion of the reaction will probably have been formed by the dimerisation of the [Ru(Triphos)H$_2$] on cooling (see Equation 7.5). The

dimerisation of the [Ru(Triphos)H_2] allows the 16-electron co-ordinatively unsaturated ruthenium complex to satisfy its stereo-chemical and electronic preference for being a six co-ordinate 18-electron species.

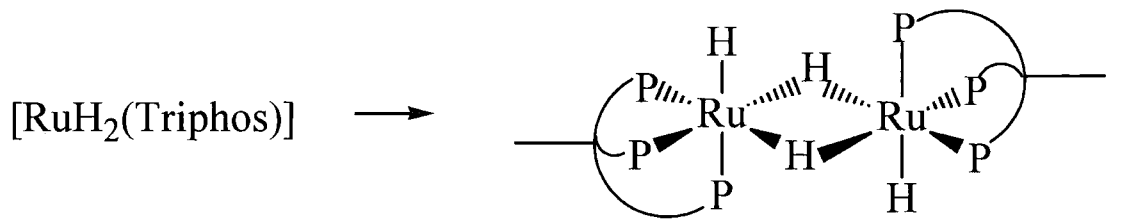

Equation 7.5

The existence of the [(Triphos)HRu(μ-H)$_2$RuH(Triphos)] provides support for the proposal that the active catalyst is [Ru(Triphos)H_2] (see Chapter 2). The investigation of the reactivity of [Ru(H_2)H_2(PPh_3)$_3$] by Kubas *et al* resulted in the isolation of [(PPh_3)$_3$Ru(μ-H)$_3$RuH(PPh_3)$_2$].[40] They proposed that loss of dihydrogen from [Ru(H_2)H_2(PPh_3)$_3$] produced the intermediate [RuH_2(PPh_3)$_3$], which dimerised into [(PPh_3)$_3$HRu(μ-H)$_2$RuH(PPh_3)$_3$] and after subsequent loss of triphenylphosphine and formation of a third bridging hydride gave [(PPh_3)$_3$Ru(μ-H)$_3$RuH(PPh_3)$_2$] (see Scheme 7.1).[40]

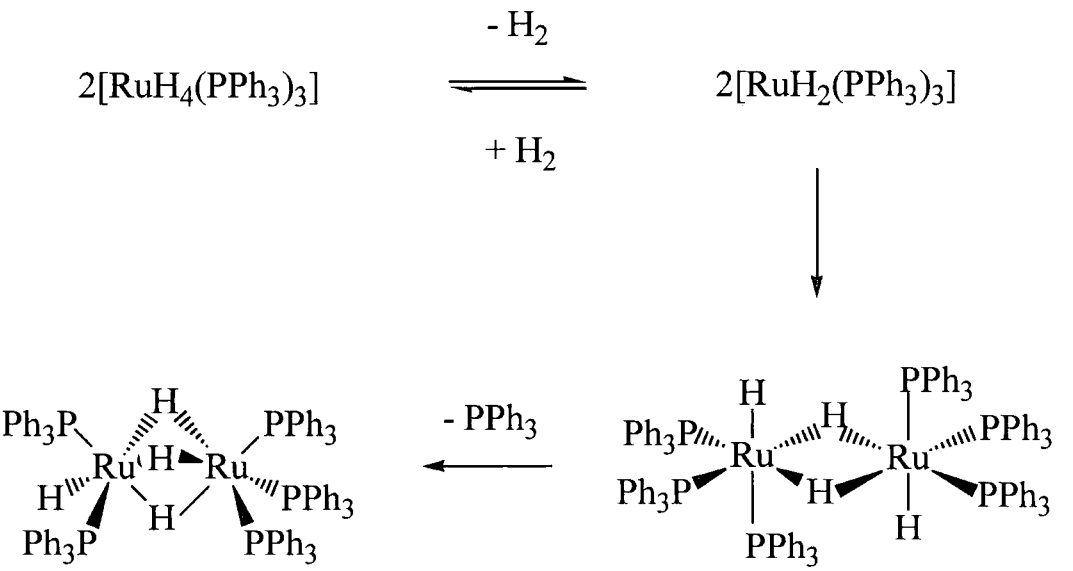

Scheme 7.1

The results of Kubas *et al* corroborate the suggestion that the [(Triphos)HRu(μ-$H)_2$RuH(Triphos)] was the result of the dimerisation of [Ru(Triphos)H_2], and that therefore the active catalyst is [Ru(Triphos)H_2]. In a medium, this catalytic intermediate would add a ligand to form [Ru(Triphos)H_2L], where L is a labile ligand such as dihydrogen or a solvent or substrate molecule (see Equation 7.6).

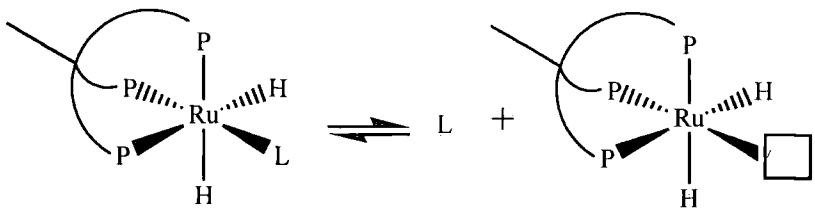

Equation 7.6
Note : L = H_2 or a solvent or substrate molecule.

7.2.2 Hydrogenation of Nitrogen Compounds

The hydrogenation of the nitrogen compounds by the $Ru(acac)_3$ and Triphos catalytic system was investigated in a solvent comprised of THF and water. The solvent was chosen because propionamide, was selected for study, and the -CONHR functional group was deemed potentially capable of catalyst deactivation. The water was included to facilitate any requirement for the catalyst reactivation, *via* the water gas shift reaction (WGS). The reaction temperature used was 140°C. The THF and water solvent and a temperature of 140°C were used in all the nitrogen compound investigations, so as to create consistency in the catalytic system used for the hydrogenations. A reaction period of 16 hours using a $p(H_2)$ 6.8 MPa was chosen.

7.2.2.1 Hydrogenation of Nitrotoluene

Nitrotoluene can exist in three different isomers (see Fig. 7.5). The hydrogenation of equal amounts of each compound was investigated by their simultaneous inclusion in the same reaction.

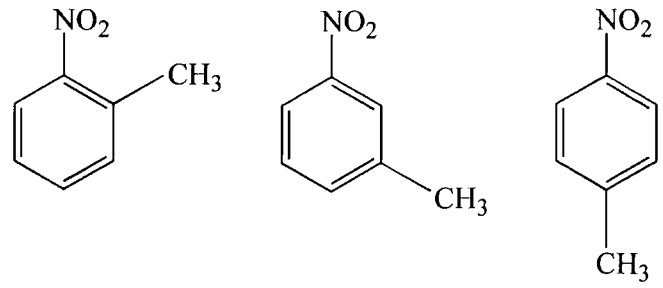

o-Nitrotoluene (2-Nitrotoluene) | *m*-Nitrotoluene (3-Nitrotoluene) | *p*-Nitrotoluene (4-Nitrotoluene)

Figure 7.5 Nitrotoluene Configurations

The catalytic system was able to hydrogenate each of the configurations equally, with no discernible difference in levels of conversion being obtained for any of the three forms, as no trace of nitrotoluene was observed on completion. The different stereo-chemical and electronic properties had no apparent effect on their catalysis. Hydrogenation produced a mixture of many products, analysed by GCMS, but due to the presence of a significant number of unidentified compounds the analysis was qualitative only.

The catalyst not only hydrogenated the nitro group to the respective amine, but also proceeded to remove the amine completely to produce toluene, which in turn was also hydrogenated to methyl-cyclohexane. Also identified in the products were methyl-cyclohexanol (all three configurations), which will have been produced by hydrolysis of the amine, due to the presence of the water in the solvent. The result of the nitrotoluene hydrogenation demonstrated that the catalytic system was able to carry out the reduction. However, the catalyst under the conditions investigated lacked any specificity and proceeded to completely reduce the nitrotoluene eventually to the respective hydrocarbon.

7.2.2.2 Hydrogenation of Propionitrile

The hydrogenation of propionitrile was also achieved by the same catalytic system, complete conversion of the propionitrile being achieved. The products included propylamine, dipropylamine, tripropylamine, *n*-methyldipropylamine and propanol, as detailed in Table 7.2. The 1-propanol obtained in the products will be the result of

hydrolysis of propylamine due to the presence of water in the reaction solvent, whilst the methyl of *n*-methyldipropylamine will be from the decarbonylation of the 1-propanol.

Table 7.2 Hydrogenation Products of Propionitrile

Product	Selectivity (%)
Propylamine	11.5
Dipropylamine	38.9
Tripropylamine	19.9
n-Methyldipropylamine	5.9
1-Propanol	12.3

The mixture of products may have been avoided, or at least reduced, had the reaction been carried out in the absence of water to avoid product hydrolysis and in the presence of an excess of ammonia, which is used industrially to suppress the production of secondary and tertiary amines.[19, 29] The major product would then be more likely to be the primary amine propylamine.

7.2.2.3 Hydrogenation of Propionamide

The hydrogenation of propionamide by the same catalytic system was not as successful as the hydrogenations of nitrotoluene or propionitrile. The level of conversion achieved for propionamide was only 38 %. The products included dipropylamine and 1-propanol with the by-product of *n*-propylpropionamide, as detailed in Table 7.3. An indication of the presence of ammonia was detected in the product solution by GCMS. However, due to the volatility of ammonia, the majority was lost when the headspace gas of the reaction was vented on completion.

Table 7.3 Hydrogenation Products of Propionamide

Product	Selectivity (%)
Propylamine	0.0
Dipropylamine	1.2
1-Propanol	37.0
n-Propylpropionamide	13.4

The presence of dipropylamine, 1-propanol and ammonia in the products indicates that the hydrogenation of propionamide is possible. The 1-propanol and ammonia in the products, suggest that the propionamide hydrogenation by the catalytic system favours alcohol production, rather than that of amines (see Equation 7.7). It might be, that an investigation of the reaction conditions might yield a better level of conversion for amines, if that was the desired product. The dipropylamine present in the product mixture indicates that the catalytic system is susceptible to the problem of producing a mixture of primary, secondary and tertiary amines, which is a common problem for the hydrogenation of unsubstituted amides. Side reactions such as the creation of secondary amines from primary amines, or hydrogenolysis of secondary and tertiary amines are a problem for catalytic hydrogenation of amides.[37]

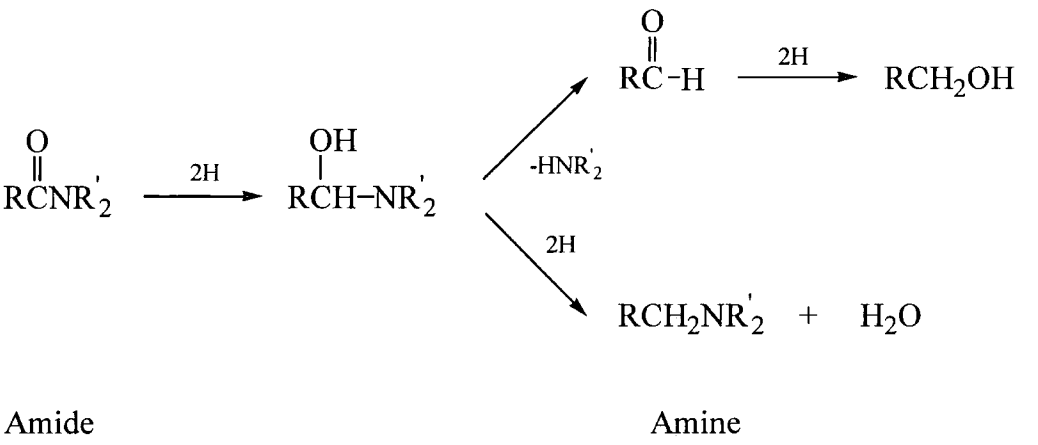

Equation 7.7

7.2.3 Conclusion

Exploratory studies using the catalyst, generated *in-situ* from $Ru(acac)_3$ and Triphos, have shown that it will hydrogenate alkenes, both terminal and cyclic, and the nitrogen compounds, nitrotoluene, propionitrile and propionamide. As with previous catalysts the reduction of nitrotoluene was achieved with ease, as could be seen from the products which included the respective hydrocarbon, methyl-cyclohexane. The more difficult amide reduction resulted in a lower level of conversion than that obtained for nitrotoluene and propionitrile, and even then the major product obtained was 1-propanol.

The hydrogenation of 1-hexene to hexane resulted in the isolation of the ruthenium dimer [(Triphos)HRu(μ-H)$_2$RuH(Triphos)]. From this the active catalyst and its intermediate were determined to be [Ru(Triphos)H$_2$] and [Ru(Triphos)H$_2$L] respectively.

7.3 Experimental

7.3.1 Hydrogenations

All hydrogenations were carried out using a 300-ml Hasteloy^{TM} autoclave equipped with overhead stirrer. The autoclave was loaded with the reagents (see below, 7.3.1.1) and then the air was removed by flushing three times with hydrogen. The autoclave was then pressurised at r.t. with hydrogen (4.4 MPa). The autoclave was then heated to the respective reaction temperature, at which the hydrogen mass flow controller was set to 6.8 MPa, and then heated and stirred for 16 hours. On completion of the reaction period, the heating was stopped and the autoclave allowed to slowly cool, over approximately two hours. The headspace gases within the autoclave were slowly vented and the products removed. The product solution was analysed by GC, GCMS and NMR spectroscopy. The product solid was analysed by ^{31}P NMR spectroscopy, X-ray crystallography (where appropriate), and selected samples by ^{1}H NMR spectroscopy, IR, mass spectrometry and elemental analysis.

7.3.1.1 Quantity of Reagents Used

Table 7.4 Catalyst

Reagent	Quantity
Ru(acac)$_3$	4.5 x 10^{-4} mol
Triphos	6.1 x 10^{-4} mol

Table 7.5 Alkene Hydrogenation

Reagent	Quantity
Alkene	20.0 cm^3
iPA (Solvent)	50.0 cm^3

Table 7.5 Nitrotoluene Hydrogenation

Reagent	Quantity
2-Nitrotoluene	5.1×10^{-2} mol
3-Nitrotoluene	5.1×10^{-2} mol
4-Nitrotoluene	5.1×10^{-2} mol
THF (Solvent)	40.0 cm^3
H_2O (Solvent)	10.0 cm^3

Table 7.5 Propionitrile Hydrogenation

Reagent	Quantity
Propionitrile	20.0 cm^3
THF (Solvent)	40.0 cm^3
H_2O (Solvent)	10.0 cm^3

Table 7.5 Propionamide Hydrogenation

Reagent	Quantity
Propionamide	2.7×10^{-1} mol
THF (Solvent)	40.0 cm^3
H_2O (Solvent)	10.0 cm^3

7.3.2 NMR Spectroscopy

The NMR spectra of the product solutions were measured against an external reference of chloroform-*d* containing Triphos, which was used to lock and shim the NMR spectrometer. The product solids were dissolved in the appropriate *deuterated* solvent and the NMR spectrometer locked and shimmed accordingly, prior to running the sample for the required NMR measurements.

7.4 References

1. B. R. James, *Inorg Chim. Acta Res.*, 1970, 73.
2. R. E. Harmon, S. K. Gupta and D. J. Brown, *Chem. Res.*, 1973, **73**, 1, 21.
3. E. W. Abel, F. G. A. Stone and G. Wilkinson, *Comprehensive Organometallic Chemistry*, Pergamon Press, Oxford, 1987, Vol. 4.
4. H. E. Bryndza and W. Tam, *Chem. Res.*, 1988, **88**, 1163.
5. P. S. Hallman, B. R. McGarvey and G. Wilkinson, *J. Chem. Soc. (A)*, 1968, 3143.

6. J. A. Osborn, F. H. Jardine, J. F. Young and G. Wilkinson, *J. Chem. Soc. (A)*, 1966, 1711.
7. F. H. Jardine, J. A. Osborn and G. Wilkinson, *J. Chem. Soc. (A)*, 1967, 1574.
8. R. H. Crabtree and D. G. Hamilton, *J. Am. Chem. Soc.*, 1986, **108**, 3124.
9. D. E. Linn, Jr., and J. Halpern, *J. Am. Chem. Soc.*, 1987, **109**, 2969.
10. S. Komiya and A. Yamamoto, *J. Mol. Catal.*, 1979, **5**, 279.
11. S. Komiya, A. Yamamoto and S. Ikeda, *J. Organomet. Chem.*, 1972, **42**, C65.
12. R. A. Grey, G. P. Pez and A. Wallo, *J. Am. Chem. Soc.*, 1988, **102**, 5948.
13. A. F. Borowski, D. J. Cole-Hamilton and G. Wilkinson, *Nouv. J. Chim.*, 1978, **2**, 137.
14. Z. Tóth, F. Joó and M. T. Beck, *Inorg. Chim. Acta*, 1980, **42**, 153.
15. Y. Wakatsuki and H. Yamazaki, *J. Organomet. Chem.*, 1995, **500**, 349.
16. V. Ratovelomanana-Vidal and J-P. Genet, *J. Organomet. Chem.*, 1998, **567**, 163.
17. B. R. James, D. Wang and R. F. Voight, *Chem. Commun.*, 1975, 1365.
18. R. Noyori and S. Hasiguchi, *Acc. Chem. Res.*, 1997, **30**, 97.
19. H. Beyer and W. Walter, *Handbook of Organic Chemistry*, Simon and Schuster International Group, Hemel Hempstead, 1996.
20. J. March, *Advanced Organic Chemistry*, John Wiley & Sons, New York, 4th edn., 1992.
21. T. W. G. Solomons, *Fundamentals of Organic Chemistry*, New York, 5th edn., 1997.
22. J. P. Collman, L. S. Hegedus, J. R. Norton and R. G. Finke, *Principles and Applications of Organotransition Metal Chemistry*, University Science Books, Mill Valley, CA, 2nd edn., 1987.
23. C. J. Love and F. J. McQuillin, *J. Chem. Soc., Perkin Trans.*, 1973, **1**, 2509.
24. H. Des Abbayes and H. Alper, *J. Am. Chem. Soc.*, 1977, **99**, 98.
25. H. Alper and S. Amaratunga, *Tetrahedron Lett.*, 1980, **21**, 2603.
26. M. Miura, M. Shinohara and M. Nomura, *J. Mol. Catal.*, 1984, **45**, 151.
27. J. F. Knifton, *J. Org. Chem.*, 1976, **41**, 1200.
28. F. L.'Eplattenier, P. Matthys and C. Calderazzo, *Inorg. Chem.*, 1970, **9**, 342.
29. K. Weissermel and H. –J. Arpe, *Industrial Organic Chemistry*, VCH Publishers, Inc., New York, 2nd edn., 1993.
30. A. R. Barron, J. E. Salt, G. Wilkinson, M. Motevalli and M. B. Hursthouse, *J. Chem. Soc., Dalton Trans.*, 1987, 2947.
31. D. R. Levering, U.S. Patent No. 3 152 184 1964 (assigned to Hercules Powder Co.).
32. T. Yoshida, T. Okano and S. Otsuka, *J. Chem. Soc., Chem. Commun.*, 1979, 870.
33. J. E. Bercaw, D. L. Davies and P. T. Wolczanski, *Organometallics*, 1986, **5**, 443.
34. R. A. Grey, G. P. Pez and A. Wallo, *J. Am. Chem. Soc.*, 1981, **103**, 7356.
35. K. C. Dewhirst, U.S. Patent No. 3 454 644, 1969 (assigned to Shell Oil Co.).
36. R. P. Beatty and R. A. Paciello, U.S. Patent No. 5 763 669 (assigned to DuPont).
37. M. Hudlický, *Reductions in Organic Chemistry*, American Chemical Society, Washington, DC, 2nd edn., 1996.
38. J. Fuhrop and G. Penzlin, *Organic Synthesis*, VCH Publishers, Inc., New York, 2cnd edn., 1994.
39. R. C. Larock, *Comprehensive Organic Transformations*, John Wiley & Sons, Inc., New York, 2nd edn., 1999.
40. L. S. Van Der Sluys, G. J. Kubas and K. G. Caulton, *Organometallics*, 1991, **10**, 1033.

Chapter 8

Conclusions

The homogeneous hydrogenation of esters and related compounds was achieved by a catalyst produced *in situ* from $Ru(acac)_3$ and the tripodal triphosphine 1,1,1-tris(diphenylphosphinomethyl)ethane (Triphos). The many and varied applications of homogeneous ruthenium catalysts are well documented in the literature, and the catalytic system developed for the homogeneous hydrogenations described in this thesis is a further example.[1]

The catalytic hydrogenation of unsaturated carboxylic acids to alcohols using existing catalysts requires two steps and two catalysts; firstly the hydrogenation and esterification of the carboxylic acid to the respective ester by one catalyst, and then secondly the hydrogenation of the ester to the target alcohol with a different catalyst. Conveniently the $Ru(acac)_3$ and Triphos catalytic system homogeneously hydrogenates carboxylic acids directly to the analogous alcohol both with high selectivity and conversion. Unlike previous homogeneous catalytic systems, where the catalyst was unable to reduce the acid further than the ester (because the reaction conditions favoured esterification), the $Ru(acac)_3$ and Triphos catalytic system hydrogenates esters directly to alcohols.[2, 3, 4]

The homogeneous hydrogenation of maleic and fumaric acid to produce THF was achieved in a one-pot reaction by the $Ru(acac)_3$ and Triphos catalytic system. The reduction of the maleic acid to THF proceeded *via* succinic acid to gBL and BDO to THF. The catalyst will also hydrogenate the analogous esters, dimethyl maleate, dimethyl fumarate and gBL, and has been demonstrated for the hydrogenation of other esters.

The catalytic system applied in this study has been shown to hydrogenate esters and carboxylic acids to completion, and to produce their respective alcohols with a high level of selectivity. The inclusion of H_2O into the catalytic system and the application of temperatures in excess of 140°C ensures that the catalyst, deactivated by decarbonylation of product alcohols, is reactivated *in situ* by the water gas shift

reaction. The use of the tripodal *facially* co-ordinating polyphosphine Triphos ligand, ensures the correct ruthenium geometry for the co-ordination of substrate and hydride ligands. The *facial* orientation of the remaining sites results in the necessary *cis* arrangement of the reactant ligands for hydrogenation to occur. The strong *trans* effects of the *fac* co-ordinated Triphos and the steric properties of the phenyl substituents produce the required environment for fast ligand dissociation, to provide vacant co-ordination sites essential for catalysis to occur.

The isolation of the complex [(Triphos)HRu(μ-H)$_2$RuH(Triphos)] from the hydrogenation of 1-hexene suggests that the active catalyst is [Ru(Triphos)H$_2$]. The dimer was obtained when the catalyst had consumed the available unsaturated substrate, and in the absence of alcohols to decarbonylate the complex dimerised to form [(Triphos)HRu(μ-H)$_2$RuH(Triphos)], which was characterised by X-ray crystallography.

The Ru(acac)$_3$ and Triphos catalytic system can decarbonylate primary alcohols either stoichiometrically or catalyticaly, in the presence of water. This catalyst demonstrates the ability of many ruthenium complexes to extract CO from primary alcohols or aldehydes. The decarbonylation of the primary alcohol probably proceeds *via* the dehydrogenation of the alcohol to the respective aldehyde, which undergoes subsequent decarbonylation. The complex formed from the stoichiometric decarbonylation was identified by X-ray crystallography, mass spectrometry and NMR spectroscopy as [Ru(Triphos)H$_2$(CO)], also identified as the deactivated catalyst. The [Ru(Triphos)H$_2$(CO)] is catalyticaly inactive, because the CO ligand effectively blocks a co-ordination site and therefore inhibits the catalyst's ability to hydrogenate any further substrate. The CO ligand can be removed from [Ru(Triphos)H$_2$(CO)] by the introduction of H$_2$O. The CO is removed as CO$_2$ by the water gas shift reaction, which reactivates the catalyst. The presence of H$_2$O in the reaction media facilitates the catalytic decarbonylation of primary alcohols.

$$RCH_2OH \longrightarrow RCHO \longrightarrow RH$$

$$CO + H_2O \longrightarrow CO_2 + H_2$$

The separation of the homogeneous hydrogenation products and recovery of the catalyst was achieved by distillation. The recycling of the recovered catalyst in a series of ten batch reactions indicated no catalyst degradation or loss of performance. The initial catalyst charge was generated from the $Ru(acac)_3$ and Triphos precursors and recovered as a solution based concentrate.

The catalytic system's properties as a hydrogenating agent were illustrated by the reduction of the amine-based compounds of propionitrile, propionamide, nitrotoluene and the amino acid (+/-) 2-phenylglycine. The products obtained indicate that the catalyst will continue to hydrogenate, dehydrate and decarbonylate any susceptible substrate and products capable of further reaction.

Importantly the catalytic system investigated in this study for the hydrogenation of carboxylic acids and esters, has been shown capable of providing an alternative to the presently used heterogeneous system.

8.1 References

1. B. R James, *Inorg. Chim. Acta, Res.*, 1970, 73.
2. J. E. Lyons, *Chem. Commun.*, 1975, 412.
3. M. Bianchi, F. Piacenti, P. Frediani, U. Matteoli, C. Botteghi, S. Gladiali and E. Benedetti, *J. Organomet. Chem.*, 1977, **141**, 107.
4. M. Bianchi, G. Menchi, F. Francalanci, F. Piacenti, U. Matteoli, P Frediani and C. Botteghi, *J. Organomet. Chem.*, 1980, **188**, 109.

Addendum

Temperature Calibration

Subsequent to completion of the PhD. Study, and during experimentation with a different autoclave to demonstrate the repeatability of the results, it was discovered that for the autoclave used for the thesis work , the reaction temperature was controlled *via* the head space gas and not the reaction solution. This arose because the thermocouple had been incorrectly fitted to the autoclave, and was located above the reaction solution at a bend in the thermocouple well. Consequently, all temperatures recorded as temperatures of reaction solutions in this thesis are subject to systematic errors, and should be considered as headspace temperatures. A temperature calibration has been undertaken to relate the head space gas temperature to the corresponding solution temperature (see Figure A.1, page 176), and all recorded reaction temperatures should be adjusted upwards accordingly. Repeat of a selection of reactions detailed in this thesis, using the solution temperatures derived from the calibration graph, in both the original autoclave and a different autoclave, confirmed the precision of the calibration graph.

As the thermocouple was not removed from the autoclave throughout the period of the thesis work, all the reported reaction temperatures are subject to the same systematic error.

Figure A.1 Temperature Calibration Graph, Headspace to Solution

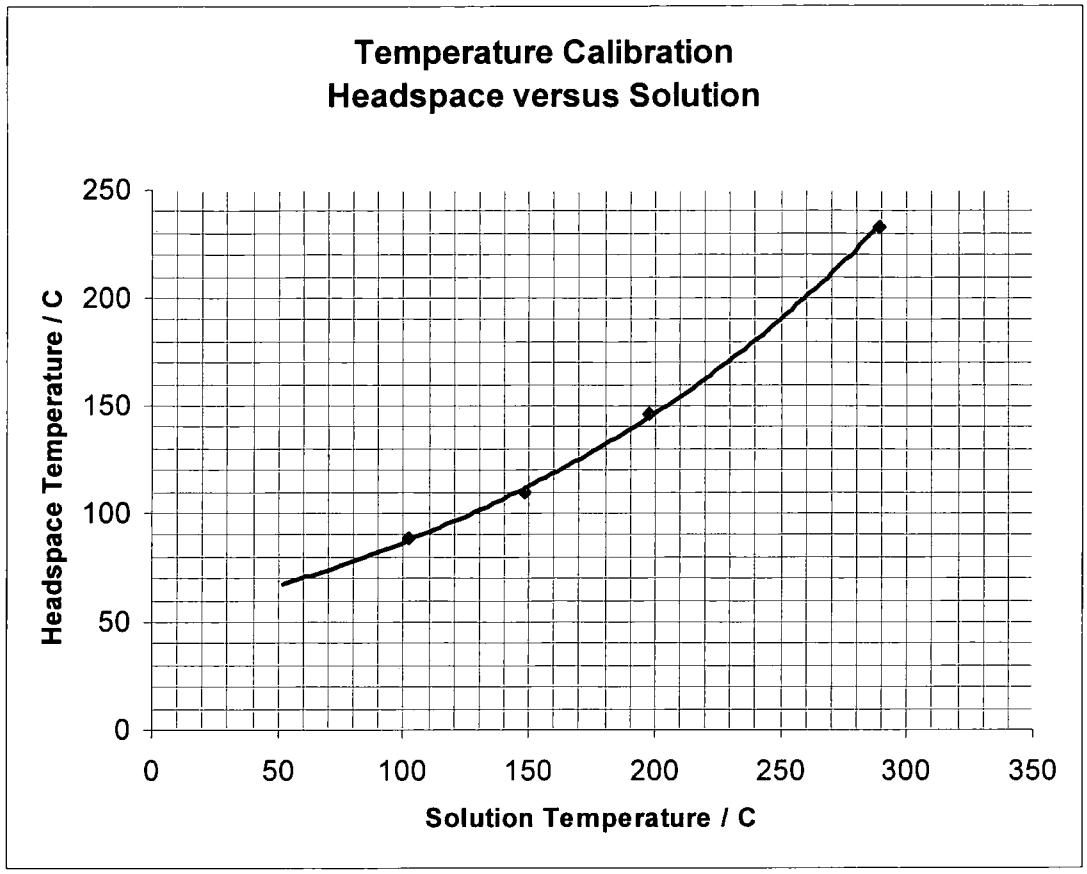

Appendix 1

Experimental Parameters

Unless otherwise stated, all reactions were carried out under a dry, oxygen free nitrogen atmosphere, using standard vacuum line and Schlenk techniques. Solvents used were dried, using the appropriate drying agents, and freshly distilled before use. All reagents were purchased commercially.

Complex characterisation and high pressure hydrogenation reaction products were performed, using a model CE-440 elemental analyser manufactured by Exeter Analytical Inc., by IR spectroscopy using a Paragon 1000 series FTIR spectrometer, by NMR spectroscopy using Varian Mercury 200, Bruker AM-250, Varian VXR-400 and Varian Inova-500 MHz spectrometers. Spectra were obtained for protons referenced to the chemical shifts of the solvents and reported with respect to $SiMe_4$. Spectra were obtained for ^{31}P nuclei referenced to an external frequency lock and reported with respect to 85% H_3PO_4. Products were determined using a HP 6890 GC System gas chromatograph and HP 6890 GC System coupled to a HP 5973 Mass Selective Detector. Headspace gas analysis was by a Pye-Unicam refinery gas analyser and CO and CO_2 Draeger tube. Water content was determined by Orion AF8 volumetric Karl Fischer titrator.

High pressure testing was performed in a Parr Instrument Co., Hastelloy 300 cm^3 Autoclave with overhead stirring, controlled by a Parr 4842 control box.

Appendix 2

Supplementary Data for Chapter 2

Table 1. Crystal data and structure refinement for [Ru(Triphos)H_2(CO)]

Empirical formula	C42 H39 O P3 Ru	
Formula weight	753.71	
Temperature	293(2) K	
Wavelength	0.71073 Å	
Crystal system	orthorhombic	
Space group	Pna2 (1)	
Unit cell dimensions	a = 20.873(3) Å	$\alpha = 90^{\circ}$.
	b = 10.3167(12) Å	$\beta = 90^{\circ}$.
	c = 16.929(2) Å	$\beta = 90^{\circ}$.
Volume	3645.5(7) $Å^3$	
Z	4	
Density (calculated)	1.373 Mg/m^3	
Absorption coefficient	0.594 mm^{-1}	
F(000)	1552	
Crystal size	0.5 x 0.2 x 0.08 mm^3	
Theta range for data collection	1.95 to 25.01 °.	
Index ranges	-17 <=h<=24, -12<=k<=12, -19<=l<=20	
Reflections collected	18716	
Independent reflections	6314 [R(int) = 0.1484]	
Completeness to theta = 25.01 °	99.9%	
Refinement method	Full-matrix least-squares on F^2	
Data / restraints / parameters	66314 / 1 / 425	
Goodness-of-fit on F^2	1.012	
Final R indices [I>2sigma(I)]	R1 = 0.0608, wR2 = 0.1241	
R indices (all data)	R1 = 0.1449, wR2 = 0.1615	
Absolute structure parameter	-0.01(6)	
Largest diff. Peak and hole	0.636 and –0.441 e $Å^{-3}$	

The Crystal Structure of [Ru(Triphos)H_2(CO)]

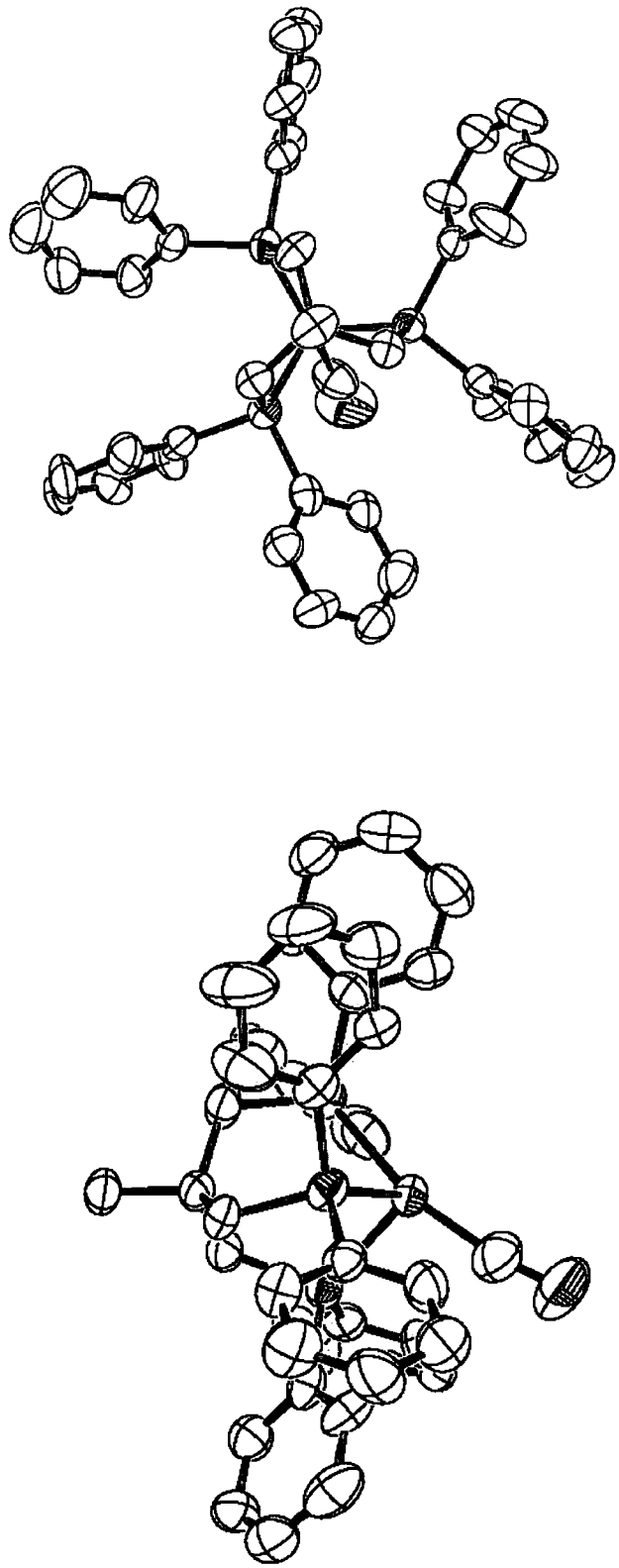

Table 2. Atomic coordinates (x 10^4) and equivalent isotropic displacement parameters ($Å^2$x 10^3). U(eq) is defined as one third of the trace of the orthogonalized U^{ij} tensor.

	x	y	z	U(eq)
C(100)	7655(7)	2642(13)	9478(9)	81(4)
C(101)	11184(10)	9712(15)	5868(11)	108(6)
C(102)	8105(6)	3226(13)	9925(8)	74(4)
C(103)	10273(8)	3070(15)	9199(7)	103(6)
C(104)	10719(7)	2125(17)	9275(9)	109(6)
C(105)	7363(6)	6731(15)	8799(8)	82(4)
C(106)	10939(7)	1418(15)	8660(10)	90(4)
C(107)	7736(6)	2626(13)	8679(8)	78(4)
C(108)	11997(7)	3351(12)	6347(9)	77(4)
P(4)	9057(1)	7524(3)	7618(2)	44(1)
P(3)	9411(1)	4602(3)	8293(1)	45(1)
P(2)	10414(1)	6157(2)	7184(2)	45(1)
Ru(1)	9335(1)	5545(1)	7030(1)	44(1)
C(1)	8924(4)	8941(9)	6978(7)	52(2)
C(2)	9156(5)	10171(9)	7109(10)	62(3)
C(3)	12117(5)	4156(13)	6938(9)	71(3)
C(4)	10616(5)	6480(11)	8240(5)	52(3)
C(5)	11287(6)	8153(11)	6871(8)	74(4)
C(6)	8335(5)	7668(10)	8229(6)	52(3)
C(7)	10697(5)	7628(9)	6685(6)	47(2)
C(8)	8719(5)	3854(10)	8764(6)	47(3)
C(9)	11649(5)	4955(11)	7228(6)	60(3)
C(10)	10354(5)	7610(12)	9497(5)	58(3)
C(11)	8264(5)	3218(12)	8325(7)	64(3)
C(12)	10350(7)	8148(12)	6075(6)	67(4)
C(13)	8532(5)	8754(10)	6313(6)	55(3)
O(1)	8120(5)	4601(11)	6275(7)	126(4)
C(15)	9678(5)	8087(10)	8302(6)	49(3)
C(16)	10249(5)	2646(11)	7832(7)	59(3)
C(17)	9617(5)	5880(9)	9019(5)	45(3)
C(18)	8629(6)	3786(11)	9585(6)	61(3)
C(19)	11047(5)	5015(10)	6879(6)	50(3)
C(20)	11399(7)	3384(14)	5960(7)	76(4)
C(21)	10717(6)	1679(12)	7936(8)	71(3)
C(23)	8188(6)	8775(12)	8659(7)	62(3)
C(24)	9014(7)	11179(11)	6602(8)	75(4)
C(25)	7260(7)	7868(14)	9230(8)	69(4)
C(26)	10941(6)	4204(11)	6233(7)	57(3)
C(27)	7664(6)	8864(14)	9131(6)	67(3)
C(28)	7914(5)	6658(11)	8317(7)	62(3)
C(200)	8573(7)	5000(12)	6631(8)	80(4)
C(30)	10026(5)	3351(10)	8449(6)	47(3)
C(31)	8642(6)	10963(12)	5973(7)	67(4)
C(32)	10581(8)	9227(13)	5655(8)	85(4)
C(33)	11535(8)	9226(15)	6472(10)	97(5)
C(37)	8386(6)	9772(12)	5826(6)	60(3)
C(38)	10057(5)	6970(11)	8737(6)	47(3)

Table 3. Bond lengths [Å] and angles [°].

C(100)-C(102)	1.349(17)		
C(100)-C(107)	1.364(18)	C(102)-C(100)-C(107)	118.4(13)
C(101)-C(33)	1.35(2)	C(33)-C(101)-C(32)	123.2(16)
C(101)-C(32)	1.40(2)	C(100)-C(102)-C(18)	120.7(13)
C(102)-C(18)	1.366(15)	C(104)-C(103)-C(30)	119.2(13)
C(103)-C(104)	1.354(18)	C(106)-C(104)-C(103)	123.3(14)
C(103)-C(30)	1.400(15)	C(25)-C(105)-C(28)	118.2(13)
C(104)-C(106)	1.352(19)	C(21)-C(106)-C(104)	118.6(13)
C(105)-C(25)	1.397(18)	C(100)-C(107)-C(11)	121.3(12)
C(105)-C(28)	1.413(16)	C(3)-C(108)-C(20)	120.3(12)
C(106)-C(21)	1.337(17)	C(15)-P(4)-C(6)	101.5(5)
C(107)-C(11)	1.396(15)	C(15)-P(4)-C(1)	103.1(5)
C(108)-C(3)	1.325(16)	C(6)-P(4)-C(1)	98.2(5)
C(108)-C(20)	1.409(18)	C(15)-P(4)-Ru(1)	111.7(4)
P(4)-C(15)	1.832(10)	C(6)-P(4)-Ru(1)	120.9(4)
P(4)-C(6)	1.834(11)	C(1)-P(4)-Ru(1)	118.7(4)
P(4)-C(1)	1.841(11)	C(8)-P(3)-C(30)	101.2(5)
P(4)-Ru(1)	2.344(3)	C(8)-P(3)-C(17)	101.2(5)
P(3)-C(8)	1.823(11)	C(30)-P(3)-C(17)	104.0(5)
P(3)-C(30)	1.839(10)	C(8)-P(3)-Ru(1)	121.2(3)
P(3)-C(17)	1.853(10)	C(30)-P(3)-Ru(1)	117.9(3)
P(3)-Ru(1)	2.353(2)	C(17)-P(3)-Ru(1)	108.9(3)
P(2)-C(7)	1.835(10)	C(7)-P(2)-C(19)	99.7(5)
P(2)-C(19)	1.844(11)	C(7)-P(2)-C(4)	102.7(5)
P(2)-C(4)	1.866(9)	C(19)-P(2)-C(4)	102.7(5)
P(2)-Ru(1)	2.354(3)	C(7)-P(2)-Ru(1)	118.7(4)
Ru(1)-C(200)	1.818(15)	C(19)-P(2)-Ru(1)	118.9(4)
C(1)-C(2)	1.376(13)	C(4)-P(2)-Ru(1)	111.7(3)
C(1)-C(13)	1.404(14)	C(200)-Ru(1)-P(4)	102.2(4)
C(2)-C(24)	1.381(16)	C(200)-Ru(1)-P(3)	105.6(5)
C(3)-C(9)	1.369(15)	P(4)-Ru(1)-P(3)	89.53(10)
C(4)-C(38)	1.524(13)	C(200)-Ru(1)-P(2)	164.0(5)
C(5)-C(7)	1.381(14)	P(4)-Ru(1)-P(2)	87.50(9)
C(5)-C(33)	1.396(17)	P(3)-Ru(1)-P(2)	86.88(9)
C(6)-C(28)	1.371(14)	C(2)-C(1)-C(13)	117.4(11)
C(6)-C(23)	1.389(15)	C(2)-C(1)-P(4)	125.8(10)
C(7)-C(12)	1.371(14)	C(13)-C(1)-P(4)	116.8(8)
C(8)-C(11)	1.372(14)	C(1)-C(2)-C(24)	121.3(13)
C(8)-C(18)	1.404(14)	C(108)-C(3)-C(9)	120.9(12)
C(9)-C(19)	1.389(14)	C(38)-C(4)-P(2)	114.5(7)
C(10)-C(38)	1.574(13)	C(7)-C(5)-C(33)	122.0(13)
C(12)-C(32)	1.406(17)	C(28)-C(6)-C(23)	115.2(11)
C(13)-C(37)	1.369(14)	C(28)-C(6)-P(4)	121.7(9)
O(1)-C(200)	1.193(15)	C(23)-C(6)-P(4)	123.0(9)
C(15)-C(38)	1.580(14)	C(12)-C(7)-C(5)	119.3(11)
C(16)-C(30)	1.355(14)	C(12)-C(7)-P(2)	120.0(9)
C(16)-C(21)	1.408(15)	C(5)-C(7)-P(2)	120.5(9)
C(17)-C(38)	1.528(14)	C(11)-C(8)-C(18)	114.9(10)
C(19)-C(26)	1.395(14)	C(11)-C(8)-P(3)	120.9(8)
C(20)-C(26)	1.358(16)	C(18)-C(8)-P(3)	124.0(8)
C(23)-C(27)	1.358(15)	C(3)-C(9)-C(19)	121.3(11)
C(24)-C(31)	1.337(16)	C(8)-C(11)-C(107)	121.5(10)
C(25)-C(27)	1.339(17)	C(7)-C(12)-C(32)	120.6(13)
C(31)-C(37)	1.363(17)	C(37)-C(13)-C(1)	120.5(10)

C(38)-C(15)-P(4)	114.7(7)
C(30)-C(16)-C(21)	121.4(11)
C(38)-C(17)-P(3)	117.1(7)
C(102)-C(18)-C(8)	123.0(11)
C(9)-C(19)-C(26)	116.7(10)
C(9)-C(19)-P(2)	123.9(8)
C(26)-C(19)-P(2)	119.2(8)
C(26)-C(20)-C(108)	118.7(12)
C(106)-C(21)-C(16)	119.9(13)
C(27)-C(23)-C(6)	122.8(12)
C(31)-C(24)-C(2)	119.6(12)
C(27)-C(25)-C(105)	118.8(13)
C(20)-C(26)-C(19)	122.0(11)
C(25)-C(27)-C(23)	121.9(13)
C(6)-C(28)-C(105)	122.9(12)
O(1)-C(200)-Ru(1)	170.8(14)
C(16)-C(30)-C(103)	117.6(10)
C(16)-C(30)-P(3)	120.3(8)
C(103)-C(30)-P(3)	122.1(9)
C(24)-C(31)-C(37)	121.5(11)
C(101)-C(32)-C(12)	117.4(14)
C(101)-C(33)-C(5)	117.3(16)
C(31)-C(37)-C(13)	119.6(11)
C(4)-C(38)-C(17)	112.8(9)
C(4)-C(38)-C(10)	106.8(8)
C(17)-C(38)-C(10)	106.8(8)
C(4)-C(38)-C(15)	111.6(8)
C(17)-C(38)-C(15)	112.4(8)
C(10)-C(38)-C(15)	105.8(8)

Table 4. Anisotropic displacement parameters ($Å^2 x\ 10^3$). The anisotropic displacement factor exponent takes the form: $-2\pi^2[\ h^2\ a^{*2}U^{11} + ... + 2\ h\ k\ a^*\ b^*\ U^{12}\ ]$

	U^{11}	U^{22}	U^{33}	U^{23}	U^{13}	U^{12}
C(100)	72(10)	87(10)	86(10)	-19(9)	28(9)	-20(8)
C(101)	127(16)	64(10)	133(16)	-17(11)	69(13)	-17(10)
C(102)	67(9)	81(9)	75(8)	13(8)	8(8)	-22(8)
C(103)	134(14)	121(12)	55(8)	13(8)	-7(8)	85(11)
C(104)	98(12)	144(15)	85(10)	35(10)	15(9)	69(11)
C(105)	54(9)	102(12)	90(10)	33(9)	-6(8)	-16(8)
C(106)	66(9)	95(11)	109(12)	14(10)	-6(9)	40(8)
C(107)	57(8)	83(9)	93(10)	-18(8)	15(8)	-32(7)
C(108)	68(10)	65(8)	97(10)	15(8)	24(8)	20(7)
P(4)	43(2)	45(2)	44(1)	-3(1)	-3(1)	-5(1)
P(3)	41(2)	52(2)	43(1)	6(1)	-5(1)	-1(1)
P(2)	47(1)	47(1)	41(2)	4(1)	-2(1)	-5(1)
Ru(1)	47(1)	41(1)	44(1)	0(1)	-9(1)	-3(1)
C(1)	44(5)	58(6)	55(6)	-1(8)	10(7)	-6(5)
C(2)	57(7)	54(6)	75(8)	5(8)	-2(8)	-12(5)
C(3)	52(7)	105(9)	56(7)	9(9)	-8(8)	14(7)
C(4)	42(6)	76(8)	39(5)	-4(5)	-1(5)	-13(6)
C(5)	70(8)	66(7)	85(10)	5(7)	22(8)	-23(6)
C(6)	56(7)	52(7)	47(6)	9(6)	-16(5)	-5(6)
C(7)	55(7)	46(6)	41(5)	-2(5)	11(6)	-8(6)
C(8)	45(6)	50(6)	46(6)	4(5)	-4(5)	4(5)
C(9)	46(7)	72(7)	61(8)	-7(6)	6(6)	-10(6)
C(10)	49(7)	85(8)	40(6)	-8(6)	-5(6)	-10(6)
C(11)	62(8)	84(9)	45(6)	-11(6)	5(6)	-10(7)
C(12)	91(10)	66(8)	44(6)	11(6)	18(7)	4(7)
C(13)	76(8)	36(6)	53(7)	-6(6)	-7(6)	-4(6)
O(1)	77(7)	140(10)	159(10)	-30(9)	-46(7)	-10(7)
C(15)	46(6)	50(6)	49(6)	-8(5)	-3(5)	-7(5)
C(16)	52(7)	63(8)	63(7)	-5(7)	-10(6)	13(6)
C(17)	44(6)	53(6)	39(5)	2(5)	-11(5)	-4(5)
C(18)	62(8)	63(7)	58(7)	2(6)	-9(6)	-8(6)
C(19)	54(7)	57(6)	40(7)	-2(5)	8(6)	1(5)
C(20)	79(10)	78(9)	70(8)	-20(7)	23(8)	-16(8)
C(21)	66(9)	60(8)	88(9)	6(7)	2(8)	9(7)
C(23)	58(8)	61(8)	65(7)	-3(7)	0(6)	-6(6)
C(24)	86(9)	39(7)	99(9)	25(7)	-6(8)	-15(7)
C(25)	59(9)	89(11)	59(8)	17(8)	9(7)	0(8)
C(26)	47(7)	53(7)	70(7)	6(6)	3(6)	-2(6)
C(27)	52(8)	92(9)	57(7)	-2(7)	8(6)	5(8)
C(28)	42(7)	60(7)	83(8)	24(7)	-17(7)	-4(6)
C(200)	72(9)	75(8)	92(9)	-3(7)	-22(8)	10(7)
C(30)	42(7)	48(6)	51(6)	10(6)	-2(5)	-6(5)
C(31)	82(9)	52(8)	67(8)	30(7)	7(8)	10(7)
C(32)	109(12)	65(9)	83(9)	21(8)	24(9)	4(9)
C(33)	102(13)	88(12)	100(11)	-24(10)	29(10)	-25(10)
C(37)	72(9)	65(9)	45(6)	3(6)	-9(6)	14(7)
C(38)	37(6)	61(7)	43(5)	-9(5)	0(5)	-8(5)

Table 5. Hydrogen coordinates (x 10^4) and isotropic displacement parameters ($Å^2$x 10^3).

	x	y	z	U(eq)
H(100)	7297	2259	9709	98
H(101)	11351	10402	5580	130
H(102)	8057	3249	10472	89
H(103)	10131	3526	9640	124
H(104)	10882	1954	9776	131
H(105)	7077	6042	8829	99
H(106)	11239	763	8739	108
H(107)	7434	2212	8364	93
H(108)	12308	2762	6186	92
H(2)	9413	10325	7547	75
H(3)	12525	4179	7159	85
H(4A)	10777	5686	8474	62
H(4B)	10957	7116	8259	62
H(5)	11527	7781	7275	89
H(9)	11736	5468	7667	72
H(10A)	10016	7915	9833	88
H(10B)	10621	8325	9346	88
H(10C)	10605	6979	9776	88
H(11)	8309	3181	7779	77
H(12)	9958	7784	5938	80
H(13)	8370	7934	6203	66
H(15A)	9981	8615	8011	58
H(15B)	9479	8636	8697	58
H(16)	10088	2804	7328	71
H(17A)	9221	6267	9203	54
H(17B)	9818	5467	9470	54
H(18)	8942	4139	9912	73
H(20)	11320	2854	5526	91
H(21)	10873	1224	7503	85
H(23)	8460	9487	8622	74
H(24)	9176	12004	6698	90
H(25)	6917	7932	9578	83
H(26)	10545	4226	5982	68
H(27)	7583	9638	9395	80
H(28)	7996	5890	8047	74
H(31)	8556	11641	5627	81
H(32)	10343	9603	5251	102
H(33)	11926	9591	6614	116
H(37)	8114	9651	5398	73

Appendix 3

Supplementary Data for Chapter 7

Table 1. Crystal data and structure refinement for [(Triphos)HRu(μ-H)$_2$RuH(Triphos)]

Empirical formula	C82 H82 P6 Ru2	
Formula weight	1455.44	
Temperature	105(2) K	
Wavelength	0.71073 Å	
Crystal system	Monoclinic	
Space group	$P2_1/n$ (No. 14)	
Unit cell dimensions	a = 13.026(3) Å	α= 90°
	b = 18.836(4) Å	β= 96.36(1)°
	c = 13.765(3) Å	γ = 90°
Volume	3356.6(13) Å^3	
Z	2	
Density (calculated)	1.440 g/cm^3	
Absorption coefficient	0.640 mm^{-1}	
F(000)	1504	
Crystal size	0.15 × 0.18 × 0.43 mm^3	
θ range for data collection	2.16 to 29.0°.	
Index ranges	$-17 \leq h \leq 17$, $-25 \leq k \leq 25$, $-18 \leq l \leq 18$	
Reflections collected	40447	
Independent reflections	8903 [R(int) = 0.0397]	
Reflections with I>2σ(I)	8017	
Completeness to θ = 29.0°	99.6 %	
Absorption correction	None	
Refinement method	Full-matrix least-squares on F^2	
Data / restraints / parameters	8903 / 0 / 415	
Largest final shift/e.s.d. ratio	0.004	
Goodness-of-fit on F^2	1.045	
Final R indices [I>2σ(I)]	R1 = 0.0255, wR2 = 0.0623	
R indices (all data)	R1 = 0.0300, wR2 = 0.0648	
Largest diff. peak and hole	0.559 and -0.436 e.Å^{-3}	

The Crystal Structure of [(Triphos)HRu(μ-H)$_2$RuH(Triphos)]

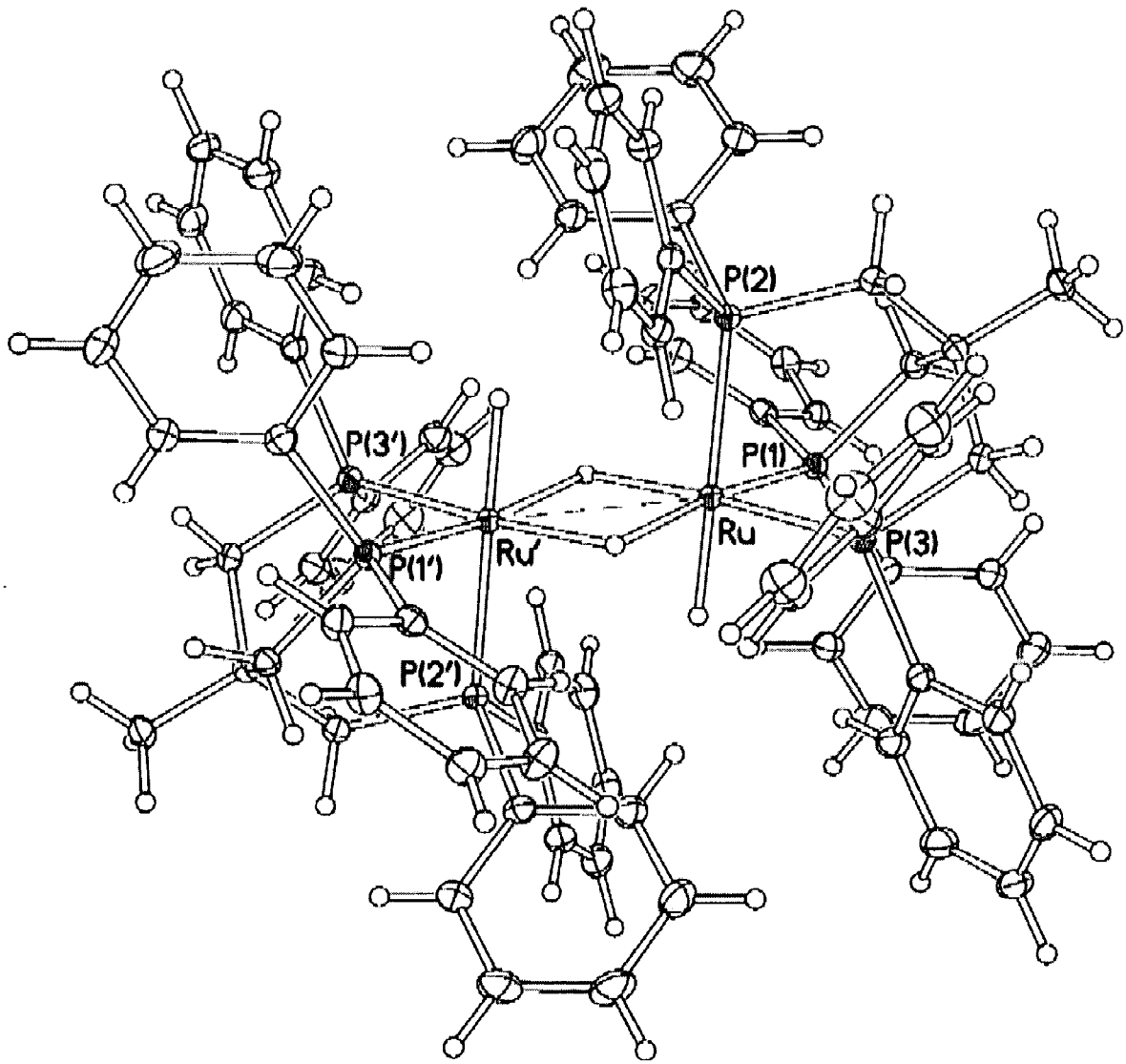

Table 2. Atomic coordinates ($\times 10^4$) and equivalent isotropic displacement parameters ($Å^2 \times 10^4$). U(eq) is defined as one third of the trace of the orthogonalized Uij tensor.

	x	y	z	U(eq)
Ru	5081.93(9)	5350.51(6)	4098.03(8)	97.1(4)
P(1)	5031.9(3)	5040.7(2)	2513.8(3)	111.3(7)
P(2)	3373.7(3)	5757.1(2)	3800.6(3)	113.2(7)
P(3)	5662.7(3)	6428.2(2)	3672.1(3)	117.0(8)
C(1)	4182(1)	5624(1)	1686(1)	134(3)
C(2)	3267(1)	6439(1)	2814(1)	139(3)
C(3)	5126(1)	6712(1)	2429(1)	132(3)
C(4)	4056(1)	6397(1)	2041(1)	128(3)
C(5)	3621(1)	6845(1)	1151(1)	171(3)
C(11)	6239(1)	4972(1)	1931(1)	143(3)
C(12)	6465(1)	5360(1)	1116(1)	181(3)
C(13)	7364(1)	5228(1)	677(1)	248(4)
C(14)	8042(1)	4701(1)	1043(1)	268(4)
C(15)	7836(1)	4317(1)	1865(1)	237(4)
C(16)	6947(1)	4454(1)	2308(1)	185(3)
C(21)	4450(1)	4192(1)	2065(1)	137(3)
C(22)	4615(1)	3915(1)	1150(1)	158(3)
C(23)	4033(1)	3346(1)	756(1)	182(3)
C(24)	3265(1)	3045(1)	1253(1)	187(3)
C(25)	3115(1)	3307(1)	2172(1)	207(3)
C(26)	3714(1)	3869(1)	2580(1)	176(3)
C(31)	2314(1)	5132(1)	3409(1)	153(3)
C(32)	1667(1)	5158(1)	2530(1)	198(3)
C(33)	870(1)	4663(1)	2331(1)	266(4)
C(34)	711(1)	4139(1)	3008(1)	277(4)
C(35)	1349(1)	4106(1)	3883(1)	238(4)
C(36)	2143(1)	4595(1)	4082(1)	184(3)
C(41)	2738(1)	6240(1)	4736(1)	137(3)
C(42)	3366(1)	6613(1)	5448(1)	161(3)
C(43)	2938(1)	7036(1)	6128(1)	202(3)
C(44)	1871(1)	7070(1)	6124(1)	216(3)
C(45)	1237(1)	6684(1)	5441(1)	223(3)
C(46)	1665(1)	6275(1)	4742(1)	183(3)

C(51)	5401(1)	7211(1)	4425(1)	147(3)
C(52)	4748(1)	7777(1)	4112(1)	188(3)
C(53)	4555(2)	8327(1)	4750(1)	239(4)
C(54)	5018(2)	8327(1)	5704(1)	256(4)
C(55)	5686(1)	7777(1)	6022(1)	233(3)
C(56)	5877(1)	7226(1)	5391(1)	188(3)
C(61)	7056(1)	6590(1)	3609(1)	147(3)
C(62)	7458(1)	7283(1)	3631(1)	184(3)
C(63)	8501(1)	7400(1)	3546(1)	214(3)
C(64)	9155(1)	6832(1)	3428(1)	227(4)
C(65)	8770(1)	6143(1)	3403(1)	215(3)
C(66)	7728(1)	6023(1)	3501(1)	172(3)

Table 3. Bond lengths [Å] and angles [°]

Ru-H(01)	1.62(2)	C(15)-C(16)	1.391(2)
Ru-H(02)	1.91(2)	C(21)-C(26)	1.393(2)
Ru-P(1)	2.2514(6)	C(21)-C(22)	1.402(2)
Ru-P(3)	2.2661(6)	C(22)-C(23)	1.388(2)
Ru-P(2)	2.3460(6)	C(23)-C(24)	1.393(2)
Ru-Ru#1	2.8412(5)	C(24)-C(25)	1.392(2)
P(1)-C(21)	1.8462(16)	C(25)-C(26)	1.395(2)
P(1)-C(11)	1.8474(16)	C(31)-C(32)	1.397(2)
P(1)-C(1)	1.8574(16)	C(31)-C(36)	1.405(2)
P(2)-C(41)	1.8459(16)	C(32)-C(33)	1.399(2)
P(2)-C(31)	1.8491(16)	C(33)-C(34)	1.389(3)
P(2)-C(2)	1.8627(16)	C(34)-C(35)	1.387(3)
P(3)-C(61)	1.8519(16)	C(35)-C(36)	1.390(2)
P(3)-C(3)	1.8543(16)	C(41)-C(42)	1.395(2)
P(3)-C(51)	1.8556(16)	C(41)-C(46)	1.400(2)
C(1)-C(4)	1.550(2)	C(42)-C(43)	1.391(2)
C(2)-C(4)	1.561(2)	C(43)-C(44)	1.391(3)
C(3)-C(4)	1.554(2)	C(44)-C(45)	1.387(3)
C(4)-C(5)	1.543(2)	C(45)-C(46)	1.395(2)
C(11)-C(12)	1.397(2)	C(51)-C(52)	1.402(2)
C(11)-C(16)	1.402(2)	C(51)-C(56)	1.403(2)
C(12)-C(13)	1.397(2)	C(52)-C(53)	1.398(2)
C(13)-C(14)	1.386(3)	C(53)-C(54)	1.384(3)
C(14)-C(15)	1.394(3)	C(54)-C(55)	1.391(3)

C(55)-C(56)	1.394(2)	C(63)-C(64)	1.389(3)
C(61)-C(66)	1.399(2)	C(64)-C(65)	1.391(3)
C(61)-C(62)	1.404(2)	C(65)-C(66)	1.397(2)
C(62)-C(63)	1.394(2)		

H(01)-Ru-H(02)	83.6(11)	C(61)-P(3)-Ru	121.12(5)
H(01)-Ru-P(1)	87.9(8)	C(3)-P(3)-Ru	113.24(5)
H(02)-Ru-P(1)	94.9(7)	C(51)-P(3)-Ru	118.68(5)
H(01)-Ru-P(3)	92.7(9)	C(4)-C(1)-P(1)	116.03(10)
H(02)-Ru-P(3)	175.5(7)	C(4)-C(2)-P(2)	117.43(10)
P(1)-Ru-P(3)	87.490(17)	C(4)-C(3)-P(3)	116.05(10)
H(01)-Ru-P(2)	176.2(9)	C(5)-C(4)-C(1)	107.85(12)
H(02)-Ru-P(2)	93.9(7)	C(5)-C(4)-C(3)	107.48(12)
P(1)-Ru-P(2)	89.454(17)	C(1)-C(4)-C(3)	110.21(12)
P(3)-Ru-P(2)	89.990(18)	C(5)-C(4)-C(2)	107.54(12)
H(01)-Ru-Ru#1	81.8(8)	C(1)-C(4)-C(2)	111.29(12)
H(02)-Ru-Ru#1	42.4(7)	C(3)-C(4)-C(2)	112.26(12)
P(1)-Ru-Ru#1	136.817(16)	C(12)-C(11)-C(16)	118.17(15)
P(3)-Ru-Ru#1	134.588(12)	C(12)-C(11)-P(1)	125.28(12)
P(2)-Ru-Ru#1	98.198(15)	C(16)-C(11)-P(1)	116.41(12)
Ru-H(02)-Ru#1	95.6(11)	C(13)-C(12)-C(11)	121.02(16)
C(21)-P(1)-C(11)	97.55(7)	C(14)-C(13)-C(12)	120.09(17)
C(21)-P(1)-C(1)	96.44(7)	C(13)-C(14)-C(15)	119.59(16)
C(11)-P(1)-C(1)	104.65(7)	C(16)-C(15)-C(14)	120.27(17)
C(21)-P(1)-Ru	121.01(5)	C(15)-C(16)-C(11)	120.82(16)
C(11)-P(1)-Ru	120.29(5)	C(26)-C(21)-C(22)	118.50(14)
C(1)-P(1)-Ru	113.10(5)	C(26)-C(21)-P(1)	119.21(12)
C(41)-P(2)-C(31)	98.01(7)	C(22)-C(21)-P(1)	121.65(12)
C(41)-P(2)-C(2)	99.56(7)	C(23)-C(22)-C(21)	120.47(15)
C(31)-P(2)-C(2)	103.51(7)	C(22)-C(23)-C(24)	120.81(15)
C(41)-P(2)-Ru	121.96(5)	C(25)-C(24)-C(23)	118.91(15)
C(31)-P(2)-Ru	120.38(6)	C(24)-C(25)-C(26)	120.40(15)
C(2)-P(2)-Ru	110.16(5)	C(21)-C(26)-C(25)	120.82(15)
C(61)-P(3)-C(3)	100.40(7)	C(32)-C(31)-C(36)	118.18(15)
C(61)-P(3)-C(51)	97.88(7)	C(32)-C(31)-P(2)	126.11(13)
C(3)-P(3)-C(51)	102.27(7)	C(36)-C(31)-P(2)	115.68(12)

C(31)-C(32)-C(33)	120.61(16)
C(34)-C(33)-C(32)	120.34(16)
C(35)-C(34)-C(33)	119.64(16)
C(34)-C(35)-C(36)	120.18(17)
C(35)-C(36)-C(31)	121.05(16)
C(42)-C(41)-C(46)	118.68(15)
C(42)-C(41)-P(2)	117.70(12)
C(46)-C(41)-P(2)	123.57(12)
C(43)-C(42)-C(41)	120.87(15)
C(44)-C(43)-C(42)	119.93(16)
C(45)-C(44)-C(43)	119.86(16)
C(44)-C(45)-C(46)	120.24(16)
C(45)-C(46)-C(41)	120.36(16)
C(52)-C(51)-C(56)	117.73(15)
C(52)-C(51)-P(3)	125.13(12)
C(56)-C(51)-P(3)	117.12(12)
C(53)-C(52)-C(51)	121.07(16)
C(54)-C(53)-C(52)	120.37(17)
C(53)-C(54)-C(55)	119.37(16)
C(54)-C(55)-C(56)	120.47(16)
C(55)-C(56)-C(51)	120.97(16)
C(66)-C(61)-C(62)	118.39(15)
C(66)-C(61)-P(3)	120.43(12)
C(62)-C(61)-P(3)	121.13(12)
C(63)-C(62)-C(61)	120.66(16)
C(64)-C(63)-C(62)	120.26(16)
C(63)-C(64)-C(65)	119.83(16)
C(64)-C(65)-C(66)	120.01(17)
C(65)-C(66)-C(61)	120.84(16)

Symmetry transformations used to generate equivalent atoms: #1 -x+1,-y+1,-z+1

Table 4. Anisotropic displacement parameters ($Å^2 \times 10^4$).

The anisotropic displacement factor exponent takes the form: $-2\pi^2[h^2 a^{*2} U_{11} + ... + 2 h k a^* b^* U_{12}]$

	U_{11}	U_{22}	U_{33}	U_{23}	U_{13}	U_{12}
Ru	97.1(6)	101.1(6)	93.0(6)	4.7(4)	10.4(4)	-2.6(4)
P(1)	115(2)	114(2)	106(2)	1(1)	15(1)	-3(1)
P(2)	104(2)	125(2)	111(2)	6(1)	10(1)	-3(1)
P(3)	117(2)	116(2)	118(2)	7(1)	11(1)	-9(1)
C(1)	133(7)	152(7)	113(6)	0(5)	5(5)	5(5)
C(2)	122(7)	150(7)	145(7)	23(5)	16(5)	15(5)
C(3)	132(7)	130(7)	134(7)	19(5)	21(5)	-13(5)
C(4)	123(7)	134(7)	124(6)	19(5)	2(5)	-4(5)
C(5)	182(7)	188(8)	142(7)	53(6)	11(6)	32(6)
C(11)	140(7)	157(7)	134(7)	-17(5)	22(5)	-9(6)
C(12)	164(7)	220(8)	161(7)	18(6)	26(6)	-5(6)
C(13)	204(8)	348(10)	207(8)	35(7)	82(6)	-18(7)
C(14)	158(8)	396(11)	263(9)	-26(8)	79(7)	19(7)
C(15)	167(8)	268(9)	274(9)	-8(7)	19(6)	60(7)
C(16)	164(7)	204(8)	185(7)	8(6)	15(6)	14(6)
C(21)	144(7)	120(7)	142(7)	2(5)	2(5)	16(5)
C(22)	174(7)	164(7)	138(7)	4(6)	28(5)	-16(6)
C(23)	237(8)	160(8)	149(7)	-20(6)	19(6)	-10(6)
C(24)	192(8)	155(8)	209(8)	-13(6)	-3(6)	-26(6)
C(25)	212(8)	189(8)	230(8)	-11(6)	75(6)	-53(6)
C(26)	211(8)	156(7)	168(7)	-21(6)	51(6)	-22(6)
C(31)	125(7)	169(7)	162(7)	-20(6)	11(5)	-20(6)
C(32)	172(8)	237(8)	176(7)	4(6)	-20(6)	-21(6)
C(33)	212(9)	347(10)	219(9)	-37(7)	-63(7)	-54(7)
C(34)	209(8)	313(10)	301(9)	-55(8)	3(7)	-128(7)
C(35)	225(8)	239(9)	252(9)	10(7)	31(7)	-87(7)
C(36)	170(7)	213(8)	167(7)	-4(6)	10(6)	-34(6)
C(41)	147(7)	132(7)	137(7)	26(5)	41(5)	15(5)
C(42)	161(7)	170(7)	157(7)	11(6)	35(6)	2(6)
C(43)	264(9)	182(8)	163(7)	-9(6)	43(6)	14(6)
C(44)	283(9)	207(8)	175(8)	26(6)	99(6)	94(7)
C(45)	173(8)	278(9)	231(8)	63(7)	78(6)	64(7)
C(46)	153(7)	210(8)	186(7)	18(6)	27(6)	14(6)

C(51)	157(7)	131(7)	157(7)	-15(5)	35(5)	-23(5)
C(52)	199(8)	159(8)	203(8)	2(6)	5(6)	-3(6)
C(53)	267(9)	163(8)	292(9)	-22(7)	45(7)	25(7)
C(54)	295(9)	213(9)	266(9)	-88(7)	60(7)	-12(7)
C(55)	243(9)	258(9)	194(8)	-64(7)	10(6)	-37(7)
C(56)	179(8)	200(8)	184(8)	-14(6)	17(6)	-16(6)
C(61)	140(7)	182(8)	117(7)	16(5)	6(5)	-29(6)
C(62)	182(8)	189(8)	180(7)	19(6)	12(6)	-31(6)
C(63)	203(8)	236(9)	199(8)	30(6)	5(6)	-99(7)
C(64)	134(7)	354(10)	189(8)	34(7)	5(6)	-55(7)
C(65)	156(8)	281(9)	208(8)	2(7)	23(6)	14(6)
C(66)	151(7)	192(8)	170(7)	-6(6)	3(6)	-19(6)

Table 5. Hydrogen coordinates ($\times 10^4$) and isotropic displacement parameters ($Å^2 \times 10^3$)

	x	y	z	U(iso)
H(01)	6234(18)	5023(13)	4263(17)	34(6)
H(02)	4689(18)	4435(13)	4527(17)	32(6)
H(1A)	4460	5640	1045	17
H(1B)	3489	5403	1580	17
H(2A)	2563	6409	2463	18
H(2B)	3336	6912	3127	18
H(3A)	5067	7236	2425	17
H(3B)	5626	6582	1967	17
H(5A)	3473	7327	1367	26
H(5B)	2983	6627	844	26
H(5C)	4130	6866	678	26
H(12)	6001	5719	856	22
H(13)	7509	5499	127	30
H(14)	8645	4603	736	32
H(15)	8304	3960	2123	28
H(16)	6819	4194	2873	22
H(22)	5129	4118	797	19
H(23)	4159	3159	139	22
H(24)	2851	2668	970	22
H(25)	2602	3102	2525	25
H(26)	3619	4034	3216	21

H(32)	1769	5515	2062	24
H(33)	436	4686	1730	32
H(34)	167	3805	2873	33
H(35)	1244	3747	4348	29
H(36)	2577	4566	4683	22
H(42)	4096	6579	5469	19
H(43)	3374	7301	6594	24
H(44)	1577	7357	6589	26
H(45)	509	6697	5449	27
H(46)	1226	6020	4267	22
H(52)	4431	7787	3457	23
H(53)	4102	8703	4526	29
H(54)	4881	8698	6138	31
H(55)	6014	7778	6673	28
H(56)	6335	6854	5618	23
H(62)	7015	7675	3705	22
H(63)	8765	7871	3569	26
H(64)	9864	6914	3363	27
H(65)	9215	5753	3321	26
H(66)	7472	5550	3494	21